Swansea University
Prifysgol Abertawe

Cronfa
Setting Research Free

Swansea University E-Theses

Automated chromosome damage analysis to investigate thresholds for genotoxic agents.

Brusehafer, Katja

How to cite:

Brusehafer, Katja (2013) *Automated chromosome damage analysis to investigate thresholds for genotoxic agents..* thesis, Swansea University.
http://cronfa.swan.ac.uk/Record/cronfa43178

Use policy:

This item is brought to you by Swansea University. Any person downloading material is agreeing to abide by the terms of the repository licence: copies of full text items may be used or reproduced in any format or medium, without prior permission for personal research or study, educational or non-commercial purposes only. The copyright for any work remains with the original author unless otherwise specified. The full-text must not be sold in any format or medium without the formal permission of the copyright holder. Permission for multiple reproductions should be obtained from the original author.

Authors are personally responsible for adhering to copyright and publisher restrictions when uploading content to the repository.

Please link to the metadata record in the Swansea University repository, Cronfa (link given in the citation reference above.)

http://www.swansea.ac.uk/library/researchsupport/ris-support/

Automated chromosome damage analysis to investigate thresholds for genotoxic agents

By

Katja Brüsehafer

A thesis submitted in partial fulfilment of the requirements for the degree of Doctor of Philosophy

DNA damage and Cancer Research Group
Institute of Life Sciences
College of Medicine
Swansea University

ProQuest Number: 10821570

All rights reserved

INFORMATION TO ALL USERS
The quality of this reproduction is dependent upon the quality of the copy submitted.

In the unlikely event that the author did not send a complete manuscript
and there are missing pages, these will be noted. Also, if material had to be removed,
a note will indicate the deletion.

ProQuest 10821570

Published by ProQuest LLC (2018). Copyright of the Dissertation is held by the Author.

All rights reserved.
This work is protected against unauthorized copying under Title 17, United States Code
Microform Edition © ProQuest LLC.

ProQuest LLC.
789 East Eisenhower Parkway
P.O. Box 1346
Ann Arbor, MI 48106 – 1346

Declaration

This work has not previously been accepted in substance for any degree and is not being concurrently submitted in candidature for any degree.

Signed ....(candidate)

Date 31/07/2013

Statement 1

This thesis is the result of my own investigations, except where otherwise stated. Other sources are acknowledged by footnotes giving explicit references. A bibliography is appended.

Signed ....(candidate)

Date 31/07/2013

Statement 2

I hereby give consent for my thesis, if accepted, to be available for photocopying and for inter-library loan, and for the title and summary to be made available outside organisations.

Signed ....(candidate)

Date 31/07/2013

Acknowledgements

I am very grateful to Professor Gareth J.S. Jenkins and Dr. Shareen H. Doak for giving me the opportunity to complete a PhD in this research group. I would like to thank them both for their constant support and advice throughout the period of this PhD. I am also grateful to Dr. Michael R. O'Donovan and Dr. Ann T. Doherty for their advice and help, especially during the extended work period performed at AstraZeneca in Cheshire, UK. Further I would like to thank Dr. Paul D. Lewis for his help with the statistical analysis of my work.

Thank you to Margaret and Sally for running the lab, ordering all the supplies needed and their general support and friendly words. A big thank you to Bella for her unshakeable support, constant advice and her friendship during my PhD. Life would be a lot less fun without you.

Thanks also to all my fellow researchers and friends, Anna, Neenu, George, James, Matt, Adam, Ben, Kulsoom, John, Kate, Bushra, Abdullah, Jatin, Jeremy and Hasan, who made this PhD pass quickly and really enjoyable. Conferences and social times with you guys will never be forgotten.

Obviously these acknowledgements would not be complete without mentioning my family. Ich möchte mich ganz herzlich bei meinen Eltern für ihre jahrelange Unterstützung bei meinem Studium und bei meiner Doktorarbeit bedanken. Sie standen mir immer mit Rat und Tat zur Seite. Danke Mama! Danke Papa! Es ist ein Geschenk euch als Eltern zu haben.

Finally huge thanks to Tom for his constant support and endurance of my bad moods, especially during the write up of this thesis. Glad to have you in my life.

This PhD was funded by MRC with a CASE award from AstraZeneca.

Summary

Genotoxicology involves the assessment of a substance's ability to induce DNA damage after exposure to humans. DNA damage is an underlying cause of mutations that are likely to initiate carcinogenesis. Furthermore, the investigation of low dose responses in genotoxicology testing helps to improve health risk assessment by establishing whether DNA reactive compounds follow linear or non-linear (thresholded) dose response relationships.
The current assumption for direct acting genotoxins is that the relationship between exposure to genotoxic chemicals, DNA damage formation and the induction of mutagenic changes is linear. However, it is known that mutations are not produced directly by DNA adducts as DNA repair activity limits the proportion of adducts processed into mutations. It is therefore possible, that no observed effect levels (NOEL) may exist for some genotoxins.

The main aim of this thesis was to improve *in vitro* genotoxicity testing by assessing the low dose response relationships for the genotoxic agents mitomycin-C (MMC), 4-nitroquinoline 1-oxide (4NQO) and cytosine arabinoside (araC). Furthermore, the automated micronucleus slide scoring system Metafer was validated and used for these studies.
In addition, the mechanism of action of each test component was further investigated by follow up experiments to gain a better understanding of the processes involved in this type of damage.

The *in vitro* micronucleus assay for the detection of chromosomal damage revealed non-linear dose response relationships following low dose exposure of MMC and araC, while 4NQO revealed a weak clastogenic potential. The semi-automated scoring protocol for the Metafer-System proved to be a rapid and accurate system for scoring micronuclei.
DNA repair plays most likely a major role in these non-linear responses by removing genetic damage induced at low levels. Furthermore, p53 was shown to be involved in the DNA damage response in human lymphoblastoid cells, through cell cycle delay and the induction of apoptosis.
In addition, this work confirmed that a proper dosing regime, accurate toxicity measurements and the appropriate choice of cell type are crucial criteria for defining the dose response relationships and the induction of genotoxicity and cytotoxicity.

Abbreviations

AE	Alkaline elution
8-AG	8-Azaguanine
AP sites	Apurinic/ apyrimidinic sites
4AQO	4-Aminoquinoline 1-oxide
araC	Cytosine arabinoside
ATP	Adenosine triphosphate
BER	Base excision repair
BMD	Benchmark dose
CA	Chromosome aberrations
CBMN	Cytokinesis-blocked micronucleus assay
CBPI	Cytokinesis-block proliferation index
cDNA	copyDNA
CDK	Cyclin-dependent kinases
CHL	Chinese hamster lung
CHO	Chinese hamster ovary
CKI	Cyclin-dependent kinase inhibitors
COM	Committee on Mutagenicity of Chemicals in Food, Consumer Products and the Environment
CPSC	US Consumer Product Safety Commission
CTP	Cytosine triphosphate
CytoB	Cytochalasin B
2,7-DAM	2,7-diaminomitosense
DAPI	4',6-diamidino-2-phenylindole
DISC	Death-inducing signalling complex
DMC	Decarbamoyl mitomycin C
DNA	Deoxyribonucleic acid
DSB	DNA double strand breaks repair
EMS	Ethyl methanesulfonate
ENDOIII	Endonuclease III
ENU	N-Ethyl-N-nitrosourea
EPA	US Environmental Protection Agency
EU	European Union
FADD	Fas-associated death domain
FCS	Forward scatter
FDA	US Food and Drug Administration
FPDG	Formamidopyrimidine DNA-glycosylase
GGR	Global genomic repair
GSH	Glutathione
GSTP1-1	Glutathione S-transferase P1-1
4HAQO	4-Hydroxyaminoquinoline 1-oxide
HAT	Hypoxanthine-aminopterin-thymidine
hOGG1	Human 8-hydroxyguanine DNA-glycosylase 1
HPRT	Hypoxanthine-guanine phosphoribosyl transferase
HR	Homologous recombination
HT	Hypoxanthine-thymidine

ICH	International Conference on Harmonization of Technical Requirements for Registration of Pharmaceuticals for Human Use
$KBrO_3$	Potassium bromate
kD	KiloDalton
LOEL	Lowest observed effect level
MeIQX	2-Amino-3,8-dimethylimidazo[4,5-f]quinoxaline
MF	Mutation frequency
MGMT	O6-methylguanine-DNA methyltransferase
MLA	Mouse lymphoma assay
MMC	Mitomycin C
MMR	Mismatch repair
MMS	Methyl methanesulfonate
MN	Micronucleus/ micronuclei
MNU	N-Methyl-N-nitrosourea
MONOMn	Mononucleated micronucleus assay
MRP	Multidrug resistance protein
NAD(P)H	Nicotinamide adenine dinucleotide (phosphate) oxide
NER	Nucleotide excision repair
NHEJ	Non-homologous end-joining
NOEL	No observed effect level
4NQO	4-Nitroquinoline 1-oxide
OECD	Organisation for Economic Co-operation and Development
8-OH-dG	8-Hydroxydeoxyguanosine
8-OxoG	8-oxo-7,8-dihydroguanine
PBS	Phosphate buffer saline
PCR	Polymerase chain reaction
PD	Population doubling
PE	Plate efficiency
PhiP	2-Amino-1-methyl-6-phenylimidazo[4,5-b]pyridine
PI	Propidium iodide
POD	Point of departure
PS	Phosphatidylserine
QO-SG	4-(glutathione-S-yl)-quinoline 1-oxide
RCC	Relative cell counts
RI	Replication index
RICC	Relative Increase in cell counts
RNA	Ribonucleic acid
ROS	Reactive oxygen species
RPD	Relative population doubling
Ppm	Parts per million
RSM	Restriction site mutation
RTU	Ready to use
SAR	Structure activity relationships
SCE	Sister chromatid exchange
SD	Standard deviation
SHE CT	Syrian hamster embryo cell transformation
SSC	Side scatter
TCR	Transcription-coupled repair

TFT	Trifluorothymidine
TNF	Tumour necrosis factor
TI	Tail intensity
6-TG	6-Thioguanine
TK	Thymidine kinase
UDS	Unscheduled DNA synthesis
UK	United Kingdom
US	United States
UV	Ultraviolet
XPRT	Xanthine-guanine phosphoribosyl transferase

Table of contents

Chapter 1

General Introduction

Genotoxicology involves the assessment of a substance's ability to induce DNA damage, which is an essential consideration for human risk assessment, because DNA damage is an underlying cause of mutations that have the potential to initiate carcinogenesis. A mutation is defined as a permanent change in the amount or structure of the genetic material of a whole organism or a single cell (Dearfield et al., 2002; COM guideline, 2011). Mutations can range from alterations in genes to modifications of the number and/or structure of chromosomes. Gene mutations are changes in the nucleotide sequence, which involve single point mutation (substitutions or frameshift mutation), or small deletions or duplications. Chromosome mutations comprise alterations in segments of chromosomes through whole chromosomes or entire sets of chromosomes (COM guideline, 2011). Mutations in germ cells can cause heritable effects, which then may also have an impact on the offspring. Thus characterising DNA damage is crucial to minimising the detrimental impact of exposure to exogenous substances (COM guideline, 2011).

Compounds, which interact with DNA and cause mutations, are called mutagens and/or genotoxins. These compounds can interact with DNA by various mechanisms, such as direct interaction of the compound with DNA, interaction of the compound with cellular components that cause indirect DNA damage and DNA damage can be induced through activation of the compound by cellular metabolism to produce products, which are capable to interact with DNA (Parry and Parry, 2012). Examples of chemicals which directly interact with the DNA helix are mitomycin C and 4-nitroquinoline 1-oxide; while the production of reactive oxygen species is a mechanism as an example of the generation of secondary active molecules which are capable to react with DNA. The metabolism of benzo(a)pyrene by arylhydrocarbon hydroxylases into a diol epoxide, which then reacts with DNA, is an example for activation of a compound by cellular metabolism into a reactive metabolite (Levin et al., 1977; Parry and Parry, 2012).

1.1 DNA damage, mutagenesis and carcinogenesis

DNA damage plays a key role in mutagenesis and carcinogenesis as an important cause of genetic disease. Chemical events that can lead to DNA damage include hydrolysis, exposure to reactive oxygen species (ROS) and electrophilic attack (Marnett and Plastaras, 2001; De

Bont and van Larebeke, 2004). These reactions are triggered through exposure to exogenous chemicals, such as environmental agents, food additives and constituents or are the result of endogenous reactive metabolites (Marnett and Plastaras, 2001).

Mutations due to DNA damage (exogenous and endogenous) play an essential role in carcinogenesis. Consequently knowledge of the types of endogenous DNA damage is crucial for the understanding of the interaction of exogenous agents and the influences of endogenous processes in the development of cancer and other diseases (De Bont and van Larebeke, 2004).

1.1.1 Endogenous DNA damage and mutation

Endogenous (spontaneous) mutations arise from a variety of sources, including DNA replication errors, spontaneous lesions and transposable genetic elements. Oxidation, methylation, deamination and depurination are major endogenous processes leading to significant DNA damage (Ames et al., 1993). Endogenous DNA damage occurs at a high rate, but specific DNA repair glycosylases for oxidative, methylated and deaminated adducts and a repair system for apurinic sites contribute to the low frequency of spontaneous mutations, which is estimated to be 10^{-9} to 10^{-12} mutations per nucleotide per cell per generation (Drake et al., 1969; Ames et al., 1993).

Errors in replication can occur due to misincorporation of bases during DNA replication leading to base substitutions (Griffiths et al., 2000). Mispairs can lead to transition mutations, in which a purine substitutes for a purine or a pyrimidine for a pyrimidine, or to transversion mutations, where a pyrimidine substitutes for a purine and vice versa (Griffiths et al, 2000). Further replication errors can lead to frameshift mutations and deletions and duplications constitute to a sizeable fraction of spontaneous mutations (Griffiths et al., 2000).

In addition to replication errors, spontaneous lesions can generate mutations, including apurinic/apyrimidic (AP) sites, deamination and oxidative DNA damage. AP sites often occur through the disruption of the glycosidic bond between the base and the desoxyribose and the subsequent loss of a base from the DNA leaving a gap in the DNA sequence (Griffiths et al., 2000). The resulting AP sites, if not repaired, cannot specify a base complementary to the original base during replication.

Deamination of DNA bases can cause transition mutations. For instance, the deamination of cytosine produces uracil, which will pair with adenine during replication if unrepaired and result in the conversion of a G-C pair into an A-T pair (Griffiths et al., 2000).

Reactive oxygen species (ROS), such as superoxide radicals, hydrogen peroxide and hydroxyl radicals are continuously formed as a consequence of metabolic and other biochemical reactions. ROS can oxidize DNA, which can lead to DNA damage, including oxidized bases and single- and double-strand breaks (De Bont and van Larebeke, 2004).

To summarize, endogenous mutations can be generated by different processes. Errors in replication and spontaneous lesions cause most of the significant DNA damage.

1.1.2 Exogenous DNA damage and mutation

Mutations can be caused through exposure to exogenous chemicals. Exogenous agents include aromatic amines, alkylating agents, radiation and other reactive chemicals.

Some chemical agents act as base analogs and are incorporated into the DNA in place of normal bases, where they can cause mispairs. For instance, 5-bromouracil is an analog of thymine, whereas 2-amino-purine is an analog of adenine (Griffiths et al., 2000). Alkylating agents, such as ethylmethanesulfonate can cause specific mispairing through alteration of a base. Ionizing radiation can lead to the formation of ionized and excited molecules that can cause damage to the DNA, including formation of AP sites or DNA strand breaks (Griffiths et al., 2000).

In conclusion, mechanisms by which these agents can cause mutation include mimicking normal bases and incorporation into the DNA, where they can mispair (Griffiths et al, 2000). The types of endogenous DNA damage are similar to those caused by exogenous agents.

1.1.3 Multiple mutations in cancer

The ability of substances to induce mutations and their ability to induce cancer are correlated, as mutations are essential for cancer to evolve (Loeb and Loeb, 2000). Cancer is a genetic disease and cancer cells contain multiple mutations, implying that tumour progression is driven by mutagenesis (Loeb and Loeb, 2000; Sarasin, 2003). It has been estimated that four to seven mutations in key genes are necessary for the induction of human cancers (Sarasin, 2003). Early events of carcinogenesis involve mutations in genes that are key in maintaining genetic stability of cells, leading as a result to genetic instability in cancer cells and resulting in a cascade of mutations which enable cancer cells to bypass regulatory processes, such as cell cycle progression, apoptosis and gene expression (Loeb and Loeb, 2000; Jackson and Loeb, 2001).

Normal mutation rates followed by the selective advantage of mutated clones might be enough to produce the multiple mutations found in human cancers (Sarasin, 2003). However,

mutations in normal cells only occur at a rate of 10^{-10} mutations per nucleotide per cell per generation. Therefore Loeb *et al.* (2003), proposed that normal mutation rates are insufficient to account for the numerous mutations found in tumours and that mutations increase the basal mutation rate and lead to multiple mutations (Loeb et al., 2003; Sarasin, 2003).

Several types of genetic modification have been identified in human tumours, including base substitutions, deletions or additions of a few nucleotides, losses or gains of whole chromosomes, chromosome translocation and gene amplification (Sarasin, 2003). The loss or gain of whole chromosomes results from a defective mitosis and leads to chromosomal non-disjunction (Jackson and Loeb, 2001), while chromosome translocations result from fusion between two non-adjacent sequences on the same chromosome or on two different chromosomes (Sarasin, 2003).

Consequently, the ability to detect substances which cause DNA mutations is essential in the risk assessment for human populations. Assessing substances for their DNA damage capability might be a useful tool as a surrogate for carcinogenicity testing. To provide comprehensive coverage of the mutagenic potential of a chemical it is necessary to supply information on three levels of DNA damage: gene mutation, clastogenicity (i.e. structural chromosome aberrations) and aneuploidy (i.e. numerical chromosomal aberrations) (COM guideline, 2011). Consequently, genotoxicity testing was established to investigate the mutagenic potential of all new synthetic chemicals and regulatory bodies developed guidelines and assays for genotoxicity testing.

1.2 Regulatory authorities and testing

Many countries have developed guidelines for testing the genotoxicity of new chemicals. No single test alone can predict the entire spectrum of inducible mutations, because of the variety of genetic events that can occur (Cimino, 2006). Non-human test systems are able to predict the intrinsic mutagenicity of test chemicals because of the universality of DNA and the genetic code, even though differences in metabolism or DNA repair may exist (Dearfield et al., 2002). Furthermore, chemicals causing genetic effects in one species or test system (e.g. bacterial, insect, rodent) show largely similar effects in other species or systems (Dearfield et al., 2002).

Initial screens for genotoxic activity include a range of *in vitro* tests to cover the three main endpoints. Advantages of *in vitro* systems include easy and rapid culture conditions, exposure of target cells and most importantly no use of live animals for the exposure of toxic compounds. However disadvantages, like poor characterisation of the metabolic capability of

cell lines or the fact that organ homogenates used in exogenous activation systems might be cytotoxic to mammalian cells in culture led to the conclusion that *in vivo* tests should be included in the standard test battery (Cimino, 2006).

1.2.1 History of testing strategies

Concerns about chemicals introducing deleterious alterations in the DNA of humans, which were demonstrated by Auerbach and Robson in the late 1940s (Auerbach and Robson, 1946) and concerns about germ line mutations, led to the formation of the Environmental Mutagen Society in 1969 in the United States. Subsequently, in the 1970s requirements for testing for mutagenic properties of chemicals were introduced (MacGregor et al., 2000). The publication of a key paper by McCann *et al*, "Carcinogens are Mutagens: Analysis of 300 Chemicals" showed a strong correlation of mutagenic activity in Salmonella with animal carcinogenicity (McCann et al., 1975; MacGregor et al., 2000). *In vitro* mutagenesis screening tests, like the Ames test, were then used to identify chemical carcinogens. Furthermore, regulatory guidelines for the bacterial gene mutation test were implemented during the 1970s and 1980s (MacGregor et al., 2000). However at that time it was also recognized that mutations could arise by multiple mechanisms and that the Ames test was not adequate to detect chromosomal interchanges or large chromosomal deletions. From this it followed that an *in vitro* test battery was devised to be able to detect all major classes of damage which could be fixed as heritable mutations (MacGregor et al., 2000). The first test batteries used included (1) a bacterial test for gene mutation, (2) an *in vitro* test for chromosomal aberrations or a mammalian cell mutagenesis test and (3) a general DNA damage test (MacGregor et al., 2000).

During the 1970s, guidelines for testing environmental chemicals (and in 1982 for food additives) were drafted in the US (MacGregor et al. 2000). In 1993 the US Food and Drug Administration (FDA)-recommended testing battery was (1) a bacterial test for gene mutation, (2) an *in vitro* mammalian gene mutation test and (3) an *in vivo* cytogenetic damage assay, with preference for a rodent bone marrow assay (MacGregor et al, 2000). Similar recommendations, but with regional differences were made by the European, Japanese and Canadian authorities. An international consensus for a testing battery for pharmaceutical registration was achieved by the International Conferences on Harmonization of the Toxicological Requirements for Registration of Pharmaceuticals for Human Use (ICH) in the late 1990s and included (1) a bacterial test for gene mutation in bacteria, (2) an *in vitro* mammalian chromosome aberration test or the L5178Y mouse lymphoma mammalian cell

mutagenesis test and (3) an *in vivo* chromosomal damage test in rodent hematopoietic cells (MacGregor et al., 2000). Since then great efforts in harmonization of testing strategies and testing standards have been undertaken. Recommendations for internationally harmonized testing protocols were developed by the Organization for Economic Cooperation and Development (OECD) (MacGregor et al., 2000).

1.2.2 Regulatory testing strategies in the United States, the United Kingdom and the European Union

Similar genotoxicity testing strategies, but with regional differences were developed for the detection of the mutagenic hazard of chemicals, which cover the endpoints of gene mutations and chromosome aberrations.

1.2.2.1 United States (US)

The regulatory agencies in the US include among others the US Environmental Protection Agency (EPA), the US Food and Drug Administration (FDA) and the US Consumer Product Safety Commission (CPSC).

The EPA evaluates environmental risks though a risk assessment process that combines analysis of a set of scientific data with the application of scientific judgement (Dearfield et al., 2002). The EPA estimates chemical risk via a four-step risk assessment paradigm (Dearfield et al., 2002; Cimino, 2006):

- Hazard identification: evaluates the inherent genotoxicity of an agent, including structure activity relationships (SAR) data to assess human genotoxicity
- Dose-response assessment: relationship between dose of an agent and the induction of an adverse effect (includes mechanisms and mode of action of the agent)
- Exposure assessment: extent of human exposure (route(s) of entry and levels of exposure)
- Risk characterization: nature and likelihood of genotoxicity risk to humans (including attendant uncertainty)

The current EPA test battery consists of a three-tiered system (Table 1.1), with the first tier including (1) the bacterial reverse mutation assay for gene mutation (*Salmonella typhimurium* and *Escherichia coli*), (2) an *in vitro* mammalian cell gene mutation assay and (3) the *in vivo*

mammalian bone marrow chromosome aberration or the in *vivo* erythrocyte MN assay (Dearfield et al., 1991; Cimino, 2006). If the first tier studies show any genotoxicity, a second tier study is employed, investigating any genotoxic effects in the reproductive tissue of the intact mammal. Tests available include the *in vivo* unscheduled DNA synthesis (UDS), alkaline elution (AE), sister chromatid exchange (SCE) and chromosomal aberration assays, done in testicular tissues and the rodent dominant lethal assay (Cimino, 2006). Third tier studies are used to determine if any mutagenic effects are transmitted to the offspring by parents who were exposed to a chemical. Tests include biochemical or visible specific locus assays (Cimino, 2006).

The FDA is compromised of the following components:

1. Centre for Biologics Evaluation and Research (CBER)
2. Centre for Drug Evaluation and Research (CDER)
3. Centre for Devices and Radiological Health (CDRH)
4. Centre for Food Safety and Applied Nutrition (CFSAN)
5. Centre for Veterinary Medicine (CVM)
6. National Centre for Toxicological Research (NCTR)
7. Office of Regulatory Affairs (ORA)
8. Office of the Commissioner (OC)

Most centres of the FDA, which are involved in regulatory testing, follow the three test battery (Table 1.1) proposed for human drugs developed by the ICH (Cimino, 2006).
CPSC is an independent regulatory agency and relies upon existing genotoxicity data, when assessing the need to regulate a consumer product (Cimino, 2006).

Table 1.1: Genotoxicity Testing Schemes for the US regulatory agencies EPA, FDA and CPSC (after Cimino, 2006)

	EPA	FDA				CPSC
	Toxics and Pesticides (Industrial and Pesticides)	CFSAN (Food additives)	CDER (Human drugs)	CVM (Veterinary drugs)	CDRH (Devices and radiologics)	
First-tier	• .....Bacterial gene mutation assay (*Salmonella typhimurium* and *Escherichia coli*).....					
	• *In vitro* mammalian cell gene mutation assay (pref., MLA)	• .... *In vitro* structural CA or in vitro MLA....		• Three *in vitro* assays	• Relies on existing test results	
	• ..... *In vivo* MN or CA assay.....					
Second-tier	• Effect in mammalian gonad *in vivo* (e.g. UDS, SCE, AE, RDL, CA in testicular					
Third-tier	• Effect in offspring of exposed parents (e.g. SLT, HT)					

AE, alkaline elution assay; CA, chromosome aberrations; HT, rodent heritable translocation; MLA, mouse lymphoma assay; MN, micronucleus assay; RDL, rodent dominant lethal; SCE, sister chromatid exchange; SLT, mouse specific locus; UDS, unscheduled DNA synthesis

1.2.2.2 United Kingdom (UK)

Regulatory bodies in the UK are advised by the Committee on Mutagenicity of Chemicals in Food, Consumer Products and the Environment (COM). COM is an independent expert advisory committee (COM, 2000). Advised regulatory bodies include:

1. UK Department of Health (DOH)
2. Food Standard Agency (FSA)
3. Department of Environment, Transport and the Regions (DETR)
4. Health and Safety Executive (HSE)
5. Pesticides Safety Directory (PSD)
6. Veterinary Medicines Directory (VMD)
7. Medicines Control Agency (MCA)
8. Scottish Executive
9. Welsh Assembly
10. Northern Ireland Executive

The current COM test strategy consists of a staged system (Table 1.2). Stage 0 includes preliminary considerations, such as physico-chemical properties of the test agent, structure activity relationships (SAR) and information from screening tests (COM guideline, 2011). Stage 1 is the core-test battery, which is based on *in vitro* tests including (1) a bacterial gene mutation assay (Ames test) combined with (2) the *in vitro* MN test to require information for gene mutation, chromosome damage and aneuploidy (COM guidelines, 2011). If any genotoxic effects were observed in Stage 1, then Stage 2 is employed.

Stage 2 investigates if any genotoxic effects are expressed in somatic or germ cells using *in vivo* testing. The assays mainly used are the rodent MN/chromosome aberration assays, to investigate aneuploidy and clastogenicity and the rodent transgenic gene mutation assay and/or comet assay for DNA damage induction (COM guideline, 2011). However based on information on the compound, the UDS assay and ^{32}P-postlabelling assays might be used on a case-by-case basis (Cimino, 2006). To measure the induction of DNA lesions i.e. as a measure of exposure, uptake and reactivity to DNA, the comet assay or the ^{32}P-postlabelling assay can be used in target tissues. The liver UDS can be used to measure the repair of DNA lesions, whereas transgenic animal models are useful to determine the induction of genetic changes (COM guideline, 2000). Assays available to analyse germ line mutations include MN induction in spermatocytes, the dominant lethal assay and mutation assays in the

reproductive tissue of transgenic mice (Cimino, 2006). To further investigate the risk for heritable mutations, assays including the mouse specific locus test and/or heritable translocation test are available.

Table 1.2: Genotoxicity Testing Scheme for the UK

Proposed UK (COM) scheme

Stage 0:	Preliminary considerations • Physico-chemical properties of test agent • Structure activity relationships (SAR) • Screening tests
Stage 1:	Two *in vitro* tests: • Bacterial gene mutation assay (Ames test) • *In vitro* MN assay
Stage 2:	*In vivo* tests (at least one) • *In vivo* MN assay • *In vivo* chromosome aberration assay • Possible other *in vivo* tests include: ➢ Comet assay ➢ ^{32}P-postlabeling assay ➢ UDS, SCE ➢ Transgenic animal models

SCE, sister chromatid exchange; UDS, unscheduled DNA synthesis

1.2.2.3 European Union (EU)

The EU test battery consists of a three-tiered test system (Table 1.3). Initial screening consists mainly of *in vitro* testing. The type and amounts of tests are based upon the chemical type. In the first tier the EU requires two *in vitro* tests for industrial products (1) a bacterial gene mutation assay and (2) a mammalian cell assay. For biocides (pesticides), cosmetic products and food additives the EU requires three *in vitro* tests, including (1) a bacterial gene mutation assay, (2) either the chromosome aberration or the *in vitro* MN assay and (3) a mammalian cell gene mutation assay. For pharmaceuticals the following three tests are required: (1) a bacterial gene mutation assay, (2) an *in vitro* mammalian cell chromosome aberrations assay or an *in vitro* gene mutation assay in mouse lymphoma cells and (3) either the *in vivo* chromosome aberration test or the *in vivo* MN assay. Five *in vitro* tests are required for hair dye ingredients. These tests include (1) the bacterial gene mutation assay, (2) a mammalian cell mutation assay, (3) a mammalian cell chromosomal aberration assay, (4) a mammalian cell MN assay and (5) a mammalian cell UDS assay (Cimino, 2006). If any of these tests show genotoxic activity further *in vivo* studies are required. However due to the 7th amendment to the EU Cosmetics Directive testing ban, it is no longer possible to follow up positive *in vitro* results with *in vivo* genotoxicity tests of cosmetic ingredients (Pfuhler et al., 2010). A second and third tier might be employed, which investigates effects in germ cells and effects in the offspring of exposed parents (Cimino, 2006).

Due to the prohibition of *in vivo* testing for cosmetic products and their ingredients in the EU and due to the general direction within the scientific community to reduce animal testing, *in vitro* genotoxicity testing will be the main tool to investigate and monitor human populations for genetic damage in the future (Kirkland et al., 2007; Pfuhler et al., 2010).

However, the sensitivity and specificity of a number of *in vitro* assays needs to be improved due to the high false positive rate observed for *in vitro* genotoxicity tests when compared with carcinogenicity in rodents (Kirkland et al., 2007; Pfuhler et al., 2010). The main areas of focus in the reduction of false positive results are: choices of cell type, toxicity measurements and maximum concentration to be tested (Pfuhler et al., 2010). Further new assays need to be developed to follow up positive results from *in vitro* assays, i.e. the use of 3D human reconstructed skin models and weight of evidence assessments (using information on the chemical itself, structural/functional analogues, metabolites, etc.) need to be conducted (Pfuhler et al.,2010).

Table 1.3: Genotoxicity Testing Schemes for the European Union (EU) (after Cimino, 2006)

EU					
(Industrial)	(Pesticides)	(Pharmaceuticals)	(Veterinary drugs)	(Cosmetics)	(Food)
First-Tier					
• ..... Bacterial gene mutation assay (*Salmonella typhimurium* and *Escherichia coli*).....					
• *In vitro* mammalian mutation assay (generally CA)	• *In vitro* mammalian gene mutation assay (pref., MLA))	• ..... *In vitro* MLA or CA	• *In vitro* mammalian gene mutation assay (pref., MLA)		
			• ... *In vitro* MN or CA	• *In vitro* CA • *In vitro* MN • *In vitro* UDS • *In vitro* SHE CT	
	• *In vitro* MN or CA				
	• ..... *In vivo* MN or CA				
	(If *in vitro* test is positive)			• An *in vivo* test if in vitro test is positive	
Second-tier					
• If positive, test for germ cell effects	• If *in vivo* positive, test for germ cell effects				
Third-tier					
• Effect in offspring of exposed parents					

CA, chromosome aberrations; MLA, mouse lymphoma assay; MN, micronucleus assay; SHE CT, Syrian hamster embryo cell transformation; UDS, unscheduled DNA synthesis

1.2.3 International Standardization

ICH and OECD attempt to standardize testing strategies for genotoxicity as well as test guidelines between different regulatory authorities and countries to produce useful and transparent data.

1.2.3.1 ICH Harmonization

The first meeting of the ICH took place in Tokyo in December 1992 (Cimino et al., 2006). The membership of the workgroup comprises two co-sponsors from each of three regions, Europe, Japan and the US. One co-sponsor represents the regulatory authority, whereas the second co-sponsor represented the pharmaceutical industry (Cimino, 2006). The six co-sponsors are:

- Commission of the European Union
- European Federation of Pharmaceutical Industries and Associations (EFPIA)
- Ministry of Health and Welfare (MHW), Japan
- Japan Pharmaceutical Manufacturers Association (JPMA)
- U.S. Food and Drug Administration (FDA)
- Pharmaceutical Research and Manufacturers of America (PhRMA)

Furthermore the World Health Organization, the European Free Trade Area and Canada act as observers (Cimino, 2006).

Over the years the ICH workgroup developed two guidances for genotoxicity testing: S2A "Guidance on specific aspects of regulatory genotoxicity tests" (ICH, 1996b) and S2B "Genotoxicity: a standard battery for genotoxicity testing of pharmaceuticals" (ICH, 1997b), which provides general advice for genotoxicity testing and assessment of pharmaceuticals (Cimino, 2006).

The current ICH test battery consists of (1) a gene mutation test in bacteria, (2) an *in vitro* mammalian chromosomal damage test or the *in vitro* mouse lymphoma assay and (3) an *in vivo* test to investigate chromosomal damage in rodent hematopoietic cells (Cimino, 2006).

1.2.3.2 OECD Test Guidelines

OECD is an international organization with the aim to develop and coordinate environmental health and safety activities on an international level (Cimino, 2006), including:

- Harmonizing chemical testing and hazard assessment procedures
- Harmonizing classification and labelling
- Developing principles for Good Laboratory Practices (GLPs)
- Cooperating on the investigation of existing chemicals
- Sharing and exploring cooperative activities on risk management

Over recent years OECD developed several guidelines for the testing of chemicals (OECD, 2005; Cimino, 2006). The guidelines are internationally accepted and used by government, industry and independent laboratories. Furthermore the data produced in studies following the guidelines are accepted by all OECD member countries (30 countries) (Cimino, 2006).

1.3 Mutation assays

A battery of mutagenicity tests is used for the detection of gene, chromosome or genome mutations to assess human risk for genetic damage. As mentioned above, a battery of *in vitro* tests for hazard identification has been developed which employs a wide variety of organisms, including bacteria, yeast and other eukaryotic microorganisms as well as mammalian cells (COM guideline, 2000). These tests include the Ames test (mutation in bacteria), the gene mutation test (mutation in mammalian cells), chromosomal aberration or MN assays in cultured human or Chinese hamster cells.

Furthermore a battery of *in vivo* tests are available for hazard characterisation and can be also used for risk assessment, including the MN assay in rodent bone marrow, blood or liver for chromosomal aberrations, the comet assay for DNA damage, DNA adduct analysis in appropriate tissues or the MutaMouse model for mutation in target genes of transgenic animals (COM guideline, 2000).

1.3.1 *In vitro* gene mutation assays

In vitro gene mutation assays are commonly used in genotoxicity testing as initial screens for mutagenicity and carcinogenesis. Tests available include the bacterial reverse mutation assay as well as the *in vitro* mammalian cell gene mutation assay.

1.3.1.1 Bacterial Reverse Mutation Test

The short-term bacterial reverse mutation assay (Ames test) allows identifying substances that lead to gene mutations. The test is used as an initial screen for the mutagenic potential of

new chemicals and drugs as there is a high predictive value for rodent carcinogenicity when the test shows a positive response (Mortelman and Zeiger, 2000).

The assay uses a number of auxotrophic amino acid-dependent strains of *Salmonella typhimurium* and *Escherichia coli*. *Salmonella typhimurium* strains have mutations in the histidine operon that leaves the bacteria unable to synthesize histidine, whereas the *Escherichia coli* strains used have mutations in the gene for the amino acid tryptophan, which leaves the bacteria unable to synthesize tryptophan (OECD, 1997a). In the absence of a histidine respectively tryptophan source, the cells are unable to grow to form colonies. Colony growth can be restored by new mutations at the site of the mutation or nearby in the genes allowing the cells to synthesize histidine or tryptophan respectively (Mortelman and Zeiger, 2000). Revertant cells grow on minimal agar that contains small amounts of histidine or tryptophan, whereas wild-type cells stop growing after depleting the traces of amino acid (OECD, 2008).

The bacterial reverse mutation test uses prokaryotic cells, which differ in certain factors, such as uptake, metabolism, chromosome structure and DNA repair processes from mammalian cells (OECD, 1997a). Therefore it is important to keep in mind that the Ames test does not provide direct information on the mutagenic and carcinogenic potency of substances in mammals (OECD, 1997a). Despite this, the Ames test is a commonly used and robust test for the initial screening of genotoxic activity.

1.3.1.2 *In vitro* mammalian cell gene mutation test

The *in vitro* mammalian cell gene mutation test identifies substances that lead to gene mutations in mammalian cells. The test detects mutated cells which are able to survive in the presence of a selective agent only after the new mutation occurs (Aaron et al., 1994).

Suitable cell lines for the test include the L5178Y mouse lymphoma cells, the CHO, AS52 and V79 lines of Chinese hamster cells and the human lymphoblastoid cell line TK6 (OECD, 1997e). Endpoints measured are mutation at thymidine kinase (TK), hypoxanthine-guanine phosphoribosyl transferase (HPRT) and a transgene of xanthine-guanine phosphoribosyl transferase (XPRT) (Aaron et al., 1994; OECD, 1997e). The HPRT locus is on the X-chromosome, whereas the TK and XPRT locus lies on an autosome. Therefore these mutation tests detect different spectra of genetic events, for example the location of TK and XPRT allows detecting large deletions not detected at the HPRT locus (OECD, 1997e).

Cells deficient in TK, due to $TK^{+/-}$ to $TK^{-/-}$ mutation, are resistant to the cytotoxic effects of the pyrimidine analogue trifluorothymidine (TFT), whereas cells deficient in HPRT or XPRT

are resistant to 6-thioguanine (6-TG) or 8-azaguanine (8-AG) (OECD, 1997e). Therefore mutant cells are able to proliferate in the presence of TFT, 6-TG or 8-AG, whereas the cellular metabolism of normal cells is inhibited and further cell divisions are put on hold (OECD, 1997e).

1.3.2 *In vitro* chromosome aberration assays

The *in vitro* chromosome aberration assays identify substances that cause chromosomal damage (OECD, 1997b), including chromosome loss or gain (aneuploidy) and/or chromosomal breakage (clastogenicity). Assays available are the *in vitro* mammalian chromosome aberration test or the *in vitro* MN assay (see section 1.4 for further detail).

1.3.2.1 The *in vitro* mammalian chromosome aberration assay

The *in vitro* mammalian chromosome aberration assay identifies substances that cause structural chromosome aberrations in cultured mammalian cells (OECD, 1997b). Suitable for the *in vitro* test are cultures of established cell lines, cell strains or primary cell cultures. These are selected by growth ability in culture, stability of karyotype, chromosome number and diversity as well as spontaneous frequency of chromosome aberrations (OECD, 1997b). Cell cultures are treated with a metaphase-arresting substance at predetermined intervals after exposure to the test compound with and without metabolic activation (Galloway et al., 1994; OECD, 1997b). This allows condensed chromosome preparations to be produced for easy analysis of chromosome defects. Afterwards cultures are harvested, stained and analysed (in the metaphase stage) microscopically for the presence of chromosome aberrations (Galloway et al., 1994; OECD, 1997b).

The *in vitro* mammalian chromosome aberration test is used to screen for possible mammalian mutagens and carcinogens since many compounds detected positive in the test are mammalian carcinogens. However it is important to keep in mind that there is not a perfect correlation between the test and carcinogenicity (OECD, 1997b). Further the assay is laborious and requires highly trained laboratory staffs, who are experienced in scoring chromosome aberrations.

1.3.3 *In vivo* assays for somatic cell gene mutation in endogenous and transgenic genes

In vivo assays for gene mutation in endogenous genes, like the mouse spot test, are not widely used for testing purposes because of the lack of effective methods and high costs (OECD,

2008). Mutation tests using endogenous genes, i.e. *Hprt*, *Aprt*, $TK^{+/-}$ and *Dlb-1* have been developed, but are not yet used for routine testing (OECD, 2008).

In vivo assays for gene mutation in transgenes are available for routine testing. With the help of transgenes, i.e. *LacZ* or *LacI*, mutations can be detected in almost every tissue. However they appear to have high background mutation rates, which are leading to relatively high background mutation frequencies that seem to lower the sensitivities for detecting induced mutations resulting from exogenous chemicals (Svenberg et al., 2008).

1.3.3.1 Mouse spot test

The mouse spot test is used to identify substances that cause gene mutations and re-combinations in somatic cells of mice. In this test developing embryos are treated with a test chemical. The target cells are mouse melanoblasts, which are heterozygous for several recessive coat colour genes (OECD, 1986b; OECD, 2008). Mutations in or loss of the dominant allele in those colour genes produces varies coloured spots in the coat of the resulting mouse as a result of the expression of the recessive phenotype (OECD, 1986b).

1.3.3.2 Transgenic mutation detection systems

The transgenic rodent gene mutation assay allows detection of mutations in a range of somatic and germ cells. The assay uses transgenic mice and rats that contain multiple copies of chromosomally integrated plasmid or phage shuttle vectors. These transgenes harbour reporter genes, for example *LacI* and *LacZ*, for the detection of gene mutations and/or chromosomal rearrangements (OECD, 2008).

Mutations arising in rodents are scored by recovering the integrated plasmid or shuttle vector and analysing the phenotype of the reporter gene in a bacterial host (OECD, 2008). The host is deficient for the reporter gene. Furthermore the mutant transgenes can be sequenced to determine the mutation spectrum (OECD, 2008). However, one of the disadvantages of the assay is the relatively high spontaneous mutant frequency in comparison with the endogenous targets (OECD, 2008).

1.3.4 *In vivo* assays for somatic cell chromosomal aberrations

The *in vivo* chromosomal aberration assays have the potential to detect substances that cause DNA damage at the chromosome level. The substances can either effect the chromosome structure or, by interfering with the mitotic apparatus, alter the chromosome number (OECD, 2008).

Tests available include the bone marrow chromosomal aberration assay and the rodent erythrocyte MN assay (see in section 1.4 for further detail).

1.3.4.1 Mammalian bone marrow chromosome aberration test

The mammalian bone marrow chromosome assay identifies substances that cause chromosome aberrations in bone marrow cells of animals (OECD, 1997d). The mammalian bone marrow chromosome aberration test is used to assess mutagenic hazard and takes *in vivo* metabolism, pharmacokinetics and DNA repair processes into consideration, although these factors may vary among species and tissues (OECD, 1997d).

Mice, rats or Chinese hamsters are used for the test and administered with a test chemical. Animals are then treated with a spindle inhibitor prior to bone marrow processing to arrest cells in metaphase (Tice et al., 1994). Chromosome preparations from the bone marrow are subsequently stained and scored for aberrations (Tice et al., 1994).

1.4 The micronucleus (MN) assay

The MN assay is one of the most common assays used in genotoxicity testing to study DNA damage at the chromosome level and is part of the initial screening batteries for mutational hazard of chemicals.

MN are expressed in dividing cells and are derived from either chromosome fragments arising from asymmetrical structural aberrations lacking centromeres (acentric fragments) or represent whole chromosomes, which are not incorporated into the nucleus during DNA replication and nuclear division (Fenech, 1997; Fenech et al., 1999; Fenech, 2000). MN can be measured in peripheral blood lymphocytes and to a lesser extent in epithelial cells, erythrocytes and fibroblasts (Fenech et al., 1999). Chromosome specific probes for centromeric, pericentromeric or telomeric regions of human, rat and mouse chromosomes allow further investigation of the origin of MN (chromosome breakage and/or chromosome loss) as well as the distribution of sister chromatids between daughter cells (chromosome loss or chromosome non-disjunction) (Figure 1.1) (Kirsch-Volders et al., 1997). Chromosome loss is caused by lagging chromosomes at the metaphase plate during the anaphase movement, while chromosome non-disjunction is the failure of two sister chromatids to segregate (Kirsch-Volders et al., 1997).

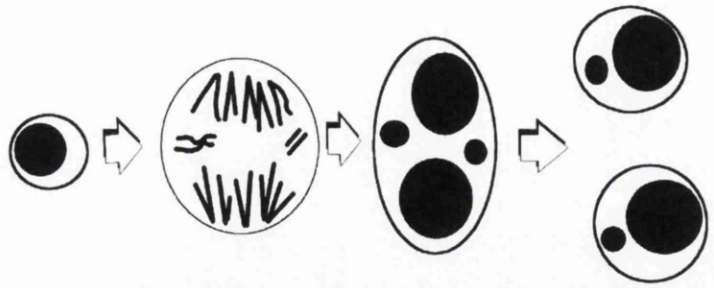

Figure 1.1: The origin of MN (chromosome breakage and/or chromosome loss) in a dividing cell at anaphase (from Fenech et al., 1999)

The advantage of using the MN assay is the relatively simple scoring procedure and the statistical power obtained from scoring large numbers of cells (Fenech et al., 2000). The diameter of the MN, which are morphologically identical to, but smaller than the main nuclei, varies between 1/16th and 1/3rd of the mean diameter of the main nuclei (Figure 1.2) (Fenech, 2000; Fenech et al., 2003).

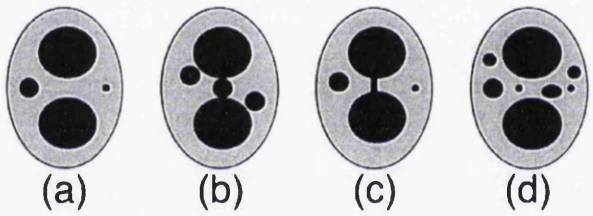

Figure 1.2: Appearance and relative size of MN in binucleated cells. a) Cell with two MN with 1/3rd and $1/9^{th}$ the diameter of the main nuclei. b) MN touching the main nuclei. c) A binucleated cell with a nucleoplasmic bridge and MN. d) Cell with MN of various sizes (from Fenech, 2000).

1.4.1 History of the MN assay

MN have been described by many scientists for more than a century. In the late 1800s and early 1900s, Howell and Jolly described Feulgen-positive nuclear bodies, which represented chromosomes separated from the mitotic spindle (Howell-Jolly bodies) to haematologists (Howell, 1890; Jolly, 1905; Decordier et al., 2006). Cytogeneticists described similar structures after *in vitro* irradiation of cells (Thoday, 1951; Evans et al., 1959) and assumed that the structures originate from acentric fragments, which were excluded from the daughter nuclei during mitosis (Decordier et al., 2006).

In the early 1970s the term MN test was used for the first time by Boller and Schmid (Boller and Schmid, 1970) and Heddle (Heddle, 1973). They showed that the MN test system is a rapid method to detect chromosomal damage after *in vivo* exposure (X-rays) of animals using bone marrow erythrocytes (Heddle, 1973; Decordier et al., 2006). In 1976, Countryman and Heddle showed that the MN test could also be used for peripheral blood lymphocytes. The advantages of peripheral lymphocytes amongst others are availability, wide body distribution for *in vivo* studies and convenient culturing methods (Countryman and Heddle, 1976). Furthermore they suggested that the MN assay could be useful as a rapid screening method.

The conventional MN methods did not discriminate between dividing and non-dividing cells. MN are expressed only in cells that have undergone a nuclear division. In the early 1980s, Fenech and Morley reported a method (cytokinesis-block micronucleus (CBMN) method), which could inhibit cytokinesis by using an inhibitor of microfilament assembly, called cytochalasin B (Fenech and Morley, 1986). Cytochalasin B is a known inhibitor of actin polymerisation, which is required for the formation of the microfilament ring that constricts the cytoplasm between the daughter nuclei during cytokinesis. This enabled reliable comparisons of chromosome damage between cell populations that may differ in their cell division kinetics by scoring binucleated cells only (Fenech and Morley, 1986; Fenech, 2000). The CBMN assay solved the problem of variation in the MN frequency caused by alterations in the proportion of dividing cells (Figure 1.3) (Fenech, 2000; Kirsch-Volders et al., 2003).

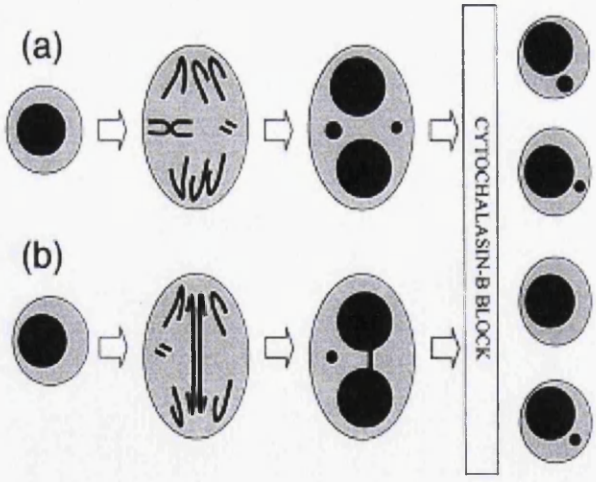

Figure 1.3: The origin of MN (A) from chromosome loss and chromosome breakage at anaphase. (B) Nucleoplasmic bridge formation from a dicentric chromosome. In the CBMN assay cells are identified by their binucleated appearance through cytochalasin B treatment. This method enables the distinction between cells that are not dividing and cells that are undergoing mitosis within a cell population (from Fenech, 2000)

In 1980, Yamamoto and Kikuchi made a first attempt to distinguish clastogens from aneugens by measuring the diameter of the MN (Yamamoto and Kikuchiu, 1980; Kirsch-Volders et al., 1997) and in 1986, Vig and Swearngrin showed that centromeres in MN could be immunologically visualized with anti-kinetochore antibodies from CREST-patients (*c*alcinosis, *R*aynaud phenomenon, *e*sophageal dismotility, *s*clerodactyly, and *t*elangiectasia) (Vig and Swearngrin, 1986; Kirsch-Volders et al., 1997). The CREST serum contains antibodies that bind specific to protein of the kinetochore region of chromosomes of mammalian cells (Kirsch-Volders et al., 1997). Further, in 1989 Vanderkerken *et al.* distinguished clastogens from aneugens with the C-banding technique, which is based on the detection of pericentromeric DNA. However the method cannot detect Y-chromosomes in mice because of its C-heterochromatin deficiency and is limited to animal species with chromosomes without intercalary C-heterochromatin (Vanderkerken et al., 1989, Kirsch-Volders et al., 1997).

In the late 1980s and in the early 1990s the use of DNA probes directed against repetitive sequences uniquely present in the centromeric region of the chromosomes became an accurate method to distinguish aneugenic from clastogenic agents (Kirsch-Volders et al., 1997). These techniques, combined with the CBMN assay, allowed identification of chromosome breakage (MN with acentric fragments) versus failure of the mitotic apparatus (MN with whole chromosomes) as mechanisms responsible for MN induction (Decordier et al., 2006).

As a result of two "International Workshops on Genotoxicity Test Procedures" in 1999 and 2002 a definite international protocol for the *in vitro* MN test was designed. At the Washington International Workshop in 1999, methodologies and data for the MN test were inspected and agreement was achieved on the following topics: cells, slide preparation, analysis, cytochalasin B, number of doses and treatment as well as harvest time (Kirsch-Volders et al., 2000). At the Plymouth International Workshop in 2002 a definite protocol for the *in vitro* MN test was finally designed after important validation studies were completed, the data were reviewed and agreement was reached on the following topics: demonstration of cell proliferation, assessment of toxicity and dose range finding, treatment schedule for cell lines, treatment schedule for lymphocytes, choice of positive controls, number of cells to be scored, repeat experiments and statistics (Kirsch-Volders et al., 2003). The harmonized protocol supported the release of guidelines for the MN assay by the OECD.

1.4.2 Methodological variations

The MN assay can be carried out *in vivo* as well as *in vitro*.

1.4.2.1 *In vivo* MN assay

The *in vivo* MN assay is the most common *in vivo* genotoxicity test in rodents. Bone marrow and peripheral blood are acceptable tissues for analysis of MN induction in mice and rats and micronucleated cells in peripheral blood samples obtained at various times can give additional information about the time course of MN induction (Hayashi et al., 2000).

Animals have to be sacrificed at appropriate times after treatment if bone marrow is used for MN analysis. Bone marrow is extracted; smears are prepared and stained for the analysis (Hayashi et al., 2000). If peripheral blood is used for analysis, blood is collected at appropriate times after and/or during treatment, followed by smear preparation and staining (Figure 1.4) (Hayashi et al., 2000).

The majority of MN can be found in the group of youngest erythrocytes, since they expel their nucleus after completion of the last mitosis and the MN remain in the cytoplasm (Schmid, 1975). Furthermore young erythrocytes stain differently from older forms, since they are polychromatic for the duration of their adolescence (lasting approximately 24h) (Schmid, 1975). However the presence of MN can be analysed in either immature or mature erythrocytes.

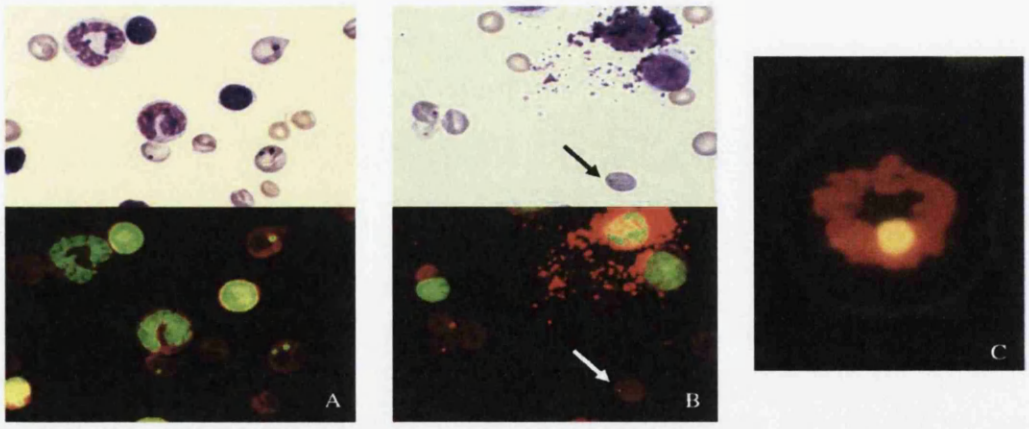

Figure 1.4: Micronucleated immature erythrocytes. (A) Mouse bone marrow cells. (B) Rat bone marrow cells. Giemsa staining (upper panel) and acridine orange (lower panel). (C) Micronucleated mouse peripheral reticulocyte (from Heddle et al., 2011)

In studies with rodents, concurrent negative control animals treated with solvent or vehicle alone, as well as untreated controls should be included (Hayashi et al., 2000). One gender is

adequate for screening unless gender-related differences in toxicokinetics are known and treated and control groups should include at least five animals per group each (Hayashi et al., 2000). The test substance is administered by gavage, via drinking water, feed, intraperitoneal injection or intravenous injection normally at least once each day and treatments of up to four weeks are acceptable (Hayashi et al., 2000). Bone marrow samples should be collected no later than 24h after the last treatment, whereas peripheral blood should be collected no later than 40h after the last treatment (Hayashi et al., 2000). At least three dose levels should be used and they should cover a range from clear toxicity to little or no toxicity (Hayashi et al., 2000).

For analysis, the proportion of immature cells among total erythrocytes is determined. Therefore, with bone marrow samples a total of at least 2000 erythrocytes should be counted for each animal, whereas for peripheral blood 1000 erythrocytes should be counted (Hayashi et al., 2000). In general at least four analysable animals and 2000 cells per animal should be scored to determine the incidence of micronucleated immature erythrocytes (Hayashi et al., 2000).

Additionally, tissues other than bone marrow and blood can be used for the MN assay. Examples are colon, skin and young rodent liver as well as male germ cells (Morita et al., 2011). These assays can be used for mechanistic studies to investigate specific issues (Hayashi et al., 2000; Hayashi et al., 2007; Morita et al., 2011).

1.4.2.2 *In vitro* MN assay

Different cell types are suitable for the *in vitro* MN assay, such as human lymphoblastoid cells, Syrian Hamster Embryo (SHE) cells or rodent cell lines, like CHO, V79 and L5178Y, which have a low and stable background frequency for MN formation (OECD, 2007). The assay can be performed with or without the actin polymerisation inhibitor cytochalasin B. When using cytochalasin B, appropriate concentrations need to be optimized for each cell type.

In the absence of a cytokinesis blocker it is necessary to demonstrate the analysed cells have undergone cell division during or after the exposure to the test substance (OECD, 2007).

For both, the *in vitro* MONOMn and the *in vitro* CBMN assay, cell lines and strains are seeded in an appropriate culture medium and incubated at 37°C. If the cells used are not metabolically competent then the use of an exogenous source of metabolic activation is needed. Often used is a co-factor-supplemented post-mitochondrial fraction (S9), which is prepared from the livers of rodents, treated with enzyme inducing agents (OECD, 2007).

The test concentrations selected should cover a range producing 50±5% cytotoxicity to little or no cytotoxicity, because higher levels may induce chromosome damage as a secondary effect of cytotoxicity. Several different methods to measure cytotoxicity in the presence and absence of cytochalasin B are available. In the presence of cytochalasin B cytotoxicity can be determined with the help of the Cytokinesis-block proliferation index (CBPI) or the Replicative index (RI). In the absence of cytochalasin B, Relative population doubling (RPD), Relative increase in cell counts (RICC) or Relative cell counts (RCC) can be used to measure cytotoxicity (Fellows and O'Donovan, 2009).

Short-term treatments as well as extended treatments can be performed. The scoring for MN is usually done manually with a light or fluorescent microscope (according to cell stains selected). However, new semi-automated systems for scoring MN exist and are frequently used. The slides can be stained using various methods, such as Giemsa or fluorescent DNA-specific dyes like DAPI or acridine orange. For scoring cytochalasin B treated cultures, a minimum of 2000 binucleated cells per dose should be scored, whereas in cultures without cytochalasin B, analysis should include a minimum of 4000 mononucleated cells per dose.

A positive result from the MN assay indicates that the test substance induces chromosomal damage; whereas a negative result indicates no induction of chromosomal damage under the used test conditions.

1.4.2.2.1 The advantages and disadvantages of the CBMN method

MN will only be expressed in a DNA damaged cell after at least one round of nuclear division. From this it follows that cells that are not dividing cannot express MN as a sign of chromosome damage and so the level of MN observed is dependent on the proportion of cells that are dividing (Fenech, 1997). Furthermore it was reported that the MN frequencies decline when cells proceed through more than one nuclear division (Fenech, 1997). It is therefore important that the kinetics of nuclear division after a DNA insult are identical and it has to be noted that an absolute value for MN frequency can only be obtained if MN are scored in cells that have divided once only (Fenech, 1997).

The most frequently used method to score MN is in cells that have passed through one mitosis, but are prevented from undergoing cytokinesis due to the use of cytochalasin B (CBMN assay). This method enables distinction between cells that are not dividing and cells that are undergoing mitosis within a cell population by scoring only binucleated cells (Fenech, 2000). Cytochalasin B is added to cultured cells before the first mitotic wave after induction of DNA damage (Fenech, 1997). The advantage of cytochalasin B is that it inhibits

cytokinesis without interfering with nuclear division (Carter, 1967; Fenech, 1997), while increased sensitivity and consistency in experiments are further advantages of the assay (Figure 1.5). Additionally, twice the numbers of mononucleated cells have to be scored to observe the same level of MN that would occur in binucleated cells (Fenech, 1997). Furthermore, the CBMN assays enables measurement of the nuclear division index, which provides information on cytostatic effects of a particular chemical or physical agent, and the test system also offers the possibility of detecting dicentric bridges as well as chromosome loss and non-disjunction events (Fenech, 1997).

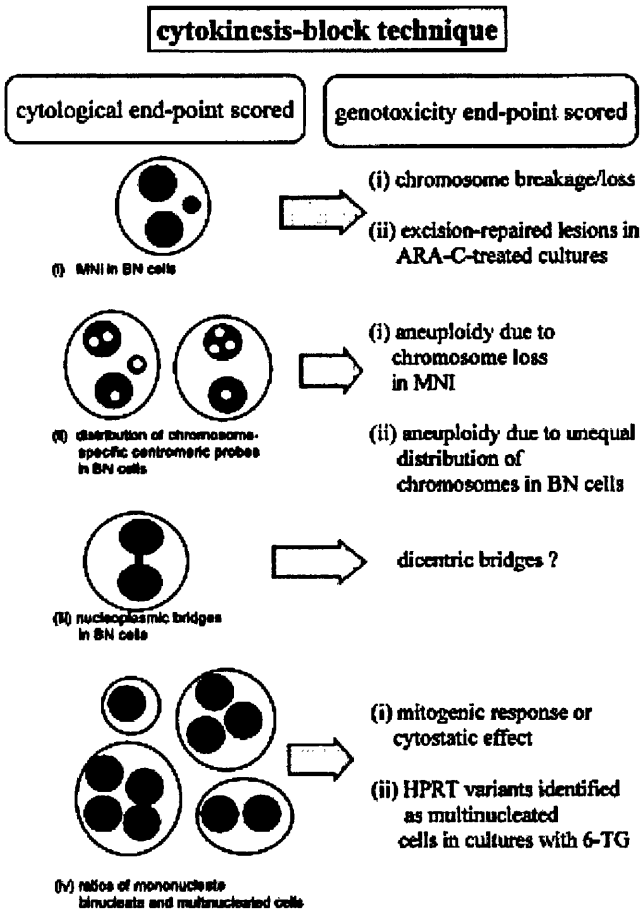

Figure 1.5: A schematic diagram to visualise the end-points that can be scored with the CBMN assay (from Fenech, 1997)

The disadvantage of the CBMN assay is that cytochalasin B itself might induce MN in binucleated cells. However, several studies have demonstrated that there is no dose-response effect for MN induction over the concentration range 1 to 6 μg/ml (Fenech, 1997). Furthermore the efficiency of cytochalasin B inhibition of cytokinesis is dependent on the

concentration used. Therefore it is important to test the optimal concentration of cytochalasin B for each cell type to ensure the maximising cytokinesis-blocking effect (Fenech, 1997). Further cytochalasin B might prevent the detection of chemicals that are also cytokinesis or microfilament polymerisation inhibitors (Fenech, 1997).

Nonetheless, in general, the CBMN technique is a robust assay that has enhanced the MN technique and enabled investigation of new parameters of genotoxicity and cell division kinetics.

1.4.3 Advent of automated technologies

Visual scoring of MN can be time consuming and the results depend on subjective interpretation. Therefore a high demand for automation of the MN assay exists. Two types of automated MN scoring are commonly used: flow cytometry and MN scoring by image analysis (Varga et al., 2004). With specific regard to image analysis, several systems are now commercially available, such as Metafer, IMSTAR and Cellomics (Decordier et al., 2011; Doherty et al., 2011).

Flow cytometry has been used to measure MN frequencies induced by ionising radiation and chemicals and in rat hepatocytes treated with carcinogens (Nüsse and Marx, 1997). In addition, this technique can be used to measure and analyse the DNA distribution of MN, which allows investigation of the mechanisms of MN induction (Nüsse and Marx, 1997). The advantages of using flow cytometry for measuring MN are that a large number of cells can be analysed in short time intervals, the objective criteria for identifying MN in suspension, or MN in erythrocytes as well as the automation during measurement and analysis of the measured data (Nüsse and Marx, 1997). Disadvantages are that the results cannot be re-checked after measurement and no data for individual cells can be obtained (Varga et al., 2004). In addition, not all particles identified as MN during the measurement are actual MN, because of the necessity to lyse cells in this protocol. Consequently, these unspecific particles might be debris developed during the preparation of a suspension of MN or nuclei or fragmented nuclei as well as apoptotic bodies induced by certain chemicals (Nüsse and Marx, 1997). Furthermore apoptotic and necrotic cells can cause MN artefacts.

Two advanced automated image analysis systems for application with the CBMN assay have been recently reported. The advantages of image analysis are that a large number of intact cells can be scored, which increases the statistical significance of the results (Verhaegen et al., 1994). In addition, repeated scoring of the same slide is possible.

The first advanced automated system, the Metafer-System, introduced by MetaSystems, uses fluorescent dyes specific for DNA (DAPI) and has been shown to be a rapid and accurate system for scoring MN (Varga et al., 2004; Doherty et al., 2011). The Metafer-System can identify mononucleated or binucleated cells and MN in the vicinity of these cells due to a set of parameters (called classifier) (Rossnerova et al., 2011). Classifier settings determine the size and shape of the cells and MN and further allow analysis of the distance of the nuclei and their size ratio (Rossnerova et al., 2011).The Metafer-System, optimised and assessed for the use on lymphocyte cell lines in our laboratory, consists of a motorised scanning stage, coupled to an Olympus BX50 fluorescent microscope (Carl Zeiss), a Dell computer hub (loaded with Metafer4 Version 3.8.5 software) and a high resolution megapixel charge coupled device (CCD) camera for image capture.

The second system, the PathFinder^{TM}Cellscan^{TM} (IMSTAR), described by Decordier *et al,* (2009), was developed for biomonitoring on Giemsa-stained slides. The detection and scoring process is separated in two steps: firstly the cells and nuclei are detected, followed by MN scoring in the detected cells (Decordier et al., 2009). The system described by Decordier *et al.* (2009) is applicable to the CBMN assay and can discriminate between mononucleated and polynucleated cells.

The visual scoring of MN of thousands of cells is time-consuming and it may result in subjective interpretation of scoring criteria (Rossnerova et al., 2011). Automation of MN analysis therefore enhances throughput and reliability of results. Furthermore, it reduces the scoring subjectivity of MN identification. However most automated systems need validation work to ensure maximum reproducibility. Minor difficulties have been encountered in our laboratory during automated scoring with the Metafer-System due to the loss of cytoplasmic boundaries. Consequently, careful attention is paid to the distance of MN from the main nuclei as well the staining pattern and intensities of the two nuclei within binucleated cells.

However, it is important to note that automated technologies allow the assessment of chromosomal damage of large numbers of cells and thus they are very powerful tools for enhancing the statistical sensitivity of the MN assay and increasing sample throughput. Consequently, they are also a promising tool for improving risk assessment of human populations, which are exposed to mutagens (Rossnerova et al., 2011).

1.5 Genotoxic thresholds

The MN assay has been extensively used in genotoxicity studies and contributed to the understanding of the dose-response relationships of aneugens and clastogens (Elhajouji et al.,

2011). It is important to investigate the biological significance of low dose exposures to improve health risk assessments, obtain sufficient safety data in the early stages of drug development and to establish if DNA reactive compounds follow linear or non-linear (thresholded) dose response relationships.

The concept of thresholds in genotoxicology has been discussed extensively and has been mainly accepted for aneuploidy based mechanistic experimental evidence (Elhajouji et al., 2011). However the assumption for direct acting genotoxins (including clastogens) is that the relationship between exposure to genotoxic chemicals, DNA damage formation and the induction of mutagenic change is linear (Henderson et al., 2000). Recent studies with alkylating agents, however, support the existence of a threshold dose-response for clastogens (Doak et al., 2007; Gocke and Mueller, 2009). However, acceptance is based on a case-by-case basis together with strong experimental evidence and supported by an understanding of the mechanisms behind the mutagen-target interaction (Elhajouji et al., 2011).

1.5.1 History of the threshold concept

During the early decades of the twentieth century the threshold model was used in establishing radiation health standards and in 1928 the "International Committee for Radiation Protection" (ICRP) recommended a tolerance dose of 1/100 of an 600r erythema dose for occupational radiation exposure (Calabrese, 2009). The second radiation standards report, published by the "National Council on Radiation Protection and Measurement" (NCRPM) in 1934, stated that a safe whole body exposure is 0.1r/day for hard x-rays (Calabrese, 2009).

Since the 1930s the linear dose response model was developed after the discovery of X-ray induced mutations in Drosophila by Hermann J. Muller (Muller, 1927; Calabrese, 2009). The hypothesis of a linear dose response relationship without a threshold at low doses was proposed for ionizing radiations on the basis of the one-hit model of action (Crebelli, 2000). The linear dose response relationship was then extended to chemical mutagens, because of the possible interaction of a single molecule of a mutagen with the DNA, which can lead to a genetic alteration and eventually trigger a carcinogenic process (Crebelli, 2000). This hypothesis was assured by demonstrating the linearity in the relationship between DNA adducts and doses over a wide exposure ranges for different mutagens, such as aflatoxin B1, benzo(a)pyrene and benzene (Crebelli, 2000). However mutations are not produced directly by DNA adducts as DNA repair activity potentially limits the proportion of adducts processed into mutational changes. A number of biological mechanisms, like metabolic

detoxification and error-free DNA repair at low doses may lead to a deviation from the linear dose response relationship and support the threshold model (Jenkins et al., 2005). However, there is limited evidence available to confirm or refute the existence of thresholds. Thus, at present, most chemicals are assumed to have non-thresholded modes of action and thresholds of genotoxic activity have to be proven for each agent on a case-by-case basis.

1.5.2 Threshold definitions

A threshold is defined as a concentration below which no effect occurs (Lovell, 2000). The threshold is characterised by the inflection point, which is the point where the change in gradient is at its maximum (Figure 1.6) (Johnson et al., 2009). The no observed effect level (NOEL) is lower than the threshold dose and defined as the highest dose that does not cause an adverse effect, whereas the lowest observed effect level (LOEL) is defined at the lowest dose that causes an adverse effect (Johnson et al., 2009).

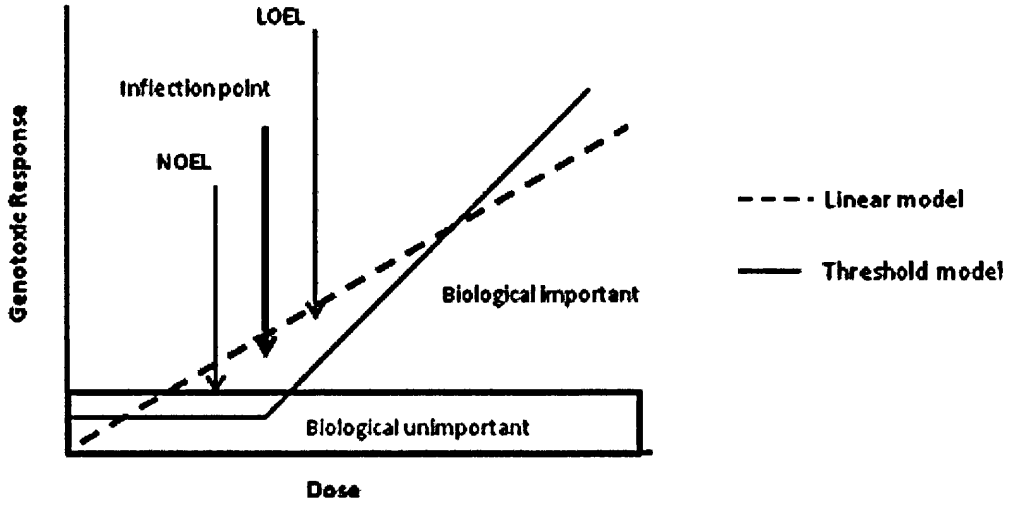

Figure 1.6: A schematic diagram of the linear and threshold dose response model. NOEL (no observed effect level); LOEL (lowest observed effect level); Inflection point = point where the change in gradient is at its maximum (after Johnson et al., 2009)

Dose response thresholds for genotoxins have implications for the setting of safe exposure levels. The European Centre for Ecotoxicology and Toxicology of chemicals (ECETOC) has defined an "absolute (true) threshold" as a concentration below which a cell would not notice the presence of the chemical, whereas a "pragmatic threshold" is considered as a concentration below which any effect is considered biologically unimportant (Lutz et al., 1998). A "statistical threshold" is the lowest concentration of a chemical that induces a statistically significant increase in the endpoint being measured (Kirsch-Volders et al., 2000),

whereas a "biologically meaningful threshold" describes the threshold dose for a substance where there is appropriate supporting evidence to conclude that there is a biological explanation of a threshold dose for mutagenicity (Kirsch-Volders et al., 2009).

1.5.3 Arguments for a threshold dose response

The choice of endpoint is an important step in mutagenicity studies. A variety of test systems can be used as an endpoint. The simplest system is where the endpoint corresponds with the target, e.g. analysis of DNA adducts, DNA breakage or modified bases (Kirsch-Volders et al., 2003). If the endpoint is different from the target three different levels can be considered at the cellular level: *proximal* is where the endpoint is close but still different, for example gene mutations or chromosomal structural mutations; *intermediate* is where the endpoint is separated by several steps from the target, e.g. analysis of repair and metabolic pathways; and *distal* is where the endpoint is a result of complex alterations of cellular activities, which happens after the initial interaction of the compound with the target, like apoptosis, necrosis and cell survival (Kirsch-Volders et al., 2003). The main endpoints analysed for threshold dose responses have been DNA adduct formation, gene mutation and chromosomal aberration. A threshold of genotoxic activity indicates that a compound will not produce mutations below a critical exposure level. Furthermore it reduces the risk for the induction of cancer or congenital abnormalities at these exposures.

Mammalian cells have a range of homeostatic mechanisms *in vivo* that provide protection to a certain extent until they become saturated and can therefore lead to threshold dose responses (Doak et al., 2007).

There are two main mechanisms which can lead to genotoxic thresholds. The first mechanism involves redundant targets. Examples for this mechanism are thresholds identified with spindle poisons, like colchicine or vinblastine (Jenkins et al., 2005). Multiple targets of tubulin monomers, of which the spindle consists, have to be damaged before a significant adverse effect occurs, thus at lower doses enough spindle fibres are intact to allow normal segregation (Jenkins et al., 2005). Non-DNA damaging substances can target mechanical components required for chromosome segregation (e.g. microtubules, kinetochores, centrioles), DNA synthesis (e.g. topoisomerases, DNA polymerases, imbalanced nucleotide pools) or DNA repair enzymes (e.g. polymerases, endonucleases, ligases) (Jenkins et al., 2005).

The second mechanism involves protective mechanisms, such as exclusion of the chemical from the cell and or nucleus through the cellular membranes and epithelial barriers,

detoxification of the genotoxic agent or DNA repair to remove damaged DNA sequences as well as apoptosis (Jenkins et al., 2005; Jenkins et al., 2010).

1.5.4 Experimental evidence for genotoxic thresholds

Experimental evidence (to date) of thresholded dose responses has only been demonstrated for spindle poisons, ionizing radiation, alkylating agents (methylmethanesulfonate (MMS), ethylmethanesulfonate (EMS)), topoisomerase II inhibitors and ROS inducers (Table 1.4).

Table 1.4: Examples of published data demonstrating genotoxic thresholds (after Jenkins et al., 2005)

Test agent	Type of agent	Test assay
Lindane, Malathion, Metacid (Kumar et al., 1995)	Pesticides	Clastogenicity, dominant lethality
Colchicine, Carbendazim, Mebendazole, Nocodazole, (Elhajouji et al., 1995; Elhajouji et al., 1997)	Spindle poisons	MN formation
Etoposide, Doxorubicin, Genistein, Ciprofloxacin (Lynch et al., 2003)	Topoisomerase II inhibitors	MN formation
Vinyl acetate (Hengstler et al., 2003)	Industrial chemical	Various
X-radiation (Koana et al., 2004)	Ionizing radiation	Drosophila somatic mutation analysis
PhIP (Fukushima et al., 2004)	Cooked meat carcinogen	DNA adduct, aberrant crypt foci
MeIQX (Wanibuchi et al., 2006)	Cooked meat carcinogen	LacI mutation, pre-neoplastic liver foci formation
MMS (Doak et al., 2007)	Alkylating agent	MN formation; HPRT assay
EMS (Doak et al., 2007; Gocke et al., 2009)	Alkylating agent	MN formation; HPRT assay

KBrO3, Bleomycin, Hydrogen peroxide (Platel, et al., 2009; Seager et al., 2012)	DNA-oxidizing agents	MN formation

Aneugens (non-DNA reactive genotoxins) show non-linear (thresholded) dose response curves. Low levels of the compounds are tolerated, because deactivation of multiple targets is required to induce aneuploidy. The non-DNA damaging substances may target mechanical components required for chromosome segregation (e.g. microtubules, kinetochores, centrioles), DNA synthesis (e.g. topoisomerases, DNA polymerases, imbalanced nucleotide pools) or DNA repair enzymes (e.g. polymerases, endonucleases, ligases) (Jenkins et al., 2005).

Spindle poisons, like colchicine or vinblastine are good examples of aneuploidy inducing agents due to inhibition of tubulin polymerisation. The spindle consists of many tubulin monomers. Therefore multiple targets have to be damaged before a significant adverse effect occurs (Elhajouji et al., 1997).

DNA reactive genotoxins are believed to induce non-threshold curves, because they directly induce DNA lesions that have the potential to be fixed as point mutations or chromosomal aberrations. However, mammalian cells have a number of defence mechanisms, such as DNA repair or detoxification, which provide protection to a certain extent and therefore can theoretically result in a NOEL (Jenkins et al., 2010).

There is now evidence to support this theory; for example a study by Doak *et al.* (2007) demonstrated that direct acting genotoxins have thresholds for mutation induction and chromosome breakage *in vitro* (Doak et al., 2007). The human lymphoblastoid cell line AHH-1 was treated with alkylating agents (MMS, MNU, EMS and ENU) that have different mechanisms of action and DNA-targets. MNU and ENU showed linear dose responses, whereas MMS and EMS showed non-linear curves containing a range of non-mutagenic low doses (Doak et al., 2007). In addition EMS showed non-linear dose responses *in vivo* using the mouse-bone marrow MN test and point mutations at the *LacZ* locus as endpoints (Gocke et al., 2009), confirming the possible existence for genotoxic thresholds.

To summarize, it is likely that genotoxic thresholds for clastogens exist. However further investigations are needed to investigate the mechanisms of action of genotoxins and how they interact with DNA at low levels (Jenkins et al., 2010). If there is no elevation of genetic

damage above background levels, safe exposure levels may exist for some clastogens, and consequently regulatory bodies may have to adapt and modify their regulatory schemes accordingly (Jenkins et al., 2010, Elhajouji et al., 2011). However, it is important to note that variability in the experimental data, intra- and inter-species variation, differences in exposure and individual susceptibility have to be taken into account for the health risk assessment (Elhajouji et al., 2011).

1.6 The present study

The main aim of this thesis was to assess low dose response relationships *in vitro* for a number of genotoxic agents and to establish if the DNA reactive compounds follow linear or non-linear (thresholded) dose responses, since it is important to investigate the biological significance of low dose exposures to improve health risk assessments.

Mitomycin C (MMC), a crosslinking agent; 4-nitroquinoline 1-oxide (4NQO), a bulky adduct inducer and cytosine arabinoside (araC), a nucleoside analogue were investigated for DNA damage induction. These agents had not been subject to robust low dose studies previously.

These studies used the newly installed semi-automated MN detection system Metafer (MetaSystems, Altlussheim, Germany) at Swansea University. RPD was used to measure cytotoxicity. In addition the mechanism of action of each test component was further investigated by follow up experiments to gain mechanistic understanding of the dose response relationships, including DNA repair assays using Real-time PCR or protein analysis using Western blotting as well as cell cycle status analysis and p53 signalling studies.

Chapter 2

Material and Methods

2.1 Materials

2.1.1 Equipment

BD FACS Aria™ Flow Cytometer	BD Biosciences
Biofreezing vessels	Bicell
Centrifuge Tubes (15ml/50ml)	Fisherbrand
Centrifuges:	
BIOFUGE fiesco	Heraeus
Centrifuge 5810R	Eppendorf
ChemiDOC™ XRS+ System	BioRad
CO_2 Air-Jacketed Incubators	Nuaire™
Comet IV capture system	Perceptive Instruments Ltd.
Cryovial®	Elkay Laboratories Products
Cytospin 4	Thermo Shandon
Fridge (4°C)	Liebherr
Freezer (-20°C)	Proline
Fume Hood	Clean Air, Limited
Haemocytometer	Hawksley
Heat block	Techne Di-Block
Hotplate & Stirrer	Jenway
Ice machine	Hoshizaki
Immun-Blot® PVDF membrane	BioRad
IQ5 Real-Time PCR System	BioRad
Microcentrifuge tubes	Eppendorf
Microscopes:	
Axio Imager Z1	Zeiss
Axiovert 40C	Zeiss
TMS	Nikon
Milli-Q Integral Water Purification System	Millipore
Mini Protean® 3 Cell	BioRad
Mini Trans-Blot® Cell	BioRad

Multipurpose Container (20ml)	Greiner bio-one
NanoDrop (ND-1000 Spectrophotometer)	Labtech
pH meter	Mettler Toledo
Pipette with tip (5ml/10ml/25ml)	Greiner bio-one
Pipettes	Gilson/ Eppendorf
Pipette tips	StarLAB
Pipettors	StarLAB/ Fisherbrand
Platform Shaker (innova™ 2100)	New Brunswick Scientific
POLARstar Omega Microplate Reader	BMG Labtech
Power Pac™ Basic Power Supply	BioRad
Purifier PCR Enclosure	Labconco
Scales:	
LA 120S	Sartorius
TE 3102S	Sartorius
T100™ Thermal Cycler	BioRad
Thick Blot Paper	BioRad
Tissue Culture Flasks ($25cm^2$/$75cm^2$/$175cm^2$)	Cellstar
Tissue Culture Hood	Scanlaf mars
Ultra Low Temperature Freezer (-80°C)	New Brunswick Scientific
Vortexer	Fisons
Windsor Incubator	Raymond A Lamb
Waterbaths:	
SUB Aqua 18	Grant
The Belly Dancer®Hybridization Water Bath	Stovall Life Sciences Inc.
Z1 Coulter Particle Counter	Beckman Coulter, Inc.

2.1.2 Reagents

Acetic acid	Fisher Scientific
Acridine orange	Sigma-Aldrich
30% Acrylamide1Bis Solution, 37.5:1	BioRad
Albumin bovine serum	Sigma-Aldrich
Ammonium persulfate	Sigma-Aldrich
Buffer Tablets „Gurr“	Gibco®
Cytochalasin B	Merck

Cytosine arabinoside	Sigma-Aldrich
Dimethyl sulfoxide	Fisher Scientific
DPX Mounting Medium	Fisher Scientific
Ethanol	Fisher Scientific
Formamide	Fisher Scientific
Giemsa' Stain Solution	Gurr®, VWR International Ltd.
Glutamine	Gibco®
Glycine	Melford
Horse serum	Gibco®
Hydrogen chloride	Fisher Scientific
Hygromycin B	Merck
Hypoxanthine-aminopterin-thymidine (HAT)	Gibco®
Hypoxanthine-thymidine (HT)	Gibco®
Isopropanol	Fisher Scientific
Magnesium chloride	Sigma-Aldrich
Methanol	Fisher Scientific
Mitomycin C (Streptomyces caespitosus)	Sigma-Aldrich
4-Nitroquinoline 1-oxide	Sigma-Aldrich
N,N,N',N'-tetramethylethylenediamine	Sigma-Aldrich
Pepsin	Sigma-Aldrich
Phosphate buffered saline	Gibco®
Phosphatase Inhibitor Cocktail 2	Sigma-Aldrich
Potassium chloride	Fisher Scientific
Propidium iodide solution	Sigma-Aldrich
Protein inhibitor cocktail	Sigma-Aldrich
Ribonuclease A	Sigma-Aldrich
RPMI 1640	Gibco®
RTU Human Pan Centromeric Probe	StarFISH (Cambio)
Sodium chloride	Sigma-Aldrich
Sodium citrate	Sigma-Aldrich
Sodium dodecyl sulfate	Sigma-Aldrich
Staurosporine	Sigma-Aldrich
6-Thioguanine	Sigma-Aldrich
Tris	Melford

Tween®20	Sigma-Aldrich
Vectashield® Mounting Medium with DAPI	Vector Laboratories
Xylene	Fisher Scientific

2.1.3 Buffer and Solutions

10x Annexin V Binding Buffer (abcam)

10% (w/v) APS	1g Ammonium persulphate ddH_2O to 10ml
BSA Blocking Buffer	20mM Tris (pH 7.6) 137mM NaCl 5% (w/v) BSA 0.1% (v/v) Tween®20
Buffer F pH 8.0	40mM HEPES 0.1M KCl 0.5mM EDTA 0.2mg/ml BSA
Electrophoresis buffer pH 13.0	1mM Na_2EDTA 0.3M NaOH
Laemmli Buffer (Sigma-Aldrich) pH 6.8	0.0004% Bromphenol blue 400mM DTT 20% Glycerol 4% SDS
Lysis solution	2.5M NaCl 100mM Na_2EDTA 10mM Tris buffer (pH10) 10% DMSO 1% Triton X-100

Neutralisation buffer pH 7.5	0.4M Tris-HCl
RIPA Buffer (Sigma-Aldrich) pH 8.0	150mM NaCl 1.0% IGEPAL®CA-360 0.5% Sodium deoxycholate 0.1% (w/v) SDS 50mM Tris
Protein Running Buffer	25mM Tris (pH8.3) 192mM Glycine 0.1% (w/v) SDS
Protein Transfer Buffer	20mM Tris (pH 8.3) 192mM Glycine 20% (v/v) Methanol 0.1% (w/v) SDS

Restore Plus Western Blot Stripping Buffer (Thermo Scientific)

10% (w/v) SDS	25g SDS ddH_2O to 250ml
20xSSC (pH 7.4)	87.6g NaCl 44.1g Na citrate ddH_2O to 500ml
10x TBS (pH 7.6)	200mM Tris 1.37M NaCl HCl to pH 7.6
TBS/Tween®20 Wash Buffer	20mM Tris (pH 7.6) 125mM NaCl 0.1% (v/v) Tween®20

1.5M Tris (pH 8.8)	45.4g Tris ddH_2O to 250ml HCl to pH 8.8
1M Tris (pH 6.8)	30.3g Tris ddH2O to 250ml HCl to pH 6.8
Tris/Glycine/SDS 10x	250mM Tris (pH 8.3) 1.92M Glycine 1% (w/v) SDS

2.1.4 Kits

DC Protein Assay	BioRad
geNorm™ Reference Gene Selection Kit	Primerdesign
Immun-Star™ WesternC™ Chemiluminescent Kit	BioRad
RNase-Free DNase Set	Qiagen
RNeasy® Mini	Qiagen
RT^2 Profiler™ PCR Array System	SAbiosciences
QuantiFast® SYBR® Green PCR Kit	Qiagen
QuantiTect® Reverse Transcription Kit	Qiagen

2.1.5 Antibodies

Anti-Annexin V antibody [VAA-33] (FITC)	Abcam
B-Actin (13E5) Rabbit mAb	Cell signalling, NEB
Goat polyclonal Secondary Antibody to Rabbit IgG- H&L (HRP), pre-adsorbed	Abcam
p53 antibody	Cell signalling, NEB
Phospho-p53 (Ser15) antibody	Cell signalling, NEB

2.1.6 Molecular Weight Marker

Biotinylated Protein Ladder Detection Pack	Cell signalling, NEB
Precision Plus Protein™ Dual Color Standard	BioRad

2.1.7 Primers

All primers were obtained from Sigma-Aldrich, UK.

Primer:	Nucleotide Sequence:
Actin Forward	5' GATGGCCACGGCTGCTTC 3'
Actin Reverse	5' TGCCTCAGGGCAGCGGAA 3'
BRCA1 Forward	5' CCTTCCTTGCAGGAAACCAGTCTCA 3'
BRCA1 Reverse	5' TCCGCTGCTTTGTCCTCAGAGTT 3'
MSH6 Forward	5' GCCCCCACCAGTTGTGACTTCTC 3'
MSH6 Reverse	5' GACAAGGCCACCAGGGGTAACC 3'
p21 Forward	5' GACTCTCAGGGTCGAAAACG 3'
p21 Reverse	5' GGATTAGGGCTTCCTCTTGG 3'
Rad51C Forward	5' AGGAGTGGCAGGTGAAGCAGTTT 3'
Rad51C Reverse	5' TCGGTGTTCCTCTCCCTTGTGTTTT 3'
XRCC3 Forward	5' GAACCCGCGGGAGGATGTGCAC 3'
XRCC3 Reverse	5' CCGCGTGTTTTTGGCTGACTTGAC 3'
XRCC6BP1 Forward	5' TGGCGTGCTCAGAGGTTCGAG 3'
XRCC6BP1 Reverse	5' TGGCTCTGTCTCGCACACAAGT 3'

2.1.8 Computer software

BD FACS Diva 6.1.3.

Metafer 4, v. 3.8.5 (MSearch)

Microsoft Excel 2010

Microsoft Word 2010

Omega, Mars Data Analysis

Quantity One

SPSS 16.0.2 and 20

2.2 Methods

2.2.1 Tissue Culture

All tissue culture manipulations were carried out in sterile Biological Safety Cabinets (Scanlaf Mars, VWR International Ltd., Leicestershire, UK). Only sterile equipment was used. Solutions, including media and PBS, were pre-warmed to 37°C in a water bath and sprayed with 70% ethanol before placing in the safety cabinets. When handling toxic chemicals appropriate safety measurements, including wearing safety equipment (lab coat, goggles and overarm gloves) and disposal of toxic waste material via incineration, were carried out.

2.2.1.1 Cell lines

In this study (at Swansea University) the human lymphoblastoid cell lines TK6, NH32, AHH-1 and MCL-5 were used.

TK6. The human lymphoblastoid cell line TK6 is a derivative of the WIL-2 cell line. The cells are heterozygous at the TK locus and contain the wild-type TP53 gene. TK6 cells were acquired from the European Collection of Cell Cultures (ECACC), Salisbury, UK (Cat.-No. 95111735).

NH32. The NH32 cell line was a kind gift from Prof. Dr. Gerald N. Wogan (MIT, Cambridge, MA, USA). Like TK6, the human lymphoblastoid cell line NH32 is a derivative of the WIL-2 cell line. The cells contain a double p53 knockout mutation.

AHH-1. AHH-1 is a human lymphoblastoid $TK^{+/-}$ cell line that constitutively expresses a high level of native CYP1A1 (Crofton-Sleigh et al., 1993). AHH-1 cells carry a heterozygous mutation in the TP53 locus (Morris et al., 1996; Dobo et al., 1997; Guest and Parry, 1999). The cells were acquired from the American Type Culture Collection (ATCC), Manassass, VA, USA (Cat. No. CRL-8146).

MCL-5. The human lymphoblastoid cell line MCL-5 is derived from AHH-1 by stable transfection with human cytochromes (CYP1A2, CYP2A6, CYP3A4 and CYP2E1) and microsomal epoxide hydrolase (Crofton-Sleigh et al., 1993). These are carried as cDNAs in plasmids and in addition the cells carry a hygromycin B resistance gene. Furthermore MCL-5 cells carry, like AHH-1 cells, a heterozygous mutation in the TP53 locus (Guest and Parry,

1999). MCL-5 cells were acquired from the American Type Culture Collection (ATCC), Manassass, VA, USA (Cat. No. CRL-10575^{TM}).

2.2.1.2 Cell culture medium

TK6, NH32, AHH-1 and MCL-5 were cultured in RPMI 1640 (Gibco®, Paisley, UK) supplemented with 10% donor horse serum (Gibco®, Paisley, UK) and 1% L-glutamine (Gibco®, Paisley, UK). For MCL-5 cells at each passage hygromycin B in acetic acid (35mM) was added to a final concentration of 200µg/ml to ensure plasmid retention (Crespi et al., 1991).

2.2.1.3 Cell culture

All cell lines used in this study were maintained in exponentially growing cultures in a humidified incubator at 37°C with 5%CO_2 in the air. The cell concentrations were maintained between 1-3 x 10^5 cells/ml and were not allowed to exceed 1.5 x 10^6 cells/ml.

Upon reaching confluency, cells were sub-cultured in order to maintain the desired concentrations in the culture flasks. Therefore the cell suspensions were transferred into multipurpose containers and spun down at 200 x g for 10min. The supernatant was removed and the cells were re-suspended in fresh media, counted with the haemocytometer (Hawksley, Sussex, UK) or the Z1 Coulter Particle Counter (Beckman Coulter Inc., High Wycombe, UK) and diluted to the final concentration of roughly 1-3 x 10^5 cells/ml.

2.2.1.4 Measurement of cell concentration

To measure the amount of cells per ml of culture media either the haemocytometer or the Z1 Coulter Particle Counter was used.

For the haemocytometer 10µl of cell suspension was removed from the culture flask after gentle shaking and placed onto the haemocytometer slide. The number of cells in each of the four large corner counting chambers (each compromised of 16 small squares) were scored, averaged and multiplied by 1 x10^4 to obtain the final cell number per ml of media.

For the Z1 Coulter Particle Counter 100µl of cell suspension were placed into a cuvette containing 10ml of dilute conducting liquid. The cuvette was placed on the Z1 coulter Particle Counter and the cell number per ml culture was measured. The particles pass through an aperture of defined size and the cell number is displayed on a screen as cells/ml of media.

2.2.1.5 Cryopreservation of cells

Cryopreservation is a process that enables storage of cell stocks over an indefinite amount of time at an ultra-low temperature. Cell cultures to be cryopreserved should be free of contamination and maintained in exponential growth phase for several days before freezing. Cell suspensions, which reached near-confluency were spun down in 20ml multipurpose containers for 10 min at 200 x g. The supernatant was removed and the pellet was re-suspended in 3 to 4 ml of horse serum containing 10% v/v dimethyl sulfoxide (DMSO). Subsequently, 1.5 to 2ml of the cell suspensions were added into cryovials® for the freeze process. The cryovials were placed in biofreezing vessels and kept overnight in the -80°C freezer before long-term storage in liquid nitrogen at -196°C.

2.2.2 The *in vitro* MN assay

The manual and the semi-automated scoring protocol, using the Metafer-System (MetaSystems, Altlussheim, Germany), were performed in this study.

2.2.2.1 The manual scoring protocol for the MN assay

2.2.2.1.1 Initiation of the assay

All cell suspensions (10ml) were seeded at $1x10^5$cells/ml for 24h at 37°C, 5%CO_2. For the CBMN-assay each cell suspension was treated with appropriately diluted chemical for different time points and 4.5 to 6 µg/ml cytochalasin B for one cell cycle. After the different incubation times the suspensions were removed from each flask and transferred into appropriately labelled tubes. The cells were spun down (10min, 200 x g) and washed with PBS to remove any residual chemical.

2.2.2.1.2 Manual harvest and scoring

After washing with PBS the cells were spun down (10min, 200 x g) and re-suspended in fresh culture medium. One hundred microliters of the cell suspensions were cytospun onto polished glass slides (5min, 1000rpm), fixed in ice-cold 90% methanol for 10min, stained in 20% Giemsa solution (VWR International Ltd., Poole, UK) and viewed under an Olympus BH2 light microscope. A minimum of two slides per replicate were prepared.

2.2.2.1.3 Giemsa staining

For manual scoring, cells were stained with a 20% Giemsa solution in phosphate buffer (pH 6.8) for 11 min. The stained cells were then washed with phosphate buffer, rinsed under tap water and air dried.

To mount the cells the slides were placed in xylene for 10 sec. Afterwards a drop of DPX mounting medium (Fisher Scientific, Loughborough, UK) was added to the slide, followed by a coverslip. The slides were allowed to set for 12h before scoring.

2.2.2.1.4 Scoring

For the CBMN assay a minimum of 1000 binucleated cells per replicate were scored, whereas for the mononucleated assay a minimum of 2000 mononucleated cells per replicate were scored (at Swansea University). The binucleated and mononucleated cells were examined for MN (Figure 2.1). Furthermore mononucleated, binucleated, trinucleated, tetranucleated and multinucleated cells were scored.

The scoring system for MN as well as the classification for MN was adapted from Fenech *et al.* (2003).

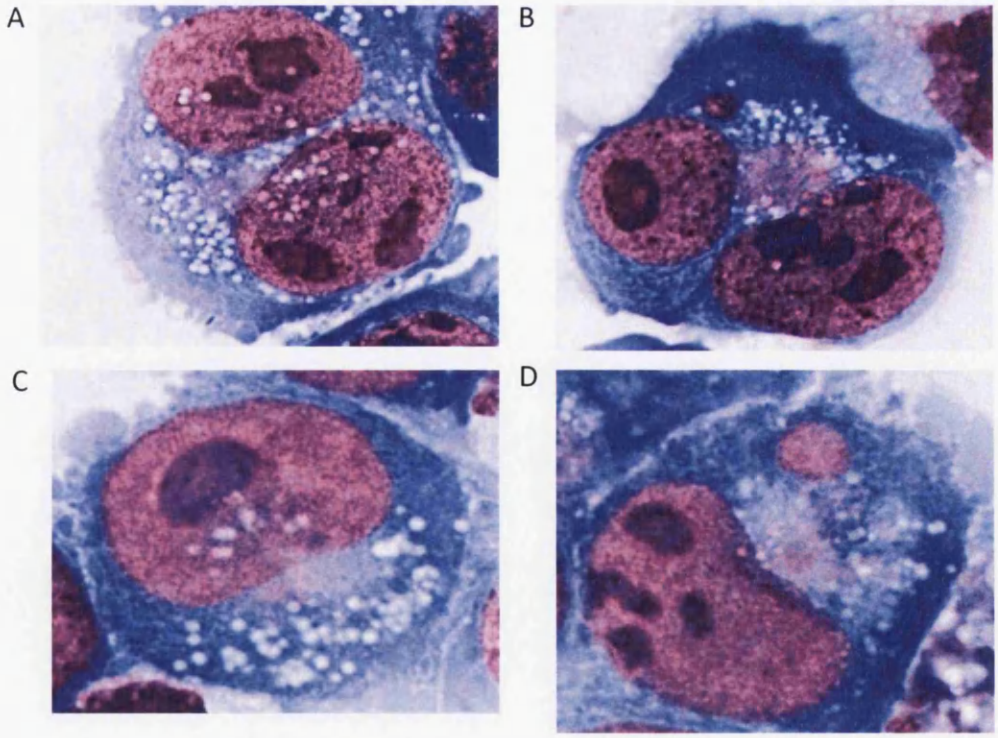

Figure 2.1: Binucleated (A and B) and mononucleated (C and D) cells without (A/C) and with (B/D) MN in TK6 cells after MMC treatment stained with 20% Giemsa solution

2.2.2.2 The Metafer-System

2.2.2.2.1 Initiation of the assay

All cell suspensions were seeded at $1x10^5$cells/ml for 24h at 37°C, 5%CO_2. For the CBMN assay each cell suspension was treated with the appropriately diluted test chemical for different time points and 4.5 to 6 µg/ml cytochalasin B for one cell cycle. Test chemicals used were mitomycin C (MMC), cytosine arabinoside (araC) and 4-nitroquinoline 1-oxide (4NQO). For the MONOMn assay only TK6 cell suspensions were treated with MMC (0-0.1 µg/ml) for 24h followed by a 24h recovery period previous to harvest.

After the different incubation times the suspensions were removed from each flask and transferred into appropriately labelled tubes. The cells were spun down (10min, 200 x g) and washed with PBS to remove any residual chemical.

2.2.2.2.2 Cell harvest

For semi-automated scoring, cells were prepared as described by Varga *et al.* (2004). Shortly, after washing the cells with PBS, the cells were treated with 0.56% KCl solution and fixed with a methanol/acetic acid/0.09% NaCl (5:1:6) solution for 10min. A second fixation step was then performed 4 times with methanol/acetic acid (5:1). The fixed cells were dropped across the length of slides and subsequently the cells were mounted in vectashield antifading solution containing 4',6-diamidino-2-phenylindole (DAPI) stain with a large coverslip.

2.2.2.2.2.1 Scanning and Classifier settings

The slides were scanned at 10x magnification with the Metafer 4 master station, coupled to an Olympus BX50 fluorescent microscope (Carl Zeiss), a Dell computer hub (loaded with the Metafer4 Version 3.8.5 software) and a high resolution megapixel charge coupled device (CCD) camera (Axiocam; Carl Zeiss) for image capture. A number of grid positions evenly distributed across the scan area determined the plane of focus and a predetermined scan area was used for all slides.

Classsifiers developed by MetaSystems were modified in order to detect mononucleated as well as binucleated cells. The search definition classifiers were used to define the size and shape of nuclei and MN (Table 2.1).

Table 2.1: Classifier settings on the Metafer-System to define binucleated/mononucleated cells and MN

	Binucleate		Mononucleate	
	Nuclei	MN	Nuclei	MN
Object threshold	30%	8%	20%	10%
Minimum area	20µm^2	1.5µm^2	10µm^2	1.0µm^2
Maximum area	400µm^2	55µm^2	400µm^2	55µm^2
Maximum relative concavity of depth	0.9	0.9	0.9	1.0
Maximum aspect ratio	1.5	4.0	2.5	3.5
Maximum distance between	30µm	25µm	-	35µm
Maximum area asymmetry	70%	-	90%	-

2.2.2.2.2.2 Scoring

The detection and scoring process for the Metafer-System was separated into 3 steps: firstly the slides were scanned and binucleated or mononucleated cells were detected. Secondly MN-positive binucleated or mononucleated cells were validated microscopically and finally manual confirmation of the MN was performed in the image gallery (Figure 2.2). A minimum of 4000 mononucleated cells or 2000 binucleated cells per replicate were scored (at Swansea University) (exceptions were stated, for details see Appendix I).

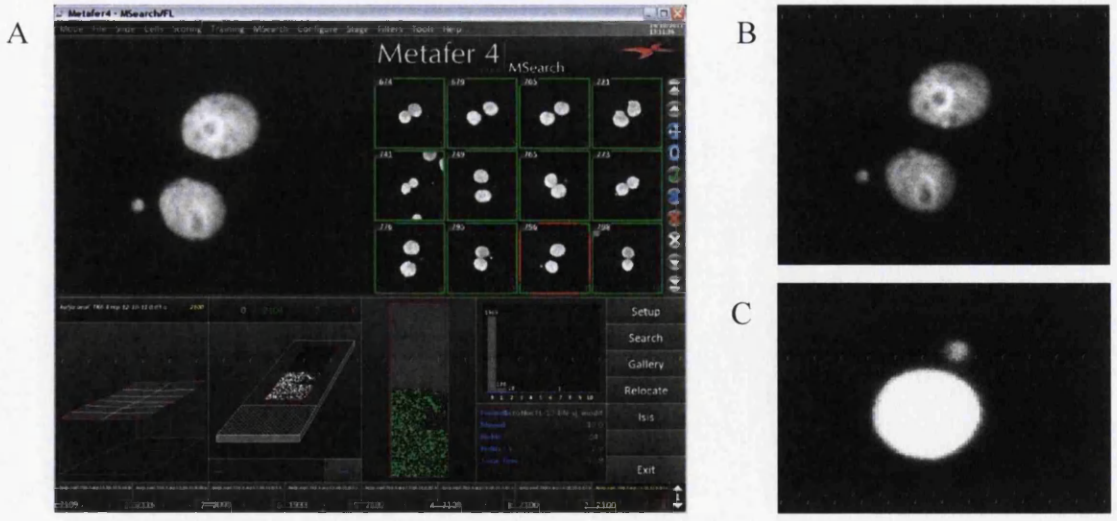

Figure 2.2: Metafer image gallery (A), Binucleated cell with MN (B), Mononucleated cell with MN (C)

2.2.3 Cytotoxicity

Different cytotoxicity methods in the absence of cytochalasin B (RPD, RICC and RCC) were compared to find the most suitable one for measurement.

RPD was determined as follows:

$$\text{RPD} = \frac{\text{Number of population doublings in treated cultures}}{\text{Number of population doublings in control cultures}} \times 100$$

where

$$\text{Population doubling (PD)} = \frac{[\log(\text{post-treatment cell number/initial cell number})]}{\text{Log2}}$$

RICC was defined as:

$$\text{RICC} = \frac{\text{Increase in number of cells in treated cultures (final count-initial count)}}{\text{Increases in number of cells in control cultures (final count-initial count)}} \times 100$$

And RCC was determined as follows:

$$\text{RCC} = \frac{\text{Final cell count in treated cultures}}{\text{Final cell count in control cultures}} \times 100$$

Cytotoxicity assessment was dependent on the measurement used. RCC slightly underestimated the level of cytostasis and cell death, when compared to RPD and RICC; while RICC slightly overestimated the level of cytostasis and cell death, when compared to RPD (see Table 2.2 as an example).

Table 2.2: Cell viability of TK6 cells treated with MMC for 4h followed by 18h of cytochalasin B using RPD, RICC and RCC

	Cell viability (%)			Standard Deviation (%)		
MMC (µg/ml)	**RPD**	**RICC**	**RCC**	**RPD**	**RICC**	**RCC**
0	100	100	100	0	0	0
0.002	85.33	77.35	85.76	12.79	9.42	3.87
0.004	93.70	91.35	95.03	5.77	10.90	8.95
0.006	106.05	98.93	95.43	11.99	15.46	8.52
0.008	91.04	85.42	90.51	3.09	7.61	9.17
0.01	87.57	85.99	93.16	4.81	7.94	5.81
0.02	77.22	72.39	85.50	8.87	5.62	3.30
0.04	75.83	63.05	75.11	8.77	7.07	3.19
0.06	57.58	48.85	71.09	21.99	18.57	6.07
0.08	55.79	43.12	64.03	11.56	9.41	5.84
0.1	54.21	41.49	62.87	9.64	8.60	5.20

In recent studies by Fellows *et al.* it was shown that RPD and RICC are the most appropriate measurements of toxicity in the absence of cytochalasin B (Fellows et al., 2008; Fellows et al., 2009).

Throughout this work it was decided to use RPD for the measurement of cytostasis and cell death.

2.2.4 Human Pan Centromeric Chromosome Painting

For the Human pan-centromeric chromosome staining TK6 cells treated with either MMC, araC or 4NQO were cytospun (5min, 1000rpm) onto polished glass slides and fixed in ice-cold 90% methanol for 10min. Afterwards the cells were pre-treated with pepsin to remove the cytoplasm and to allow better penetration of the probes. Both sample slides and 300mg/ml 0.01M HCl pepsin (pH 2.7-3) were pre-warmed for 10min to 37°C. Several drops of pepsin were applied to each slide's cytodot for 30sec to 1min. To arrest the pepsin treatment, slides were washed in PBS for 5min, followed by another wash step in PBS/50mM $MgCl_2$ for 5min. The slides were then dehydrated in 70%, 80% and 95% ethanol for 2min each to prepare them for the denaturation step.

Meanwhile, the RTU Human pan-centromeric probe (StarFISH, Cambio, Cambridge, UK) was warmed up to 37°C for 5min. A 5µl aliquot of the probe per slide was added to a microcentrifuge tube.

Afterwards the chromosomes on the slide were denatured in 70% formamide in 2xSSC for 2min at 70°C and immersed in ice-cold 70% ethanol. The slides were then dehydrated through a series of 70%, 90% and 100% ethanol washes for 5min each and air-dried at room temperature.

Meanwhile the probe was denatured for 10 min at 85°C and immediately chilled on ice. Subsequently the probe was applied to the cytodot on the slide, covered with a cover slip and hybridised for approximately 16 hours at 37°C in a humidified chamber.

After the hybridisation step the cover slip was removed and the slides were washed for 5min in 2xSSC at 37°C, followed by two washes in 50% formamide/2xSSC for 5min each time at 37°C and two washes in 2xSSC for 5min each time. The slides were dried in the dark at room temperature.

The nuclei were counterstained with a DAPI + vectashield solution and 100 MN per dose (2 replicates with 50 MN each) were scored as positive or negative for centromere(s) under an Olympus BX50 fluorescence microscope (Carl Zeiss).

2.2.5 RNA extraction

Total RNA was extracted from the human lymphoblastoid cell lines. All cell suspensions (50ml) were seeded at $1x10^5$cells/ml for 24h at 37°C, 5%CO_2. The RNA extraction was performed using the Qiagen RNeasy Mini Kit (Qiagen, Sussex, UK) according to the manufacturers` instructions. Cells were spun down in 25ml aliquots (8min, 200 x g) and the supernatant was removed. After that the pellets were re-suspended in 600µl of buffer RLT. Subsequently the samples were homogenized by passing the lysate 3 to 4 times through a needle (21G). Then one volume of 70% ethanol was added and after mixing by pipetting the samples was applied to the columns. After spinning for 15sec at ≥8000 x g the on-column DNase digestion followed. For the DNase digestion the RNase-Free DNase Set (Qiagen, Sussex, UK) was used. Therefore, 350µl buffer RW1 were added and spun down for 15sec at ≥8000 x g. Then 10µl DNase I stock solution was added to 70µl buffer RDD. Afterwards the DNase I incubation mix (80µl) was directly added to the column membrane and placed on the bench top for 15min at room temperature, followed by another washing step with 350µl buffer RW1. After spinning (15sec, ≥8000 x g) 500µl buffer RPE were added to the column. After the centrifugation (15sec, ≥8000 x g) another 500µl of buffer RPE were added to the

column followed by a centrifugation for 2min and ≥8000 x g. The column was then transferred to a fresh collection tube and spun down at full speed for 1min to be completely dry. The column was afterwards transferred to a fresh collection tube to remove the RNA from the column by adding 30µl Nuclease-free water and spun down for 1min at ≥8000 x g. After completing the RNA extraction the RNA content was measured and the purity was assessed (260:280 ratio) with a NanoDrop ND-1000 Spectrophotometer (Labtech International, Uckfield, UK). The RNA was stored at -80˚C until further use.

2.2.6 RT^2 Profiler^{TM} PCR Array System

The Human DNA Repair PCR array system (PAHS-042) was acquired from SABiosciences, Qiagen, Sussex, UK and was used to analyse a panel of genes related to DNA repair pathways. Each PCR array contained a panel of 96 primer sets for a set of 84 relevant pathway-focused genes listed below, as well as five housekeeping genes and three RNA and PCR quality controls:

Base Excision Repair (BER): *APEX1, APEX2, CCNO, LIG3, MPG, MUTYH, NEIL1, NEIL2, NEIL3, NTHL1, OGG1, PARP1, PARP2, PARP3, POLB, SMUG1, TDG, UNG, XRCC1.*

Nucleotide Excision Repair (NER): *ATXN3, BRIP1, CCNH, CDK7, DDB1, DDB2, ERCC1, ERCC2, ERCC3, ERCC4, ERCC5, ERCC6, ERCC8, LIG1, MMS19, PNKP, POLL, RAD23A, RAD23B, RPA1, RPA3, SLK, XAB2, XPA, XPC.*

Mismatch Repair (MMR): *MLH1, MLH3, MSH2, MSH3, MSH4, MSH5, MSH6, PMS1, PMS2, POLD3, TREX1.*

Double-Strand Break (DSB) Repair: *BRCA1, BRCA2, DMC1, FEN1, LIG4, MRE11A, PRKDC, RAD21, RAD50, RAD51, RAD51C, RAD51B, RAD51D, RAD52, RAD54L, XRCC2, XRCC3, XRCC4, XRCC5, XRCC6.*

Other Genes Related to DNA Repair: *ATM, ATR, EXO1, MGMT, RAD18, RFC1, TOP3A, TOP3B, XRCC6BP1.*

To complete the PCR array procedure experimental RNA samples (RNA from TK6 cells treated with MMC) were converted into first strand cDNA using the RT^2 First Strand Kit (SABiosciences, Qiagen, Sussex, UK). Firstly the Genomic DNA Elimination Mixture was

prepared. For each RNA sample, the following components were combined in a sterile PCR tube:

Total RNA	1.6	µg
GE (5x gDNA Elimination Buffer)	2.0	µl
Water to a final volume of	10.0	µl

The contents were mixed gently with a pipette followed by a brief centrifugation. Afterwards the contents were incubated at 42°C for 5min and then immediately chilled on ice for at least one minute.

Thereafter the following RT Cocktail was prepared:

RT Cocktail	1 reaction	2 reactions	4 reactions
BC3 (5x RT Buffer 3)	4µl	8µl	16µl
P2 (Primer & External Control Mix)	1µl	2µ	4µl
RE3 (RT Enzyme Mix 3)	2µl	4µl	8µ
Water	3µl	6µl	12µl
Final Volume	10µl	20µl	40µl

Afterwards the first strand cDNA synthesis reaction was performed. Therefore 10µl of RT cocktail were added to each 10µl Genomic DNA Elimination Mixture and mixed gently with a pipette. An incubation at 42°C for exactly 15min followed and then the reaction was immediately stopped by heating at 95°C for 5min. 91µl of water were added to each 20µl cDNA synthesis reaction. The finished first strand cDNA synthesis reaction was put on ice until the next step or stored overnight at -20°C.

After the first strand cDNA synthesis reaction the Real-Time PCR was performed. Firstly the Experimental Cocktail was prepared as follows:

Plate Format:	96-well
2x SABiosciences RT^2 qPCR Master Mix	1350µl
Diluted First Strand cDNA Synthesis Reaction	102µl
Water	1248µl
Total Volume	2700µl

Afterwards the loading of the 96 -Well PCR array followed. Therefore 25µl of the Experimental Cocktail were added to each well of the PCR array. To remove bubbles the plate was centrifuged for 1min at room temperature at 1000 x g. Subsequently the Real-Time PCR detection was performed. The arrays were slotted into the iCycler iQ5 Thermal Cycler (BioRad, Hertfordshire, UK) and run the following program:

1. 95°C for 10min
2. 95°C for 15sec
3. 60°C for 1min } x 40
4. 95°C for 1min
5. 55°C for 1min
6. 10sec at each 0.5°C increase in temperature from 55°C to 95°C to generate a melt curve

The 10min step at 95°C was required to activate the HotStart DNA polymerase. SYBR Green fluorescence was detected and recorded from every well during the annealing step of each cycle (Step3). Steps 4 to 6 enabled melt curve analysis.

2.2.6.1 Data analysis: $\Delta\Delta C_t$ Method

For the analysis of the data the PCR Array Data Analysis Web Portal was used (www.SABiosciences.com/pcrarraydataanalysis.php). The Web Portal automatically performed the following calculations:

1. All C_t values reported greater than 35 or as N/A were changed to 35. At this point, any C_t value equal to 35 was considered a negative call.
2. The threshold cycle values of the control wells were examined.
    a. Genomic DNA Control (GDC): calculate C_t^{GDC}; if the value is greater than 35, then the genomic DNA contamination is too low to affect gene expression profiling results
    b. Reverse Transcription Control (RTC): calculate ΔC_t=AVG C_t^{RTC}-AVG C_t^{PPC}: if this value is less than 5, then no inhibition is apparent
    c. Positive PCR Control (PPC): the average Ct^{PPC} value should be 20±2 on each PCR Array and should not vary by more than two cycles between PCR Arrays compared
3. The ΔC_t for each pathway-focused gene in each plate was calculated: $\Delta C_t = C_t^{GOI} - C_t^{AVG\,HKG}$
4. The $\Delta\Delta C_t$ for each gene across two PCR Arrays (or groups) were calculated: $\Delta\Delta C_t = \Delta C_t$ (group 2)-ΔC_t (group 1); where group 1 was the control and group 2 was the experimental
5. The fold-change for each gene from group 1 to group 2 as $2^{\wedge}(\Delta\Delta C_t)$

2.2.7 Reverse Transcription with elimination of genomic DNA for Quantitative, Real-Time PCR

The mRNA from the total RNA extractions (see section 2.2.5) were reverse transcribed into cDNA by using the QuantiTect® Reverse Transcription Kit (Qiagen, Sussex, UK). Firstly the genomic DNA elimination reaction was prepared and contained the following components:

Component	Volume/reaction	Final concentration
gDNA Wipeout Buffer, 7x	2µl	1x
Template RNA	1µg	
Rnase-free water	Variable	
Total volume	14µl	

The DNA elimination reaction were then incubated for 2min at 42˚C and immediately placed on ice.

Subsequently the reverse-transcription master mix for multiple reactions was prepared, to ensure that the same ingredient quantities were present in each reaction. The master mix contained the following components:

Component	Volume/reaction	Final concentration
Reverse transcription Master Mix		
Quantiscript Reverse Transcriptase	1µl	
Quantiscript RT Buffer, 5x	4µl	1x
RT Primer Mix	1µl	
Template RNA		
Entire genomic DNA elimination reaction	14µl	
Total volume	20µl	

The template RNA (14µl) was added to each tube containing the reverse-transcription master mix. The mix was then incubated for 15min at 42˚C followed by 3min at 95˚C to inactivate the Quantiscript Reverse Transcriptase.

If 2µg RNA was used the volumes of all reaction components were doubled to a final 40µl reaction volume.

An aliquot of each finished reverse-transcription reaction was added to a Real-time PCR mix or stored at -20˚C for further use.

2.2.8 PrimerDesign geNorm Reference Gene Assay

The geNorm Reference Gene Selection Kit from PrimerDesign Ltd., Rownhams, UK was used to select the reference gene for the Real-time PCR experiments. The Kit contained a panel of 12 candidate reference genes:

- Homo sapiens actin beta (ACTB), mRNA
- Homo sapiens glyceraldehyde-3-phosphate dehydrogenase (GAPDH), mRNA
- Homo sapiens ubiquitin C (UBC), mRNA
- Homo sapiens beta-2-microglobulin (B2M), mRNA
- Homo sapiens phospholipase A2 (YWHAZ), mRNA
- Homo sapiens 60S ribosomal protein L 13a (RPL13A)
- Homo sapiens 18S rRNA gene
- Homo sapiens cytochrome c-1 (CYC1), mRNA
- Homo sapiens eukaryotic translation initiation factor 4A. isoform 2 (EIF4A2), mRNA
- Homo sapiens succinate dehydrogenase complex (SDHA), mRNA
- Homo sapiens topoisomerase (DNA) I (TOP1), mRNA
- Homo sapiens ATP synthase, (ATP5B), mRNA

The expression of these genes was measured by quantitative Real-time PCR and the data were analysed with the help of the geNorm software.

Firstly the lyophilised primers were re-suspended in 220µl RNase/DNase water. The reactions were then set up in a PCR hood using sterile equipment. The components of each reaction included:

Component	**1 Reaction**
Resuspended primer mix	1µl
2x QuantiFast SYBR Green Master Mix	10µl
RNase/DNase free water	4µl
Final Volume	15µl

Subsequently, 15µl of the mix was pipetted into each well of the 96-well plate according to the plate set up. All samples for each reference gene were run on the same plate. Six different cDNA samples (TK6 cells treated with MMC) per reference gene were used. After this at least 132µl of cDNA were prepared by diluting the RT reactions 1:10 (20µl of RT and 180µl of water). Five µl of the diluted cDNA was then pipetted into each well of the 96-well plate

according to the plate layout. The final volume in each well was 20µl. After that the plate was slotted into the iCycler iQ5 Thermal Cycler (BioRad, Hertfordshire, UK) and run the following program:

1. 95°C for 10min
2. 95°C for 15sec
3. 60°C for 60sec } X 50
4. 95°C for 1min
5. 55°C for 1min
6. 10sec at each 0.5°C increase in temperature from 55°C to 95°C to generate a melt curve

2.2.8.1 GeNorm analysis in qBase^{PLUS}

The geNorm analysis software is incorporated in to qBase^{Plus}, which is a Real-time PCR analysis software provided with the Kit. The identities of the genes analysed were put into the software, the run files were uploaded and annotated. After the analysis was complete the results appeared in the main window.

The analysis revealed the best reference gene for accurate normalisation in the experimental system by ranking the candidate reference genes according to their expression stability. It was shown that beta actin (ACTB) would be the best reference gene to use for the Real-time PCR experiments (Figure 2.3).

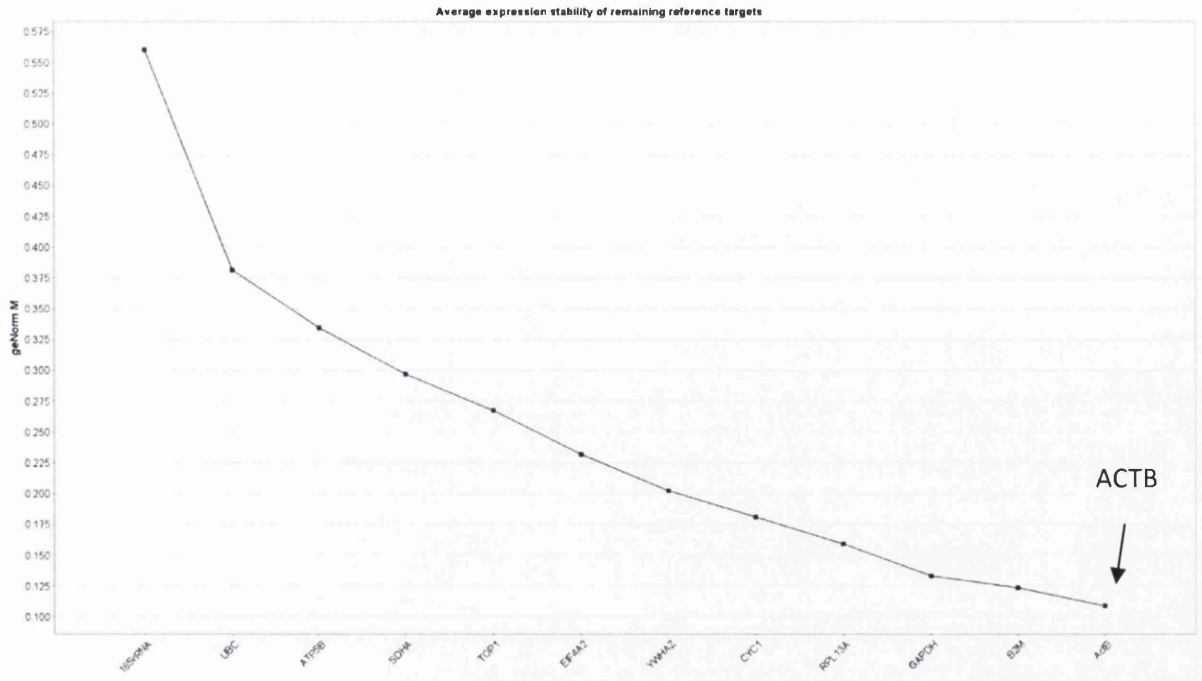

Figure 2.3: Graph indicates the average expression stability value (M) of the reference targets at each step during stepwise exclusion of the least stably expressed reference gene. *ACTB* was the most stable gene, as can be seen on the right site of the graph (black arrow).

2.2.9 Real-Time PCR

For the Real-time PCR experiments the QuantiFast™ SYBR® Green PCR Kit (Qiagen, Sussex, UK) was used.

2.2.9.1 The reaction

The reactions were set up in the PCR hood using sterile equipment. The components of each reaction included:

Component	Volume/reaction (96 well block)
2x QuantiFast SYBR Green PCR Master Mix	12.5µl
Primer A	0.25µl
Primer B	0.25µl
Template DNA or cDNA	1.5µl
RNase-free water	10.5µl
Total reaction volume	25µl

Firstly master mixes were prepared, containing the QuantiFast SYBR Green master mix; primers and water to ensure that the same ingredient quantities were present in each reaction. These master mixes were sub-divided into aliquots of three reactions, because all samples were run in triplicate. Sample cDNA (1.5µl per reaction; 4.5µl in total) was added to each

sub-divided master mix. At least 25µl of each resultant mix was aliquoted into wells of a sterile 96-well 0.2ml PCR plate (Sarstedt, Nuembrecht, Germany). Standard samples as well as negative controls were also included for each primer pair. In negative controls the cDNA was replaced with water.

The plates were sealed with Absolute QPCR Seal sheets (Thermo Scientific, Surrey, UK) after all 25µl reactions were loaded into the wells, they were briefly centrifuged to bring all the contents to the bottom of the wells. After that the plates were slotted into the iCycler iQ5 thermal Cycler (BioRad, Hertfordshire, UK) and run the following program:

1. 95°C for 5min
2. 95°C for 10sec } X 40
3. 60°C for 30sec
4. 95°C for 1min
5. 55°C for 1min
6. 10sec at each 0.5°C increase in temperature from 55°C to 95°C to generate a melt curve

The first step activates the HotStarTaq *Plus* DNA polymerase. Steps 2 and 3 represent the PCR reaction, while steps 4 to 6 enabled melt curve analysis.

For the amplification reaction the fluorescent data were collected at step 3 as well as analysed in real-time, whereas for the melt curve analysis the data were collected at step 6 and analysed in real-time.

2.2.9.2 Data analysis

The iCycler iQ5 software version 2.1 (BioRad, Hertfordshire, UK) was used to analyse the data. Each sample was individually analysed.

To assign the specificity of the PCR reaction products that had been generated, the melt curves for all samples were analysed. When the melt temperature (Tm) was incorrect for any sample, this sample was removed from the analysis.

For the relative quantitation of gene expression the standard curve method was used. Standard samples with known template amounts were defined in the "sample setup" view. Therefore stock cDNA samples were diluted (10-fold dilutions with the dilution values: 1, 10, 100 and 1000). The results from wells defined as Standards were used to generate a standard curve. The crossing points (C_Ts) were plotted against the log of the template amount,

resulting in a straight line. Threshold cycle (C_T) values for these samples and the standard curve were then used to calculate the amount of starting template in the experimental samples.

The samples were normalized by their respective endogenous control results to calculate a normalized target value:

Normalized target = Target/Endogenous control

The normalized target values were then divided by one another to calculate the fold-difference in target quantity:

Fold difference in target = Normalized target (treated sample)/ Normalized target (untreated control)

N-fold differences observed were considered as changes in gene expression if <0.5 or >1.5 as defined by Doak *et al.* (2004) and statistical analysis was conducted.

2.2.10 The mammalian cell *HPRT* gene mutation assay

The *hypoxanthine phosphoribosyl transferase (HPRT)* gene mutation assay detects mutations which destroy the functionality of the *HPRT* gene and/or protein by positive selection (Johnson, 2012).

The first step of the HPRT assay was the mutant cleansing stage. Therefore 1ml of hypoxanthine-aminopterin-thymidine (HAT) was added to the TK6 culture (4-5x10^5 cells/ml) and the cells were grown for 3 days. The aminopterin in HAT medium blocks the salvage pathway for the production of dNTPs for DNA synthesis. That means the cells had to rely on the endogenous pathway (HPRT and TK) and mutant $HPRT^-$ and $TK6^{-/-}$ mutants were selectively killed (Johnson, 2012). After 3 days the HAT medium was washed off with PBS. Therefore the cells were spun down (10min, 200 x g), the supernatant discarded and the pellet washed with PBS. Afterwards the cells were re-suspended in 50ml fresh medium and 1ml of hypoxanthine-thymidine (HT) was added to the culture medium for 24h, to ensure that the de novo nucleotide biosynthesis pathways as well as the salvage pathway were able to function from this step onward (Johnson, 2012). After washing off the HT medium with PBS, the TK6 cell suspensions (10ml) were seeded at 1x10^5cells/ml for 24h at 37°C, 5%CO_2. The cell suspensions were then treated with the chemical and after the treatment period the chemical

was washed off with PBS, new medium was added and the cells were sub-cultured to 1.2-1.5x10^5cells/ml in 50ml flasks (day 1). The cells were left to grow for thirteen days to enable expression of the $HPRT^-$ mutants. Cells were sub-cultured at days 1, 3, 5, 7, 9 and 11 and can be cryogenically frozen down at days 5 and 7. After the phenotypic expression period at day 13, the cells were added to 96-well micro plates.

For mutation frequency (MF), TK6 cells with 2.4x 10^7 cells in 60ml were treated with 240µl of 6-thioguanine (0.6µg/ml) (6-TK) for selection. Five plates per dose were used with 100µl of cell suspension in each well. $HPRT^+$ cells incorporate 6-TG into the DNA and consequently die, whereas $HPRT^-$ cells cannot incorporate the toxic analogue into their DNA and consequently survive (Johnson, 2012).

For plating efficiency (PE) approximately 200 cells in 100µl were added to the plate per well with no selection. Five plates per dose were used.,

Plates were scored for colony formation after 14 days of incubation at 37°C, 5%CO_2. Scoring criteria specified that only colonies with 20+ cells in diameter were scored. Furthermore it was ensured that separate colonies were clearly apart, taking clonal expansion into account. The experiment was carried out in triplicate.

2.2.10.1 6-Thioguanine (6-TG)

Working solutions of 1x 6-TG were prepared at 0.15mg/ml to minimise freeze/thaw cycles. The 30x stock of 6-TG (4.5mg/ml) was therefore diluted to a 1x working solution by adding 1ml of 30x 6-TG to 29ml of 0.1M NaOH (1g NaOH in 250ml distilled water). The 1x 6-TG solution was then filter sterilized with 0.2µM filters and kept as 5ml aliquots at -20°C until use.

2.2.11 The *in vitro* comet assay +/-hOGG1

The comet assay is also known as the single cell gel electrophoresis assay. Cells were treated with the test chemical, which was then washed off with PBS and the cells were re-suspended in fresh media. The cell number was adjusted to 1.5x10^5cells/ml. After that 1ml of the cell suspensions were sampled into labelled eppendorf tubes, centrifuged at 720rcf for 3min, the supernatant discarded and the cells re-suspended in 1ml cold 1xPBS. After centrifugation (720rcf for 3min) the supernatant was removed from the pellet and the cells were re-suspended with 200µl low-melting agarose and 3 x 40µl drops, resulting in 3 gels, were added per glass slide (pre-coated with agarose) and covered with a coverslip. Slides were then placed on a cold tray, which allowed for gels to set after which the coverslips were

removed and the slides were placed in cold lysis solution (2.5M NaCl, 100mM Na_2EDTA, 10mM Tris buffer (pH 10), 10% DMSO, 1% Triton X-100) in a dark container over night at 4°C. Following lysis, the slides were washed twice for 5min in 1x buffer F (40mM HEPES, 0.1M KCl, 0.5mM EDTA and 0.2mg/ml BSA (pH 8.0)) at room temperature. hOGG1 (+hOGG1) or buffer F (-hOGG1) (60µl) were then added to each slide, topped up with a coverslip and incubated in a humidified box at 37°C for 10min. After removing the coverslips the slides were placed in an electrophoresis platform and covered with electrophoresis buffer (1mM Na_2EDTA, 0.3M NaOH (pH 13)) for 20min at 4°C to allow for the DNA to unwind. Afterwards the electrophoresis was performed at 0.7V/cm, 300mA for further 20min at 4°C.
To neutralise, the slides were removed from the electrophoresis platform and immersed in three changes of neutralisation buffer (0.4M Tris-HCl (pH 7.5)) for 5min each time at room temperature.
Finally the slides were stained with 60µl propidium iodide (20µg/ml) for 30min, before scoring using a Comet IV capture system (Perceptive Instruments Ltd., Haverhill, UK). Fifty nuclei per gel were scored and the tail intensity (TI), which is defined as the percentage of DNA migrated from the head of the comet into the tail, was measured for each nucleus scored (Smith et al., 2006). The experiment was run in duplicate.

2.2.12 Protein extraction

All steps for the protein preparation were performed at 4°C; pre-cooled buffers and equipment were used.
For the total protein extraction all cell suspensions were seeded at $1x10^5$cells/ml for 24h at 37°C, 5%CO_2. Subsequently the cells were treated with the appropriately diluted test chemical for different time points. After chemical treatment the cell suspensions were transferred to centrifuge tubes and spun down at 200 x g for 8min. The cells were then washed with 5ml ice-cold PBS and again spun down at 200 x g for 8min. After re-suspending the cell pellet, 200µl ice-cold 1x radioimmuno-precipitation lysis (RIPA) buffer (Sigma-Aldrich, Dorset, UK) supplemented with 2µl protease inhibitor cocktail (Sigma-Aldrich, Dorset, UK) and 2µl phosphatase inhibitor cocktail 2 (Sigma-Aldrich, Dorset, UK) were added and the cell suspensions were transferred to pre-chilled micro-centrifuge tubes. After 5min incubation at 4°C, the cells were lysed by vortexing thoroughly and spun down for 10min at 10000 x g in a centrifuge pre-cooled to 4°C. Finally the supernatant was transferred to a new micro-centrifuge tube and after protein quantification (see section 2.2.13) aliquots of the protein samples were stored at -80°C.

2.2.13 Protein quantification

The BioRad DC Protein Assay (BioRad, Hertfordshire, UK) was used for the protein quantification and the assay contained the reagents A, B and S. For the quantification dilutions of a BSA protein standard (BioRad, Hertfordshire UK) containing 0 to 2.5mg/ml of BSA, as well as the working reagent A were prepared, by adding 20µl of reagent S per ml of reagent A. All protein quantification steps were run in duplicate.

Subsequently 5µl of the protein standards and protein samples were pipetted into a clean, dry 96-well plate. Then 25µl of the working reagent A, followed by 200µl of reagent B were added to each well. Afterwards the plate was gently agitated to mix the reagents for 15min. After the incubation, absorbance was read at 750nm with the POLARstar Omega Microplate Reader (BMG Labtech Ltd., Aylesbury, Bucks, UK) and the Mars Data Analysis Software (version 1.20.R2) was used for quantification.

2.2.14 Western blotting

With the help of the sodium dodecyl sulphate-polyacrylamide gel electrophoresis (SDS-PAGE) proteins could be analysed.

2.2.14.1 SDS-PAGE

The proteins were separated according to their size following denaturation (as described below) on a polyacrylamide gel. The gel consisted of two layers, the resolving and the stacking gel. The gels were prepared as seen in Table 2.3 below:

Table 2.3: Gel composition for the SDS-PAGE

	Stacking Gel	Resolving Gel
	4%	10%
	4 Gels	4Gels
30% Acrylamide	1.3ml	10ml
ddH_2O	6ml	12ml
1.5M Tris (pH 8.8)		7.5ml
1M Tris (pH 6.8)	2.5ml	
10% SDS	100µl	300µl
10% APS	50µl	150µl
Temed	10µl	30µl

The Mini Protean® 3 Cell system from BioRad (BioRad, Hertfordshire, UK) was used for the SDS-PAGE. After assembling of the casting stand, the resolving gel was applied to the cast and left to polymerise for 30 to 60min. Subsequently the stacking gel and the comb were applied to the cast and again left to polymerise for 30 to 60min. The polymerised gel was placed into the electrode assembly and clamping frame, the comb was removed and the assembly filled with running buffer (25mM Tris (pH 8.3), 192mM glycine, 0.1% (w/v) SDS). In parallel the protein samples (40µg) were mixed in a 1:1 ratio with Laemmli Buffer (Sigma-Aldrich, Dorset, UK), sonicated three times for 10sec with 10sec breaks in between and afterwards incubated for 5min at 95°C.

Subsequently 8µl of the Dual Colour Standard and Biotinylated Ladder were loaded onto the gels as well as the protein samples.

The proteins were separated on the gel at 120V until the dye front reached the bottom of the gel.

2.2.14.2 Protein blotting

After the SDS-PAGE was completed the proteins were electroblotted onto an Immun-Blot PVDF membrane (BioRad, Hertfordshire, UK).

For the protein blotting the Mini Trans-Blot® Cell system (BioRad, Hertfordshire, UK) was used. The BioRad Immun-Blot PVDF membrane was immersed in 100% methanol until translucent. Afterwards fibre pads, blot paper (BioRad, Hertfordshire, UK), the polyacrylamide gel and the PVDF membrane were equilibrated for 10min in transfer buffer (20mM Tris (pH 8.3), 192mM glycine, 20% (v/v) methanol, 0.1% (w/v) SDS)) pre-cooled to 4°C. The transfer cassette was assembled as below:

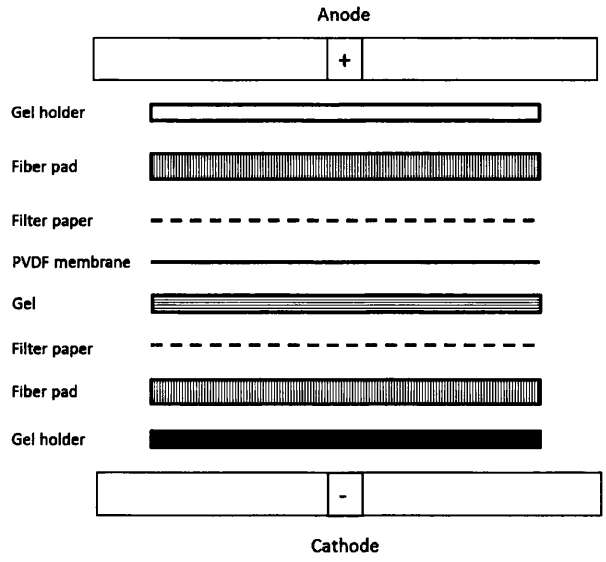

The proteins were transferred onto the membrane at 400mA for 1hr at 4°C.

2.2.14.3 Membrane blocking and antibody incubations

After removing the PVDF membrane from the transfer cassette and washing briefly in TBS/T (20mM Tris (pH 7.6), 125mM NaCl, 0.1% (v/v) Tween®20) the membranes were incubated in blocking buffer (20mM Tris (pH 7.6), 137mM NaCl, 5% (v/v) BSA, 0.1% (v/v) Tween®20) for 1hr at room temperature with gentle agitation.

Subsequently the blocking buffer was removed and the membranes were incubated in with 1:1000 dilutions (p53/phospho-p53) or 1:2000 dilutions (beta-actin) of primary antibodies specific to p53, phospho-p53 (Ser15) and beta-actin (Cell Signalling, New England Biolabs, Herts, UK), diluted in 8ml blocking buffer over night at 4°C with gentle agitation.

Afterwards the membranes were washed in TBS/T for 4x5min at room temperature with strong agitation, then they were incubated for 1h in HRP conjugated goat polyclonal secondary antibody to rabbit IgG (1:1000 dilution; Abcam, Cambridge, UK) and Anti-biotin, HRP linked antibody (1:1000 dilution; Cell Signalling, New England Biolabs, Herts, UK) with gentle agitation at room temperature.

Before protein detection the membranes were washed again for 4x5min in TBS/T at room temperature with strong agitation.

2.2.14.4 Protein detection

The BioRad Immun-Star WesternC Chemiluminescent kit (BioRad, Hertfordshire, UK) was used for protein detection. The lumino/enhancer solution and the peroxide buffer solution were mixed in a 1:1 ratio. The membranes were then incubated with the mixture and visualised using the Chemidoc XRS system (BioRad, Hertfordshire, UK). Average band densitometry was determined using the Quantity One version 4.6.3 software (BioRad, Hertfordshire, UK) and the test band densities were normalised against the corresponding beta-actin band density to compensate for variations in protein loading.

2.2.14.5 Stripping Membranes for Re-probing

The membranes were briefly washed in TBS/T, before incubating in 8ml Restore Western Blot Stripping Buffer (Thermo Scientific, Northumberland, UK) for 10min with gentle agitation at room temperature. After removing the stripping buffer and briefly washing the membranes in TBS/T, the membranes were ready for re-use.

2.2.15 Apoptosis analysis using flow cytometry

The induction of apoptosis in cells treated with test chemicals was investigated by using an AnnexinV-FITC antibody (Abcam, Cambridge, UK). After the initiation of apoptosis, cells translocate membrane phosphatidylserine (PS) from the inner layer of the plasma membrane to the cell surface, where it can be detected by staining with a fluorescent conjugate of AnnexinV, a protein with a high affinity to PS (Elmore, 2007). Propidium iodide (PI) (Sigma-Aldrich, Dorset, UK) was used as a counterstain for the detection of dead cells.

All cell suspensions (10ml) were seeded at $1x10^5$cell/ml for 24h at 37°C, 5%CO_2 and treated with the test chemicals. After the different incubation times the suspensions were removed from each flask and transferred into appropriately labelled tubes. The cells were spun down (10min, 200 x g), washed with PBS to remove any residual chemical and re-suspended in PBS, before determining the cell concentration using the Beckman Coulter Counter (Beckman Coulter Inc., High Wycombe, UK). The right amounts of cells ($1x10^6$) were transferred to each tube and the cells were spun down for 10min at 200x g at 4°C. After removing all of the supernatant, the cell pellets were washed with 1ml of 1x AnnexinV binding buffer (Abcam, Cambridge, UK) and spun down for 10min at 200 x g. Afterwards the cell pellets were re-suspended in 100µl of 1x AnnexinV binding buffer, 10µl of AnnexinV-FITC antibody was added into each tube and incubated for 15min in the dark at room temperature. Subsequently the excess antibody was washed off with 1x AnnexinV

binding buffer, the cell pellets were re-suspended in 200µl PBS and 5µl of PI (1mg/ml) was added to each tube for 5min at a final concentration of 5µg/ml, before analysing the samples with a BD FACS Aria™ flow cytometer (BD Biosciences, Oxford, UK).

2.2.15.1 Quantification by flow cytometry

The BD FACS Diva™ software (BD Biosciences, Oxford, UK) was used for quantification and AnnexinV-FITC (Ex = 488nm; Em = 530nm) was analysed using a FITC signal filter (530/30), while PI (Ex = 536nm; Em = 617nm) was analysed using the 585/42 filter.

The forward scatter (FSC) and side scatter (SSC) were used to identify the cells (Figure 2.4, A). Afterwards AnnexinV-FITC was plotted on the Y-axis against PI on the X-axis, which distinguished viable cells (negative for both AnnexinV-FITC and PI), early apoptotic cells (AnnexinV-FITC positive, PI negative), late apoptotic cells (AnnexinV-FITC and PI positive) and dead cells (PI positive, AnnexinV-FITC negative) (Figure 2.4,B).

Staurosporine (1µM, 4h treatment) was used as a positive control for apoptosis induction.

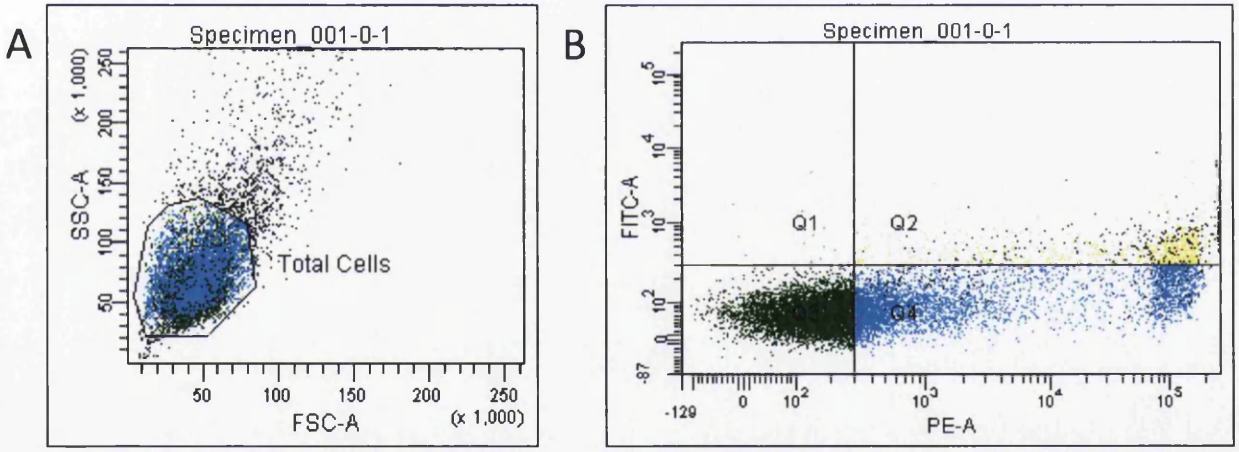

Figure 2.4: Apoptosis analysis. A: Forward vs. side scatter to identify cells. B: AnnexinV-FITC and PI staining of TK6 cells. Q1; early apoptotic cells (AnnexinV-FITC positive, PI negative), Q2; late apoptotic cells (AnnexinV-FITC and PI positive), Q3; viable cells (negative for both AnnexinV-FITC and PI), Q4; PI positive, AnnexinV-FITC negative)

2.2.16 Cell cycle analysis using propidium iodide (PI) staining

The cell cycle status, in cells treated with the test chemicals, was analysed by quantitation of DNA content using flow cytometry.

All cell suspensions (10ml) were seeded at $1x10^5$cells/ml for 24h at 37°C, 5%CO_2 and treated with test chemicals. After the different incubation times the suspensions were removed from each flask and transferred into appropriately labelled tubes. The cells were spun down (10min, 200 x g), washed with PBS to remove any residual chemical and re-suspended in

PBS, before determining the cell concentration using the Beckman Coulter Counter (Beckman Coulter Inc., High Wycombe, UK). The right amounts of cells ($1x10^6$) were transferred to each tube and they were spun down at 4°C for 10min at 200 x g. After removing the supernatant, the cells were re-suspended in 300µl ice-cold PBS. To fix the cells, 700µl cold ethanol (70%) were added drop-wise to the tube containing 300µl of cell suspension in PBS, while vortexing gently. The cells were left for 1h on ice or up to a few days at 4°C. Subsequently the cells were spun down, washed once with cold PBS, before re-centrifugation and removal of the supernatant. Afterwards the cell pellet was re-suspended in 250µl PBS, 5µl of 10mg/ml RNase A were added at a final concentration of 0.2 to 0.5mg/ml and the cells were incubated at 37°C for 1h.

Finally 10µl of 1mg/ml PI solution at a final concentration of 10µg/ml were added and the cells were kept in the dark at 4°C until analysed.

The DNA content was quantified using the BD FACS Aria™ flow cytometer (BD Biosciences, Oxford, UK) and the BD FACSDiva software (BD Biosciences, Oxford, UK) was used for analysis. The forward scatter (FSC) and side scatter (SSC) were measured to identify single cells and a suitable filter (PE-A: 585/42) was chosen to measure PI (Ex = 536nm; Em = 617nm). Cell count was plotted on the Y-axis, while PI was plotted on the X-axis. PI binds in proportion to the amount of DNA present in the cell. The flow cytometric data were acquired in logarithmic scale and gates for G0/G1, S-phase and G2/M were set within the analysis program.

2.2.17 Statistical analysis

The Kruskal-Wallis test was used to determine significant differences between groups. When the Kruskal-Wallis test led to significant results ($p<0.05$), the Mann-Whitney U test was used for pairwise comparisons (between the control samples and the treated samples). As the final step the Bonferroni-Holm method was used for adjustment of the p-values for multiple testing.

The Chi-squared test with Yates' continuity correction was used for the analysis of the MN data. Again the Bonferroni-Holm method was used afterwards for adjustment of the p-values for multiple testing.

Pearson's r correlation analysis was performed for the comparison of the automated system Metafer and the conventional manual scoring.

Chapter 3

The dose regime determines the genotoxicity of mitomycin C (MMC)

3.1 Introduction

The investigation of low dose responses in genotoxicology testing helps to improve health risk assessments by establishing if DNA reactive compounds follow linear or non-linear (thresholded) dose response relationships. The current assumption is that the relationship between exposure to genotoxic chemicals, DNA damage formation and the induction of mutagenic change is linear (Henderson et al., 2000). However, mutations are not produced directly by DNA adducts as DNA repair activity limits the proportion of adducts processed into mutational change. It is therefore possible that no observed effect levels (NOEL) may exist for some genotoxins (Jenkins et al., 2005). Furthermore natural defence mechanisms, like epithelial barriers to genotoxin entry, chemical detoxification, DNA redundancy or DNA repair corroborate the theory of genotoxic thresholds (Jenkins et al., 2010).

Biological thresholds for genotoxic mutagens or carcinogens are accepted for some genotoxic mechanisms, such as aneuploidy or indirect modes of action (Greim and Albertini, 2012). Further mechanisms, such as disruption of cell division and chromosome segregation, inhibition of DNA synthesis or overloading of oxidative defence mechanism might permit the identification of a non-linear (thresholded) genotoxic effect (Greim and Albertini, 2012).

However, thresholds of genotoxic activity have to be proven for each agent on a case-by-case basis

3.1.1 Mitomycin C (MMC)

MMC is an antineoplastic antibiotic discovered in the 1950s and was isolated from the industrial microorganism *Streptomyces caespitosus* (Hata et al., 1956; Tomasz, 1995). MMC has been used for clinical cancer treatments since the 1960s, because of its effectiveness against solid tumours (Tomasz and Palom, 1997; Paz, 2008). Examples are adenocarcinoma of the stomach or pancreas, superficial bladder cancer, epidermoid anal carcinomas and oesophageal carcinomas (Paz, 2008). MMC is in particular selective against the hypoxic regions of solid tumours, because these tumours are short of oxygen in comparison to normal tissues (Paz et al., 1999). The activation of MMC is inhibited by an oxidizing environment.

From this it follows, that MMC has selective toxicity for solid tumours (Tomasz, 1995). The antibiotic is used in combination treatments with other anti-tumour drugs.

However MMC causes severe secondary effects, like myelosuppression and severe toxicities, such as leucopenia and anaemia (Paz, 2008). Clinical use of MMC is therefore limited.

Further MMC is known for its wide range of specific biological effects in mammalian cells and microorganisms. Examples are selective inhibition of DNA synthesis, mutagenesis, and induction of DNA repair in bacteria (SOS response), sister-chromatid exchange, signal transduction and chromosome breakage (Tomasz, 1995; Tomasz and Palom, 1997; Mao et al., 1999). In addition MMC cross-links the complementary strands of the DNA double helix, first shown in 1963 (Iyer and Szybalski, 1963; Tomasz, 1995).

3.1.1.1 Mechanism of action

MMC itself can not react with DNA. However, upon enzymatic or chemical reduction of the quinone it is converted to a DNA-reactive species (Iyer and Szybalski, 1964; Tomasz and Palom, 1997; Paz, 2008). MMC consists of a pyrrolo indole ring system with an aziridine ring (Figure 3.1) and requires an enzymatic activation by a one-electron pathway to a semiquinone or by a two-electron reduction pathway to a hydroquinone (Danshiitsoodol et al., 2006).

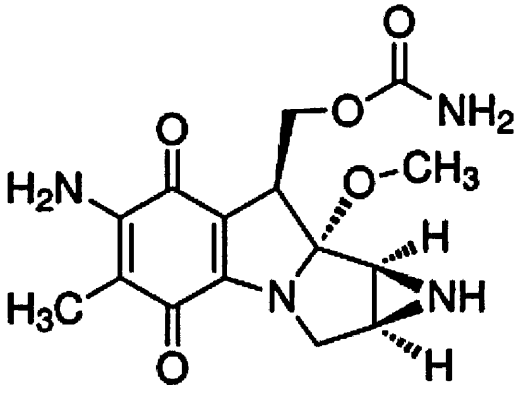

Figure 3.1: Structure of MMC (from www.sigma-aldrich.com/catalog/product/sigma/m4287)

Activation of MMC by a one-electron pathway involves enzymes such as NADPH-cytochrome P450 reductase, xanthine oxidase and cytochrome b_5 reductase; whereas enzymes such as NAD(P)H dehydrogenase, quinone 1 (DT-diaphorase) and xanthine oxidase activate MMC by a two-electron pathway (Snodgrass et al., 2010).

As a result of the reduction of the quinone and the spontaneous elimination of methanol an indole hydroquinone is formed, where the C1 aziridine and the C10 carbamate groups are

highly reactive towards nucleophiles (Tomasz and Palom, 1997; Paz, 2008). The interstrand cross-link is then formed by the reaction of this intermediate with the 2-amino group of guanines in complementary strands of duplex DNA (Paz, 2008). During this process the initial monoadduct formation occurs at the C1 group of activated MMC, whereas the second arm reaction links the C10 group to a guanine in the opposite DNA strand (Paz, 2008) (Figure 3.2). These cross-links are formed specifically at CpG sequences, because of the orientation of the initial monoadduct towards the 3' end of the opposite strand and the reactivity of guanine at the CpG steps (Paz, 2008).

In addition to the interstrand cross-links MMC also causes damage to DNA by monoadducts as well as DNA intrastrand cross-links at GpG sites (Paz et al., 1999; Paz, 2008) (Figure 3.2). In the case of monofunctional alkylation of DNA the C1 aziridine function reacts only with a guanine-N_2 nucleophile while the less reactive C10 carbamate remains intact or is hydrolysed (Paz et al., 2004). However, the main cause of cytotoxicity is interstrand MMC-DNA cross-links.

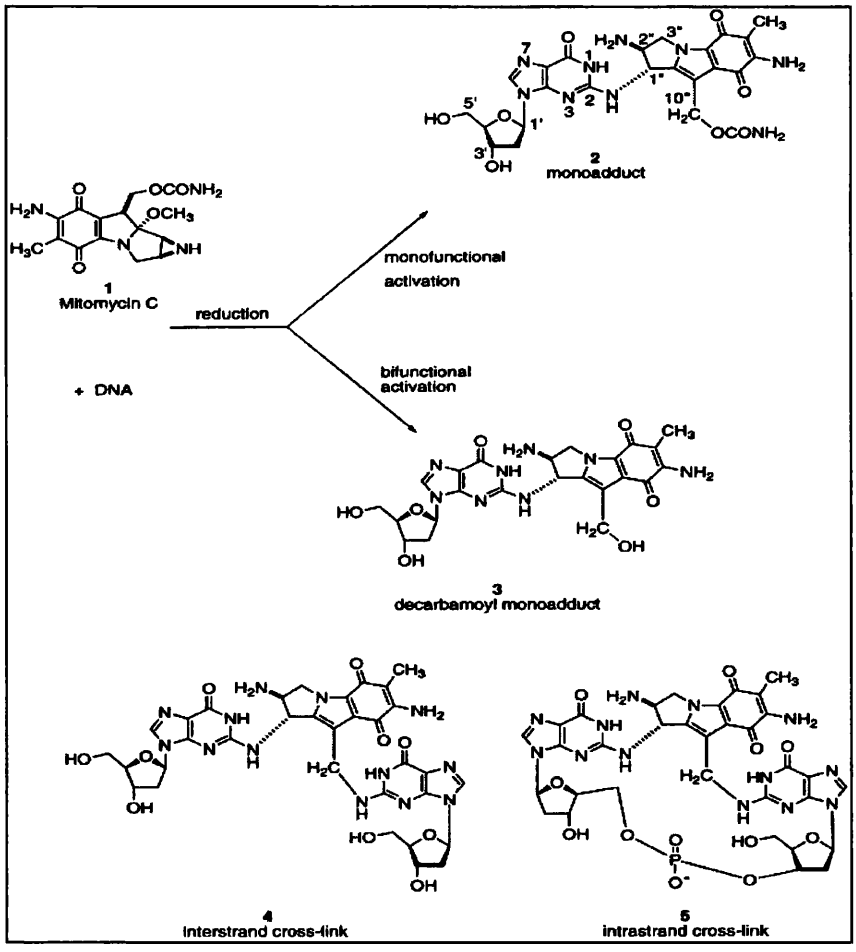

Figure 3.2: MMC adducts: (1) MMC; (2,3) MMC-guanine monoadducts; (4,5) MMC-DNA interstrand and intrastrand cross-links (from Paz et al., 1999)

It has been shown, that various adducts of MMC are capable of inducing different cell death pathways in cancer cells (Champeil et al., 2010). The evidence was deduced by a study of MMC and its derivatives 2,7-diaminomitosense (2,7-DAM) and decarbamoyl mitomycin C (DMC). 2,7-DAM is the main metabolite of MMC and forms two monoadducts with the DNA, whereas DMC alkylates and cross-links DNA, predominantly with chirality opposite to that of the DNA adducts of MMC (Champeil et al., 2010). MMC and DMC are cytotoxic and able to activate the p53 pathway, whereas 2,7-DAM is neither cytotoxic nor able to activate the p53 pathway. In comparison to MMC, DMC is more cytotoxic. Furthermore it kills p53-deficient cells by inducing degradation of Checkpoint 1 protein (Abbas et al., 2002; Bargonetti et al., 2010; Champeil et al., 2010). DNA adducts of DMC have a different signalling pathway, which explains the difference in the cell death pathways activated by MMC and DMC (Abbas et al., 2002; Bargonetti et al., 2010; Champeil et al., 2010).

3.1.1.2. Previous genotoxicity studies with MMC

The anticancer drug MMC is a known genotoxin. In previous studies MMC was therefore often used as a positive control in the chromosome aberration assay as well as the MN assay. Furthermore MMC is known to show positive responses at non-cytotoxic concentrations (Schuler et al., 2010). Therefore MMC was used as part of a collaborative evaluation study to investigate the toxicity measures recommended in the draft OECD Test Guideline 487 for the *in vitro* MN test (Elhajouji, 2010; Fowler et al., 2010; Schuler et al., 2010).

From this it follows that MMC is a useful chemical for development and validation of the *in vitro* MN assay in different cell lines as a strong inducer of MN (Sobol et al., 2012).

3.1.1.2.1 Examples of *in vitro* and *in vivo* studies

In the studies of Elhajouji (2010), Fowler *et al.* (2010) and Schuler *et al.* (2010) MMC was used as a one of the reference genotoxic agents tested in the *in vitro* MN test. The aims of these studies were to investigate and evaluate various cytotoxicity measurements recommended in the draft OECD Test Guideline 487 on "*In Vitro* Mammalian Cell Micronucleus Test" (Elhajouji, 2010; Fowler et al., 2010 and Schuler et al., 2010). These studies were part of an international collaborative evaluation.

In the study of Elhajouji (2010) the human lymphoblastoid cell line TK6 were treated with MMC for 3h followed by 27h recovery. Various concentrations between 0 to 2.0µg/ml were tested in the presence and absence of cytochalasin B, with at least 2000 cells per concentration analysed. The results showed statistically significant increases in MN

frequencies at all analysed concentrations in the presence and absence of cytochalasin B. Furthermore the 50 to 60% toxicity target at the top dose was not reached (Elhajouji, 2010). Cytotoxicity measurements without cytochalasin B at the top dose resulted in reduction in RCC, RICC or RPD as low as 25.64%, 34.48% or 21.77% respectively (Elhajouji, 2010).

In the study of Schuler *et al.* (2010) Chinese hamster ovary (CHO) cells were treated with MMC for 24h in the presence and absence of cytochalasin B. Various concentrations between 0 to 4µg/ml were used. The results demonstrated that MMC induced significant MN formation at all concentrations tested with and without cytochalasin B. A range of 9.8 to 61.8% increase in cytostasis was observed over the range of concentrations (Schuler et al., 2010).

In the study of Fowler *et al.* (2010) Chinese hamster lung (CHL) cells were treated with MMC for 3h followed by a 21h recovery period. A range of concentrations between 0 to 1.0µg/ml was selected. Significant increases in MN induction were observed at all concentrations tested. RPD, RICC and RI measurements showed 50-60% toxicity at 0.5µg/ml, whereas RCC showed 50-60% toxicity at 0.1µg/ml (Fowler et al., 2010).

The purpose of the study by Sobol *et al.* (2012) was the evaluation and validation of the *in vitro* MN assay in TK6 cells, which are p53 competent. Three treatment conditions were used for the evaluation of MMC. The 27h continuous treatment with concentrations between 0 to 0.1129µg/ml showed a dose-related and statistically significant increase in MN induction. In addition both 4h treatments with 24h recovery period (0 to 0.630µg/ml) or 48h recovery period (0 to 0.250µg/ml) showed significant increases in MN induction over the dose range. Furthermore it was shown that an extended recovery period produced higher MN frequencies (Sobol et al., 2012).

An example of an *in vivo* study is a paper published by Grawé *et al.* (1998), where low dose effects of MMC were assessed by the flow cytometric *in vivo* MN assay. For the experiment male mice (7 to 8 weeks old, weight around 25g) were used. All treatments were injected by a single intraperitoneal injection. Various concentrations between 0 to 0.183mg/kg were used and the optimum sampling time for MMC was 45h after treatment. The results showed a linear dose response relationship over the dose range, even in the very low dose range, which was defined as the dose region where the frequency of micronucleated erythrocytes was less than twice the baseline frequency (Grawé et al., 1998).

Previous studies with MMC, which looked at dose response relationships *in vitro* and *in vivo* showed linear dose responses. However concentrations and dose regime chosen in various studies differed depending on cell lines and cytotoxicity measurements. Further MMC was

mainly used as a positive control and for validation purposes. Therefore no studies investigated the low dose response relationships of MMC with the aim of finding if NOEL might exist for this genotoxin. For MMC to act as a mutagen, it needs to avoid DNA repair and other natural defence mechanisms, such as epithelial barriers for genotoxin entry.

3.1.2 DNA repair

The integrity and stability of DNA depends on processes like DNA damage recognition, repair, replication, transcription and cell cycle regulation. Furthermore apoptosis contributes to genetic integrity by removing damaged cells (Krokan et al., 2000).

The human genome is constantly attacked by endogenous and exogenous DNA damaging agents, examples are environmental mutagens, endogenous reactive metabolites and replication errors (Christmann et al., 2003). This causes instability of the DNA, thus DNA repair systems are vital to maintain the genome stability.

DNA repair genes (and proteins) are either associated with signalling and regulation of DNA repair or with distinct repair mechanisms (Christmann et al., 2003). The main repair pathways are direct repair, base excision repair (BER), nucleotide excision repair (NER), mismatch repair (MMR) and DNA double strand break (DSB) repair.

Direct DNA repair is the simplest response to DNA damage. The lesions are removed or reversed in a single-step reaction. Consequently the local sequence is restored to its original state (Yu et al., 1999). Examples for direct DNA repair mechanisms are photoreactivation or the O6-methylguanine-DNA methyltransferase (MGMT) enzyme. Several photolyases in bacteria and yeast are known to directly reverse DNA damage resulting from UV or cisplatin treatment in a light-dependent way (Sancar, 1996; Yu et al., 1999). MGMT removes alkyl adducts from the O6-position of guanine in DNA and protect cells against the mutagenic and carcinogenic effects of alkylating agents (Danam et al., 2005). MGMT is expressed in all human cells and tissues, but its activity varies several fold between different individuals, organs and cell types within organs (Drabløs et al., 2004).

Base excision repair (BER) targets "non-bulky" base adducts, examples are those produced by methylation, oxidation, reduction or fragmentation of bases (Yu et al., 1999). The lesions removed from DNA include incorporated uracil, fragmented pyrimidines, N-alkylated purines, like 7-methylguanine, 3-methyladenine and 3-methylguanine, 8-oxo-7,8-dihydroguanine (8-OxoG) and thymine glycol (Christmann et al., 2003). BER is a multistep process, which is initiated by a damage-specific DNA glycosylase (Krokan et al., 2000). The

DNA glycosylase removes the damaged base, which leaves an abasic site, which is then further processed until the correct DNA sequence is restored (Krokan et al., 2000).

Nucleoside excision repair (NER) targets bulky DNA adducts, like UV induced photolesions, photoproducts (6-4PPs), cisplatin-guanine, cyclobutane pyrimidine dimers, intrastrand crosslinks and large chemical adducts (Yu et al., 1999; Christmann et al., 2003). NER consists of two pathways: global genomic repair (GGR) and transcription-coupled repair (TCR) (Christmann et al., 2003). GGR removes lesions from non-transcribed domains of the genome and from the non-transcribed strand of transcribed regions, whereas TCR removes lesions only from the transcribed strand of expressed genes (Christmann et al., 2003).

Mismatch repair (MMR) targets the removal of base mismatches, which are caused by spontaneous and induced base deamination, oxidation, methylation and replication errors (Modrich and Lahue, 1996; Umar and Kunkel, 1996; Christmann et al., 2003). Furthermore mismatched base pairs arise through formation of heteroduplexes and secondary structure such as imperfect palindromes (Bishop et al., 1985; Yu et al., 1999).

DNA double strand break repair (DSB) arises under physiological conditions, which include somatic recombinations or the overlapping of extensive excision repair tracts (Lieber, 1998; Yu et al., 1999). Defective DSB repair can lead to toxicity and genotoxic effects, like chromosomal breaks and exchanges as well as cell death (Christmann et al., 2003). Two main pathways are involved in DSB repair: homologous recombination (HR) and non-homologous end-joining (NHEJ). NHEJ occurs mainly in the G0/G1 phase of the cell cycle, whereas HR occurs during the late S and G2 phases of the cell cycle (Johnson and Jasin, 2000; Takata et al., 1998; Christmann et al., 2003).

To study the role that DNA repair plays in MMC induced DNA damage, assays are required to sensitively study DNA integrity and stability. In addition to the direct measurement of DNA damage with test assays, such as the *in vitro* micronucleus method, it is important to consider other genetic perturbations, like those involved in aberrant signalling, because they allow detection of abnormal gene expression.

3.1.3 The MN assay

The MN assay *in vitro* and *in vivo* is frequently used to study DNA damage at the chromosome level. MN are an accepted cytogenetic endpoint in mutagenicity testing. They are derived from chromosome fragments arising from asymmetrical structural aberrations (acentric fragments) or represent whole chromosomes that are not incorporated into the nucleus at cell division (Fenech et al., 1999; Varga et al., 2004). With the development of

chromosome specific probes for centromeric, pericentromeric or telomeric regions of human, rat and mouse chromosomes the micronucleus assay became a useful tool to investigate the origin of MN (chromosome breakage and/or chromosome loss) as well as the distribution of sister chromatids between daughter cells (chromosome loss or chromosome non-disjunction) (Kirsch-Volders et al., 1997).

The MN test is described in detail in chapter 1 (section 1.4).

An important feature of the MN assay is how to set robust toxicity parameters to avoid the confounding effect of toxicity on chromosome breakage and/or whole chromosomes, which were unable to incorporate into the main nuclei during cell division.

3.1.4. Cytotoxicity measurements in the *in vitro* MN assay

Cytostasis and cell death together define the overall cytotoxicity of an agent in cell culture (Lorge et al., 2008). Cytostasis prevents cells from cellular growth and multiplication by inhibition of cell division and/or cell cycle delay. Depending on the end point (necrosis, apoptosis and cytostasis) estimates of cytotoxicity are known to differ (Fellows et al., 2008). However cytotoxicity measurements in total are mainly used for the selection of test concentration for genotoxicity assessment rather than to investigate the method by which cytotoxicity is induced (Fellows et al., 2008).

Appropriate measurements of cytotoxicity are necessary when selecting for test concentrations in *in vitro* genotoxicity assays, as underestimation of toxicity might lead to a selection of inappropriate toxic concentrations for analysis, which then have the potential to generate irrelevant positive results in the chosen assay (Fellows et al., 2008).

In the MN test different methods for measurement of cytotoxicity in the presence and absence of cytochalasin B are available. In the presence of cytochalasin B two main methods are recommended: the first one is based on the cytokinesis-block proliferation index (CBPI), whereas the second one is the measurement of the replication index (RI), which allows to measure directly the extent of cell replication in treated cultures relative to control (Lorge et al., 2008).

Several methods to measure cytotoxicity in the absence of cytochalasin B exist, but no clear recommendations have been made. Methods available are RCC, RPD and RICC.

Selection of the top concentration, when measuring for cytotoxicity, should be similar in the presence or absence of cytochalasin B (Lorge et al. 2008).

To correlate genotoxicity with changes in cell biology relevant to DNA integrity methods are needed to study cell biology endpoints, in particular changes in gene expression due to signal transduction.

3.1.5 Real-time PCR

Real-time PCR was first described in the mid-1990s and is a variation of the standard PCR technique. The technique combines the amplification of a DNA sequence with the detection of the amplified products during each reaction cycle (Bonetta, 2005).

The advantages of the Real-time PCR method over the standard PCR technique are its speed, sensitivity and specificity in a homogenous assay (Bustin et al., 2009).

Examples for applications of the method are gene expression and copy number analysis, calculations of viral titers and single-nucleotide analysis (Bonetta, 2005).

Target DNA or cDNA are used as template during repeated cycles of heat denaturation, primer annealing and primer extension (Bonetta, 2005). The amount of template DNA doubles with each cycle until one of the reagents becomes saturated and the reaction reaches a plateau (Bonetta, 2005). Probes and dyes are used as detection reagents. They produce a fluorescent signal each time a double-stranded product is made (Bonetta, 2005).

Fluorescent dyes, like SYBR Green bind to double stranded DNA and become fluorescent. More fluorescent dye binds to DNA as the amount of PCR product increases (Bonetta, 2005).

Probes, like TaqMan probes, consist of a single stranded oligonucleotide that is complimentary to a sequence within the target template. On its 5' end it has a fluorescent dye, whose signal is stifled by a quencher moiety at the 3' end (Bonetta, 2005). The probe hybridizes to one of the template DNA strands and is there as it extends the amplification primers digested by the exonuclease activity of the TaqDNA polymerase. Consequently the probe releases the fluorescent dye from the quencher (Bonetta, 2005).

Fewer amplification cycles are required the more copies of nucleic acid are present at the start of the reaction to make a sufficient product. Therefore the cycle in which a significant increase in fluorescence above the threshold is measured, called C_T-value, is used to calculate the quantity of DNA per sample (Bonetta, 2005). The calculation can be either done by absolute or relative quantification. Absolute quantification is using a standard curve of C_T-values, which is obtained by a serially diluted standard solution, whereas relative quantification compares the difference in the C_T-values of two samples (Bonetta, 2005).

3.1.6 Aim of study

The study was designed to assess the low dose response relationships of MMC in human lymphoblastoid cells using the *in vitro* MN assay and to compare the newly installed semi-automated MN detection system Metafer at Swansea University to the conventional manual scoring.

Further the mechanism of action of MMC was investigated by testing if DNA repair up-regulation influences genotoxic responses.

3.2 Material and Methods

3.2.1 Cell lines

The cell lines used in this study were TK6 and AHH-1. The human lymphoblastoid cell line TK6 is a derivative of the WIL-2 cell line. The cells are heterozygous at the thymidine kinase (TK) locus and contain the wild-type TP53 gene (Schwartz et al., 2004). AHH-1 is a human lymphoblastoid $TK^{+/-}$ cell line that constitutively expresses a high level of native CYP1A1 (Crofton-Sleigh et al., 1993). Furthermore AHH-1 cells carry a heterozygous mutation in the TP53 locus (Guest and Parry, 1999).

3.2.2 Cell culture

The cell lines were cultured in RPMI 1640 (GibCo®, Paisley, UK) supplemented with 10% donor horse serum (GibCo®, Paisley, UK) and 1% L-glutamine (GibCo®, Paisley, UK) at 37°C, 5%CO_2.

The cells were sub-cultured as described in chapter 2 (section 2.2.1).

3.2.3 Test chemical

MMC was acquired from Sigma-Aldrich, Dorset, UK. Before using, the chemical was freshly diluted from a stock solution (1mg/ml MMC dissolved in water) with water.

3.2.4 Test chemical dosing regime

For the *in vitro* MN assay TK6 cells were treated with MMC over a range of concentrations between 0 and 0.1µg/ml for 4h, 18h or 24h respectively, whereas AHH-1 cells were only treated with MMC for 4h (Table 3.1).

Table 3.1: Dilutions of stock MMC (1mg/ml) to result in the final concentrations (0-0.1µg/ml) of MMC to be applied to TK6 and AHH-1 cells

MMC Dose (µg/ml)	10ml flask- µg MMC needed	Volume diluted MMC (µl)	Volume water (final vol. 100µl)
0	0	0	100
0.002	0.02	20 (1:1000)	80
0.004	0.04	40 (1:1000)	60
0.006	0.06	60 (1:1000)	40
0.008	0.08	80 (1:1000)	20
0.01	0.1	100 (1:1000)	0
0.02	0.2	20 (1:100)	80
0.04	0.4	40 (1:100)	60
0.06	0.6	60 (1:100)	40
0.08	0.8	80 (1:100)	20
0.1	1	100 (1:100)	0

For the PCR-Array study TK6 cells were treated with MMC for 2h (0, 0.004 and 0.08µg/ml), 4h (0, 0.004 and 0.08µg/ml) and 24h (0 and 0.02µg/ml), whereas for the Real-time PCR study the cells were treated with MMC for 4h over a range of concentrations above and below the identified level of MN induction. Furthermore 4h treatments of MMC (Table 3.1) were also used for the pan-centromeric staining study.

3.2.5 The *in vitro* MN assay

The manual and the semi-automated scoring protocol, using the Metafer-System for the *in vitro* MN assay, were performed as described in chapter 2 (section 2.2.2). For the CBMN assay 1000 (manual) to 2000 (Metafer-System) cells per replicate were scored, whereas for the mononucleated assay 2000 (manual) to 4000 (Metafer-System) cells per replicate were scored (exceptions where stated; for details see Appendix I). At least two independent replicates were carried out for each experiment.

All cell suspensions (10ml) were seeded at $1x10^5$cells/ml for 24h at 37°C, 5%CO_2. For the CBMN assay each cell suspension was treated with appropriately diluted MMC for different time points and 4.5 to 6 µg/ml cytochalasin B for one cell cycle. For the MONOMn assay

TK6 cell suspensions were treated with MMC (0-0.1 μg/ml) for 24h followed by a 24h recovery period previous to harvest.

3.2.6 Cytotoxicity

RPD was used to measure cell death and cytostasis as described in chapter 2 (section 2.2.3).

3.2.7 Pan-centromeric painting

Centromeres were stained to classify if MMC was a clastogenic or aneugenic chemical with the RTU Human pan centromeric probe. The method is described in detail in chapter 2 (section 2.2.4). Nuclei were counterstained with DAPI and 100 MN per dose were scored as positive or negative for the centromeric probe under a BX50 fluorescent (Carl Zeiss) microscope (exceptions where stated, for details see Appendix IV).

3.2.8 RNA extraction

Total RNA was extracted from the human lymphoblastoid cell line TK6 after MMC treatment. Details of the method are described in chapter 2 (section 2.2.5).

3.2.9 RT^2 Profiler^{TM} PCR Array System

The method for the PCR array system is described in detail in chapter 2 (section 2.2.6).

3.2.10 Reverse Transcription with elimination of genomic DNA for Quantitative, Real-Time PCR

The reverse transcription reactions are described in detail in chapter 2 (section 2.2.7).

3.2.11 PrimerDesign geNorm Reference Gene Assay

The geNorm Reference Gene Selection Kit from PrimerDesign Ltd., Rownhams, UK was used to select the reference gene for the Real-time PCR experiments. Details of the assay are described in chapter 2 (section 2.2.8)

3.2.12 Real-Time PCR

Real-time PCR was performed to quantify the gene expression of *MSH6*, *BRCA1*, *Rad51C*, *XRCC3* and *XRCC6BP1*. For the Real-time PCR experiments the QuantiFast™ SYBR® Green PCR Kit (Qiagen, Sussex, UK) was used (the method is described in detail in chapter 2 (section 2.2.9).

Each sample in the Real-time PCR was run with primers for the β-actin housekeeping gene respectively with primers for MSH6, BRCA1, XRCC3, Rad51C and XRCC6BP1.

3.2.13 Statistical analysis

The analysis method of the data sets is described in detail in chapter 2 (section 2.2.17). Further assessment of data used BMD modelling (Gollapudi et al., 2013).

3.3 Results

3.3.1 Dose and time dependent genotoxic effects of MMC in TK6 cells

To explore the dose relationships of genotoxins at low doses, human lymphoblastoid cells were treated with the known genotoxic agent MMC and the *in vitro* MN assay was performed to investigate chromosomal damage. The *in vitro* MN assay can be performed with or without the actin polymerisation inhibitor cytochalasin B. The scoring for MN is usually done visually with a light or fluorescent microscope. However there are also new automated systems for scoring MN. One of the advanced automated systems, called the Metafer-System, uses fluorescent dyes specific for DNA and is used in our laboratory. A semi-automated scoring protocol for the Metafer-System was used for the assessment of MN preparations and compared to the visual Giemsa stained protocol.

As stated in the OECD guideline 487 (OECD, 2007) the test concentrations selected for the MN assay should cover a range of producing 50±5% toxicity to little or no toxicity. Higher levels may induce chromosome damage as a secondary effect of cell death. Several different methods to measure cytotoxicity in the presence and absence of cytochalasin B are available. In our studies, RPD was used to measure cell death and cytostasis (for further details see chapter 2 section 2.2.3).

For the comparison of the Metafer-System with manual scoring and for investigation of the low dose responses of MMC, TK6 cells were treated with MMC (0-0.1µg/ml) for different time points. Extended treatments as well as short-term treatments were performed. For the extended 24h treatments of MMC, the mononucleated as well as binucleated assay were carried out, whereas for the extended continuous treatment of MMC and cytochalasin B as well as the short-term treatment only the CBMN assay was conducted (Figures 3.3 to 3.6).

For the MONOMn assay concentration-related increases in MN with both the manual and semi-automated method were shown from 0 to 0.04µg/ml MMC in TK6 cells. No clear NOEL was observed. The increase in percentage of micronucleated cells at higher concentrations (0.04µg/ml and above) of MMC was likely due to excessive cell death and cytostasis (Figure 3.3). Cytotoxicity measurements at 0.02 and 0.04µg/ml resulted in reduction in RPD as high as 31.2% and 62.5%.

Significant increases in MN frequency at 0.006µg/ml and 0.01 to 0.04µg/ml for the Metafer-System and at 0.008µg/ml and above for manually scoring were demonstrated (Figure 3.3). Higher concentrations were not analyzed through excessive toxicity.

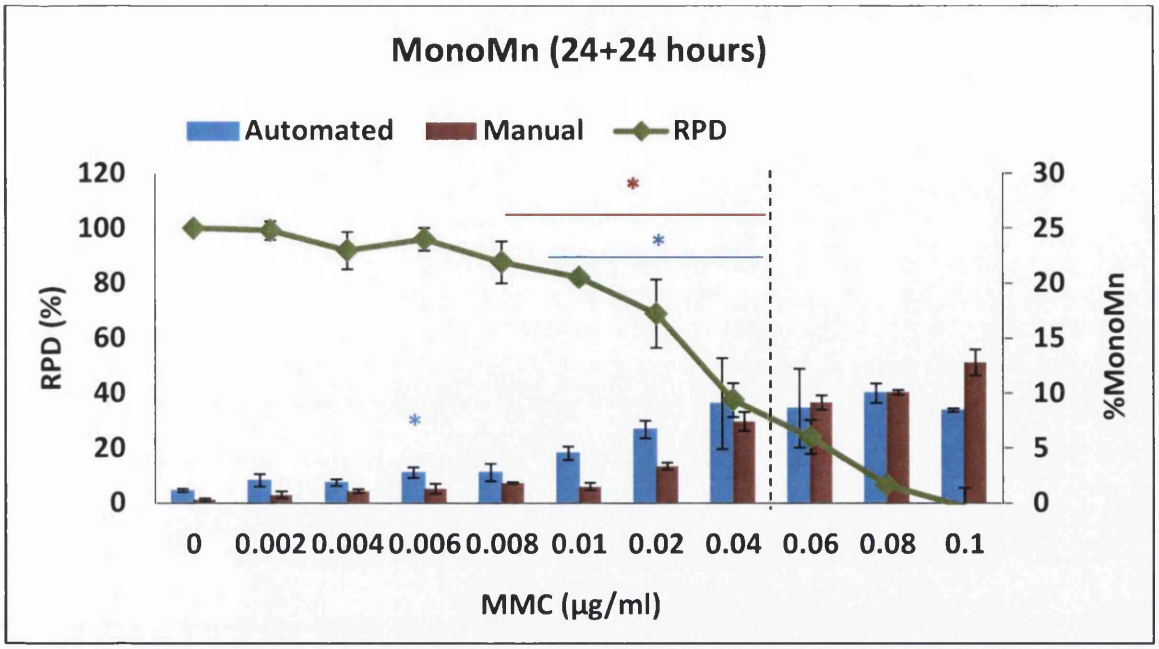

Figure 3.3: Effect of MMC on TK6 cells using the *in vitro* MN assay. TK6 cells were treated with MMC for 24h, followed by a 24h recovery period. Blue: Automated scoring, red: Manual scoring, green: Relative population doubling (RPD). Values represent mean and range of duplicate experiments. (*) Represents $p<0.05$.

For the CBMN assay TK6 cells were treated with MMC for 24h followed by one cell cycle of cytochalasin B (18h). As for the mononucleated assay an incremental increase in MN induction could be seen with each increase in concentration until 0.04µg/ml. A significant increase in MN frequency at 0.008µg/ml for the Metafer-System and at 0.02µg/ml for manual scoring was shown. The sharp increase in % micronucleated cells at higher doses (0.04µg/ml and above) of MMC was again likely due to excessive cell death and cytostasis (Figure 3.4). Cytotoxicity measurements at 0.02 and 0.04µg/ml resulted in reduction in RPD as high as 30.6% and 60.5%.

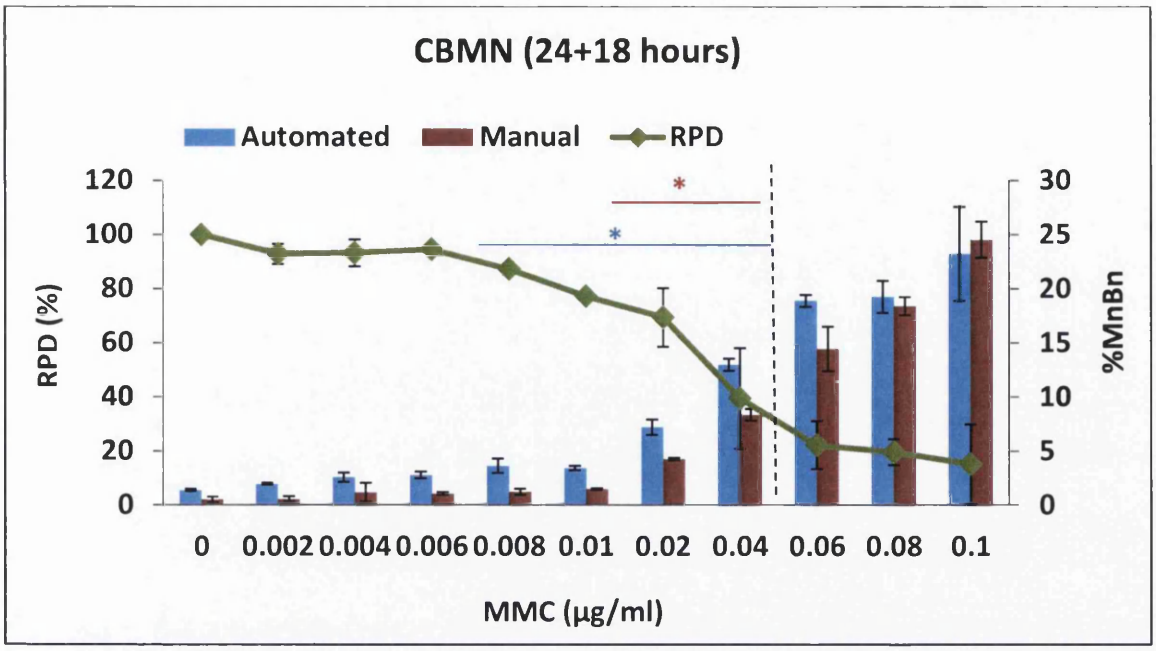

Figure 3.4: Effect of MMC on TK6 cells using the CBMN assay. TK6 cells were treated with MMC for 24h, followed by 18h of cytochalasin B. Blue: Automated scoring, red: Manual scoring, green: Relative population doubling (RPD). Values represent mean and range of duplicate experiments. (*) Represents $p<0.05$.

When comparing the MN frequencies for the mononucleated versus the CBMN assay for the extended treatment it was shown that the % of MN induction at the higher concentrations in the mononucleated assay was about half the % of MN induction in the CBMN assay (Figure 3.3 and 3.4).

TK6 cells, which were continuously treated with both MMC and cytochalasin B for 18h (one cell cycle; Figure 3.5), showed no significant increases in MN frequency at any concentration using both methods. In addition, treatments at higher concentrations with MMC (0.06µg/ml and above) showed exaggerated cell death and cytostasis (68.1% to 90.5%) (Figure 3.5).

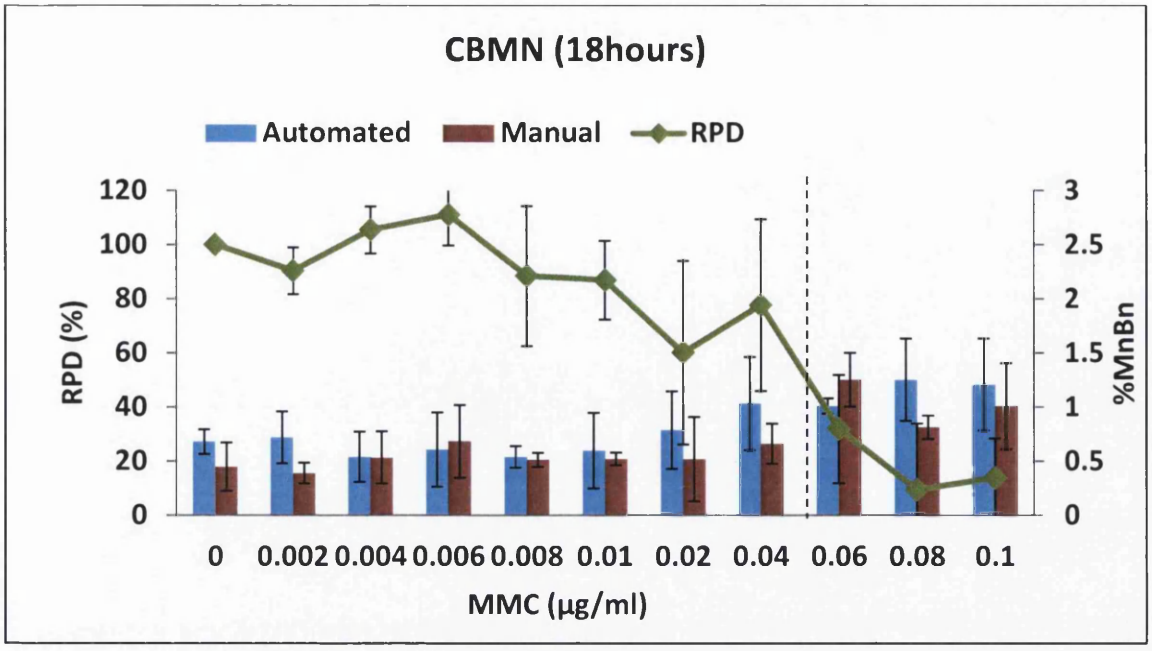

Figure 3.5: Effect of MMC on TK6 cells using the CBMN assay. TK6 cells were treated with MMC and cytochalasin B for 18h. Blue: Automated scoring, red: Manual scoring, green: Relative population doubling (RPD). Values represent mean ± SD (n=3).

An increase in MN induction over the background frequency level was only observed at the higher range of concentrations (0.02/0.04µg/ml to 0.1µg/ml) in TK6 cells treated with 4h MMC followed by one cell cycle (18h) of cytochalasin B (Figure 3.6). Furthermore the cells showed 50±5% (45.8%) cell death and cytostasis at the highest test concentration (0.1µg/ml) compared to the excessive cytotoxicity at 0.04µg/ml and above for the longer treatments (Figure 3.3 and 3.5).

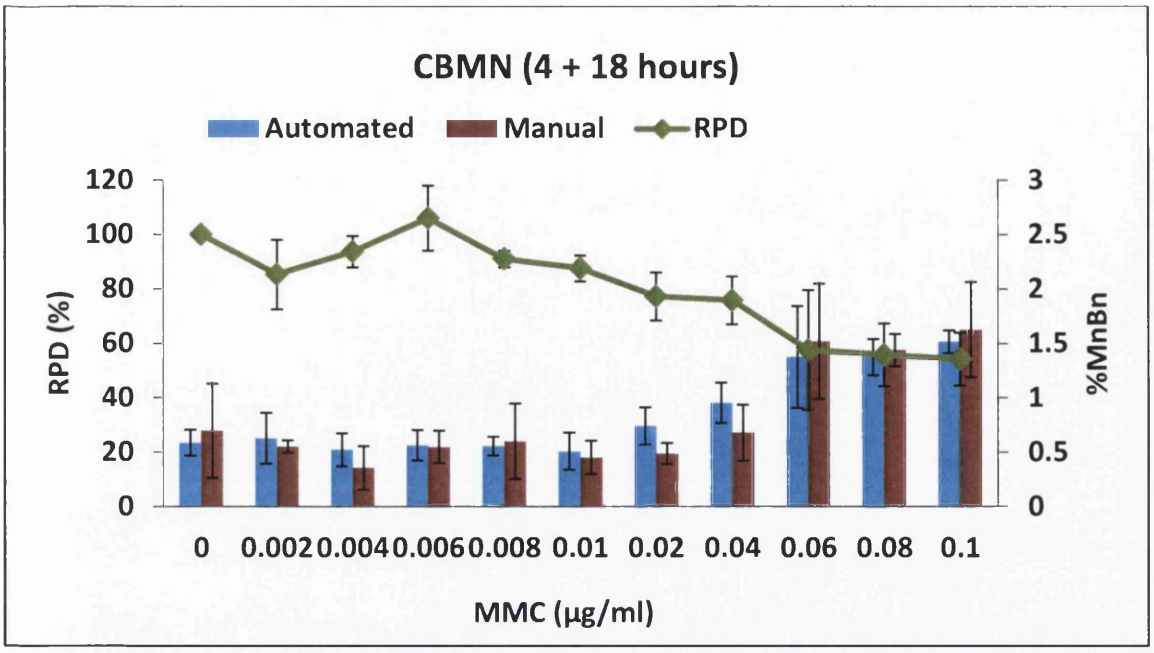

Figure 3.6: Effect of MMC on TK6 cells using the CBMN assay. TK6 cells were treated with 4h MMC followed by 18h of cytochalasin B. Blue: Automated scoring, red: Manual scoring, green: Relative population doubling (RPD). Values represent mean ± SD (n≥3).

TK6 cells treated with MMC for all different time points showed very similar dose responses and MN frequencies when comparing the manual scoring with the semi-automated system Metafer. Pearson's r correlation analysis was performed to investigate the correlation of both methods and reported highly positive correlation between the manual scoring and the semi-automated system (Table 3.2). The Metafer-System proved to be an adequate system to produce biologically relevant results. Therefore all further work was based on semi-automated analysis.

Table 3.2: Comparison of the Metafer-System versus manual scoring in TK6 cells treated with MMC using Pearson's r correlation analysis

MMC treatment	Correlation coefficient r	p-value
24h+18h (CBMN assay)	0.98	1.32E-07
24h+24h (MonoMN assay)	0.90	1.37E-04
18h (CBMN assay)	0.75	0.008972
4h+18h (CBMN assay)	0.96	2.76E-06

Furthermore depending on the dose regime, TK6 cells treated with MMC showed linear and non-linear dose responses at the low concentration range. Therefore the dosing regime is crucial in describing the dose response.

3.3.2 Effect of short-term treatment of MMC in AHH-1 cells

To compare the short-term dose response seen in TK6 cells, as well as to further investigate the low dose response relationships of MMC, the human lymphoblastoid cell line AHH-1 was treated with MMC for 4h followed by one cell cycle (22h) of cytochalasin B and the CBMN assay was performed (Figure 3.7).

An increase in MN frequency was observed only at 0.1µg/ml, when compared to the control sample. No increases in MN were found at the lower range of concentrations. Similarly to TK6 cells, AHH-1 cells treated with 4h of MMC showed up to 40% cell death and cytostasis only at the highest test concentration.

Like TK6 cells, AHH-1 cells treated with short-term MMC showed a similar dose-response at the low concentration range.

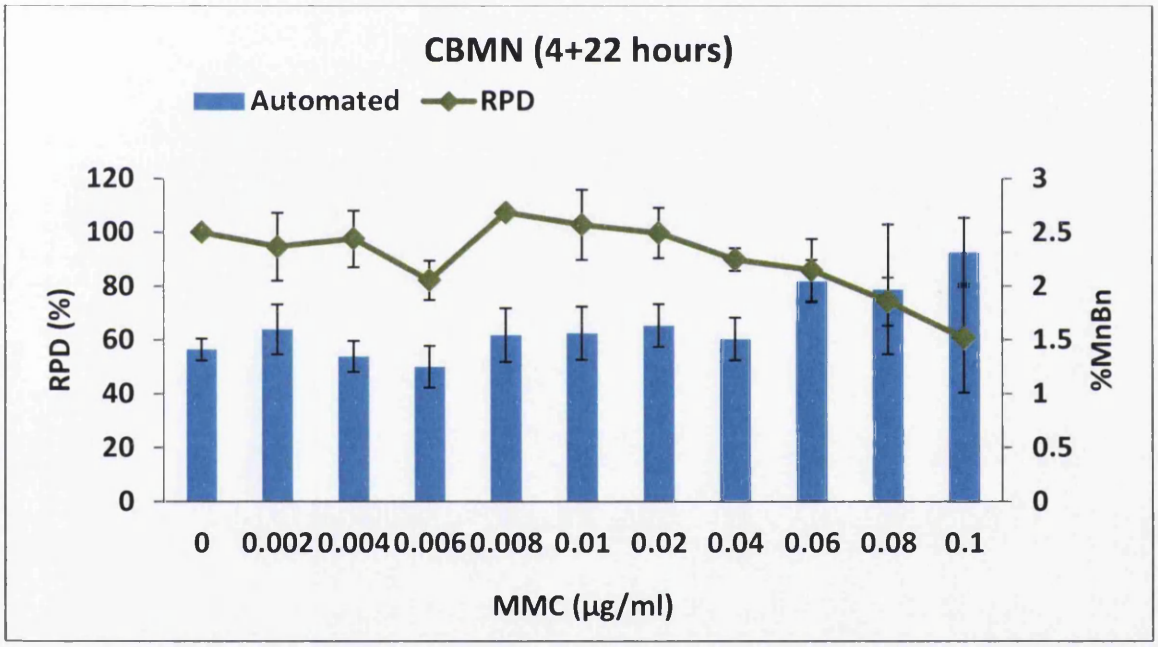

Figure 3.7: Effect of MMC in AHH-1 cells using the CBMN assay. AHH-1 cells were treated with MMC for 4h followed by cytochalasin B for 22h. Blue: percentage micronucleated binucleated cells, green: Relative population doubling (RPD). Values represent mean ± SD (n=3).

3.3.3 Assessment of the short-term dose response relationship of MMC in TK6 and AHH-1 cells

TK6 cells treated with MMC for 4h followed by 18h of cytochalasin B showed increases in MN frequencies only at the higher concentrations, whereas at the lower concentration range no increases in MN could be found (Figure 3.6). A similar dose response was observed for AHH-1 cells treated with MMC for 4h followed by one cell cycle of cytochalasin B (Figure 3.7). Therefore the dose response curves were further assessed by quantitative means using BMD modelling.

The BMD approach estimates a dose that produces a pre-determined increase in the response over the control values and the $BMDL_{10}$ refers to the lower 90% confidence interval of a dose that produces a 10% increase over the fitted background level (Gollapudi et al., 2013).

For the manual TK6 data the BMD was calculated at 0.007µg/ml with its confidence intervals between 0.006µg/ml ($BMDL_{10}$) and 0.01µg/ml, whereas for the automated data the BMD was calculated at 0.008µg/ml with its confidence intervals between 0.007µg/ml ($BMDL_{10}$) and 0.01µg/ml.

The AHH-1 data set revealed a BMD at 0.02µg/ml with its confidence intervals between 0.016µg/ml ($BMDL_{10}$) and 0.03µg/ml.

The results are summarized Table 3.3 and Figures 3.8 and 3.9.

Table 3.3: The BMD analysis for the MN endpoint induced by MMC

Cell line	MMC	Units	BMD	$BMDL_{10}$	$BMDU_{10}$
TK6	Manual data	µg/ml	0.007	0.006	0.01
TK6	Metafer data	µg/ml	0.008	0.007	0.01
AHH-1	Metafer data	µg/ml	0.02	0.016	0.03

A

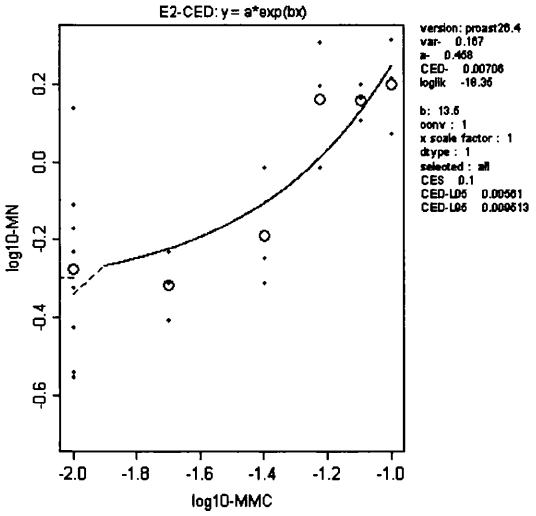

B

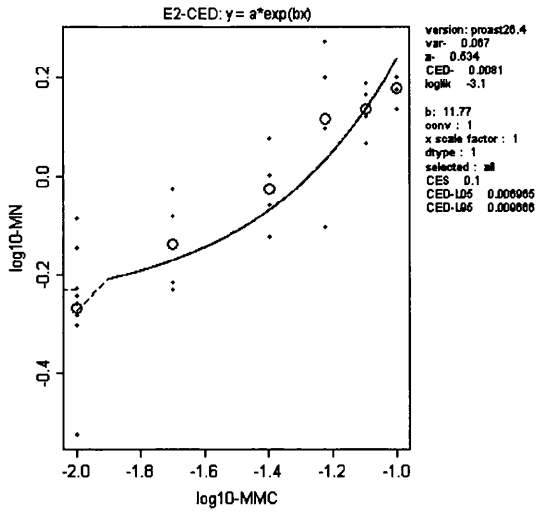

Figure 3.8: BMD dose response modelling results for MN induction in TK6 cells treated with MMC (4h+18h), using the manually and automated generated data set. (A) For the manual data the BMD was calculated at 0.007µg/ml with its confidence intervals between 0.006 and 0.01µg/ml, whereas for (B) the automated data the BMD was calculated at 0.008µg/ml with its confidence intervals between 0.007 ($BMDL_{10}$) and 0.01µg/ml.

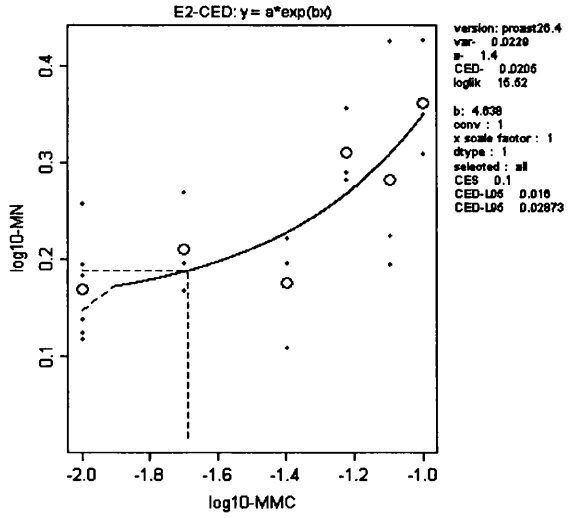

Figure 3.9: BMD dose response modelling results for MN induction in AHH-1 cells treated with MMC (4h+22h), using the automated analysis data set. The BMD was calculated at 0.02µg/ml with its confidence intervals between 0.016 and 0.03µg/ml.

3.3.4 MMC - a clastogenic chemical

Human chromosome pan-centromeric staining was subsequently performed to determine if the MN induced by MMC originate from chromosome fragments lacking a centromere (clastogenicity) or whole chromosomes which were unable to incorporate into the main nucleus during cell division (aneuploidy).

Human chromosome pan-centromeric staining of TK6 cells (Figure 3.10 and 3.11) treated with 4h MMC followed by 18 h of cytochalasin B showed that MMC was a clastogenic chemical. The MN induced by MMC originate predominantly from chromosome fragments lacking a centromere and not aneuploidy, which was particularly demonstrated over the concentration range that presented increased MN frequencies (Figure 3.10).

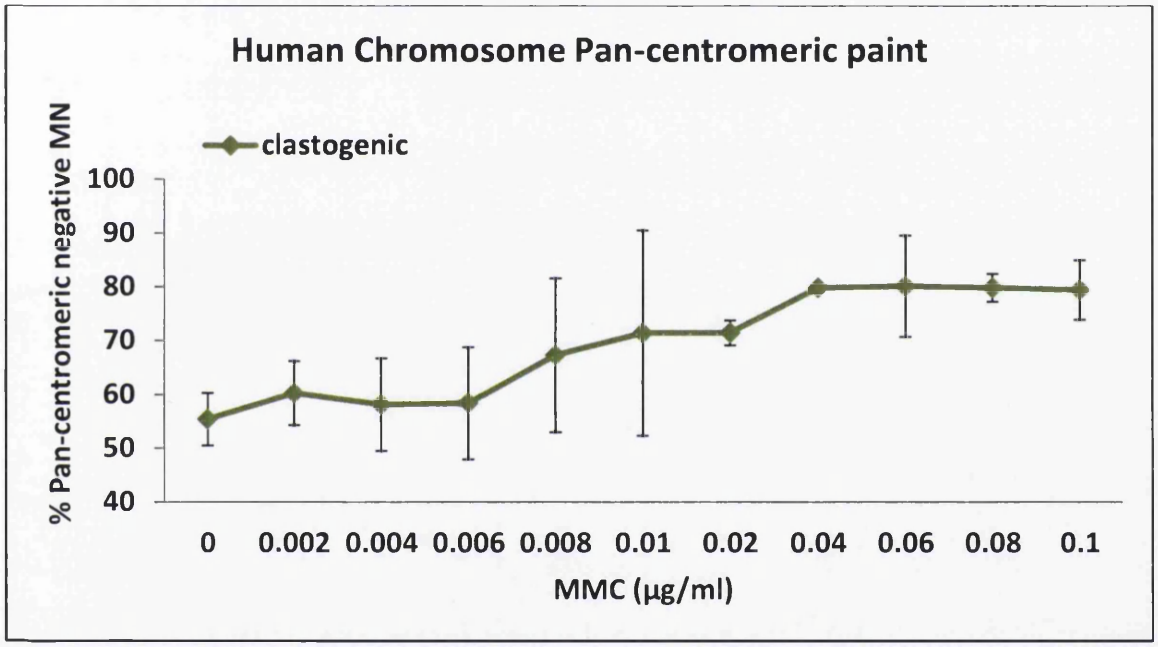

Figure 3.10: Human chromosome pan-centromeric staining of TK6 cells treated with 4h MMC followed by 18h of cytochalasin B. Values represent mean and range of duplicate experiments.

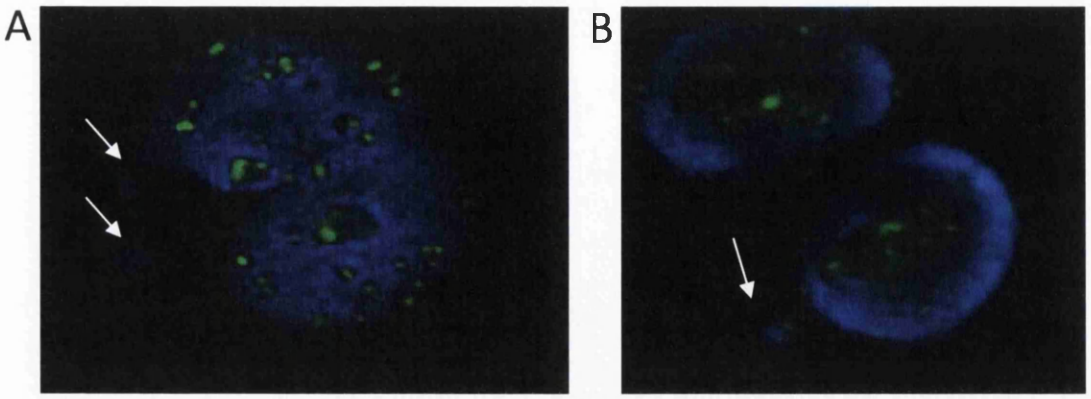

Figure 3.11: Examples of human chromosome pan-centromeric staining. (A) clastogenic MN with no signal (white arrows); (B) aneugenic MN with signal (white arrow).

3.3.5 DNA repair- a mechanistic study of MMC

DNA repair is believed to be mainly responsible for NOELs at low levels of DNA damage (Jenkins et al., 2010). Due to various DNA repair mechanisms, low levels of DNA damage at low concentrations can be tolerated by the cell. However at higher concentrations these mechanisms become saturated (Jenkins et al., 2010).

To investigate if DNA repair pathways play a role in the short-term treatment of MMC in TK6 cells, PCR arrays as well as Real-time PCR were performed to look at relative changes in gene expression of a panel of DNA repair genes.

It was hypothesized that important repair pathways may have been up-regulated in response to DNA damage and hence this up-regulation was sought.

The DNA Repair RT^2 Profiler^{TM} PCR Array (SABiosciences, Qiagen, Sussex, UK) profiled the expression of 84 genes, which are involved in various DNA repair pathways, like BER, NER, MMR or DSB repair.

Different treatment times for MMC (2h, 4h and 24h) and concentrations below and above the increases for MN induction were chosen. However, the 2h and 24h treatments showed no changes in gene expression when comparing the control with the MMC treated samples (data not shown; for details see Appendix V). Low gene expression changes in a couple of genes could be observed when TK6 cells were treated with MMC for 4h (Figure 3.12).

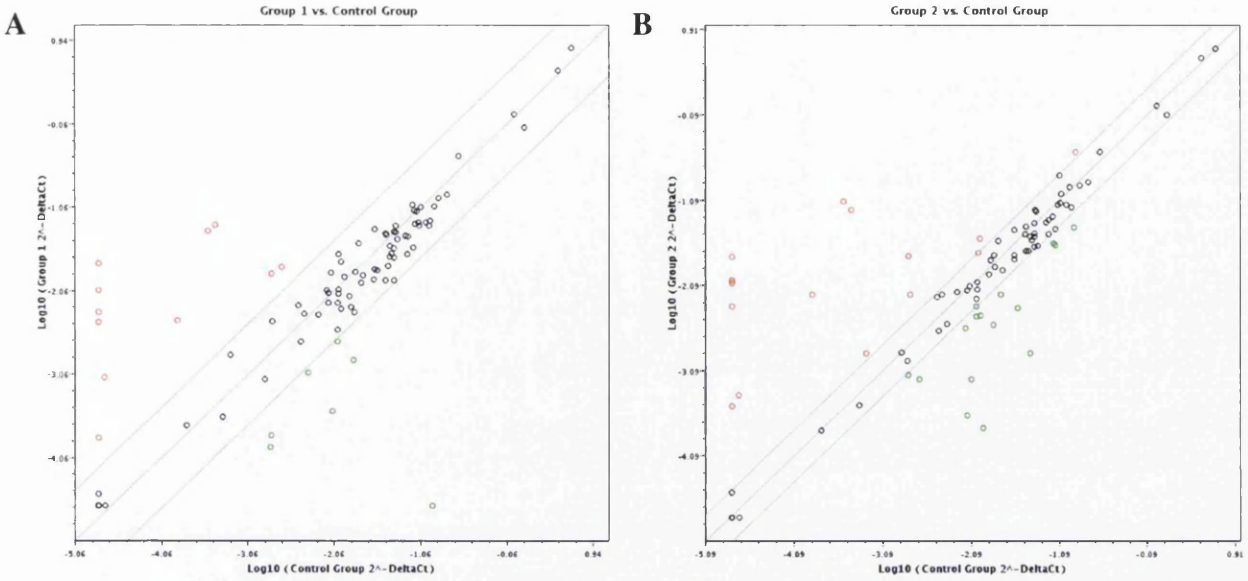

Figure 3.12: DNA Repair RT^2 Profiler^{TM} PCR Array Scatter Plot. Normalized expression of every gene of the array was compared between the control group and treated group 1 A: 0.004µg/ml or group 2 B: 0.08µg/ml. Black dots: Genes with no changes in gene expression; red dots: Genes with up-regulation of gene expression; green dots: Genes with down-regulation in gene expression.

Based on changes at the average delta C_T values (Figure 3.13) the following genes were chosen for further analysis by Real-time PCR: *MSH6*, *BRCA1*, *Rad51C*, *XRCC3* and *XRCC6BP1*.

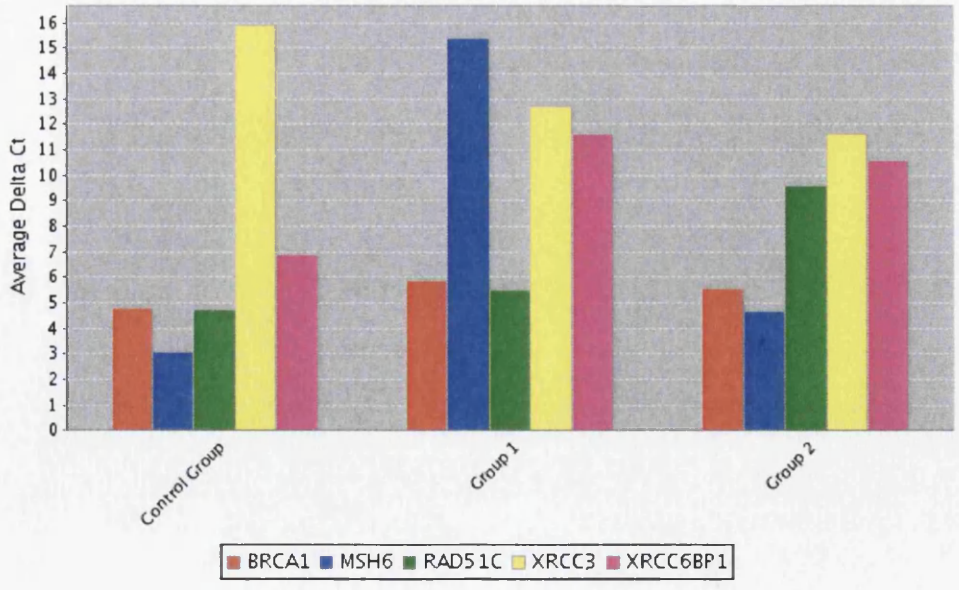

Figure 3.13: DNA Repair RT^2 Profiler^{TM} PCR Array Multigroup Plot. Expression changes of a selected set of genes across the control group and the treated groups 1 (0.004µg/ml) and 2 (0.08µg/ml).

When looking at the average C_T values, *MSH6* was increased in TK6 treated with 0.004µg/ml MMC, but seemed back to control levels when treated with 0.08µg/ml. *Rad51C* showed an increase in the average C_T values over the control levels only in TK6 treated with 0.08µg/ml, whereas *XRCC6BP1* showed increases in the average C_T value in both treated MMC groups of 0.004 and 0.08µg/ml. On the other hand *XRCC3* showed a decrease in the average C_T values in the treated groups with MMC, when compared to the control group. Further *BRCA1* showed no changes in the average C_T values, when comparing the control group with the treated MMC groups of 0.004 and 0.08µg/ml (Figure 3.13).

Short-term treatments with selected concentrations above and below the increased levels of MN induction were chosen for the Real-time PCR study. However, as can be seen in Figure 3.14, no significant changes in gene expression of the selected genes could be observed. This may be because of some variation in the replicates, as can be seen with the wide error bars.

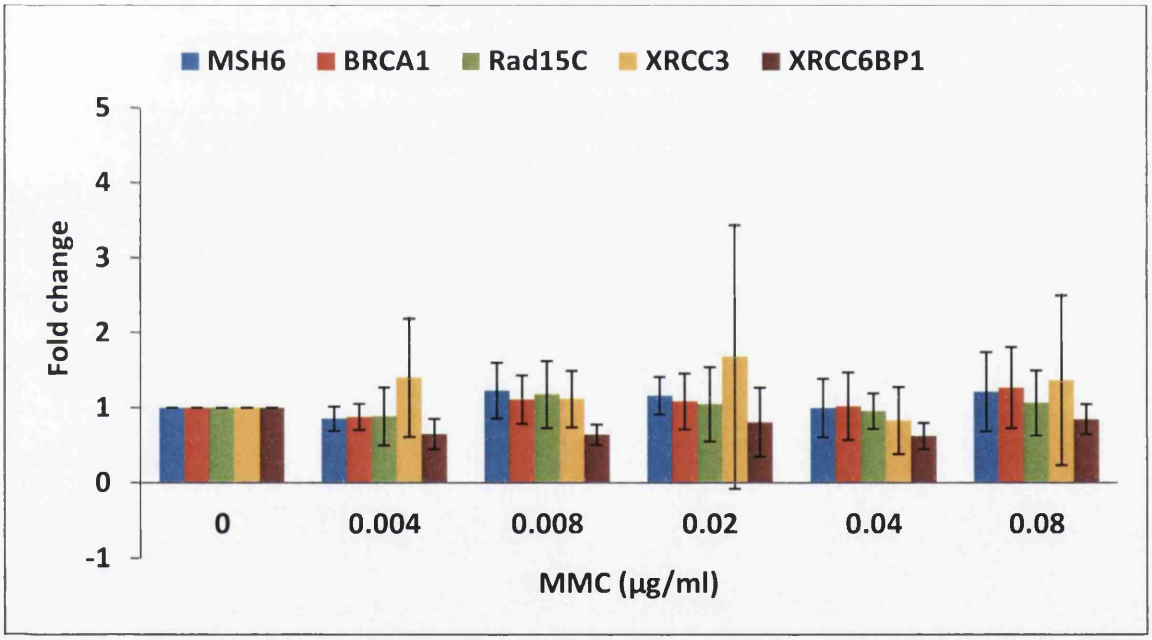

Figure 3.14: Relative fold changes in *MSH6*, *BRCA1*, *Rad51C*, *XRCC3* and *XRCC6BP1* gene expression, following exposure (4h) to increasing concentrations of MMC. Error bars represent SD (n=3)

3.4 Discussion

Genetic toxicology testing is a basic component of the pre-clinical safety assessment of drug candidates, industrial chemicals and cosmetics. Therefore genotoxicology helps to identify compounds that are a potential risk for carcinogenicity and heritable mutations. It is important to improve health risk assessments by investigating if DNA reactive compounds follow linear or non-linear (thresholded) dose response relationships after exposure to low doses. This will allow more scientific assessment of actual risks and help to understand how the cells can tolerate some exposures.

In this study human lymphoblastoid cells (TK6 and AHH-1) were treated with the known genotoxin MMC. Chromosomal damage was quantified with the *in vitro* MN assay and further investigations into the mode of action of MMC were undertaken.

3.4.1 The Metafer-System versus manual scoring

The *in vitro* MN test is widely used for the assessment of genotoxic potential of drug substances. MN are an important endpoint in the quantification of chromosome damage. They are derived from chromosome fragments arising from asymmetrical structural aberrations (acentric fragments) or represent whole chromosomes that are not incorporated into the nucleus at cell division (Fenech et al., 1999; Varga et al., 2004).

Visual scoring of MN can be time consuming and the results depend on subjective interpretation. Therefore a high demand for automation of the MN test has been existed.

In our studies, the automated slide scoring platform Metafer, developed by MetaSystems in 2004 was used. This advanced automated system uses fluorescent dyes specific for DNA.

For comparison purposes of the system with manual scoring, the dose response curves and MN frequencies obtained with the Metafer-System after treatment of TK6 cells with MMC were compared to the conventional manual scoring of Giemsa stained slides. This was for both the mono- and binucleate version of the MN assay.

TK6 cells treated with different concentrations of MMC (0-0.1µg/ml), for different time points, showed very similar dose responses and MN frequencies, when comparing the manual scoring with the Metafer-System. Further, Pearson's r correlation analysis revealed high correlation between both methods with highly significant p-values (see Table 2 for further details).

When looking at the Figures 3.3 to 3.6 it is notable that the mean response for the MN frequencies obtained with the Metafer-System was generally higher than for the manual scoring. However that is possibly due to subjective manual scoring and allowance of the

system to score higher total numbers of cells as well as the classifier settings. Classifiers determine the parameters for the identification of the mononucleated and binucleated cells and the MN.

This study clearly demonstrated that the results gained with the Metafer-System are comparable with the results gained through visually scoring. Therefore it can be concluded that the Metafer-System used in our laboratory is an adequate system to produce biologically relevant results.

Furthermore, it is likely that the automated system can reduce the scoring subjectivity of MN identification. In addition, the Metafer-System allows scoring of a higher number of cells in a short time, when compared to manual scoring, which potentially advances the statistical power of the assay.

3.4.2 Dose relationships of MMC

Dependent on the treatment regime, different genotoxic responses for MMC could be observed. TK6 cells treated with MMC for 24h in the mononucleated as well as in the binucleated assay showed incremental increases in MN induction at all concentrations tested. Previous studies in different cell lines treated with MMC showed linear dose responses at relatively low concentrations of MMC (Elhajouji, 2010; Fowler et al., 2010; Schuler et al., 2010, Sobol et al., 2012). The results are not unexpected since MMC is a cross-linking agent as well as an alkylating agent and therefore known to induce chromosomal aberrations (Abbas et al., 2002; Greenwood et al., 2004; Schuler et al., 2010). Alkylating agents induce DNA strand breaks as a result of the processing of lesions by various repair pathways, such as excision, homologous or non-homologous recombination and mismatch repair (Morales-Ramirez et al., 2004).

As expected, the frequency of micronucleated cells is higher in the CBMN assay than in the mononucleated assay. Cell division is required after damage induction for the development of MN. The CBMN assay detects chromosome breakage as well as chromosome loss in once divided binucleated cells, because cytochalasin B inhibits the actin furrow during anaphase (Kirsch-Volders and Fenech, 2001), whereas the mononucleated assay detects MN in mononucleated cells which may have gone through division.

TK6 cells continuously treated with MMC and cytochalasin B for 18h showed no increases in MN frequency at the chosen dose regime. It might be possible that cytochalasin B interacts with MMC in the continuous treatment resulting in no genotoxic effects. That cytochalasin B can reduce MN induction in combined treatments was shown for spindle poisons, like

colchicine (Minissi et al., 1999). It was suggested that cytochalasin B treatment interferes with chromosome missegregation in human lymphocytes (Minissi et al., 1999). Further it was assumed that in cytokinesis-blocked cells the absence of the actin ring interferes with anaphase-B, which consequently leads to a shorter distance between the poles (Minissi et al., 1999).

Another important factor is the cell cycle time. The average doubling time of TK6 cells used in our lab was approximately 16 to 18 hours. It seems to be very likely that the treatment time and cell cycle length of TK6 cells are crucial to produce genotoxic effects. It is therefore possible that the treatment time of 18h with no recovery time might not have been long enough to produce genotoxic effects. Another important factor here might be the time required for a lesion to be fixed as a mutation. As mentioned before MMC is an alkylating agent and a DNA cross-linker, which causes severe chromosomal damage and requires multiple DNA repair pathways including NER, DSB repair (homologous recombination) and/or translesion bypass repair (Drabløs et al., 2004; Lee et al., 2006). It was shown that genotoxicity and cytoxicity of the O^6-methylguanine lesion caused by MMS, an alkylating agent, is mainly due to the recognition of mispairs by the MMR system and the induction of futile repair cycles, resulting in the final stage in double strand breaks (Margison and Santibanez-Koref, 2002; Drabløs et al., 2004). More than one cell cycle might be therefore needed for MMC to cause MN induction due to multiple rounds of error-prone lesion repair. Further Morales-Ramirez et al. (2004) showed that MMC induces MN *in vivo* mainly in the first division, but maybe not exclusively.

TK6 cells treated with MMC for 4h followed by 18h with cytochalasin B showed increases in MN frequency only at the higher concentrations. Furthermore AHH-1 cells treated with MMC for 4h and one cell cycle of cytochalasin B showed a similar dose response to TK6 cells, with only the top concentration of 0.1µg/ml showing increases in MN induction.

As mentioned earlier it is assumed that the relationship between exposure to genotoxic chemicals, DNA damage formation and the induction of mutagenic change is linear (Henderson et al., 2000). However mutations are not produced directly by DNA adducts as DNA repair activity limits the proportion of adducts processed into mutational change. It is therefore possible that NOEL may exist for some genotoxins (Jenkins et al., 2005). Furthermore natural defence mechanisms can reduce the entry and interaction of the genotoxin with the DNA.

Concentrations selected should have covered a range of 50±5% toxicity at the top dose to no toxicity in the control cultures. However extended treatments of MMC (18h and 24h) in TK6

cells reached ≥50% toxicity at around 0.04μg/ml. Increases in MN induction at higher doses of 0.04μg/ml were likely due to excess cell death as necrotic and apoptotic cells often contain chromosome fragments. MMC gave increases in MN frequency at or below the target range of 50±5% toxicity with the short-term treatments.

In addition pan-centromeric staining revealed that with increases in concentration, the proportion of centromere negative MN increased, confirming that MMC predominantly induces MN via chromosome breakage and not aneuploidy.

3.4.3 Dose response relationship assessment of MMC

The data for TK6 cells treated with 4h of MMC followed by 18h of cytochalasin B were further assessed for quantitative dose responses.

The short-term treatment data sets generated in TK6 and AHH-1 cells were analysed by the BMD approach, which estimates a dose that produces predetermined, biologically relevant, increases in the response over control (Gollapudi et al., 2013). The $BMDL_{10}$ refers to the estimate of lower 90% confidence interval of a dose that produces a 10% increase over the fitted background level for continuous endpoints and is considered an adequate point of departure (POD) for the extrapolation of dose response data (Gollapudi et al., 2013).

Table 3.3 summarizes the BMD values generated for each dataset tested and the ratio of $BMDU_{10}$ to $BMDL_{10}$ values provides information on the uncertainty around the BMD estimate. The data lined up well with the dose responses.

BMD modelling is widely used in risk assessment for other fields of toxicology to define POD values for cancer and non-cancer endpoints (Gollapudi et al., 2013). Determination of BMD values in genotoxic studies allows readily comparison to BMD values calculated for other toxicological endpoints and BMD modelling might therefore become the preferred approach when analysing genotoxic data (Gollapudi et al., 2013).

3.4.4 Mechanistic studies of MMC

Mechanistic experiments aimed to clarify if a possible NOEL over the background for MMC exists or not and also to understand how the cells tolerate low doses. MMC is a DNA interstrand cross-linking agent. As mentioned before, interstrand DNA cross-links are repaired by multiple repair pathways, including NER, BER and homologous recombination (Dronkert and Kanaar, 2001). Thus, the NOEL over the background could be due to DNA repair, which seems to be efficient at low doses of chemical compounds.

DNA repair PCR arrays were used for the expression analysis of a panel of genes involved in DNA repair. However only in TK6 cells treated with 4h of MMC slight changes in gene expression in a small number of genes could be observed. *MSH6, BRCA1, Rad51C, XRCC3* and *XRCC6BP1* were then chosen for further analysis by Real-time PCR. These genes are involved in different repair pathways. However no significance changes in gene expression of any genes investigated could be observed.

Limited access of the PCR arrays reduced the number of experiments to 1 replicate. It is most likely that more replicates are needed to get reliable results from the PCR arrays. Furthermore the base level expression of genes involved in DNA repair might be adequate to repair the damage caused by MMC to reduce DNA damage to background levels. Repair proteins can be modified by post-translational changes and these would not be picked up by gene expression approaches.

Furthermore if DNA repair does not play the crucial role in the NOEL of MMC other mechanisms, like cell cycle delay and apoptosis induction might. Further follow up experiments of the mode of action of MMC are needed to investigate the dose response.

3.5 Summary

In this chapter the dose response relationships after MMC treatment were explored at the low concentration range. Depending on the treatment regime different genotoxic effects were observed.

Furthermore the automated slide scoring platform Metafer, developed by MetaSystems was validated by comparing the MN frequencies obtained with the Metafer-System with the MN frequencies obtained with conventional manual scoring of Giemsa stained slides. The Metafer-System proved to be an adequate system for scoring MN.

Mechanistic studies of the short-term MMC treatment were undertaken to get a better understanding of the dose response relationship observed. DNA repair (at least up-regulation of expression) does not seem to play the crucial role in the NOEL of MMC. Further follow up experiments are needed to investigate the dose response.

Finally it was shown that MMC is a clastogenic chemical, which induces MN mainly due to chromosomal breakage and not through aneuploidy.

Chapter 4

Detection of chromosomal damage and mutation induction after exposure to 4-nitroquinoline 1-oxide (4NQO)

4.1 Introduction

As mentioned before, the investigation of the dose responses of genotoxins, especially in the low dose region helps to improve health risk assessments. In the previous chapter MMC, an alkylating and cross-linking agent was analysed, whereas in this chapter 4NQO, a genotoxin that causes bulky adducts, was investigated.

4.1.1 4-Nitroquinoline 1-oxide (4NQO)

4NQO is a known mutagen and carcinogen. It was first synthesized in 1942 and its carcinogenicity was first demonstrated in 1957 by Nakahara and his colleagues (Nakahara et al., 1957; Endo et al., 1971). Since then 4NQO was widely used in experimental oncology as a potent carcinogen (Sugimura et al., 1966). 4NQO has two polar groups in the molecule, the N-oxide and nitro group. It is therefore susceptible to nucleophilic attack in chemical reactions (Endo H., Ono T. and Sugimura T., 1971). Furthermore 4NQO behaves as an electron acceptor in the charge transfer complex formation (Endo et al., 1971) (Figure 4.1).

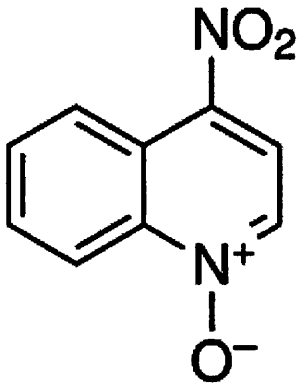

Figure 4.1: The Structure of 4NQO (www.sigmaaldrich.com/catalog/product/aldrich/n8141)

4NQO induces cancer in various tissues of mice and rat, examples of which are lung, pancreas and stomach (Bailleul et al., 1989). The enzymatic reduction of its nitro group is

believed to cause 4NQO's carcinogenic action. 4NQO is converted into 4-hydroxyaminoquinoline 1-oxide (4HAQO) and 4-aminoquinoline 1-oxide (4AQO) (see Figure 4.2). However, only 4HAQO is believed to be carcinogenic (Bailleul et al., 1989). DT diaphorase, a NAD(P)H-quinolineoxidoreductase, catalyses the reaction. DT diaphorase is a flavoprotein, which can use either NADH or NADPH as cofactors for the reduction of quinone substrates (Tedeschi et al., 1995) (Figure 4.2).

4NQO and its reduced metabolite 4HAQO are able to bind to cellular macromolecules, such as nucleic acid and protein (Tada and Tada, 1975). Seryl-tRNA synthetase is the enzyme that activates 4HAQO to bind to cellular macromolecules in the presence of ATP, L-serine and Mg^{2+} (Tada and Tada, 1975). The activated 4HAQO gives rise to three main adducts by reacting with purines but not with pyrimidines (Tada and Tada, 1975), thus of the adducts two are located within the guanine base and another adenine adduct is formed (Figure 4.2). The structures of the adducts identified were nucleic acid bases, nucleosides or nucleotides of N-(deoxyguanosin-8-yl)-4AQO, 3-(desoxyguanosin-N^2-yl)-4AQO and 3-(deoxyadenosin-N^6-yl)-4AQO (Bailleul et al., 1989; Kohda et al., 1991). The dGuo-C8-AQO adduct results from an attack of the nitrenium ion on the C8 position of guanine, whereas the dGuo-N2-AQO and the dAdo-N6-AQO adducts results from a carbocation attack on the guanine N2 and the adenine N6 positions, respectively (Bailleul et al., 1989).

4NQO reacts primarily with DNA at the N2 and C8 position of guanosine, and to a smaller extent at the N6 position of adenosine, and it was shown that NER operates on all these lesions (Jones et al., 1989).

Furthermore 8-hydroxydeoxyguanosine (8-OH-dG) formation was observed in cellular DNA treated with 4NQO (Kohda et al., 1991; Arima, et al., 2006) and it was shown that 4NQO induces oxidative stress and generates ROS, such as superoxide radicals or hydrogen peroxide, via induction of superoxide response operon (Nunoshiba and Demple, 1993; Kanojia and Vaidya, 2006). Consequently, a combination of reactive ROS formation and glutathione (GSH) depletion is involved in the 8-OH-dG formation by 4NQO (Arima et al., 2006, Stankowsi Jr., et al., 2011) (Figure 4.2).

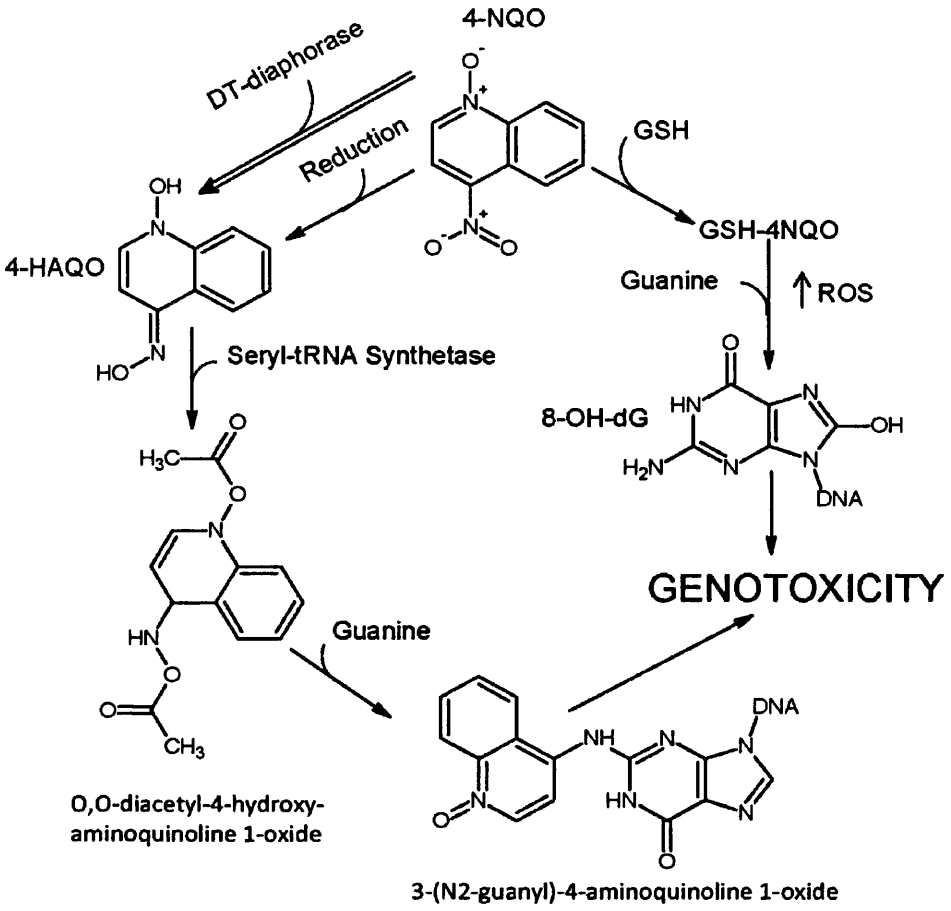

Figure 4.2: Mechanism of 4NQO's reaction with DNA. Metabolic reductions to 4-Hydroxyaminoquinoline-1-oxide (4HAQO) results in adduct formation, while 8-hydroxy-deoxyguanosine (8-OH-dG) formation occurs through glutathione (GSH) depletion and reactive oxygen species (ROS) formation. The double arrow indicates the predominant pathway for genotoxicity (from Stankowski Jr. et al., 2011).

Morrow *et al.* (1998) showed that the resistance to 4NQO induced genotoxicity and cytotoxicity is affected by the Multidrug resistance protein (MRP) and glutathione S-transferase P (GSTP1-1) proteins (Kanojia and Vaidya, 2006). GSTP1-1 utilizes, amongst other GSTs, gluthathione for conjungation and 4NQO is a substrate for GSTP1-1 (Kanojia and Vaidya, 2006). The resultant conjugate is called 4-(glutathione-S-yl)-quinoline 1-oxide (QO-SG) (Morrow et al., 1998) and can be pumped out of the cell by MRP (Kanojia and Vaidya, 2006).

In addition, 4NQO has been referred to as a UV mimetic agent, because UV light causes pyrimidine dimer formation, which are bulky adducts, that are repaired by NER (Kanojia and Vaidya, 2006). Similarly, 4NQO causes bulky DNA adducts, but differences in the UV and 4NQO induced damages and repair response to these adducts have been reported in previous studies (Jones et al., 1989; Snyderwine and Bohr, 1992; Kanojia and Vaidya, 2006).

4.1.1.1 Examples for previous genotoxicology studies with 4NQO

4NQO is primarily used as positive control in various genotoxicology assays and has been shown to give clear positive results in the Ames test (Searle, 1976) and *in vivo* rodent studies (Nomura et al., 1974).

Further Jenkins *et al.* (1998) used the restriction site mutation (RSM) assay for the analysis of mutations induced by two potent genotoxins ENU and 4NQO. Human fibroblasts were treated with 4NQO to assess the role of DNA lesions in induced mutagenesis *in vitro* by the RSM assay and the ^{32}P-post-labelling assay (Jenkins et al., 1998). The cells were treated with 5μM 4NQO for 4h and DNA was extracted 24h and 4 days post-treatment. Further DNA extractions followed from sub-culturing flasks (sampled 24h and 4 days after sub-culturing) and then the process was repeated until day 80 (Jenkins et al., 1998). The results showed two peaks of DNA mutations at day 4 and day 46 post-exposure. The mutations then declined after 46 days with no mutations detected in the 64- to 80-day period (Jenkins et al., 1998). The base substitutions detected by RSM were GC→ AT transitions on the non-transcribed strand (Jenkins et al., 1998).

Valentin-Severin *et al.* (2003) performed a study to compare the sensitivity of the MN assay and the comet assay with HepG2 cells towards direct and indirect mutagens. HepG2 cells were treated with 1.5, 3 and 7.5μM 4NQO for 4h. 4NQO induced DNA-damage at the lowest range of concentrations (1-10μM) in the comet assay and showed a significant concentration-dependent increase between 0.1 and 2μM to reach a 3.5-fold increase of MN (Valentin-Severin et al., 2003).

An *in vivo* study by Ribeiro *et al.* investigated the genomic instability on blood cells during 4NQO-induced rat tongue carcinogenesis with the help of the single cell gel (comet) and MN assay (Ribeiro et al., 2008). Male Wistar rats were treated with 50ppm 4NQO solution through their drinking water for 4, 12 and 20 weeks (Ribeiro et al., 2008). A statistically significant ($P<0.05$) increase of DNA damage was found at 4 and 20 weeks administration of 4NQO by the mean tail moment (Ribeiro et al., 2008). Furthermore a gradual increase of MN frequency was observed at all period's evaluated (Ribeiro et al., 2008).

Dertinger and colleagues evaluated two endpoints of genetic toxicity, mutation at the Pig-a gene and chromosomal damage in the form of micronucleated reticulocytes (MN-RET) in the context of a 28-day repeat-dosing study (Dertinger et al., 2010). Male Wistar Han rats were treated in 24h intervals on days 1 through 28 with one of the five following genotoxins: ENU, 7, 12-dimethyl-benz[a]anthracene, 4NQO, benzo(a)pyrene and MNU. The dose levels for 4NQO were 1.25, 2.5 and 5mg/kg/day. Flow cytometric scoring of CD59-negative

SWANSEA LIBRARY UNIVERSITY

erythrocytes (indicative of glycosylphosphatidylinositol anchor deficiency and hence Pig-a mutation) was performed using blood specimens obtained on days -1, 15, 29 and 56 (Dertinger et al., 2010). On days 4 and 29 blood specimens were collected and evaluated for MN-RET frequency (Dertinger et al., 2010). 4NQO showed no significant effect on MN-RET frequency, whereas Pig-a mutation was evident in the erythroid lineage (Dertinger et al., 2010).

Most previous studies showed that 4NQO induces DNA damage. However no investigations into the low dose response curve of 4NQO have been undertaken.

Assays, such as the *in vitro* MN method, the HPRT assay and/or the comet assay allow direct measurement of DNA damage. The *in vitro* MN test is described in detail in chapter 1 (section 1.4).

4.1.2. The mammalian cell *HPRT* gene mutation assay

The ability to detect substances that cause DNA damage is essential for human risk assessment, as DNA damage is an underlying cause of mutations that have the potential to initiate carcinogenesis. A mutation is a permanent change in the amount or structure of the genetic material of an organism (COM guideline, 2000) and can involve individual genes, blocks of genes or whole chromosomes.

The *in vitro* mammalian cell gene mutation test is used to screen for possible mammalian mutagens and carcinogens (OECD, 1997e) and allows identification of substances that lead specifically to point mutations. The test detects cells which are able to survive in the presence of a selective agent only after a new functional mutation occurs (Aaron et al., 1994).

Suitable cell lines for the test include the L5178Y mouse lymphoma cells, the CHO, AS52 and V79 lines of Chinese hamster cells and the human lymphoblastoid cell line TK6 (OECD, 1997e). Endpoints measured are mutation at TK, HPRT and a transgene of XPRT (Aaron et al., 1994; OECD, 1997e).

The *HPRT* gene is on the X chromosome of mammalian cells, which means male cells only carry a single copy of the gene and consequently it is easy to select for loss of functions mutants in cells derived from males, which are heterozygous for sex chromosomes (Johnson, 2012). Mutation, that destroy the functionality of the *HPRT* gene and/or protein are detected by positive selection using a toxic analogue (Johnson, 2012). Cells deficient in HPRT are resistant to 6-TG (a guanine analogue), whereas HPRT proficient cells are poisoned by 6-TG, so mutant cells are able to proliferate in the presence of 6-TG, whereas the cellular metabolism of normal cells is inhibited and further cell divisions are put on hold (OECD,

1997e). Consequently, HPRT$^-$ mutants result in viable cell colonies after continued sub-culturing (Johnson, 2012).

4.1.3 The comet assay

The comet or single cell gel electrophoresis assay is used in genotoxicology testing to measure DNA damage in eukaryotic cells at a single cell level.

Under alkaline conditions single- and double-strand breaks, incomplete repair sites, DNA cross-links and alkali-labile sites in single cell suspensions can be detected (Burlinson et al., 2007; OECD, 2008; Kumaravel et al., 2009).

Electrophoresis of DNA causes it to migrate in an agarose gel matrix. Thus, cells with and without DNA damage can be distinguished by the fact that damaged cells take a distinctive comet-like shape with a nuclear region and a tail region containing DNA fragments or DNA strands (OECD, 2008).

Two versions of the comet assay exist. The first version was introduced by Singh *et al.* (1988) and uses alkaline electrophoresis to analyse DNA damage. The method is capable of detecting single-strand breaks and alkali labile sites in individual cells (Singh, et al., 1988; Rojas et al., 1999). The second version introduced by Olive *et al.* (1990) involves lysis in alkali treatment followed by electrophoresis at either neutral or mild alkaline conditions to detect single-strand breaks (Olive at al., 1990, Rojas et al., 1999).

The standard alkaline method gives limited information on the type of DNA damage, since it is not possible to determine if the DNA damage measured is a consequence of the direct action of the damaging agent or of indirect effects, such as oxidative damage or DNA repair (Smith et al., 2006). However the standard method can be improved by incubating the lysed cells with lesion-specific endonucleases, such as formamidopyrimidine DNA-glycosylase (FPDG), endonuclease III or human 8-hydroxyguanine DNA-glycosylase 1 (hOGG1) (Smith et al., 2006). This allows recognition of particular damaged bases and creation of additional breaks (Smith et al., 2006). The modified comet assay can therefore be used to specifically detect oxidative DNA damage.

4.1.4 Aim of study

This study was designed to assess the low dose response relationships of 4NQO and to investigate, if the genotoxin follows linear or non-linear (thresholded) dose response relationships.

Chromosomal damage was investigated using the *in vitro* MN assay, while further gene mutation and DNA damage studies were carried out using the *in vitro* HPRT and comet assays.

This research was carried out at Swansea University, Swansea, UK as well as during an extended visit at AstraZeneca, Cheshire, UK. This allowed comparison of data generated in two laboratories as well as usage of a broad range of methods for the investigation into the low dose region of 4NQO.

4.2 Material and Methods

4.2.1 Cell lines

At Swansea University the human lymphoblastoid cell lines TK6, AHH-1 and MCL-5 were utilized. TK6, AHH-1 and MCL-5 cells were described in detail in chapter 2 (section 2.2.1).
For the experiments carried out at AstraZeneca the human lymphoblastoid cell line TK6 as well as the mouse lymphoma cell line L5178Y were used. L5178Y cells are known for their dysfunctional p53 activity (Storer et al., 1997; Clark et al., 2004).
The average doubling time of TK6 cells in both laboratories was approximately 16h to 18h. The doubling time of AHH-1 and MCL-5 cells was approximately 22h to 24h, whereas the L5178Y doubling time was around 11.5h.

4.2.2 Cell culture

Cell culture at Swansea University was performed as described in chapter 2 (section 2.2.1).
TK6 cells at AstraZeneca were cultured in RPMI 1640 (Sigma-Aldrich, Dorset, UK) supplemented with 10% heat inactivated donor horse serum (Gibco®, Paisley, UK), 2mM L-glutamine (Gibco®, Paisley, UK), 2mM sodium pyruvate (Gibco®, Paisley, UK), 200IU/ml penicillin (Gibco®, Paisley, UK) and 200µg/ml streptomycin (Gibco®, Paisley, UK) at 37°, 5%CO_2. L5178Y cells were cultured in RPMI 1640 supplemented with 10% heat inactivated donor horse serum, 2mM L-glutamine, 2mM sodium pyruvate, 1% Pluronic F68 (Gibco®, Paisley, UK), 200IU/ml penicillin and 200µg/ml streptomycin at 37°, 5%CO_2.

4.2.3 Test chemical

4NQO was acquired in both laboratories from Sigma-Aldrich, Dorset, UK. Before use, the chemical was freshly diluted from a stock solution (2.5mg/ml aliquots at Swansea University and 0.019mg/ml aliquots at AstraZeneca) with DMSO.

4.2.4 Test chemical dosing regime

At Swansea University the following 4NQO dosing regimens were used:
For the *in vitro* MN assay TK6 cells were treated with 4NQO over a range of concentrations between 0 and 0.03µg/ml for 4h, 24h or 48h respectively, followed by different recovery times. AHH-1 and MCL-5 cells were treated with 4NQO over a dose range of 0 to 0.7µg/ml for 4h with 22h or 46h recovery time. For the pan-centromeric staining study TK6 cells were treated with 4NQO for 24h over a range of concentrations between 0 and 0.03µg/ml. Further,

TK6 cells were treated for 24h with 4NQO for the HPRT assay study with 0.0009, 0.003, 0.01 and 0.02µg/ml 4NQO. Water was used as negative control, whereas DMSO was used as the solvent control. The experiment was carried out in triplicate.

The following NQO dosing regimens were used at AstraZeneca:
For the *in vitro* MN assay TK6 cells were treated with 4NQO for 4h plus 40h recovery period and 24h plus 24h recovery time over a range of concentrations between 0 to 0.03µg/ml. Further L5178Y cells were treated with 4NQO for 4h, followed by 24h recovery time over a range of concentrations between 0 and 0.05µg/ml. For the comet assay TK6 cells were treated with 4NQO for 3h over a range of concentrations between 0 and 0.06µg/ml 4NQO.

4.2.5 The *in vitro* MN assay

At Swansea University the semi-automated scoring protocol for the Metafer-System was used for the CBMN assay studies. The method is described in detail in chapter 2 (section 2.2.2). For the CBMN assay a minimum of 3000 cells per replicate were scored (exceptions where stated, for details see Appendix I). Three independent experiments were carried out.
AstraZeneca also uses the Metafer-System developed by MetaSystems for scoring MN. The *in vitro* MN test (mononucleated assay) procedure at AstraZeneca was performed as described below. Automated as well as manual scoring was carried out.

4.2.5.1 Initiation of the assay

All cell suspensions (10ml) were seeded at $2x10^5$ cells/ml and immediately dosed with 1% v/v solvent control and the test chemical as described above (section 4.2.4) at 37°C, 5%CO_2. After the different incubation times the cell suspensions were removed from each flask and transferred into appropriately labelled tubes. The cells were centrifuged (5min, 200 x g), the supernatant discarded and the pellets washed with PBS, before re-suspending the cells in 10ml fresh media.

4.2.5.2 Harvest and scoring

The cells were cytospun onto polished glass slides. Shandon mega-funnels (8min, 1000rpm) were used to harvest cells for the Metafer-System, whereas micro-funnels (8min, 800rpm) were used for the harvest for manual scoring. An appropriate volume of cells sub-cultured to $1x10^5$ cells/ml was used to prepare the slides. Five hundred microliter of the cell suspension

was used for the mega-funnels, whereas 100µl of cell suspension was used for the micro-funnels. The cells were fixed in 100% methanol for 15min.

For the automated scoring system the slides were stained with a vectashield antifading solution containing DAPI stain, while acridine orange (Sigma-Aldrich, Dorset, UK) staining was used for manual scoring under a fluorescent microscope (Carl Zeiss).

4.2.5.3 Scanning and Classifier settings for the Metafer-System

The slides were scanned at 20x magnification using the Metafer 4 master station, coupled to a fluorescent microscope (equipped with a Maerzhaeuser stepping motor stage; Carl Zeiss), a Dell computer hub (loaded with the Metafer4 Version 3.4.102 software) and a high resolution megapixel charge coupled device (CCD) camera (Axiocam; Carl Zeiss) for image capture. A number of grid positions evenly distributed across the scan area determined the plane of focus and a predetermined scan area was used for all slides.

Classifiers developed by MetaSystems were optimised in order to detect mononucleated cells. The search definition classifiers were used to define the size and shape of nuclei and micronuclei (Table 4.1).

Table 4.1: Classifier settings on the Metafer-System to define mononucleated cells and MN

	Mononuclear	
	Nuclei	Micronuclei
Object threshold	20%	10%
Minimum area	10µm^2	1.0µm^2
Maximum area	400µm^2	55µm^2
Maximum relative concavity of depth	0.9	1.0
Maximum aspect ratio	2.5	3.5
Maximum distance between	-	35µm
Maximum area asymmetry	90%	-

4.2.5.4 Acridine orange staining

For manual scoring slides were stained with acridine orange. The fixed cells on the slides were submerged in phosphate buffer (0.66% w/v potassium phosphate monobasic + 0.32% w/v sodium phosphate dibasic, pH 6.4-6.5) and stained in a solution of acridine orange (AO)

(12mg AO/100ml phosphate buffer) for 1min. The slides were transferred into phosphate buffer for 10min, then the buffer was re-freshed and the slides were left in buffer for a further 15min. Finally the slides were air-dried and stored protected from light.

4.2.5.5 Scoring

All experiments carried out at AstraZeneca were run in duplicate. 1000 mononucleated cells were scored per replicate for both manual and automated scoring. The manual scoring system for MN was as described by Fenech *et al.* (2003).

4.2.6 Cytotoxicity

RPD was used at Swansea University as well as AstraZeneca to measure cell death and cytostasis. The method is described in detail in chapter 2 (section 2.2.3).

For the Z1 Coulter Particle Counter (Beckman Coulter Inc., High Wycombe, UK) at AstraZeneca 1ml of cell suspension were placed into a cuvette containing 19ml of dilute conducting liquid.

4.2.7 Pan-centromeric painting

Centromeres were stained to classify 4NQO as a clastogenic or aneugenic chemical with RTU human pan-centromeric probe. The method is described in detail in chapter 2 (section 2.2.4). Nuclei were counterstained with DAPI and 100 MN per dose were scored as positive or negative for the centromeric stain under a BX50 fluorescent microscope (Carl Zeiss) (exceptions where stated, for details see Appendix IV).

4.2.8 The mammalian cell *HPRT* gene mutation assay

The *HPRT* gene mutation assay detects mutations which destroy the functionality of the *HPRT* gene and/or protein by positive selection (Johnson, 2012). The assay is described in detail in chapter 2 (section 2.2.10). TK6 cells were treated with 4NQO for 24h over a range of concentrations between 0 and 0.02µg/ml 4NQO.

4.2.9 The *in vitro* comet assay +/-hOGG1

For the comet assay TK6 cells were treated with 4NQO for 3h with a range of concentrations between 0 and 0.06µg/ml. Details of the assay are described in chapter 2 (section 2.2.11).

4.2.10 Statistical Analysis

The statistical analysis is described in detail in chapter 2 (section 2.2.17).

4.3 Results

4.3.1 Chromosomal aberration induction at low doses of 4NQO in TK6 cells

Short-term and extended treatments were used for the investigation of the dose response curve for 4NQO at Swansea University. The work was based on semi-automated analysis with the Metafer-System.

TK6 cells treated for 4h with 4NQO followed by one cell cycle of cytochalasin B (18h) showed no significant increases in MN induction over the treatment range chosen (0 to 0.03µg/ml). However, ≥50±5% (60.1% to 84.7%) cell death and cytostasis was observed at 0.02µg/ml of 4NQO (Figure 4.3).

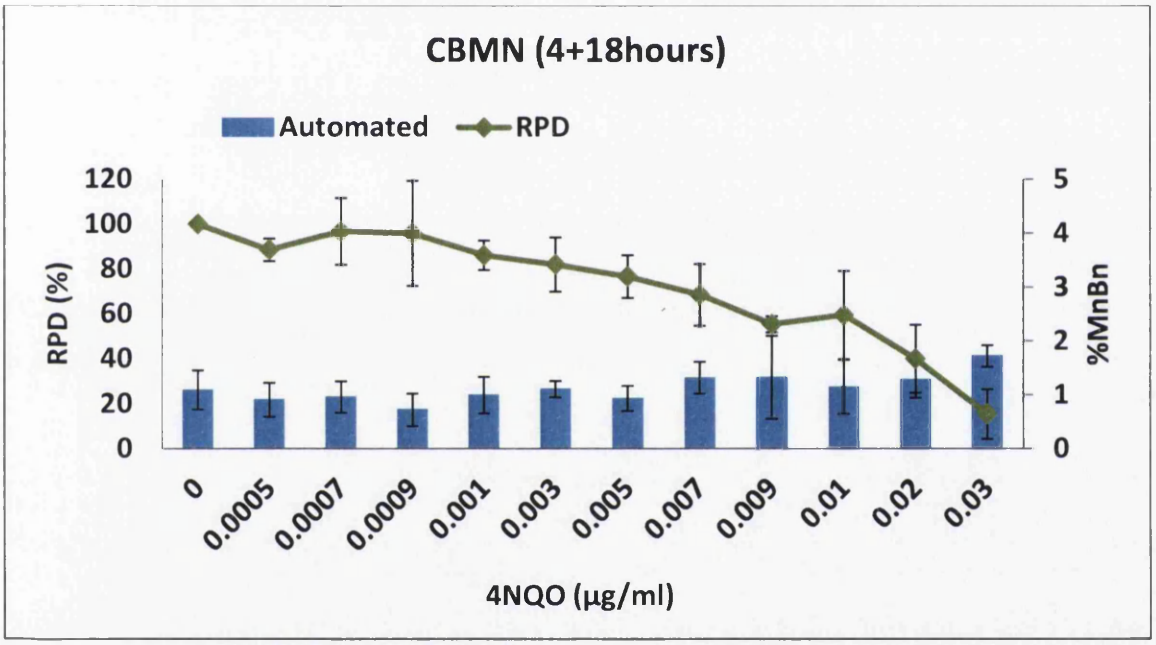

Figure 4.3: Effect of 4NQO on TK6 cells using the CBMN assay. TK6 cells were treated with 4NQO for 4h, followed by 18h of CytoB. Blue: percentage micronucleated binucleated cells, green: Relative population doubling (RPD). Values represent mean ± SD (n=3).

Extended treatments of 24h and 48h exposure to 4NQO, followed by one cell cycle of cytochalasin B (18h) were subsequently performed.

TK6 cells treated with 4NQO for 24h, followed by 18h of cytochalasin B showed no significant increases in MN frequencies. Further, ≥50±5% (55.5%) toxicity was observed at 0.02µg/ml of 4NQO (Figure 4.4).

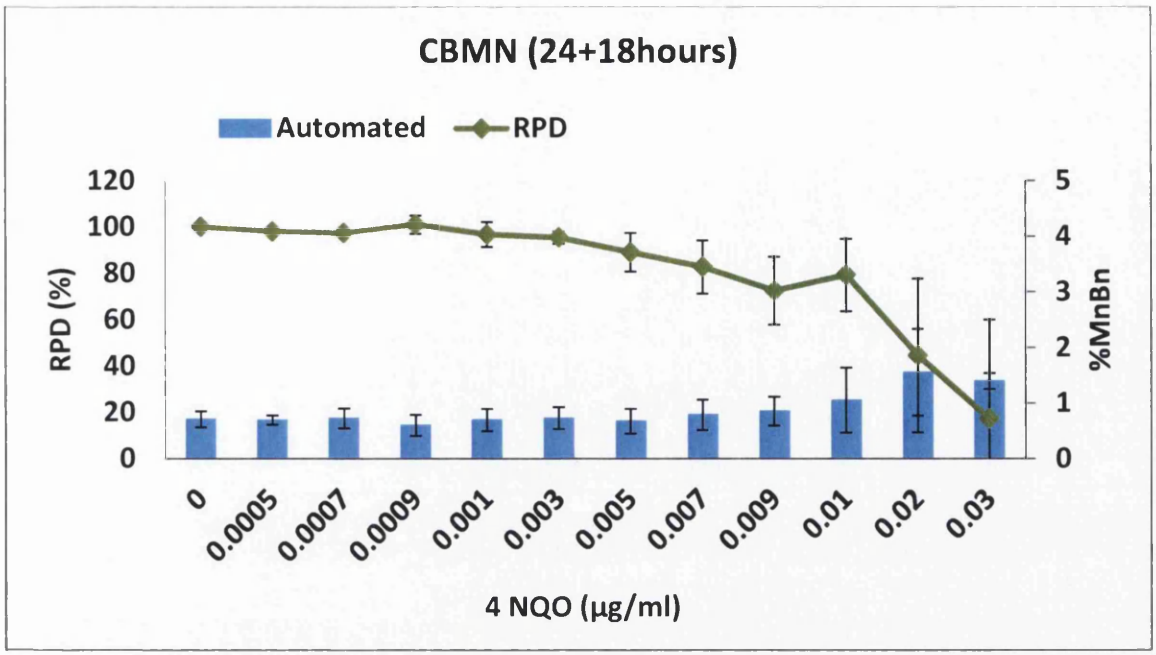

Figure 4.4: Effect of 4NQO on TK6 cells using the CBMN assay. TK6 cells were treated with 4NQO for 24h, followed by 18h of CytoB. Blue: percentage micronucleated binucleated cells, green: Relative population doubling (RPD). Values represent mean ± SD (n=3).

No significant increases in MN induction were observed when TK6 cells were treated for 48h with 4NQO, followed by one cell cycle of cytochalasin B (18h). At the top dose chosen (0.03µg/ml), only 29.5% cell death and cytostasis were observed (Figure 4.5).

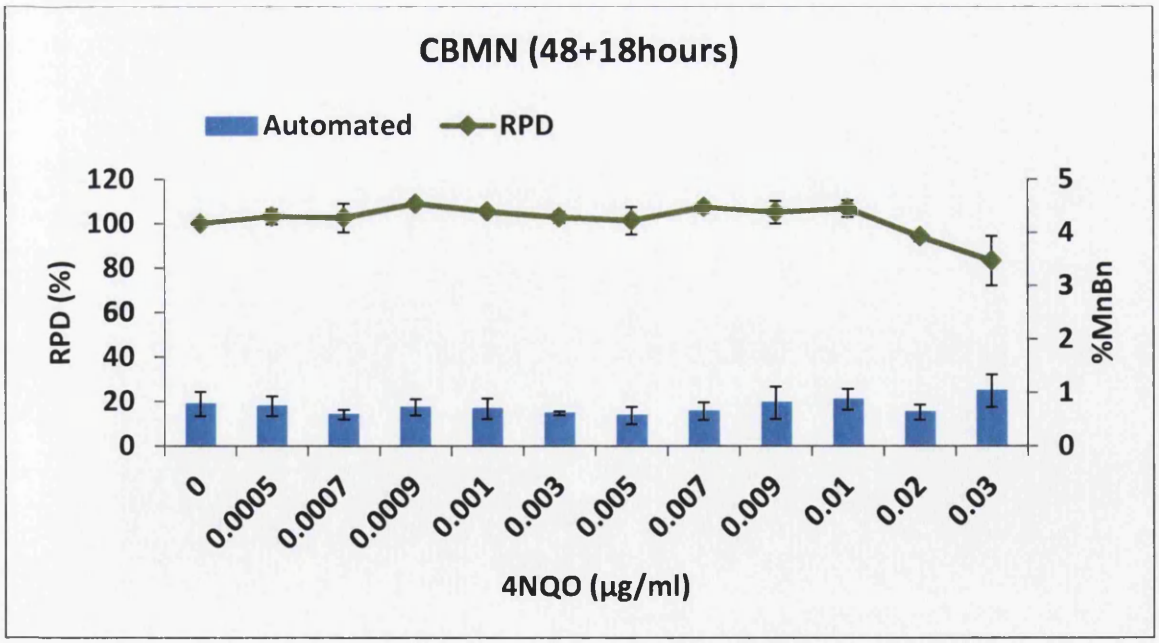

Figure 4.5: Effect of 4NQO on TK6 cells using the CBMN assay. TK6 cells were treated with 4NQO for 48h, followed by 18h of CytoB. Blue: percentage micronucleated binucleated cells, green: Relative population doubling (RPD). Values represent mean ± SD (n=3).

In previous studies (Sobol et al., 2012), it was proposed that an extended recovery time might play a critical role in MN induction. Therefore TK6 cells were treated with 4NQO for 4h, followed by a 24h recovery period, before adding cytochalasin B for another 18h (one cell cycle). Increases in MN induction only at 0.03µg/ml 4NQO could be observed. In addition at the top dose 60.6% toxicity was reached (Figure 4.6).

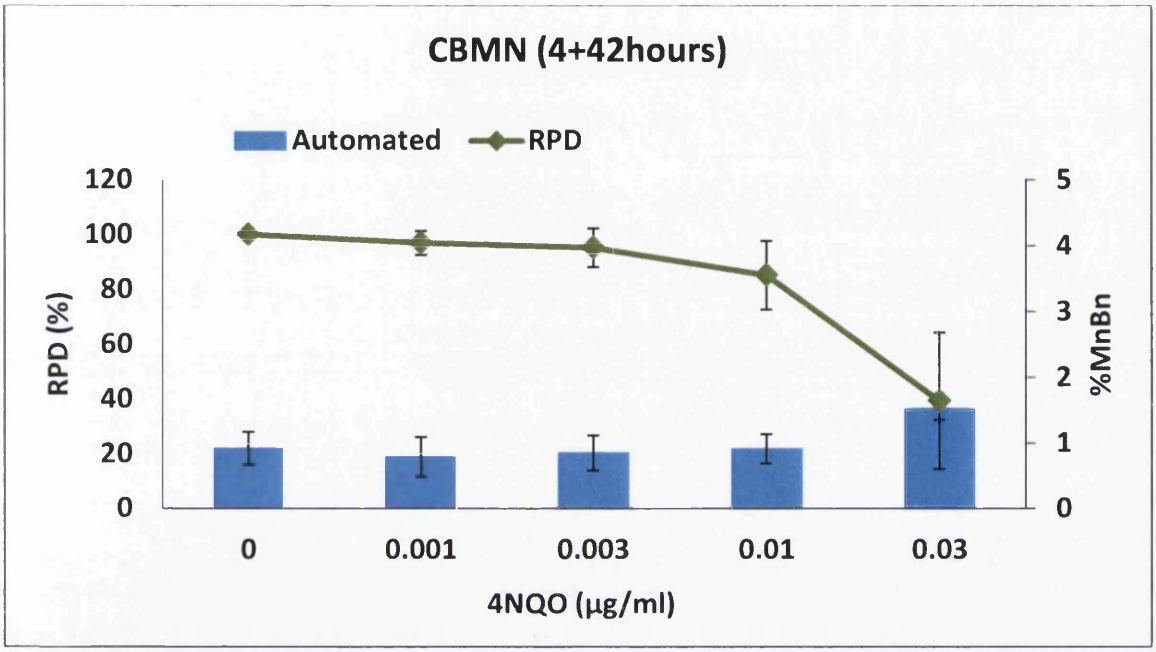

Figure 4.6: Effect of 4NQO on TK6 cells using the CBMN assay. TK6 cells were treated with 4NQO for 4h, followed by a 24h recovery period and 18h of CytoB. Blue: percentage micronucleated binucleated cells, green: Relative population doubling (RPD). Values represent mean ± SD (n=3).

To compare the results gained at Swansea University and for further investigations into the dose response curves of 4NQO, similar experiments were carried out in a second laboratory at AstraZeneca, Cheshire, UK. At AstraZeneca the mononucleated MN assay was carried out. Cells were scored with the semi-automated system Metafer as well as manual analysis by visual inspection under a fluorescent microscope.

As with the previous extended treatment, TK6 cells were treated with 24h of 4NQO, followed by a 24h recovery period before harvesting. No significant increases in MN induction were observed over a range of concentrations between 0 and 0.03µg/ml 4NQO with the manual scoring and the Metafer-System. About 40% (38.8%) cell death and cytostasis were observed at the top concentration (0.03µg/ml) (Figure 4.7).

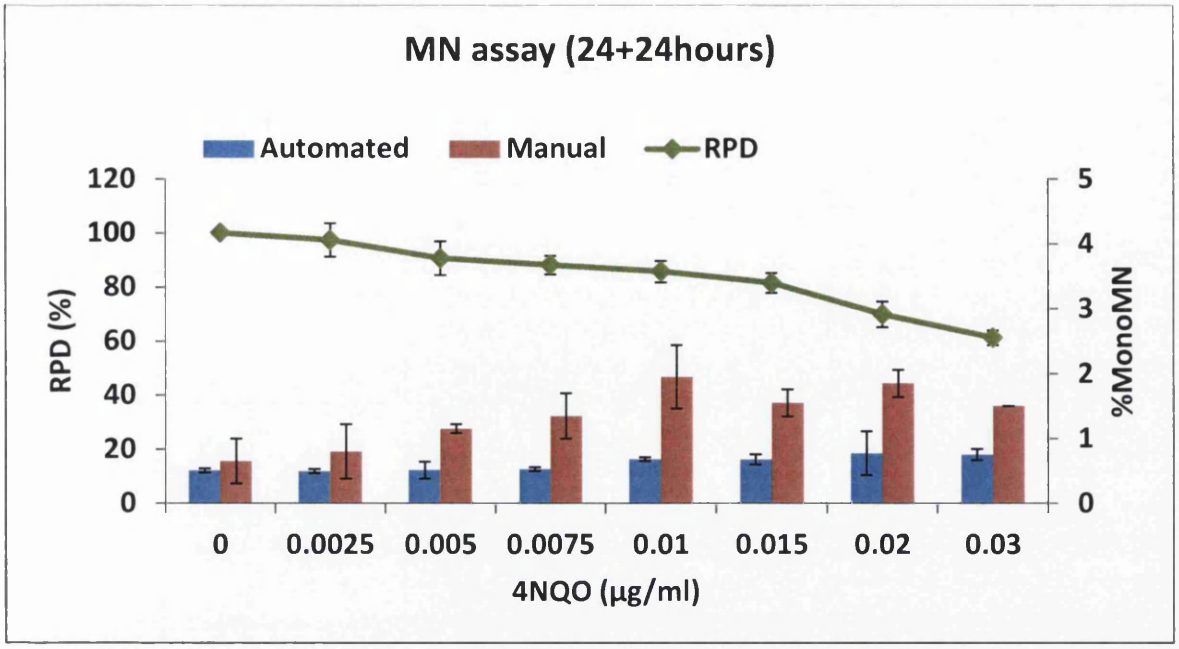

Figure 4.7: Effect of 4NQO on TK6 cells using the *in vitro* MN assay. TK6 cells were treated with 4NQO for 24h, followed by a 24h recovery period. Blue: Automated scoring, red: manual scoring, green: Relative population doubling (RPD). Values represent mean and range of duplicate experiments.

Further, a short-term treatment of 4h with an extended recovery period of 40h was performed. Significant increases in MN induction were observed at 0.02 and 0.03µg/ml 4NQO with the manual scoring, whereas increases in MN induction were shown with the Metafer-System at 0.02µg/ml and above. At the highest dose, 39.5% toxicity was reached (Figure 4.8).

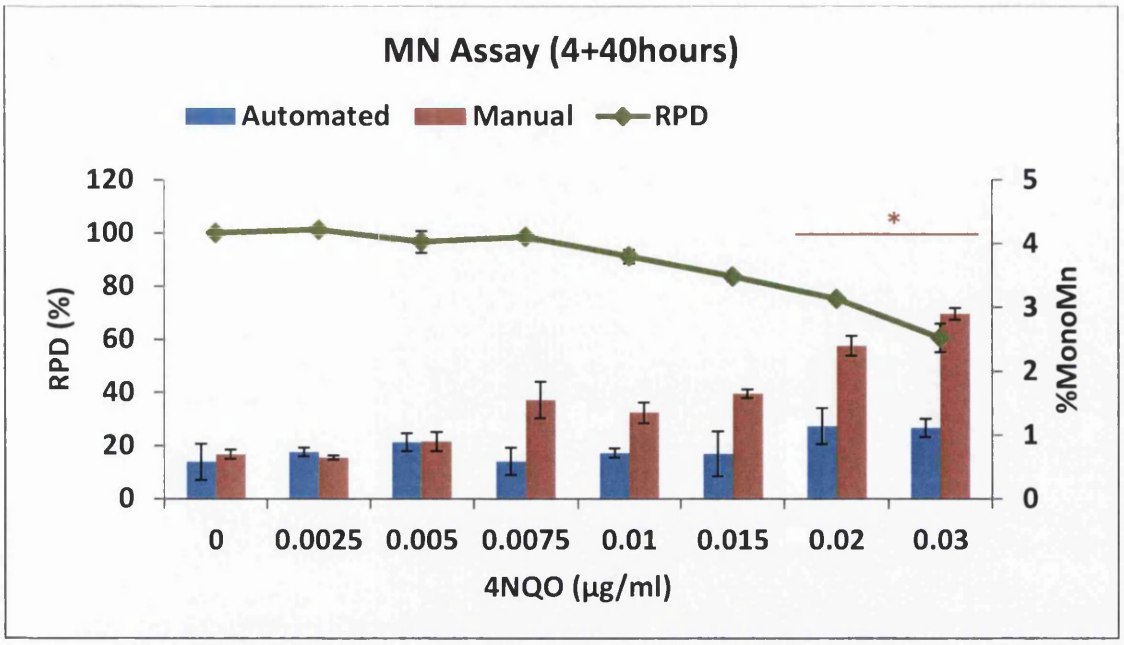

Figure 4.8: Effect of 4NQO on TK6 cells using the *in vitro* MN assay. TK6 cells were treated with 4NQO for 4h, followed by a 40h recovery period. Blue: Automated scoring, red: manual scoring, green: Relative population doubling (RPD). Values represent mean and range of duplicate experiments. (*) Represents $p<0.05$.

The work carried out at AstraZeneca, Cheshire, UK supported the studies carried out at Swansea University, Swansea, UK. Similar dose response curves of TK6 cells treated with 4NQO were obtained in both laboratories. In addition Pearson's r correlation revealed highly positive correlation between the manual scoring and the semi-automated system Metafer at AstraZeneca (Table 4.2).

4.3.2 MN induction by 4NQO in the human lymphoblastoid cell lines AHH-1 and MCL-5 as well as the mouse lymphoma cell line L5178Y

To compare the results gained in TK6 cells against other cell lines, the human lymphoblastoid cell lines AHH-1 and MCL-5 were treated with 4NQO at Swansea University, whereas at AstraZeneca the mouse lymphoma cell line L5178Y was treated with 4NQO.

Short-term treatments with and without prolonged recovery times were used at Swansea University.

AHH-1 cells treated with 4NQO for 4h over a concentration range between 0 and 0.7µg/ml, followed by one cell cycle of cytochalasin B (22h) showed no significant increases in MN induction. Further, MCL-5 cells showed no significant increases in MN induction for the short-term treatment over the dose range chosen. At 0.7µg/ml ≥50±5% toxicity in AHH-1 as

well as MCL-5 (61% in AHH-1 and 53.5% in MCL-5) cells were observed (Figures 4.9 and 4.10).

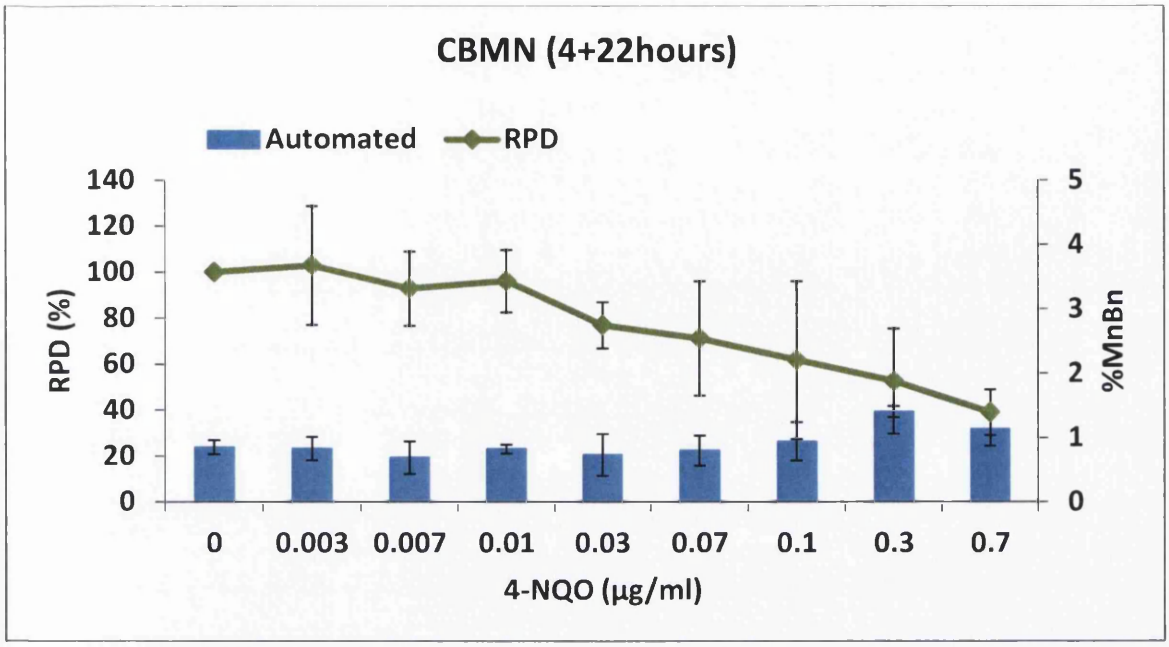

Figure 4.9: Effect of 4NQO on AHH-1 cells using the CBMN assay. AHH-1 cells were treated with 4NQO for 4h, followed by 22h of CytoB. Blue: percentage micronucleated binucleated cells, green: Relative population doubling (RPD). Values represent mean ± SD (n=3).

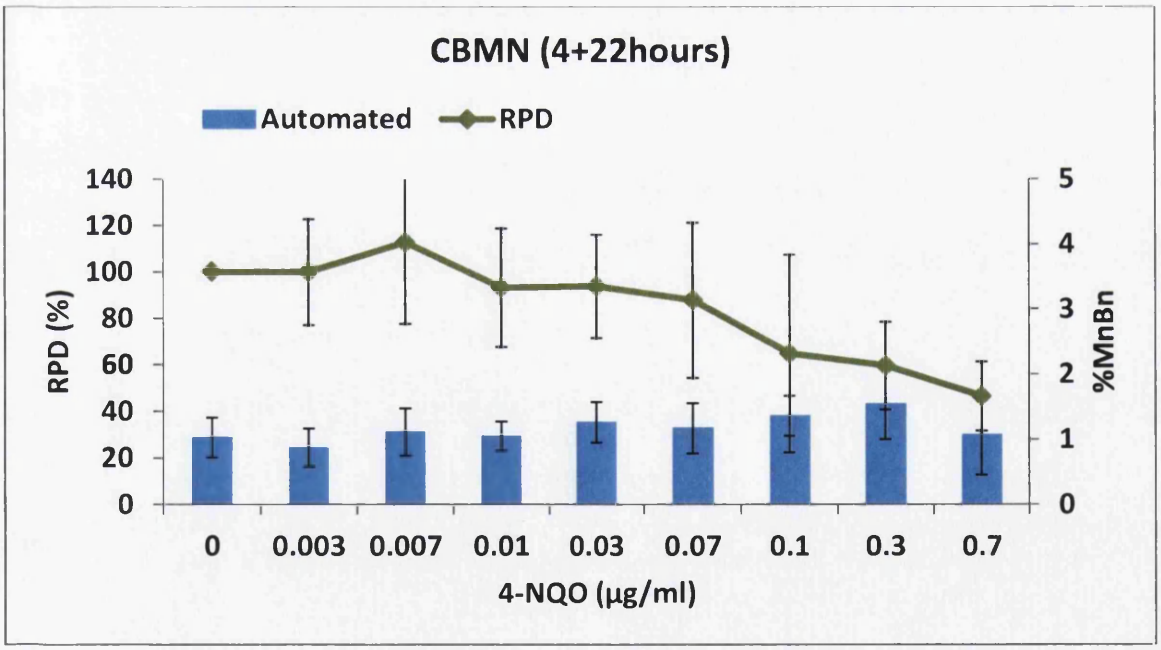

Figure 4.10: Effect of 4NQO on MCL-5 cells using the CBMN assay. MCL-5 cells were treated with 4NQO for 4h, followed by 22h of CytoB. Blue: percentage micronucleated binucleated cells, green: Relative population doubling (RPD). Values represent mean ± SD (n=3).

After prolonging the recovery time for 24h, AHH-1 cells showed increases in MN induction at 0.1µg/ml of 4NQO and MCL-5 cells showed increases in MN induction at 0.3µg/ml 4NQO (Figure 4.11).

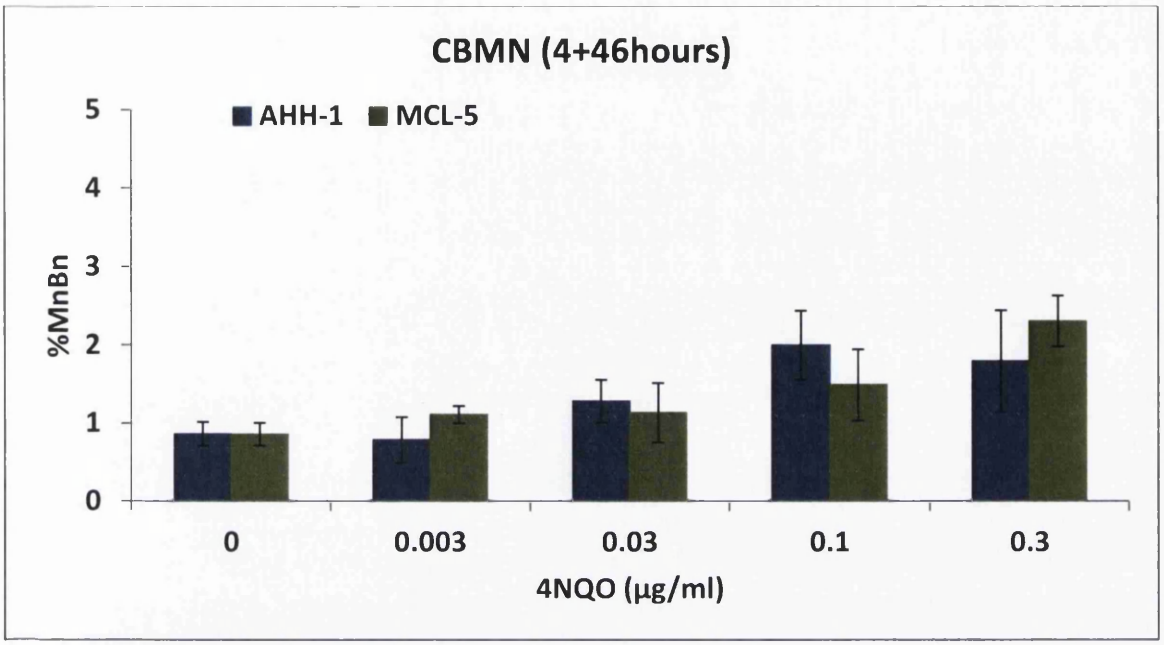

Figure 4.11: Effect of 4NQO on AHH-1 and MCL-5 cells using the CBMN assay. AHH-1 and MCL-5 cells were treated with 4NQO for 4h, followed by a 24h recovery period and 22h of CytoB. Blue: AHH-1 cells, green: MCL-5 cells. Values represent mean ± SD (n=3).

L5178Y cells are frequently used at AstraZeneca and other laboratories for genotoxicology studies. The cells were treated with 4NQO for 4h followed by a prolonged recovery time of 24h prior to harvesting, over a concentration range between 0 and 0.05µg/ml. The average doubling time of L5178Y cell was 11.5h, hence they grow much faster than the other cell lines used. The cells showed significant increases in MN induction at 0.0075µg/ml and above with the Metafer-System and at 0.03µg/ml and above with the manual scoring. No reduction in cell viability could be observed over the dose range (Figure 4.12).

Pearson's r correlation revealed again highly positive correlation between the manual scoring and the semi-automated system Metafer (Table 4.2).

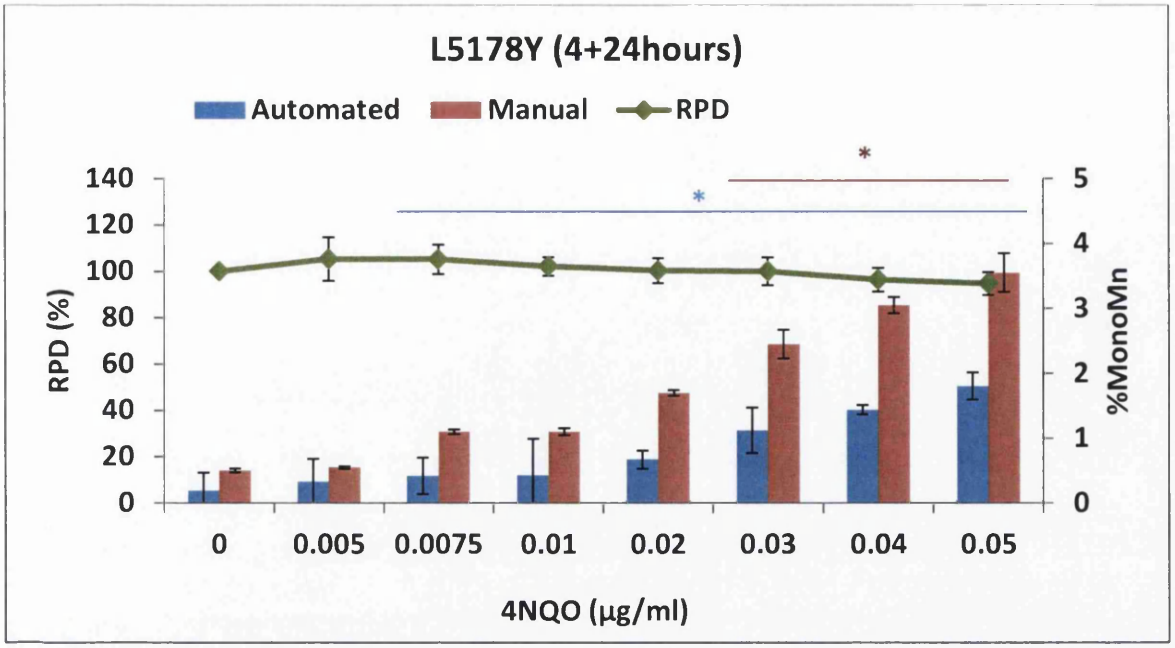

Figure 4.12: Effect of 4NQO on L5178Y cells using the *in vitro* MN assay. L5178Y cells were treated with 4NQO for 4h, followed by a 24h recovery period. Blue: Automated scoring, red: manual scoring, green: Relative population doubling (RPD). Values represent mean and range of duplicate experiments. (*) Represents $p<0.05$.

Table 4.2: Comparison of the Metafer-System (AstraZeneca) versus manual scoring in TK6 cells treated with 4NQO using Pearson's r correlation analysis

4NQO treatment	Correlation coefficient r	p-value
24h+24h (TK6 cells)	0.82	0.01246
4h+40h (TK6 cells)	0.74	0.03535
4h+24h (L5178Y cells)	0.99	1.933E-06

In summary, 4NQO showed little to no significant increases in MN induction in the human lymphoblastoid cell lines TK6, AHH-1 and MCL-5, even up to 50±5% toxicity. However, a linear dose response relationship was observed in the mouse lymphoma cell line L5178Y after 4NQO treatment, even at concentrations with no reduction in cell viability.

4.3.3 4NQO- A clastogen or an aneugen?

Human chromosome pan-centromeric staining was used to determine if the MN induced by 4NQO were predominantly due to whole chromosomes unable to incorporate into the main nuclei (aneuploidy) or due to chromosome breaks (clastogenicity).

TK6 cells treated with 4NQO for 24h and 18h of cytochalasin B showed increases in pan-centromeric negative MN over the range of concentrations (Figure 4.13). From this it

followed that the MN induced by 4NQO mainly originated from chromosome fragments lacking a centromere (clastogenicity).

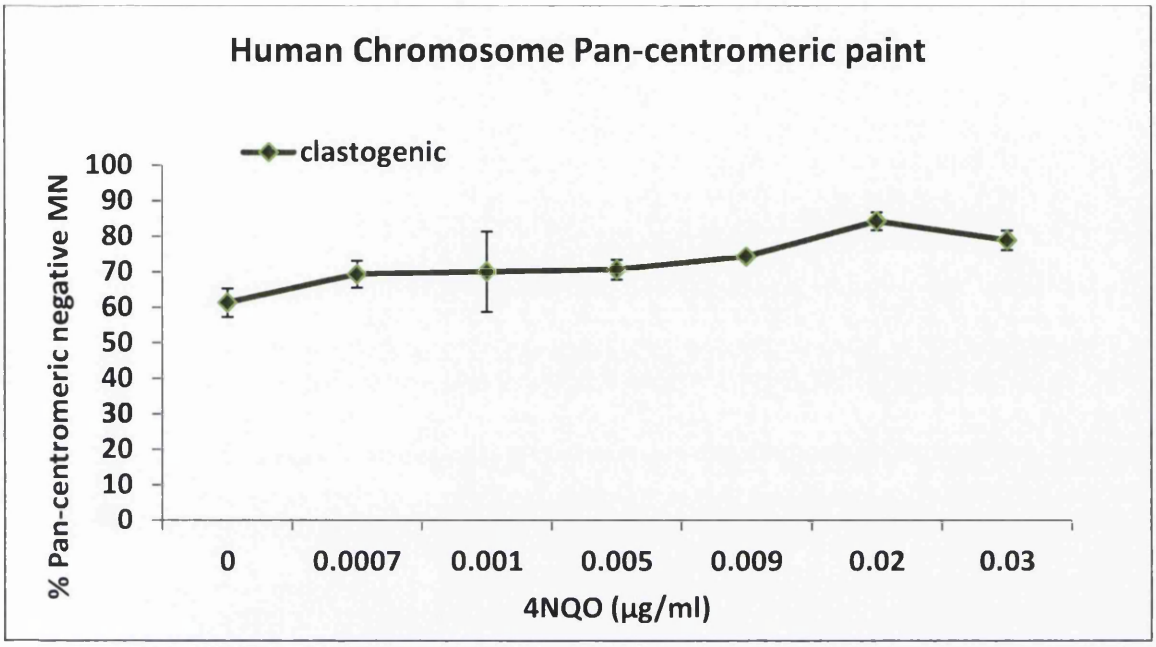

Figure 4.13: Human chromosome pan-centromeric painting of TK6 cells treated for 24h with 4NQO followed by 18h with CytoB. Values represent mean and range of duplicate experiments.

4.3.4 Gene mutation and DNA damage induction by 4NQO in TK6 cells

After investigating chromosomal damage of 4NQO in TK6 cells and observing somewhat little damage, the HPRT assay and the comet assay were performed to investigate the induction of gene mutations and DNA damage by 4NQO.

For the HPRT assay TK6 cells were treated with 4NQO for 24h between 0 and 0.02µg/ml. Water was used as negative control, while DMSO served as solvent control. Increases in gene mutations were observed at 0.01 and 0.02µg/ml 4NQO (Figure 4.14).

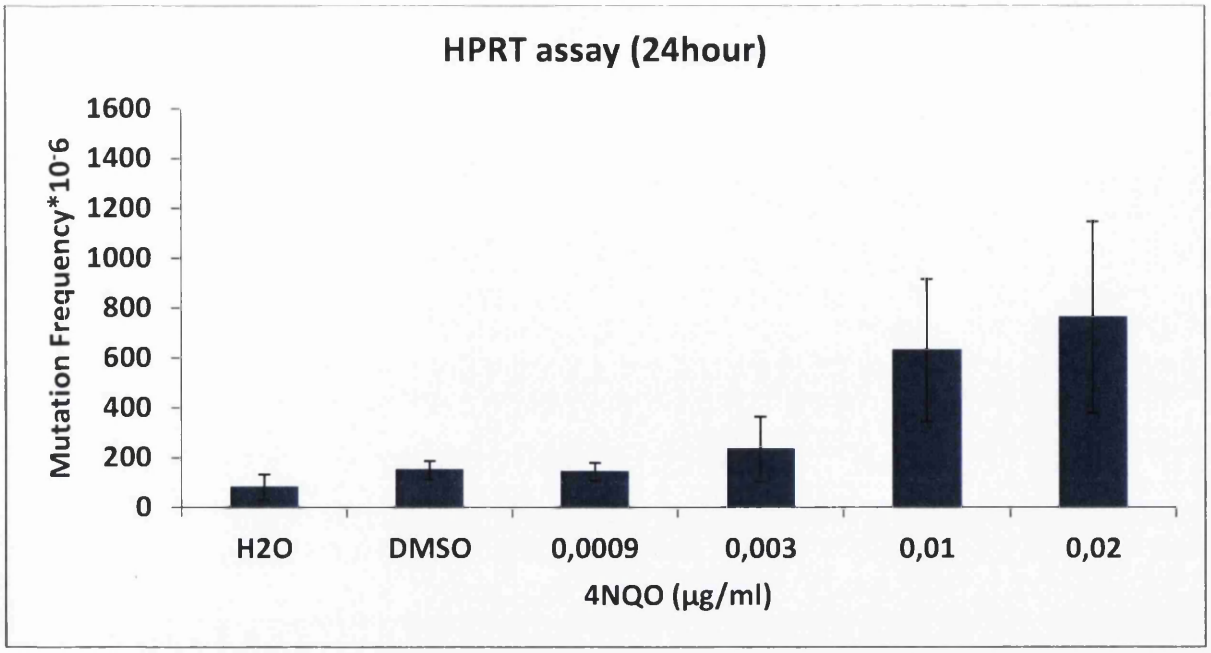

Figure 4.14: *HPRT* gene mutation frequency (number of 6TG resistant clones/10^6 clone-forming cells) in TK6 cells treated with 24h of 4NQO. Values represent mean ± SD (n=3).

The modified comet assay was performed at AstraZeneca, Cheshire, UK. With the comet assay low levels of DNA damage can be detected. The assay was performed with and without hOGG1. hOGG1 is an endonuclease, that recognizes oxidative DNA damage (Smith et al., 2006). TK6 cells treated with 4NQO for 3h showed increases in DNA damage at 0.04 and 0.06µg/ml 4NQO without hOGG1 and at 0.06µg/ml 4NQO with hOGG1 (Figure 4.15). At 0.06µg/ml 4NQO, the DNA damage induced by 4NQO was higher in the samples with hOGG1.

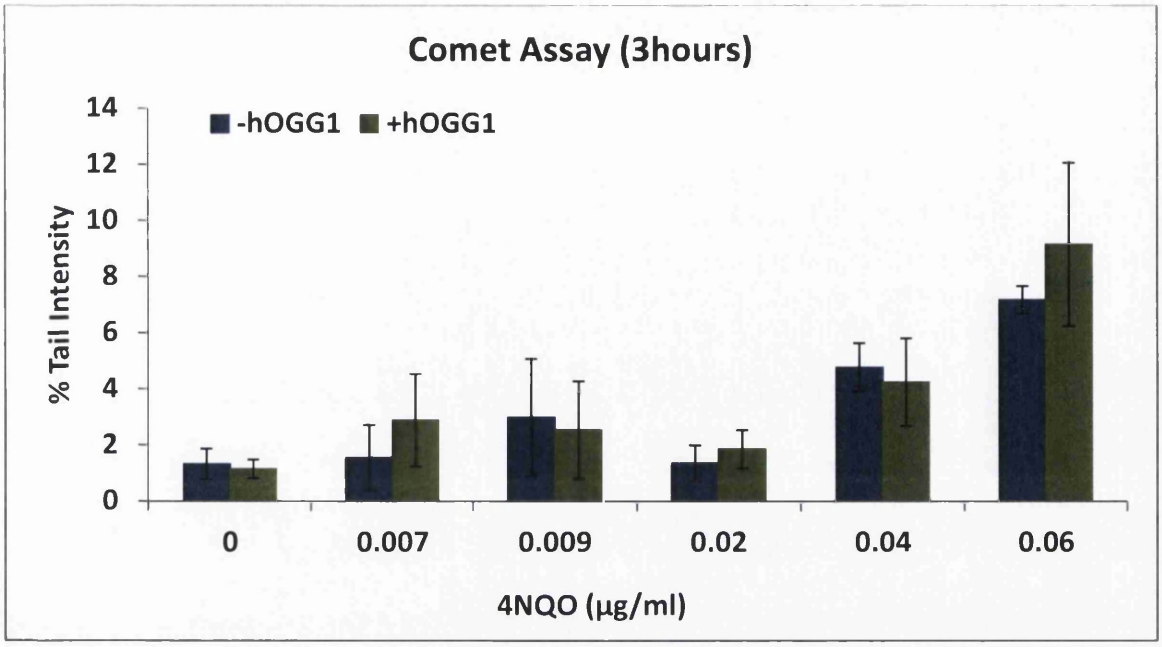

Figure 4.15: The *in vitro* comet assay. The effect of hOGG1 on DNA tail intensity, following treatment of TK6 cells with 3h of 4NQO. Values represent mean and range of duplicate experiments.

4.4 Discussion

4NQO is a known mutagen and carcinogen that forms stable monoadducts with purine bases after enzymatic reduction of its nitro group (Stankowski Jr. et al., 2011). The carcinogen is used as a model chemical in genotoxicology studies. However this study investigated the dose response relationship of 4NQO after low dose exposures.

Human lymphoblastoid cell lines (TK6, AHH-1 and MCL-5) as well as the mouse lymphoma cell line L5178Y were treated with low doses of 4NQO. Chromosomal damage was quantified with the *in vitro* MN assay. Further studies included the investigation of mutation and DNA damage induction by 4NQO.

4.4.1 Chromosomal aberration induction by 4NQO

The *in vitro* MN assay was used to investigate chromosomal damage. The semi-automated scoring protocol for the CBMN assay was carried out at Swansea University, whereas at AstraZeneca the mononucleated assay was used for manual and semi-automated scoring.

The *in vitro* MN assay can be performed with or without the actin polymerisation inhibitor cytochalasin B. Actin polymerisation is required for the formation of the microfilament ring that constricts the cytoplasm between the daughter nuclei during cytokinesis. This enables reliable comparisons of chromosome damage between cell populations that may differ in their cell division kinetics (Fenech and Morley, 1986; Kirsch-Volders et al., 2003). In the absence of a cytokinesis blocker it is necessary to demonstrate the analysed cells have undergone cell division during or after the exposure to the test substance.

MN will only be expressed in a DNA-damaged cell after at least one round of nuclear division. From this it follows, that cells that are not dividing cannot express MN as a sign of chromosome damage and so the level of MN observed is dependent on the proportion of cells that are dividing (Fenech, 1997). Furthermore it was reported that the MN frequencies decline when cells proceed through more than one nuclear division (Fenech, 1997). It is therefore important that the kinetics of nuclear division after a DNA insult is identical. Furthermore it has to be noted that an absolute value for MN frequency can only be obtained if MN are scored in cells that have divided once only (Fenech, 1997).

The CBMN assay at Swansea University and the mononucleated MN assay at AstraZeneca gave similar results. From this it follows that both assays gave reliable and comparable results and that both assay variants are a useful tool for genotoxicology studies.

The research at Swansea University was based on the semi-automated scoring protocol with the Metafer-System (MetaSystems), whereas at AstraZeneca both the semi-automated scoring protocol with the Metafer-System and manual scoring were performed. The results gained with the Metafer-System were comparable to the results gained through manual scoring, proving that the Metafer-System was a rapid and accurate method to score MN. Pearson's r correlation demonstrated highly positive correlation between manual scoring and the semi-automated system Metafer. It was noted that the Metafer-System detects slightly fewer MN than does the manual scoring, which might be due to the intensity of staining of the main nuclei and the small size of MN (Doherty et al., 2011). However, the differences were consistent in all studies and the concentrations that caused increases in MN induction after 4NQO treatment were similar.

Short-term treatments with and without prolonged recovery time and long term treatments were carried out over a concentration range of 0 to 0.03µg/ml 4NQO in TK6 cells. Short-term treatments (4h) without prolonged recovery time and the extended treatments (24h and 48h) showed little to no chromosomal damage induction up to 50±5% toxicity.

However, extending the recovery time after the short-term treatments in the CBMN assay from 18h to 42h and in the mononucleated assay from 24h to 40h increased the magnitude of MN induction at the top doses.

A study from Sobol *et al.* (2012) recently showed that an extended recovery time after treatment with compounds with direct DNA reactivity in TK6 cells increased the magnitude of MN induction. Further it was proposed by Islaih *et al.* (2005) that TK6 cells have prolonged cell cycle delay in response to genotoxins. Therefore it might be possible that damaged cells are rather stalled than eliminated through apoptosis (Sobol et al., 2012). Consequently the extended recovery period would allow the stalled cells to progress into mitosis and hence to fix damage as a MN.

In support of this, it was further noted in the present study that toxicity appeared to be higher in cells with the shorter recovery time than in cells with the extended recovery time, demonstrating higher cytostasis, which supports the proposition made by Islaih *et al.* (2005) and the findings from Sobol *et al.* (2012).

In addition pan-centromeric staining revealed that 4NQO predominantly induces MN via chromosome breakage and not aneuploidy.

To compare the results gained in TK6 cells against other cell lines, the human lymphoblastoid cell lines AHH-1 and MCL-5 were treated with 4NQO for 4h and the mouse lymphoma cell line L5178Y was treated with 4NQO for 4h.

Like TK6 cells, AHH-1 and MCL-5 cells were treated with 4NQO for 4h with and without extended recovery time over a range of concentrations between 0 and 0.7µg/ml. 4NQO showed little to no significant increases in MN induction, even up to 50±5% toxicity. However, slight increases in the magnitude of MN induction were again seen after prolonging the recovery time.

Further, in comparison to TK6 cells, AHH-1 and MCL-5 cells could be treated with a 10x higher dose of 4NQO without reaching the 50±5% toxicity threshold. MCL-5 is a derivative of the AHH-1 cell line. Both cell lines are heterozygous for a p53 mutation at the interface between the codons 281 and 282 of exon 8, whereas TK6 cells are p53 competent (Guest and Parry, 1999).

The mouse lymphoma cell line L5178Y was treated with 4NQO for 4h (0 to 0.05µg/ml) and a recovery period of 24h before harvesting. The cells showed highly significant increases in MN induction with the Metafer-System and at 0.02µg/ml and above with the manual scoring. Further no decrease in cell viability could be observed. L5178Y cells are known for their dysfunctional p53 activity, since they have a missense mutation in exon 5 on chromosome 11a (amino acid change from a cysteine to an arginine) and a nonsense mutation in exon 4 on chromosome 11b (changing a glutamine to a stop codon) (Storer et al., 1997; Clark et al., 2004). From this it follows that the mouse lymphoma cells have no wild-type p53 allele.

The tumour suppressor gene TP53 plays an important role in cellular integrity, with an integral function in transducing signals from damaged DNA to genes that control the cell cycle and lead to apoptosis (Guest and Parry, 1999). Abnormal DNA binding properties and/or transcriptional activation through p53 mutation causes mal-functions in the DNA damage dependent cell death pathway (Guest and Parry, 1999). Consequently, the effects of DNA damaging agents could become significant at low doses, where p53 competent cell lines would induce DNA damage dependent cell death (Guest and Parry, 1999).

In conclusion, TK6 cells showed a smaller magnitude of MN induction and more cytotoxicity than the human lymphoblastoid cell lines AHH-1 and MCL-5 and particular the mouse lymphoma cell line L5178Y. The sensitivity to MN induction and cytotoxicity is dependent on the cell type. However, cell lines with a p53 mutation are more likely to survive and replicate with DNA damage, which can lead to higher MN frequencies (Hashimoto et al., 2011), since p53 plays an important role in cell responses, like cell cycle arrest at the G1 or G2 phases, apoptosis and DNA repair in response to DNA damage (Hashimoto et al., 2011). p53 function is therefore most likely to be a key factor for the cell-type sensitivity for genotoxicity and cytotoxicity (Hashimoto et al., 2011).

The human lymphoblastoid cell lines showed little to no significant increases in MN induction over the background even up to 50±5% toxicity, whereas the mouse lymphoma cell line showed a linear dose response after 4NQO treatment at concentrations with no reduction in cell viability. From this it follows that 4NQO is a weak inducer of chromosomal damage in human lymphoblastoid cells. Therefore further investigations into the induction of gene mutations by 4NQO were undertaken.

4.4.2 Gene mutation and DNA damage induction by 4NQO

The *HPRT* gene mutation assay was used to investigate if 4NQO induces point mutations. Further, the comet assay was carried to investigate the DNA damage induction by 4NQO.

Increases in point mutations over the solvent control were observed in the HPRT assay, even at concentrations lower than MN induction. Mutagenesis caused by 4NQO has been shown to be specific for base-pair substitutions, predominantly as G to A transitions, but also G to T conversions and rare substitutions of adenines (Bailleul et al., 1989). 4NQO induces three main adducts: dGuo-N2-AQO, dGuo-C8-AQO and dAdo-N6-AQO, with relative proportions in double stranded DNA to be around 50%, 30% and 10% respectively (Inga et al., 1994), which can be fixed as mutations. Further, it was shown that 4NQO induces apurinic/apyrimdinic sites and single-strand breaks, which originated probably from unstable adducts (Inga et al., 1994) and could be converted to double strand breaks and fixed as MN.

To our knowledge, this is the first time that 4NQO was used in the HPRT assay with TK6 cells. But, this compound has been tested before in both normal (AA8) and 4NQO-sensitive (UV5) Chinese hamster ovary cells to investigate the mutation spectra of 4NQO (Inga et al., 1994). Mutation induction at the *hprt* locus increased linearly with 4NQO in UV5 cells over the tested range of concentrations (0 to 4μM 4NQO), similar to the results gained in TK6 cells, while it levelled off at high concentrations (0 to 12μM 4NQO) in AA8 cells (Inga et al., 1994). Mutations induced in the study by Inga et al. (1994), were base substitutions involving G residues localized at the splice sites on the non-transcribed strand. From this it follows that further sequence analysis of 4NQO induced mutations at the *hprt* locus in TK6 cells needs to be performed to determine the mutation spectra induced. However, it is most likely that the mutations induced by 4NQO are base substitutions.

The comet assay was used for detecting of low levels of DNA damage. Increases in DNA damage induction in the comet assay were observed (see Figure 4.15). The assay can detect single-strand breaks as initial damage as well those developed from alkali-labile sites under

alkaline conditions (Kawaguchi et al., 2010). As mentioned above 4NQO causes apurinic/apyrimdinic sites and single-strand breaks (Inga et al., 1994).

In previous studies high levels of 8-hydroxydeoxyguanosine were found in 4NQO treated cells, which implicated the involvement of ROS in the mutagenicity of 4NQO (Bailleul et al., 1989; Arima et al., 2006; Stankowski Jr. et al., 2011). Therefore the lysed cells in the comet assay were incubated with the lesion-specific endonuclease hOGG1 to detect any oxidative DNA damage. TK6 cells treated with 4NQO for 3h showed increases in DNA damage at 0.04 and 0.06µg/ml 4NQO without hOGG1 and at 0.06µg/ml 4NQO with hOGG1. At 0.06µg/ml the DNA damage induction was slightly higher with hOGG1 than without hOGG1, implying that oxidative DNA damage might be involved in the mutagenicity of 4NQO. However further experiments have to be undertaken to investigate the role of ROS in the mutagenicity of 4NQO.

4.4.3 Comparative investigations between the genotoxicity assays after 4NQO treatment

The MN assay provides a tool for detecting chromosomal damage that presents as MN, whereas the HPRT assay allows detection of point mutation and the comet assay detects DNA damage in the form of alkali-labile lesions and strand breaks.

In TK6 cells treated with 4NQO, the HPRT assay showed DNA damage at lower doses than the MN assay and the comet assay, while the MN assay was more sensitive than the comet assay. From this it follows that it is most likely that 4NQO predominantly induces gene mutations, more so than chromosomal damage. The difference between effects in the comet and MN assay could be due to variations in the type of DNA alterations that the test detects, while the comet assay detects primarily DNA lesions that are repairable, the MN assay detects irreparable lesions (Valentin-Severin et al., 2003). Furthermore DNA re-synthesis and re-joining events following single-strand formation can reduce the sensitivity of the comet assay in detecting DNA damage, like bulky base adducts (Kawaguchi et al., 2010).

4.5 Summary

In this study the dose response relationships of 4NQO at the low dose range were investigated. The work was carried out at Swansea University, Swansea, UK as well as during an extended stay at AstraZeneca, Cheshire, UK. This allowed comparisons between laboratories as well as usage of different methods.

The human lymphoblastoid cell lines TK6, AHH-1 and MCL-5 as well as the mouse lymphoma cell line L5178Y were used in this study.

The *in vitro* MN assay was used for investigation of chromosomal damage. Short-term as well as extended treatments of 4NQO showed little to no significant increases in MN induction. However prolonging of the recovery time increased the magnitude of MN induction.

Further gene mutation induction of 4NQO was observed in the *in vitro* HPRT assay and the *in vitro* comet assay revealed DNA damage induction by 4NQO at the higher range of concentrations. In addition oxidative damage might be a cause for the mutagenicity of 4NQO.

Chapter 5

Induction of chromosome damage by cytosine arabinoside (araC) using the CBMN assay

5.1 Introduction

In the previous two chapters the low dose responses for DNA damage of MMC, an alkylating and cross-linking agent, and 4NQO, a synthetic chemical that causes bulky adducts, were investigated. The research in this chapter examines the low dose response for DNA damage induction of the nucleoside analogue araC, using the *in vitro* MN assay described previously. AraC is used as a chemotherapeutic agent for acute non-lymphocytic leukemias and acute lymphoblastic leukemia.

5.1.1 Cytosine arabinoside (araC)

AraC was first synthesized in 1950 and introduced into clinical use in 1963 (Henderson, 1982). It is a nucleoside analogue of both cytidine and deoxycytidine (Figure 5.1).

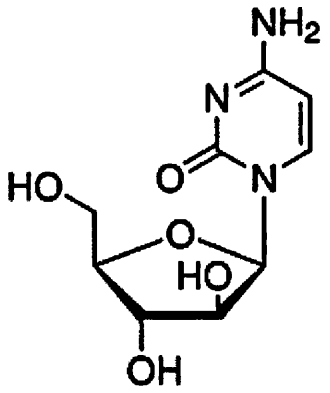

Figure 5.1: Structure of araC (http://www.sigmaaldrich.com/catalog/product/sigma/c1768)

AraC is an important drug in the treatment of acute non-lymphocytic leukemias. Further the component is also active against acute lymphoblastic leukemia and to a smaller extent in chronic myelocytic leukemia and non-Hodgkin lymphomas (Henderson, 1982). AraC is known as a "phase-specific" anti-cancer agent, because of its ability to inhibit de novo DNA synthesis effectively only when cells are in S-phase of the cell cycle and because of its rapid *in vivo* detoxification (Henderson, 1982).

Cellular effects of araC include: inhibition of cell growth, inhibition of DNA synthesis, proliferation-dependent cytotoxicity, progression delay and unbalanced growth (Valeriote, 1982). The S-phase specificity of araC implicates that its cytotoxic effects should be limited to proliferating cells and that non-proliferating cells should be insensitive to araC (Valeriote, 1982). Furthermore it was shown that araC slows down S-phase passage at low concentrations, whereas at higher concentrations araC inhibits the cell movement from G1 to S-phase (Valeriote, 1982). Unbalanced growth occurs when one of the three macromolecule syntheses (DNA, RNA, protein) are inhibited. In the case of araC it was shown, that at concentration at which araC inhibits DNA synthesis, both RNA and protein synthesis continue undiminished (Valeriote, 1982).

5.1.1.1 Mechanism of action of araC

Two mechanisms are responsible for the transport of araC through the cell membrane: a carrier mediated process and simple diffusion (Cheng and Capizzi, 1982). AraC is metabolized primarily by enzymes that metabolize deoxycytidine or cytidine, upon entry of araC into the cell (Cheng and Capizzi, 1982). AraC is phosphorylated with ATP as the phosphate donor (araC → araCMP → ara-CDP → araCTP) and the triphosphate, araCTP, inhibits DNA replication (Kufe and Majot, 1982).

Two mechanisms for the inhibition of DNA replication by araC are proposed. The first model proposes that araC directly inhibits the enzyme DNA polymerase after its conversion to the 5´-triphosphate (araCTP), whereas the second model proposes polynucleotide chain termination through incorporation of araCTP into DNA, which blocks further addition of deoxyribonucleotides (Momparler, 1982).

It was shown that araCTP does not induce functional alterations in the DNA polymerase itself, and from this it follows that araC inhibits DNA synthesis by reversible displacement of dCTP from the binding site on the enzyme (Kufe and Major, 1982).

Either of the two mechanisms mentioned above can produce cellular damage through any of the following events: faulty processing of DNA, chromosomal breaks, re-initiation of previously replicated DNA segments, inhibition of chain initiation and inhibition of chain ligation (Kufe and Major, 1982).

In addition, it was shown by Fenech and Neville (1992) that araC inhibits the gap-filling step during excision repair, which results in the formation of single-stranded breaks at repair sites. These breaks can then be converted to chromatid or chromosome breaks (Fenech and Neville, 1992; Fenech et al., 1994).

5.1.1.2 Examples of previous genotoxicology studies of araC

In previous studies, araC was often used as a positive control in the *in vitro* MN assay as well as for validation purposes.

For example, in 2010 araC was used as part of a collaborative evaluation study in different laboratories to investigate the toxicity measurements recommended in the draft OECD Test Guideline 487 for the *in vitro* MN test. Different cell lines were assessed. In the study of Schuler *et al.* (2010) Chinese hamster ovary (CHO) cells were treated with araC for 24h in the presence and absence of cytochalasin B. Various concentrations between 0 to 1000µg/ml were used. The results demonstrated that araC induced significant MN formation between 0.014 to 1000µg/ml with and without cytochalasin B. Furthermore it was shown, that araC does not require cytotoxic concentrations to produce positive responses in the *in vitro* MN assay (Schuler et al., 2010).

L5178Y cells were used in the study of Cariou *et al.* (2010). The cells were treated with araC for 24h with no recovery time over a range of concentrations between 0 and 0.5µg/ml. A concentration-dependent reduction in survival was observed. Further, a significant increase in MN induction above the concentrations of 0.05 and 0.075µg/ml araC were shown (Cariou et al., 2010).

In the study of Whitwell *et al,* (2010) Chinese hamster V79 cells were treated with araC for 24h+0h over a range of concentrations between 0 and 0.015µg/ml. In the absence of cytochalasin B, significant increases in MN induction were observed at 0.004µg/ml araC, inducing reductions in RCC, RICC or RPD of 24%, 33% or 21% respectively (Whitwell et al., 2010). In the presence of cytochalasin B significant increases in MN induction were observed at 0.008µg/ml (Whitwell et al., 2010)

The human lymphoblastoid cell line TK6 was used in the study of Nesslany and Marzin (2010). TK6 cells were treated with araC for 27h+0h or 27h+27h over a range of concentrations between 0 and 0.094µg/ml araC. In the 27h treatment with no recovery period, significant increases in MN induction were only seen at concentrations of about 65% toxicity and more (Nesslany and Marzin, 2010). In the 27h treatment, followed by a 27h recovery period significant increases in MN induction were observed at concentrations giving about 50% toxicity or less as measured by all endpoints (Nesslany and Marzin, 2010).

All the evaluation studies mentioned above showed that RICC and RPD are useful tools for measuring cytotoxicity for the *in vitro* MN assay. In addition the studies crystallised the idea that different cell lines needed to be treated with different concentrations of araC to reach

genotoxic and cytotoxic level. Furthermore, in most cell lines tested, significant increases in MN induction were only seen at the higher dose range.

From this it follows that studies into the low dose range of araC could reveal that a NOEL might exist for this genotoxin.

5.1.2 Aim of study

The study was designed to assess the low dose response relationships of the direct acting genotoxin araC. Human lymphoblastoid cells (TK6, AHH-1 and MCL-5) were used for this study. Chromosomal damage was investigated, using the *in vitro* MN assay and RPD was used to measure toxicity.

5.2 Material and Methods

5.2.1 Cell lines

The human lymphoblastoid cell lines TK6, AHH-1 and MCL-5 were used in this study. MCL-5 cells are a derivative of AHH-1 cells. The cell lines were described in detail in chapter 2 (section 2.2.1).

5.2.2 Cell culture

Cell culture and sub-culturing was performed as described in chapter 2 (section 2.2.1).

5.2.3 Test chemical

AraC was acquired from Sigma-Aldrich, Dorset, UK. Before use, the chemical was freshly diluted from a stock solution (1mg/ml aliquots) with water.

5.2.4 Test chemical dosing regime

For the *in vitro* CBMN assay TK6 cells were treated with araC over a range of concentrations between 0 and 0.1µg/ml for 24h and 48h respectively, followed by one cell cycle (18h) with cytochalasin B (4.5µg/ml). AHH-1 and MCL-5 cells were treated for 24h with araC, followed by one cell cycle (22h) with cytochalasin B (4.5 to 6µg/ml). The dose range selected for AHH-1 cells was between 0 and 0.2µg/ml araC, whereas MCL-5 cells were treated over a range of concentrations between 0 and 0.1µg/ml araC.

5.2.5 *In vitro* MN assay

The semi-automated scoring protocol for the Metafer-System was used for all CBMN assay studies. The method is described in detail in chapter 2 (section 2.2.2). For the CBMN assay a minimum of 4000 cells per replicate were scored (exceptions where stated, for details see Appendix I). Three independent experiments were carried out.

5.2.6 Cytotoxicity

RPD was used to measure cell death and cytostasis. The method is described in detail in chapter 2 (section 2.2.3).

5.2.7 Pan-centromeric staining

Centromeres were stained to classify araC as a clastogenic or aneugenic chemical with RTU human pan-centromeric probe. The method is described in detail in chapter 2 (section 2.2.4). Nuclei were counterstained with DAPI and 100 MN per dose were scored as positive or negative for the centromeric stain under a BX50 fluorescent microscope (Carl Zeiss) (exceptions where stated, for details see Appendix IV).

5.2.8 Statistical analysis

Statistical analysis is described in detail in chapter 2 (section 2.2.17). Further assessment of data used the BMD model (Gollapudi et al., 2013).

5.3 Results

The *in vitro* CBMN assay was used to investigate the low dose response relationships of araC induced DNA damage. AraC is a nucleoside analogue and used as a chemotherapeutic agent (Fenech et al., 1994; Cariou et al., 2010).

5.3.1 Chromosome aberration induction by araC in human lymphoblastoid cells

Extended treatments were used for the investigation of the low dose response curve for araC, due to the mechanism of action of araC, more than one cell cycle is needed for chromosome damage to be expressed. In this study all the work was based on automated analysis with the Metafer-System.

TK6 cells treated with araC for 24h over a range of concentrations between 0 and 0.1µg/ml, followed by one cell cycle of cytochalasin B showed significant increases in MN induction at the top doses, at 0.03 and 0.07µg/ml araC. Furthermore ≥50±5% cell death and cytostasis was observed at around 0.07µg/ml (62.5% at 0.07µg/ml and 74.1% at 0.1µg/ml) araC and above (Figure 5.2).

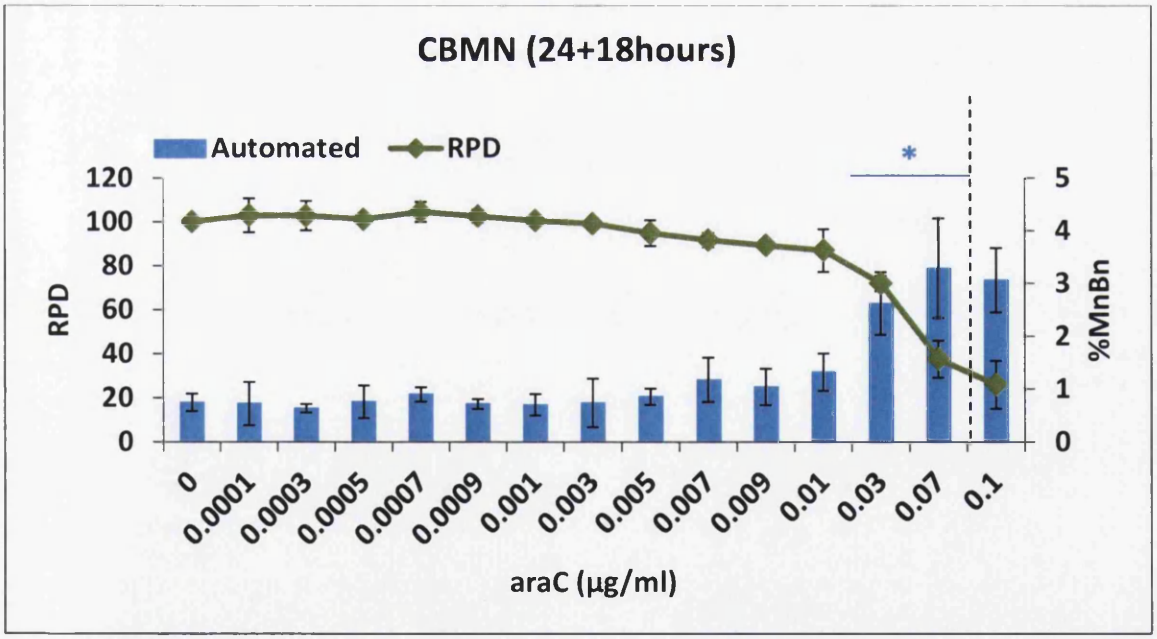

Figure 5.2: Effect of araC on TK6 cells using the CBMN assay. TK6 cells were treated with araC for 24h, followed by 18h of CytoB. Blue: percentage micronucleated binucleated cells, green: Relative population doubling (RPD). Values represent mean ± SD (n=3). (*) Represents $p<0.05$.

Further, TK6 cells treated with araC for 48h with 0 to 0.1µg/ml araC, followed by 18h of cytochalasin B showed similar results to the 24h treatment experiment. A significant increase in MN induction was only seen at 0.07µg/ml araC. In addition, 50±5% (49.3%) toxicity were observed around 0.07µg/ml (Figure 5.3)

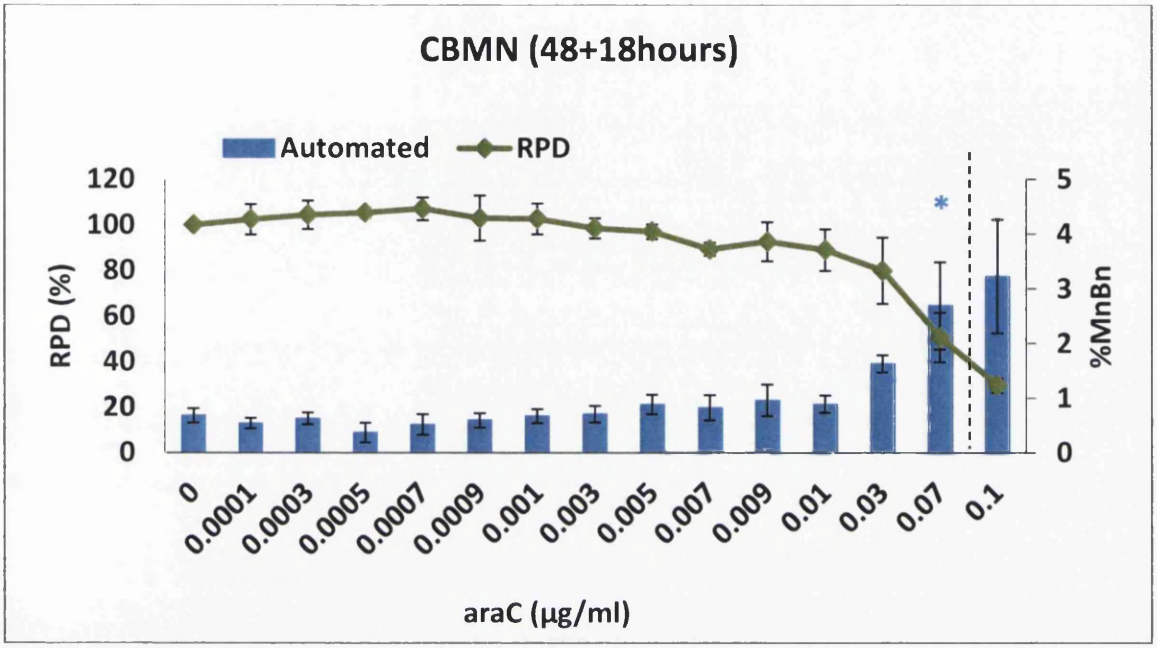

Figure 5.3: Effect of araC on TK6 cells using the CBMN assay. TK6 cells were treated with araC for 48h, followed by 18h of CytoB. Blue: percentage micronucleated binucleated cells, green: Relative population doubling (RPD). Values represent mean ± SD (n=3). (*) Represents $p<0.05$.

To compare the results gained in TK6 cells to other cell backgrounds, the human lymphoblastoid cell lines AHH-1 and MCL-5 were treated with low concentrations of araC. These cell lines have a heterozygous p53 mutation at codon 282 on exon 8. MCL-5 cells are a derivative of AHH-1 cells with metabolic capacity.

AHH-1 cells treated with araC for 24h over a range of concentrations between 0 and 0.2µg/ml araC followed by one cell cycle of araC (22h) showed increases in MN induction at the top doses. At 0.2µg/ml 22% toxicity were observed (Figure 5.4). These cells were able to tolerate slightly higher concentrations of araC before toxicity and MN induction was seen.

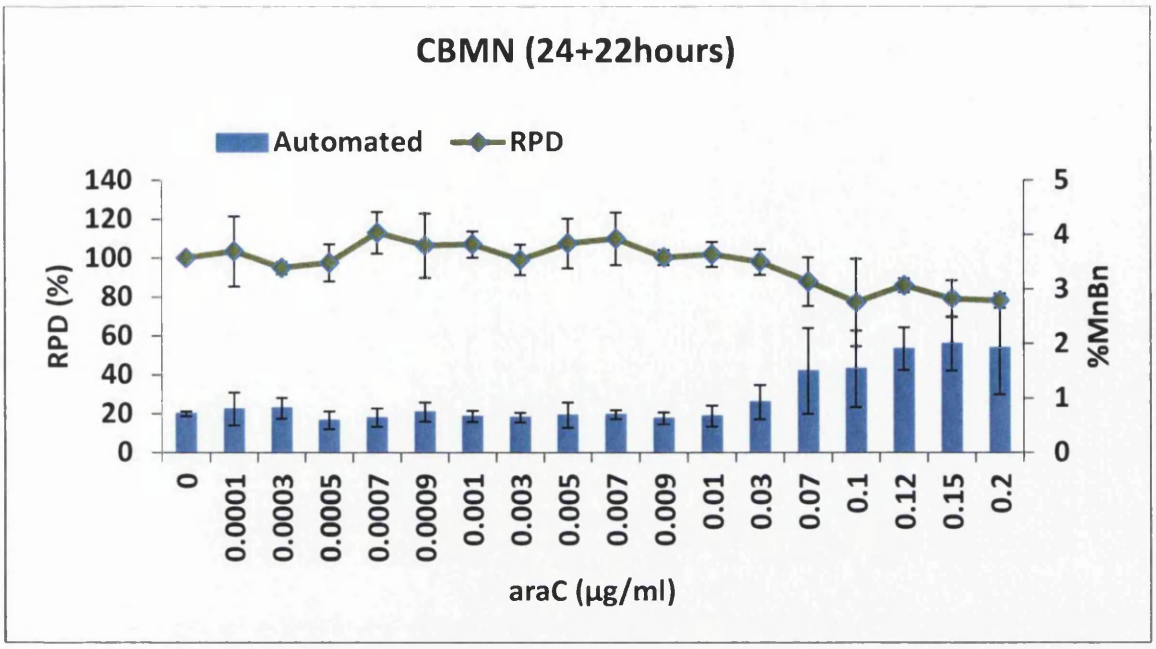

Figure 5.4: Effect of araC on AHH-1 cells using the CBMN assay. AHH-1 cells were treated with araC for 24h, followed by 22h of CytoB. Blue: percentage micronucleated binucleated cells, green: Relative population doubling (RPD). Values represent mean ± SD (n=3).

Further, MCL-5 cells treated with araC over a range of concentrations between 0 and 0.1µg/ml, followed by 22h (one cell cycle) of cytochalasin B showed, like TK6 cells, significant increases in MN induction around 0.07µg/ml araC and above. In addition, 40.7% cell death and cytostasis were reached at 0.1µg/ml araC (Figure 5.5), which was at a slightly higher concentration than in TK6 cells.

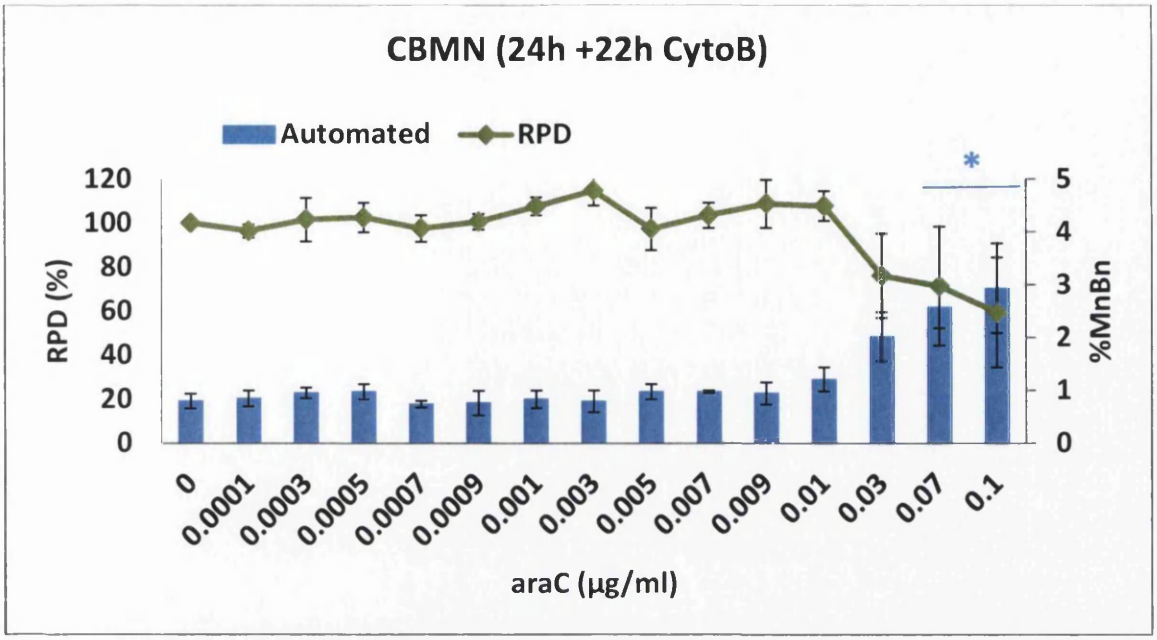

Figure 5.5: Effect of araC on MCL-5 cells using the CBMN assay. MCL-5 cells were treated with araC for 24h, followed by 22h of CytoB. Blue: percentage micronucleated binucleated cells, green: Relative population doubling (RPD). Values represent mean ± SD (n=3). (*) Represents $p<0.05$.

The human lymphoblastoid cell lines TK6 and MCL-5 showed similar low dose responses after treatment with the nucleoside analogue araC. Significant increases in MN induction were only observed at the higher end of the concentration range with increases in cell death and cytostasis, whereas at the lower range of concentrations no increases in MN induction and/or toxicity over the background level were observed. NOELs and LOELs identified in TK6 and MCL-5 cells after araC treatment are summarized in Table 5.1. Further AHH-1 cells treated with TK6 showed only increases in MN induction at the higher range of concentrations.

Table 5.1: NOELs and LOELs identified after araC treatment

Treatment	NOEL	LOEL
TK6: 24h + 18h	0.01µg/ml	0.03µg/ml
TK6: 48h + 18h	0.03µg/ml	0.07µg/ml
MCL-5: 24h + 22h	0.03µg/ml	0.07µg/ml

5.3.2 AraC- A clastogenic or aneugenic chemical?

Human chromosome pan-centromeric staining was used to determine if the MN induced by araC were predominantly due to incorporation of whole chromosomes, which were unable to incorporate into the main nuclei (aneuploidy) or due to chromosome breaks (clastogenicity). TK6 cells treated with 24h of araC, followed by one cell cycle of cytochalasin B showed a slight increase in pan-centromeric negative MN over the range of concentrations (0 to 0.03µg/ml) within an acceptable toxicity range (Figure 5.6). From this it followed, that the MN induced by araC were predominantly originating from chromosome fragments lacking a centromere (clastogenic).

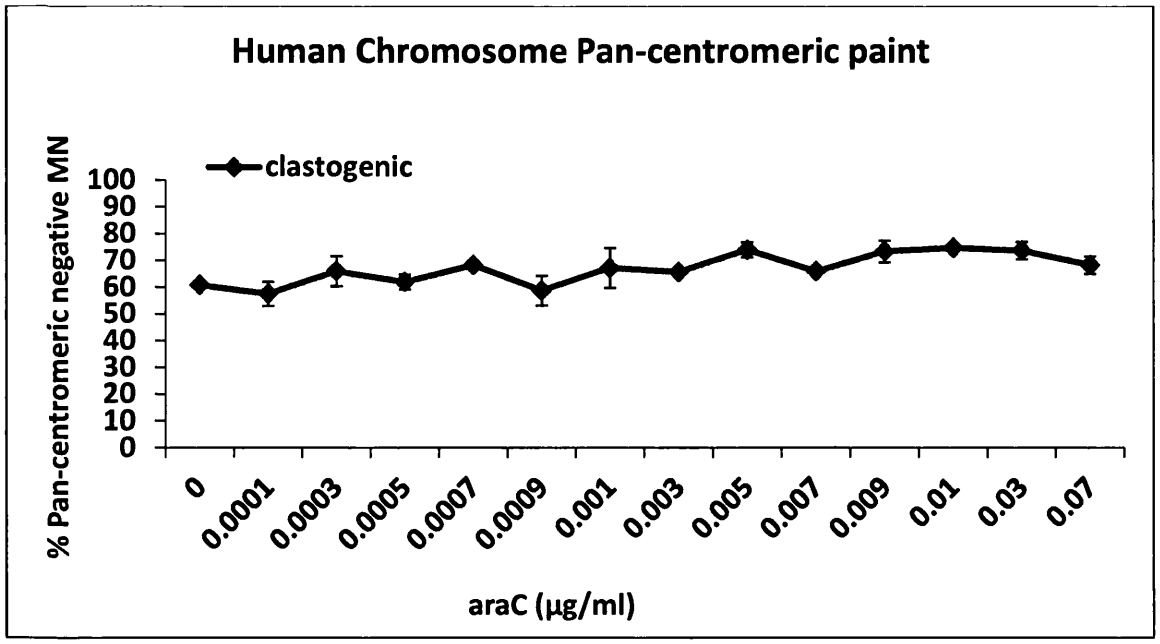

Figure 5.6: Human chromosome pan-centromeric staining of TK6 cells treated with 24h of araC, followed by 18h of cytochalasin B. Values represent mean and range of duplicate experiments.

5.3.3 Assessment of the low dose response relationship of araC in human lymphoblastoid cells

Human lymphoblastoid cells treated with araC and one cell cycle of cytochalasin B showed significant increases in MN frequencies only at higher concentrations, whereas at the lower range of concentrations no increases in MN could be found over the background level (Figure 5.2 to 5.5). Therefore the dose responses were further assessed by quantitative means using BMD modelling.

The BMD for the dose response data in TK6 cells treated with 24h of araC followed by 18h of cytochalasin B was calculated at 0.001µg/ml with its confidence intervals between 0.0007 ($BMDL_{10}$) and 0.002µg/ml (Figure 5.7).

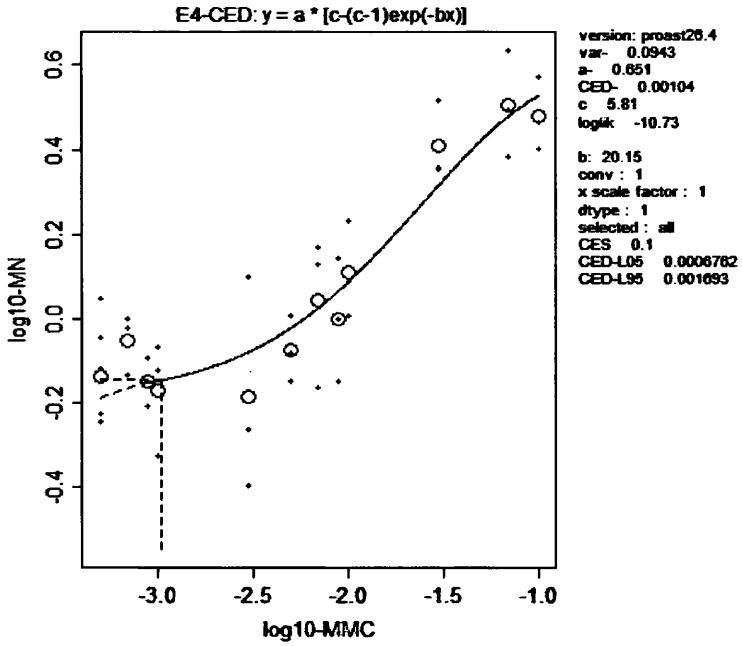

Figure 5.7: BMD dose response modelling results for MN induction in TK6 cells treated with araC for 24h. The BMD was calculated at 0.001µg/ml with its confidence intervals between 0.0007 and 0.002µg/ml.

The BMD for the dose response data in TK6 cells treated with 48h araC was calculated at 0.001µg/ml, same as the 24h treatment, with its confidence intervals between 0.0008 ($BMDL_{10}$) and 0.002µg/ml (Figure 5.8).

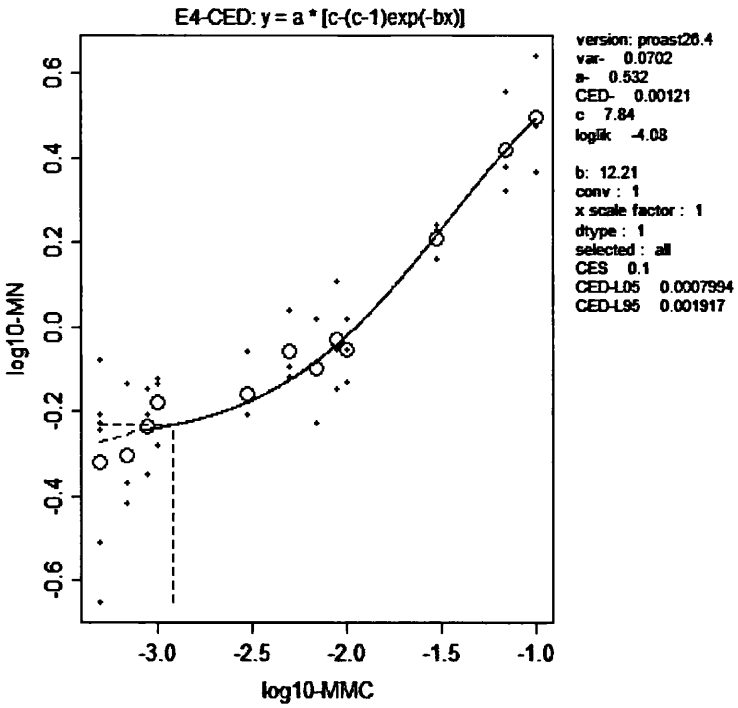

Figure 5.8: BMD dose response modelling results for MN induction in TK6 cells treated with araC for 48h. The BMD was calculated at 0.001µg/ml with its confidence intervals between 0.0008 and 0.002µg/ml.

The BMD for the dose response data generated in AHH-1 cells was calculated at 0.007µg/ml with its confidence intervals between 0.004 ($BMDL_{10}$) and 0.01µg/ml (Figure 5.9).

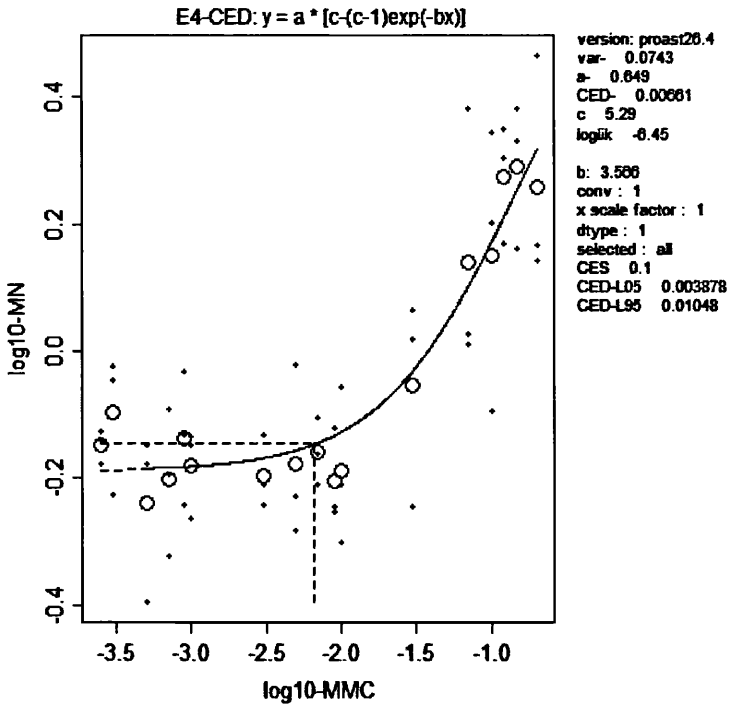

Figure 5.9: BMD dose response modelling results for MN induction in AHH-1 cells treated with araC for 24h. The BMD was calculated at 0.007µg/ml with its confidence intervals between 0.004 and 0.01µg/ml.

The BMD for the dose response data in MCL-5 cells was calculated at 0.005µg/ml with its confidence intervals between 0.003 ($BMDL_{10}$) and 0.008µg/ml (Figure 5.9).

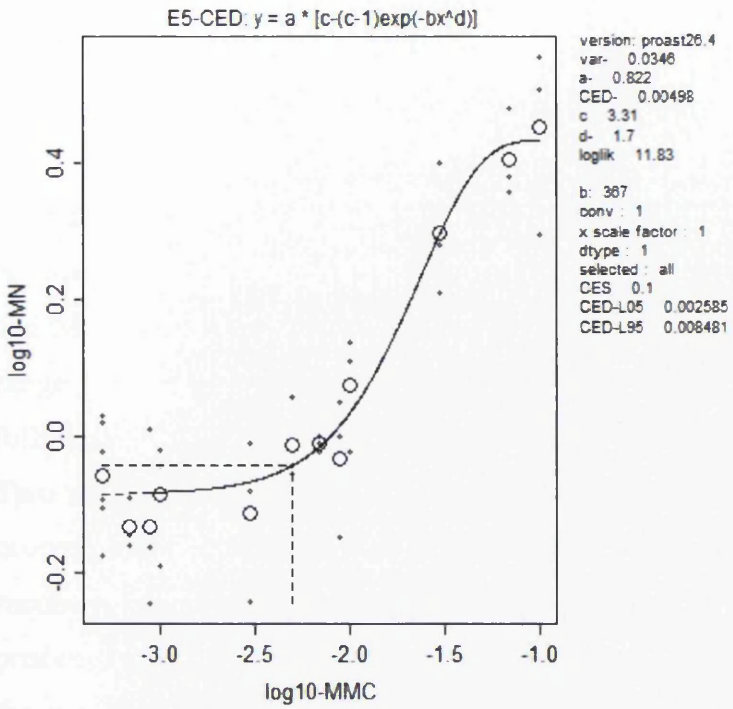

Figure 5.10: BMD dose response modelling results for MN induction in MCL-5 cells treated with araC for 24h. The BMD was calculated at 0.005µg/ml with its confidence intervals between 0.003 and 0.008µg/ml.

The assessment of the low dose response relationship of araC in the human lymphoblastoid cells TK6, AHH-1 and MCL-5 provided similar results. Non-linear dose responses after araC treatment were observed. The assessment results are summarized in Table 5.2.

Table 5.2: The BMD analysis for the MN endpoint induced by araC

araC	Cell line	Units	BMD	$BMDL_{10}$	$BMDU_{10}$
24+18h	TK6	µg/ml	0.001	0.0007	0.002
48+18h	TK6	µg/ml	0.001	0.0008	0.002
24+22h	AHH-1	µg/ml	0.007	0.004	0.01
24+22h	MCL-5	µg/ml	0.005	0.003	0.008

5.4 Discussion

The human lymphoblastoid cell lines TK6, AHH-1 and MCL-5 were treated with araC to investigate the low dose response for this chemical, using the *in vitro* MN assay.

5.4.1 Low dose response relationships of araC

Non-linear dose responses of araC were observed after extended treatments in TK6, AHH-1 and MCL-5 cells. Significant increases in MN induction were only seen at the higher dose range. TK6 cells treated with araC for 24h or 48h and MCL-5 cells treated with 24h of araC, followed by one cell cycle of cytochalasin B showed a LOEL at 0.03 to 0.07 µg/ml araC.

Two mechanisms are responsible for the transport of araC into the cell: a carrier-mediated process and simple diffusion (Cheng and Capizzi, 1982). The carrier-mediated transport mechanism predominates at low concentrations of araC. However the efficiency of this process depends on the binding affinity of araC for the carrier, the number of molecules of the carrier in the membrane and the presence of competing nucleosides (Cheng and Capizzi, 1982). Simple diffusion is the predominant mechanism for cell entry at higher concentration of araC (Cheng and Capizzi, 1982). Therefore, at low concentrations of araC cells might be resistant to araC due to the decreased efficiency of the carrier-mediated transport, whereas at higher concentrations araC might simply pass though the cell membrane by diffusion.

Furthermore two main hypotheses for the inhibitory effect of araCTP on DNA synthesis were proposed. The first one proposes that araC inhibits the DNA polymerase by competing with the binding of dCTP to this enzyme (Kufe and Major, 1982). However kinetic studies revealed that araCTP is a weak competitive inhibitor, with the binding affinity of araCTP and dCTP for the catalytic site of DNA polymerase being the same (Momparler, 1982). From this it follows that at low concentrations of araC the inhibition of DNA syntheses might be low.

The second hypotheses proposes the inhibition of DNA synthesis by araCTP through its incorporation into the DNA strand, which could result in either chain termination or slowing of chain elongation (Kufe and Major, 1982). However, it was shown that low concentrations of araC can inhibit DNA synthesis without producing cell death (Momparler, 1982). From this it follows that DNA repair mechanisms may exist, which can reduce the cytotoxic action of this chemical by removing it enzymatically from DNA (Momparler, 1982). In conclusion, NOELs may exist for the nucleoside analogue araC.

Increases in MN induction were observed at the higher range of concentrations chosen in all cell lines tested. It was shown by Fenech and Neville (1992) that araC inhibits the gap-filling

step during excision repair, which results in the formation of single-strand breaks at repair sites. The single-strand breaks could then be converted to chromatid or chromosome breaks and subsequently into MN on completion of nuclear division (Fenech and Neville, 1992; Fenech et al., 1994). Two possible ways of MN induction through araC were proposed. Excision-repairable DNA lesions on the DNA, caused endogenous or exogenous, are repaired in the presence of araC, which inhibits the gap-filling step, resulting in a single-strand break at the lesion side. The single-strand break can then be converted to a double-strand break at S-phase or can be converted to a double-strand break following endonuclease attack following S-phase, resulting in acentric chromatid fragments, which can be expressed as a micronucleus (Fenech et al., 1994). Further araC can induce MN directly by inhibiting the repair and/or re-joining of DNA strand breaks (Fenech et al., 1994).

Furthermore Fenech *et al.* (1994) showed that the majority of araC induced MN originate from acentric fragments using anti-kinetochore antibodies. This was confirmed in this study through pan-centromeric painting. With increases in concentration, the proportion of centromere negative MN increased, even though there was overall low MN induction, confirming that araC predominantly induces MN via chromosome breakage and not aneuploidy.

In addition, the study revealed that TK6 cells were a more sensitive test system compared to MCL-5 and particularly AHH-1 cells. MCL-5 and AHH-1 cells showed less cytotoxicity than TK6 cells. TK6 cell are p53 competent, whereas AHH-1 and its derivative MCL-5 are heterozygous for TP53 (Guest and Parry, 1999). The tumour suppressor gene TP53 is an important regulatory molecule, because of its involvement in the response to DNA damaging agents (Morris et al., 1996). p53 is involved in maintaining the integrity of the G_1 checkpoint in the cell cycle by up-regulating the synthesis of $p21^{WAF\text{-}1/IP\text{-}1}$ gene product and further in the signalling of damaged or unwanted cells into apoptosis (Morris et al., 1996). It is therefore likely that MCL-5 and AHH-1 cells are less susceptible to the induction of cell death (apoptosis). However Guest and Parry (1999) showed that the presence of the mutation in AHH-1 and MCL-5 cells has no influence of the DNA damage induced cell death pathway and that the reduced capacity of the G0/G1 checkpoint after p53 induction through a chemical exposure may not mean that the TP53 gene has lost its function. Further it is known that sensitivity to MN induction and cytotoxicity are highly dependent on the cell type.

5.4.2 Dose response relationship assessment of araC

The data for all the cell lines tested were further assessed for quantitative dose using BMD modelling (Table 5.2 and Figures 5.7 to 5.10).

As previously mentioned, BMD modelling estimates a dose that produces predetermined biologically relevant increases in the response over the control and the $BMGL_{10}$ refers to the estimate of lower 90% confidence interval of a dose that produces a 10% increase over the fitted background level for continuous endpoints (Gollapudi et al., 2013). The $BMGL_{10}$ in TK6 cells treated with araC was 0.0007/0.0008µg/ml, in AHH-1 0.004µg/ml and in MCL-5 cells 0.003µg/ml, which was in line with the observed genotoxicity data gained in this study (Figures 5.2 to 5.5).

In conclusion, the dose response data in this study for TK6, MCL-5 (and MCL-5) cells treated with araC showed clear NOELs and LOELs. Mechanistic experiments have to be applied to prove if araC causes no adverse effects over the background at the low dose range.

5.5 Summary

In this chapter the dose response relationships after araC treatment were explored at the low dose range in the human lymphoblastoid cell lines TK6, AHH-1 and MCL-5. Non-linear dose responses, with increases in MN induction only at the higher dose range, were observed in all cell lines tested. Further clear NOELs and LOELs were identified in TK6 and MCL-5 cells treated with araC.

RPD was used to set robust toxicity parameters to avoid the confounding effect of toxicity on chromosome breakage and/or whole chromosomes, which were unable to incorporate into the main nuclei during cell division.

In addition, it was observed that araC is a clastogenic chemical that induces MN mainly due to chromosomal breakage and not through aneuploidy.

Chapter 6

The role of p53 in the low dose mutagenic relationships of MMC and araC

6.1 Introduction

The human lymphoblastoid cell lines TK6, AHH1 (and MCL-5) showed non-linear dose responses in DNA damage induction after treatment with MMC and araC at the low dose range (see chapter 3 and 5).

Natural defence mechanisms, like epithelial barriers to genotoxin entry, chemical detoxification, DNA redundancy or DNA repair corroborate the theory of genotoxic thresholds (Jenkins et al., 2010). In addition the tumour suppressor gene *TP53* plays a key role in cellular integrity, because of its involvement in the response to DNA damaging agents, with an integral function in transducing signals from damaged DNA to genes that control the cell cycle and/or lead to apoptosis (Guest and Parry, 1999).

Therefore in this chapter, the role and involvement of p53 in the low dose response relationships after treatment with MMC and araC was investigated.

6.1.1 p53

The tumour suppressor gene *TP53* plays an essential role in cellular integrity and inactivation of the gene by mutations is the most frequent alteration in human cancers (Kato et al., 2003). p53 is a transcriptional activator that regulates the expression of various genes involved in cell cycle arrest and apoptosis in response to genotoxic and cellular stress, which prevents damaged DNA from being replicated (Arrowsmith, 1999).

The *TP53* gene encodes a 53kD phospho-protein, which is involved in cellular processes, such as gene transcription, DNA repair, cell cycle regulation, genomic stability, chromosomal segregation, senescence and apoptosis (Harris, 1996).

The human p53 protein consists of 393 amino acids with 4 highly conserved domains, which contribute to the DNA damage response (Harris, 1996; Amundson et al., 1998; Joerger and Fersht, 2007).

The N terminal region (residues 1-62), which is required for transcriptional transactivation, contains the transactivation domain, followed by a proline-rich region (residues 63-94) (Amundson, 1998; Joerger and Fersht, 2007). The transactivation domain interacts with regulatory proteins, like MDM2 (a regulator of cellular levels of p53), or components of the

transcription initiation complex and acetyltransferases, which act as co-activators and regulate p53 function through acetylation of the p53 C-terminus, while the proline-rich region contains SH3-domain binding motifs (Joerger and Fersht, 2007). The central core domain (residues 94-292) is a sequence-specific DNA binding domain and binds specifically to double-stranded DNA, while the C-terminus, which interacts directly with single-stranded DNA, contains the tetramerization domain (residues 325-356) and the negative auto-regulatory domain. The tetramerization domain regulates the oligomerization state of p53, while the negative auto-regulatory domain contains acetylation sites and binds DNA non-specifically (Amundson et al., 1998; Joerger and Fersht, 2007). The cellular p53 protein levels are tightly regulated and post-translational modification of the protein as well as alternative splicing and binding of regulatory proteins modulate the activity of p53 (Pucci et al., 2000; Joerger and Fersht, 2007). Thus, mutations in the gene disrupt the ability of p53 to bind to DNA and consequently to transactivate downstream genes (Kato et al., 2003).

p53 predominately acts at the DNA damage checkpoint in the cell cycle, influencing cell proliferation. p53 is activated by DNA damage and initiates the transcription of p21, which results in G1 cell cycle arrest (Schafer, 1998; Pucci et al., 2000). It can also act at the G2/M checkpoint, inducing cell-type specific G2 arrest. The G2/M checkpoint seems to be activated when DNA synthesis is blocked to prevent segregation of damaged or incompletely synthesised DNA (Pucci et al., 2000).

Furthermore p53 is involved in the spindle checkpoint through inhibition of entry into S-phase and plays a role in centrosome duplication, by preventing mitotic failure through regulation of the number of centrosomes (Pucci et al., 2000).

In addition, p53 plays a major role in inducing apoptosis by DNA damage, hypoxia or withdrawal of growth factors (Pucci et al., 2000).

6.1.2 The cell cycle

The cell cycle is a complex process involved in cell growth and proliferation, regulation of DNA repair, tissue hyperplasia as a result of injury and diseases like cancer (Schafer, 1998).

Numerous mechanisms control the cell cycle to ensure correct cell division. Cell division is characterised by DNA replication and segregation of replicated chromosomes into two separate cells (Vermeulen et al., 2003). Cell division consists of two stages: mitosis (M-phase) and interphase.

Mitosis is the process of nuclear division and stages of mitosis include prophase, metaphase, anaphase and telophase. During mitosis the chromosomes condense and after spindle

assembling they attach to the spindle, align at the cell equator and move as spindle microtubules retreat towards opposite poles of the cell, where they get surrounded by a nuclear membrane, resulting in two identical daughter cells (Nature Education, 2012).

The interphase is composed of the G1, S and G2 phase. S-phase is preceded by a gap (G1) during which the cells prepare for DNA synthesis and is followed by another gap (G2) during which the cells prepare for mitosis (Vermeulen et al., 2003). During S-phase DNA gets synthesized and therefore cells have a DNA content between 2N and 4N (Schafer, 1998).

Furthermore cells can enter a resting state (called G0) in G1 before commitment to DNA replication. Cells in G0 are non-growing and non-proliferating cells (Vermeulen et al., 2003).

6.1.2.1 Regulation of the cell cycle

The standard cell cycle consists of the phases G1, S, G2 and M and the transition from one phase to another occurs in order and is regulated by cellular proteins. Cyclin-dependent kinases (CDK) are the key regulatory proteins of the cell cycle (Vermeulen et al., 2003). CDKs, a family of serine/threonine protein kinases, are activated at specific points in the cell cycle, through cyclins. The CDK protein levels remain stable, while cyclin protein levels rise and fall during the cell cycle, resulting in periodical activation of CDK (Vermeulen et al., 2003).

Different cyclins are required at different phases of the cell cycle (Figure 6.1). Cells can only enter the next cell cycle stage, if the appropriate cyclin of the previous phase is degraded, and the cyclin of the next phase is synthesized (Schafer, 1998).

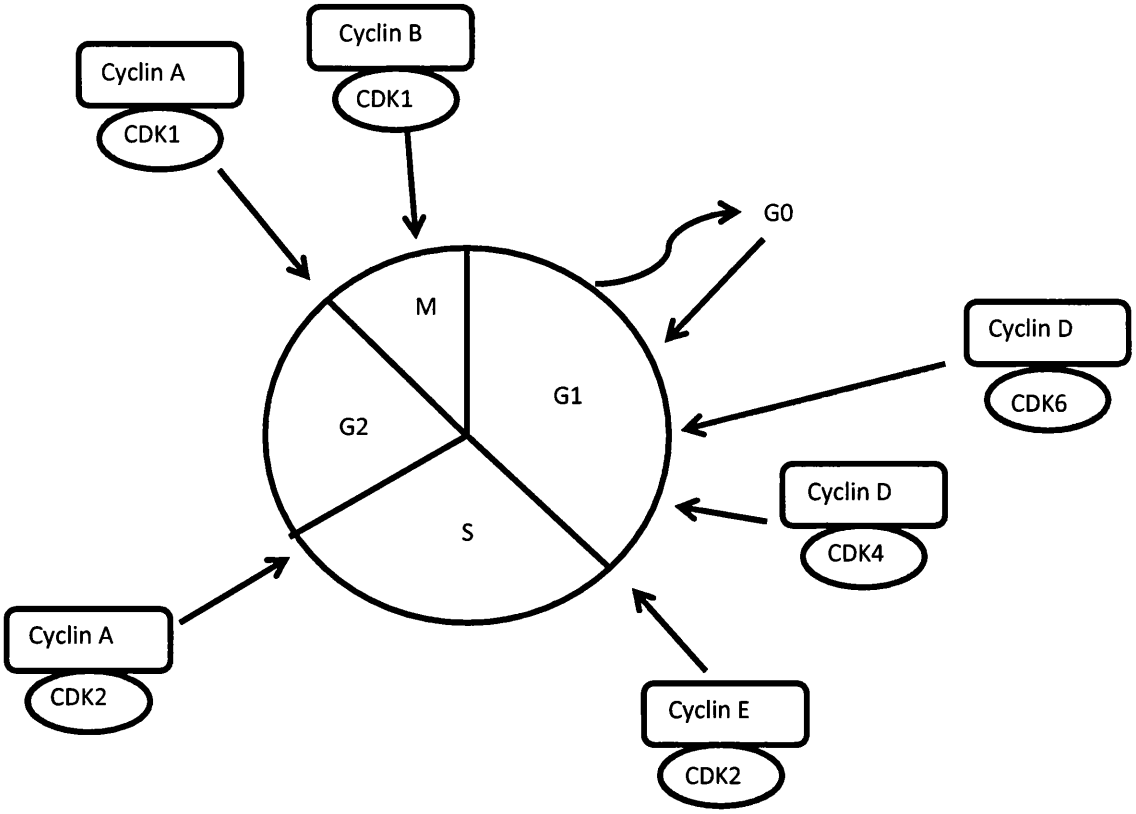

Figure 6.1: Regulation of the cell cycle by cyclin dependent protein kinases (CDKs) and cyclins

The CDK-cyclin D complexes are essential for the entry in G1, while cyclin E, which associates with CDK2, regulates the progression from G1 into S phase. Further the CDK2-cyclin A complex is required during S phase, while in late G2 and early M, the CDK1-cyclin A complex promotes the entry into mitosis and the CDK1-cyclin B complex regulates mitosis (Vermeulen, et al., 2003).

Further CDK inhibitors (CKI) can regulate CDK activity through binding to CDK alone or CDK-cyclin complexes. Two families of CKIs have been discovered: the INK4 family and Cip/Kip family. The INK4 family (p15, p16, p18 and p19) forms stable complexes with the CDK enzyme before cyclin binding, while the Cip/Kip family (p21, p27, p57) inactivate CDK-cyclin complexes (Vermeulen et al., 2003).

6.1.2.2 Cell cycle restriction point and checkpoints

After passing the restriction point, which is a point of no return in G1, the cell is committed to enter the cell cycle. Cell cycle checkpoints (DNA damage and spindle checkpoints) then monitor progression through the cell cycle and act as gatekeepers to ensure the process occurs accurately at all stages (Vermeulen et al., 2003).

Cell cycle arrest in response to DNA damage provides time for DNA repair. There are two main DNA damage checkpoints, which are positioned before the cell enters the S phase (G1-S checkpoint) and/or after DNA replication (G2-M checkpoint) (Vermeulen et al., 2003). Arrest in G1 allows repair before DNA replication, while arrest in G2 allows repair before chromosome separation in mitosis. In addition cells can also arrest in S-phase, resulting in a prolonged S-phase with slowed DNA synthesis (Schafer, 1998).

The cell cycle arrest induced by DNA damage at the G1-S checkpoint is p53 dependent. Activated p53 stimulates the transcription of important genes, such as *p21*, *Mdm2* and *Bax*, which leads in the case of p21 (a CKI) to CDK inhibition and cell cycle arrest, preventing the replication of damaged DNA (Vermeulen et al., 2003). However in cases of severely damaged cells, p53 induces apoptosis by activating genes, like *Bax*, which are involved in apoptotic signalling (see Figure 6.2) (Vermeulen et al., 2003).

Cell cycle arrest at the G2-M checkpoint can be initiated in the presence or absence of p53. The entry into mitosis is inhibited through inhibitory phosphorylation or by sequestration of components of the CDK1-cyclin B complex outside the nucleus by protein kinases Chk1 and Chk2, which are activated by DNA damage (Vermeulen et al., 2003).

The spindle checkpoint arrests the cell cycle in metaphase after detecting improper alignment of the chromosomes on the mitotic spindle (Vermeulen et al. 2003). It was shown, that the mitotic arrest deficient (Mad) and the budding uninhibited by benomyl (Bub) proteins are activated after defects in microtubule attachment, resulting in the inhibition of the Cdc20 subunit of the anaphase-promoting complex, preventing metaphase-anaphase transition (Vermeulen, et al., 2003).

6.1.3 Apoptosis

Apoptosis or programmed cell death occurs normally during development, ageing and as a homeostatic mechanism to maintain cell populations in tissues (Fulda and Debatin, 2006; Elmore, 2007). Further apoptosis is also used as a defence mechanism in immune reactions or after cell damage by disease or noxious agents (Elmore, 2007).

Morphological changes of the cell include shrinkage and pyknosis, which is the result of chromatin condensation (Majno and Joris, 1995; Elmore, 2007). Furthermore plasma blebbing occurs, followed by karryorrhexis and separation of cell fragments into apoptotic bodies, which are then phagocytosed by macrophages, parenchymal cells or neoplastic cells (Elmore, 2007).

The apoptosis process is energy-dependent and involves the activation of a group of cysteine proteases (caspases). Caspases have proteolytic activity, they are synthesized as inactive proforms, but upon activation they cleave proteins at aspartic residues (Fulda and Debatin, 2006). The proteases are categorized into initiators (caspase-2,-8,-9,-10), effectors (caspase-3,-6,-7) and inflammatory caspases (caspase-1,-4,-5) (Elmore, 2007).

Two main apoptotic pathways are described: the extrinsic or death receptor pathway and the intrinsic or mitochondrial pathway (Elmore, 2007).

Transmembrane receptor-mediated interactions are involved in the extrinsic pathway (Figure 6.2), including death receptors, which are members of the tumour necrosis factor (TNF) receptor gene superfamily, containing more than 20 proteins with various biological functions (Fulda and Debatin, 2006; Elmore, 2007). The best characterised ligands and corresponding death receptors are FasL/FasR, TNF-α/TNFR1, Apo3L/DR3, Apo2L/DR4 and Apo2L/DR5 (Elmore, 2007). Upon ligand binding to the receptors, cytoplasmic adapter proteins are recruited. In the case of Fas ligand binding to Fas receptor, the adapter protein Fas-associated death domain (FADD) is recruited, whereas TNF ligand binding to the TNF receptor results in binding of the adapter protein TRADD (Elmore, 2007). Subsequently FADD associates with procaspase-8 and the death-inducing signalling complex (DISC) is formed, resulting in auto-catalytic activation of procaspase-8 (Elmore, 2007). The execution phase of apoptosis is then triggered, after caspase-8 is activated, by activating downstream effector caspases, such as caspase-3 (Fulda and Debatin, 2006).

The intrinsic pathway (Figure 6.2) involves non-receptor stimuli, specifically mitochondrial-initiated events that produce intracellular signals and act directly on target (Elmore, 2007). Negative signals, such as absence of growth factors or hormones and/or positive stimuli, like radiation or viral infection, can trigger apoptosis. The stimuli cause changes in the inner mitochondrial membrane, resulting in an opening of the mitochondrial permeability transition pore and releasing of two main groups of pro-apoptotic proteins from the intermembrane space into the cytosol (Elmore, 2007).

The first group contains cytochrome C, Smac/DIABLO and the serine protease HTrA2/Omi and activates the caspase-dependent mitochondrial pathway by cytochrome C binding and activation of Apaf-1 and procaspase-9, which leads to caspase-9 activation (Elmore, 2007). Caspase-3 activation is triggered through the formation of the cytochrome C/Apaf-1/caspase-9 apoptosome complex (Fulda and Debatin, 2006).

The second group of pro-apoptotic proteins (AIF, endonuclease G and CAD) are released from the mitochondria during apoptosis and cause DNA fragmentation and/or chromatin condensation after translocation to the nucleus (Elmore, 2007).

Members of the Bcl-2 protein family control and regulate the apoptotic mitochondrial events, while the tumour suppressor protein p53 plays a crucial role in regulating the proteins of the Bcl-2 family (Elmore, 2007). The Bcl-2 proteins regulate mitochondrial membrane permeability by cytochrome C release and can be either pro-apoptotic (Bax, Bak, Bid) or anti-apoptotic (Bcl-2, Bcl-x, BAG) (Elmore, 2007).

Furthermore the extrinsic and intrinsic pathway can also interact (Figure 6.2). An example is that mitochondrial damage in the Fas pathway is mediated by the caspase-8 cleavage of Bid (Elmore, 2007).

Both pathways end at the execution phase, which is considered the final pathway of apoptosis. Effector caspases, such as caspase-3 and caspase-6 activate the cytoplasmic endonuclease, which results in DNA fragmentation, degradation of cytoskeletal and nuclear proteins, formation of apoptotic bodies, expression of ligands for phagocytic cell receptors and lastly uptake by phagocytic cells (Elmore, 2007).

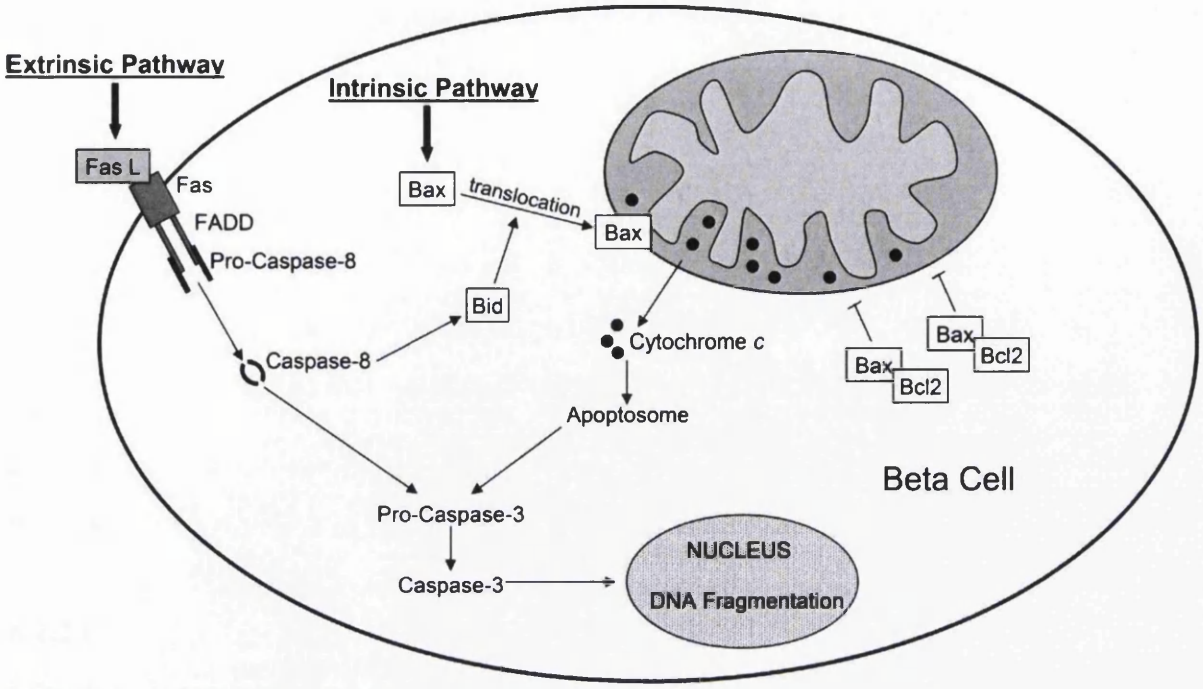

Figure 6.2: Schematic presentation of the extrinsic and the intrinsic pathway of apoptosis. The extrinsic pathway involves transmembrane receptor-mediated interactions, where upon ligand binding to the receptors, cytoplasmic adapter proteins are recruited; in the case of Fas ligand binding to Fas receptor, the adapter protein FADD is recruited and subsequently FADD associates with procaspase-8 and the DISC complex is formed, resulting in auto-catalytic activation of procaspase-8, which causes activation of either caspase-3 or truncation of Bid. The intrinsic pathway involves activation of the caspase-dependent mitochondrial pathway by cytochrome C binding and activation of Apaf-1 and procaspase-9, which leads to caspase-9 activation; caspase-3 activation is then triggered through the formation of the cytochrome C/Apaf-1/caspase-9 apoptosome complex (from Bruin et al., 2008).

6.1.4 Aim of study

The previous chapters assessed the low dose response relationships of MMC and araC in human lymphoblastoid cells, which were either p53 proficient (TK6) or heterozygous for p53 (AHH-1 and MCL-5), using the *in vitro* MN assay.

This study was designed to investigate the role of the tumour suppressor gene TP53 in the low dose relationships of MMC and araC, using *p21* gene and p53/phospho$^{(Ser15)}$-p53 protein expression analysis, as well as flow cytometry for analysis of apoptosis and cell cycle status. Furthermore DNA damage induction in MMC and araC treated cultures were compared in TK6 and NH32 cells (TK6 cells, which are p53 deficient), using the *in vitro* MN assay.

6.2 Material and Methods

6.2.1 Cell lines

The human lymphoblastoid cell lines TK6 (proficient for p53), AHH-1 (heterozygous for p53), MCL-5 (derivative of AHH-1, metabolically active, heterozygous for p53) and NH32 (TK6 cells deficient in p53) were used in this study. The cell lines were described in detail in chapter 2 (section 2.2.1).

NH32 cells are a derivative of TK6 cells with a double p53 knockout through a promoterless gene targeting approach (Chuang, et al., 1999; Hashimoto et al., 2011). The NH32 cell line was a kind gift from Prof. Dr. Gerald N. Wogan (MIT, Cambridge, MA, USA).

6.2.2 Cell culture

Cell culture and sub-culturing was performed as described in chapter 2 (section 2.2.1). NH32 cells were cultured in the same manner as TK6 cells.

6.2.3 Test chemical

MMC and araC were freshly diluted from a stock solution (1mg/ml aliquots) with water.

6.2.4 Test chemical dosing regime

For the Real-time PCR and Western Blot sections of work, TK6 and AHH-1 cells were treated with MMC for 4h with 0, 0.004, 0.008, 0.02, 0.04 and 0.08µg/ml MMC, whereas TK6, AHH-1 and MCL-5 cells were treated with araC for 24h with 0, 0.007, 0.005, 0.01, 0.07 and 0.1µg/ml araC.

Flow cytometry was used for the analysis of apoptosis and cell cycle status in TK6 cells. Therefore TK6 cells were treated with MMC for 4h and araC for 24h (with and without recovery time of 18h for the cell cycle study) over a range of concentrations between 0 and 0.1µg/ml.

For the *in vitro* CBMN assay NH32 cells were treated with MMC for 4h and with araC for 24h, followed by one cell cycle of cytochalasin B. NH32 cells were treated with MMC over a range of concentrations from 0 to 0.06µg/ml and araC with a dose range between 0 and 0.03µg/ml.

6.2.5 *In vitro* MN assay

The semi-automated scoring protocol for the Metafer-System was used for all CBMN assay studies. The method is described in detail in chapter 2 (section 2.2.2). For the CBMN assay a minimum of 4000 cells (NH32 cells) per replicate was scored (exceptions where stated, for details see Appendix I).Three independent experiments were carried out.

6.2.6 Cytotoxicity

RPD was used to measure cell death and cytostasis. The method is described in detail in chapter 2 (section 2.2.3).

6.2.7 RNA extraction

Total RNA was extracted from the human lymphoblastoid cell lines TK6 and AHH-1 after MMC treatment and TK6, AHH-1 and MCL-5 cells after araC treatment. The method is described in detail in chapter 2 (section 2.2.5).

After completing the RNA extraction the RNA content was measured and the purity was assessed (260:280 ratio) with a NanoDrop ND-1000 Spectrophotometer (Labtech International, Uckfield, UK). The RNA was stored at -80°C until further use.

6.2.8 Reverse Transcription with elimination of genomic DNA for Quantitative, Real-Time PCR

The mRNA from the total RNA extractions (see section 6.2.7) were reverse transcribed into cDNA by using the QuantiTect® Reverse Transcription Kit (Qiagen, Sussex, UK). The method is described in detail in chapter 2 (section 2.2.7).

6.2.9 Real-Time PCR

Real-time PCR was performed to quantify the gene expression of *p21*. For the Real-time PCR experiments the QuantiFast™ SYBR® Green PCR Kit (Qiagen, Sussex, UK) was used. The method is described in detail in chapter 2 (section 2.2.9).

6.2.10 Total protein extraction

All steps for the protein preparation were performed at 4°C; pre-cooled buffers and equipment were used. Details of the method are described in chapter 2 (section 2.2.12).

6.2.11 Protein Quantification

The BioRad DC Protein Assay (BioRad, Hertfordshire, UK) was used for the protein quantification and the details of the assay are described in chapter 2 (section 2.2.13).

6.2.12 Western blotting

With the help of the sodium dodecyl sulphate-polyacrylamide gel electrophoresis (SDS-PAGE) proteins could be analysed. They were separated according to their size and details of the method are described in chapter 2 (section 2.2.14).

6.2.13 Apoptosis analysis using flow cytometry

The induction of apoptosis in TK6 cells treated with either MMC or araC was investigated by using an AnnexinV-FITC antibody (Abcam, Cambridge, UK). After the initiation of apoptosis, cells translocate membrane phosphatidylserine (PS) from the inner layer of the plasma membrane to the cell surface, where it can be detected by staining with a fluorescent conjugate of AnnexinV, a protein with a high affinity to PS (Elmore, 2007). PI was used as a counterstain for the detection of dead cells.

The method is described in detail in chapter 2 (section 2.2.15).

6.2.14 Cell cycle analysis using PI staining

The cell cycle status, in TK6 cells treated with the test chemicals MMC and araC, was analysed by quantitation of DNA content using flow cytometry. Details of the method are described in chapter 2 (section 2.2.16).

6.2.15 Statistical analysis

The analysis of the data sets is described in detail in chapter 2 (section 2.2.17).

6.3 Results

In the previous chapters it was shown that human lymphoblastoid cell lines (TK6, AHH-1 and MCL-5) treated with MMC and/or araC follow non-linear dose responses for DNA damage induction, using the *in vitro* MN assay.

To summarize, TK6 and AHH-1 cells treated with MMC (0 to 0.1μg/ml) for 4h, followed by one cell cycle of cytochalasin B (see Figures 3.6 and 3.7), as well as TK6, AHH-1 and MCL-5 cells treated with araC (0 to 0.1μg/ml and up to 0.2μg/ml for AHH-1 cells) for 24h, followed by one cell cycle of cytochalasin B (see Figures 5.2, 5.4 and 5.5), showed increases in MN induction only at the higher concentrations, whereas at the lower range of concentrations no increases were observed. Further follow up experiments of the mechanism of action of the chemicals were needed for a better understanding of the dose response relationships. Consequently, in this chapter, the role and involvement of p53 was investigated.

6.3.1 p53 activation after MMC treatment

p53 stimulates the transcription of different genes, such as *p21*. The induction of p21, a cytokine kinase inhibitor (CKI), results in cytokine dependent kinase (CDK) inhibition and cell cycle arrest (Vermeulen et al., 2003). Thus, p53 activation was investigated by *p21* gene expression and p53/phospho-p53 (Ser15) protein expression analysis.

TK6 and AHH-1 cells were treated with MMC for 4h over a range of concentrations (0, 0.004, 0.008, 0.02, 0.04 and 0.08μg/ml) below and above the increase in MN induction observed in TK6 cells and below the increase in MN induction observed in AHH-1 cells for chromosome damage induction. No significant increases in *p21* gene expression were observed in either TK6 or AHH-1 cells (Figure 6.3).

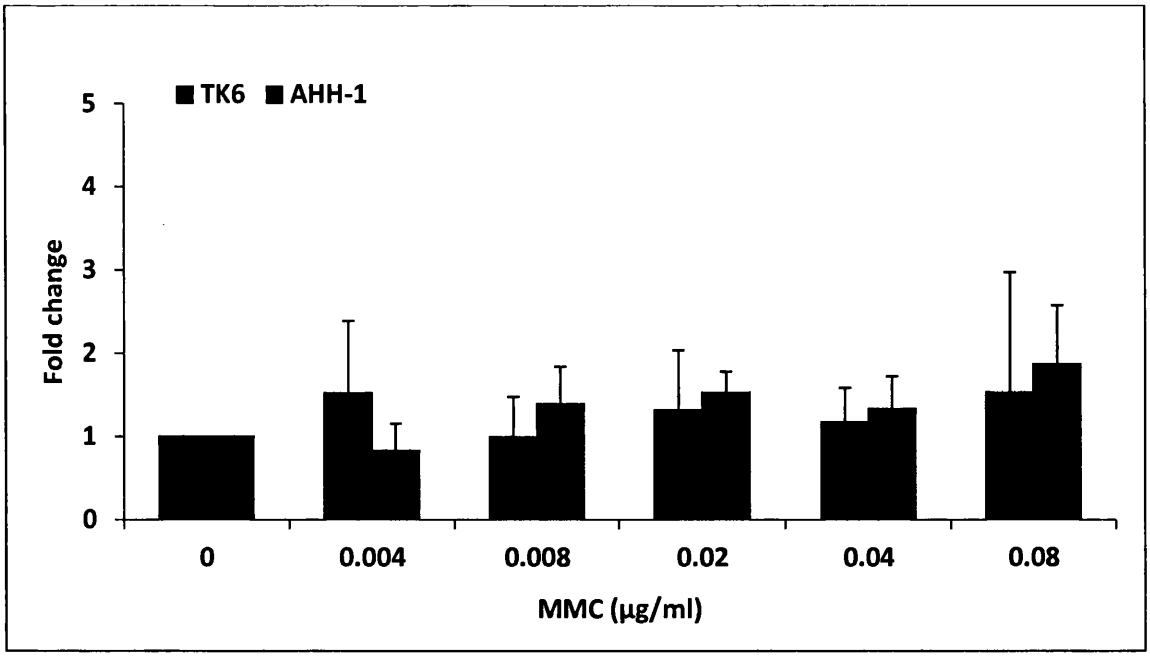

Figure 6.3: Relative fold change in *p21* gene expression in TK6 and AHH-1 cells, following exposure to increasing concentrations of MMC. Values represent mean ± SD (n=3)

However, an overall increase in phospho-p53 in TK6 cells with increasing doses of MMC was noticed (Figure 6.4). No increases in protein expression of either p53 and/or phospho-p53 (Ser15) were observed in AHH-1 cells (Figure 6.5).

A:

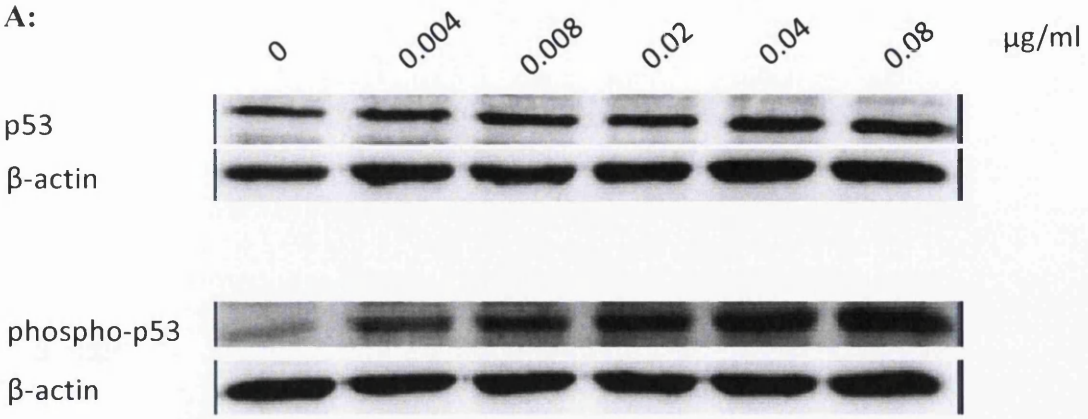

B:

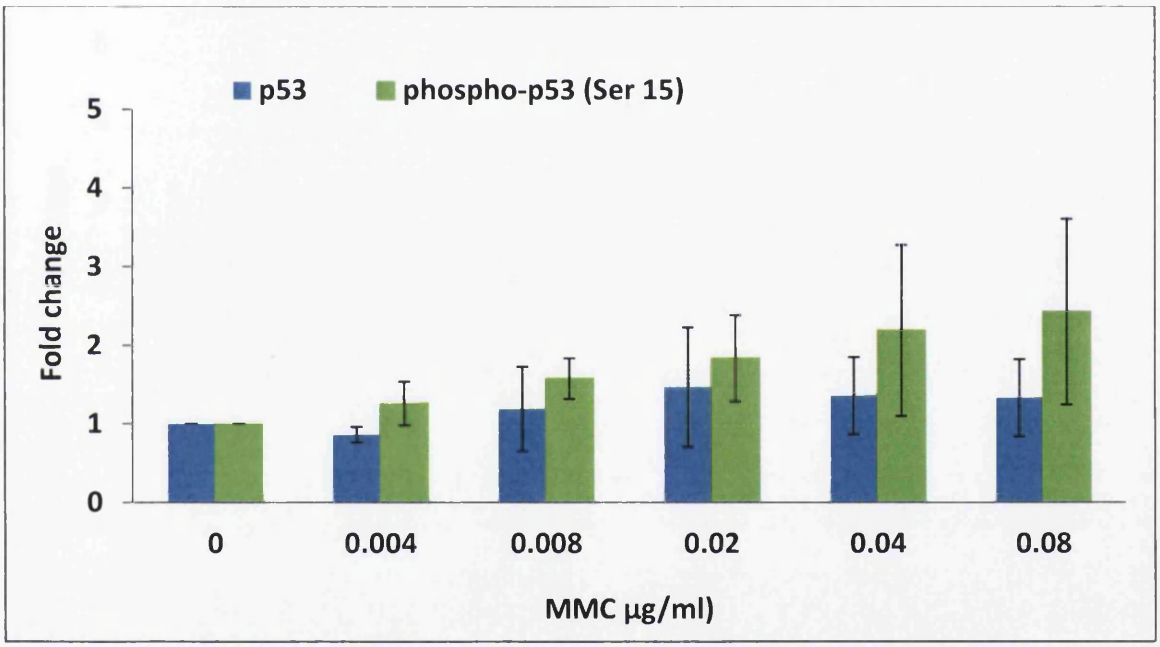

Figure 6.4: TK6 cells. A: Representative Western Blot for p53 and phospho-p53 (Ser15) following MMC treatment. B: Relative fold change in protein expression (represents the ratio of β-actin normalised treated band density to the untreated control band density. Values represent mean ± SD (n=3)

A:

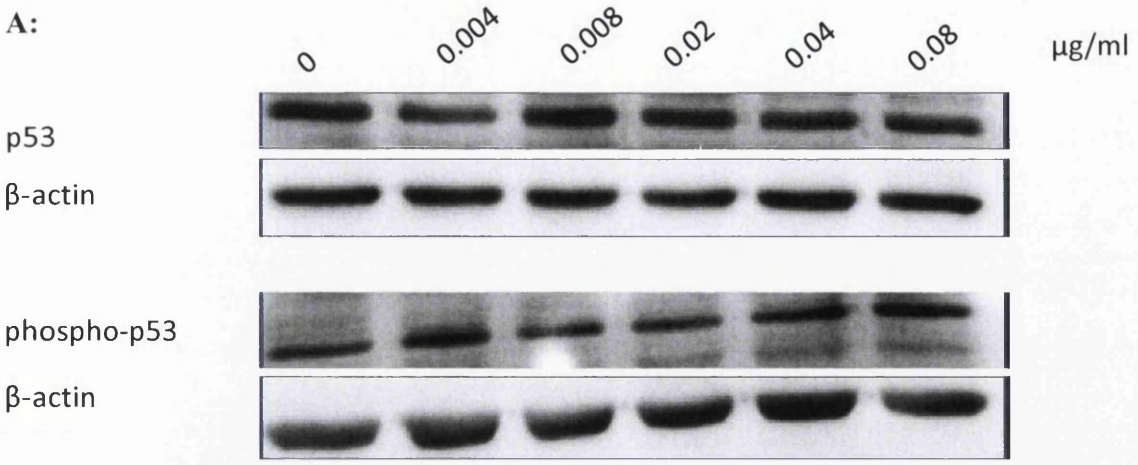

B:

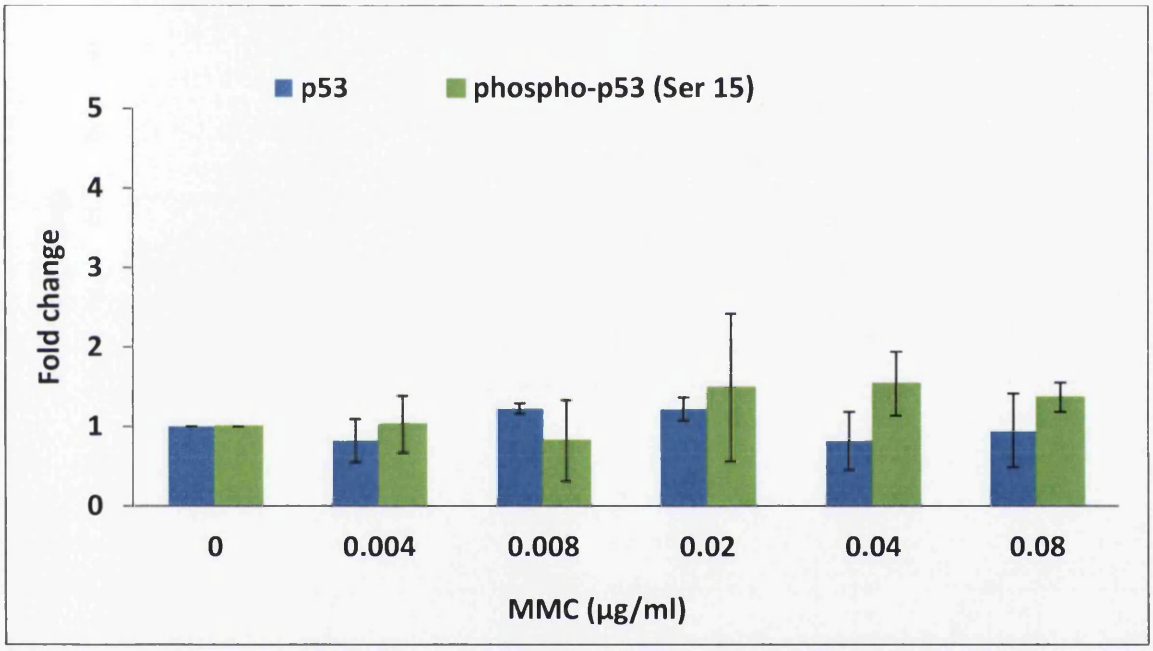

Figure 6.5: AHH-1 cells. A: Representative Western Blot for p53 and phospho-p53 (Ser15) following MMC treatment. B: Relative fold change in protein expression (represents the ratio of β-actin normalised treated band density to the untreated control band density). Values represent mean ± SD (n=3)

No p53 activation was observed in AHH-1 cells at doses which caused no chromosomal damage induction in the *in vitro* MN assay (see Chapter 3), whereas an overall increase in phospho-p53 (Ser15) was observed in TK6 cells at doses which caused increases in MN induction (see Chapter 3).

6.3.2 p53 activation after araC treatment

p53 activation was, as above, investigated by *p21* gene expression and p53/phospho-p53 (Ser15) protein expression analysis following exposure of cells to araC.

TK6, AHH-1 and MCL-5 cells were treated with araC for 24h over a range of concentrations (0, 0.0007, 0.005, 0.01, 0.07 and 0.1µg/ml) below and above the LOEL observed in TK6 and MCL-5 cells for chromosomal damage induction.

No significant increases in *p21* gene expression were observed in any of the cell lines investigated (Figure 6.6). However, an overall increase in *p21* gene expression, in particular in TK6 cells, was noticed with increasing doses of araC.

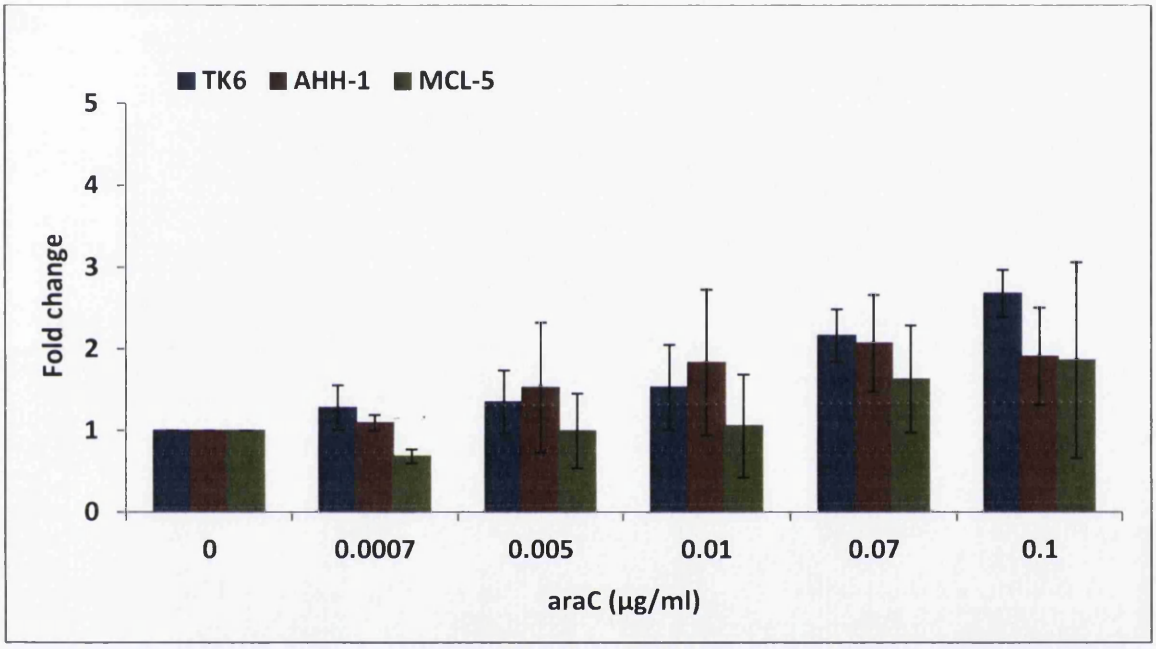

Figure 6.6: Relative fold change in *p21* gene expression in TK6, AHH-1 and MCL-5 cells, following exposure to increasing concentrations of araC. Values represent mean ± SD (n=3)

In addition, TK6 cells treated with araC for 24h showed high increases in p53 and phospho-p53 (Ser15) protein expression over the range of concentrations (Figure 6.7), whereas AHH-1 cells showed only increases in p53 protein expression at 0.1µg/ml araC (Figure 6.8), while MCL-5 cells treated with araC for 24h showed increases in p53 and phospho-p53 (Ser15) protein expression at the top concentrations of 0.07 and 0.1µg/ml (Figure 6.9).

A:

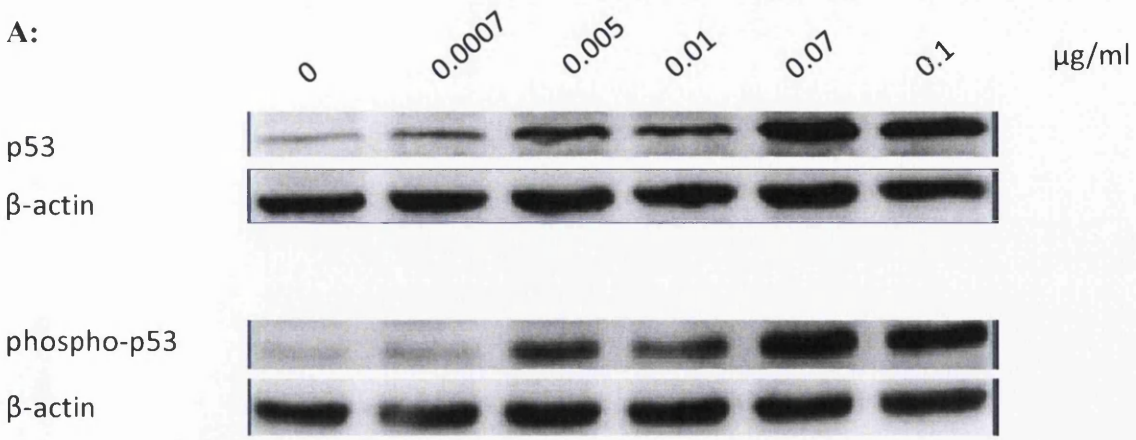

B:

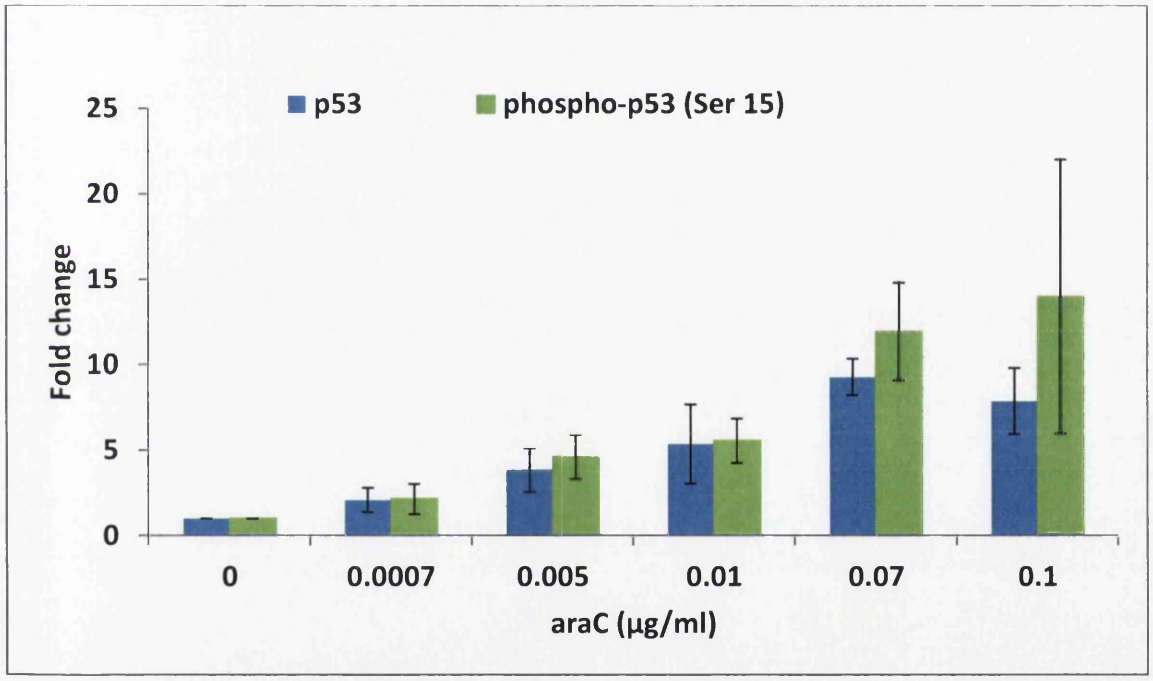

Figure 6.7: TK6 cells. A: Representative Western Blot for p53 and phospho-p53 (Ser15) following araC treatment. B: Relative fold change in protein expression (represents the ratio of β-actin normalised treated band density to the untreated control band density). Values represent mean ± SD (n=3)

A:

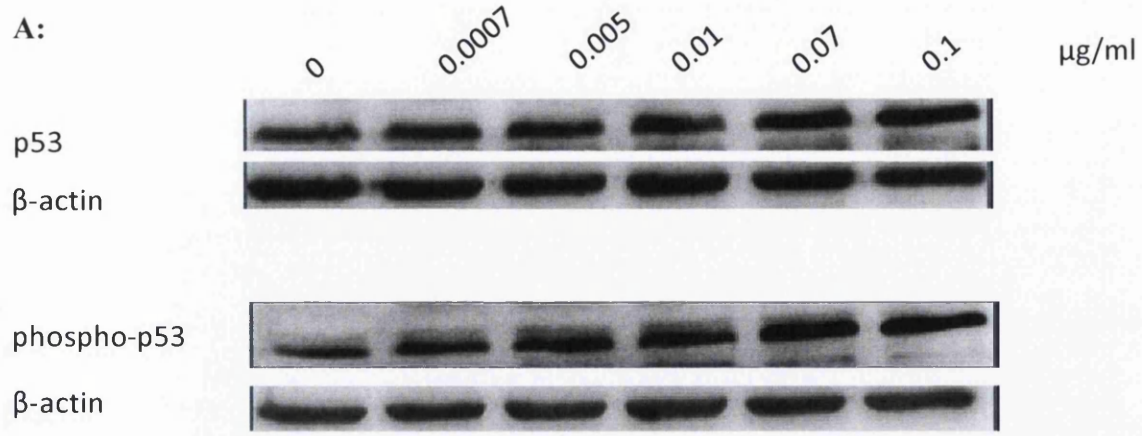

B:

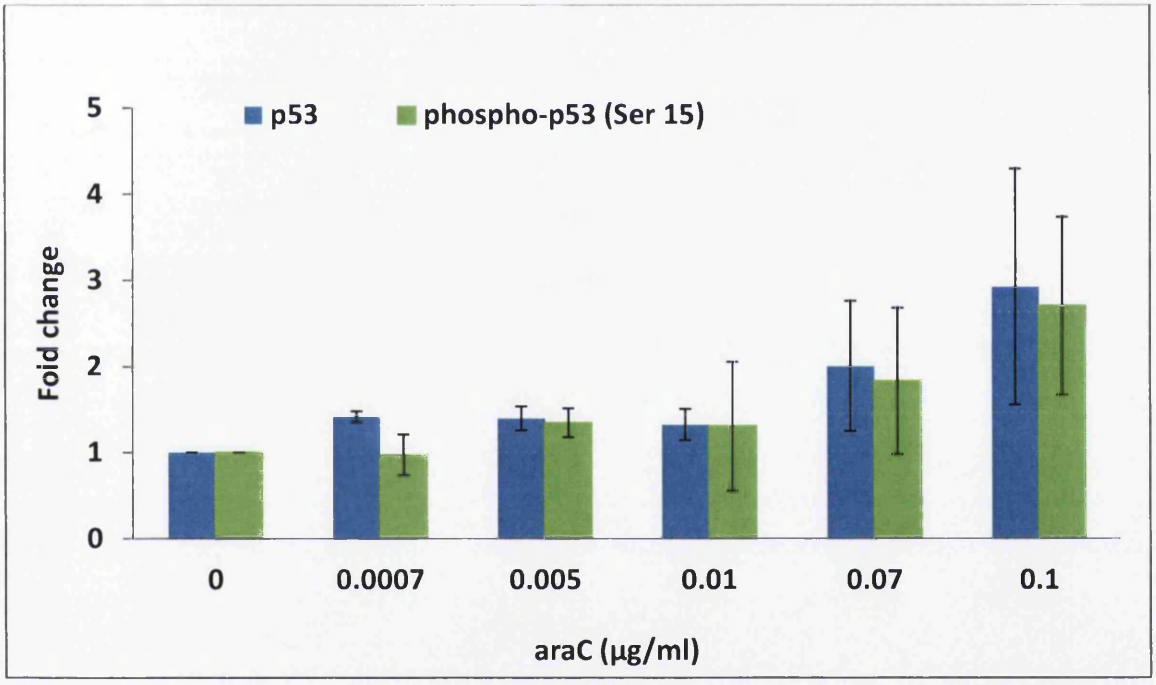

Figure 6.8: AHH-1 cells. A: Representative Western Blot for p53 and phospho-p53 (Ser15) following araC treatment. B: Relative fold change in protein expression (represents the ratio of β-actin normalised treated band density to the untreated control band density). Values represent mean ± SD (n=3)

A:

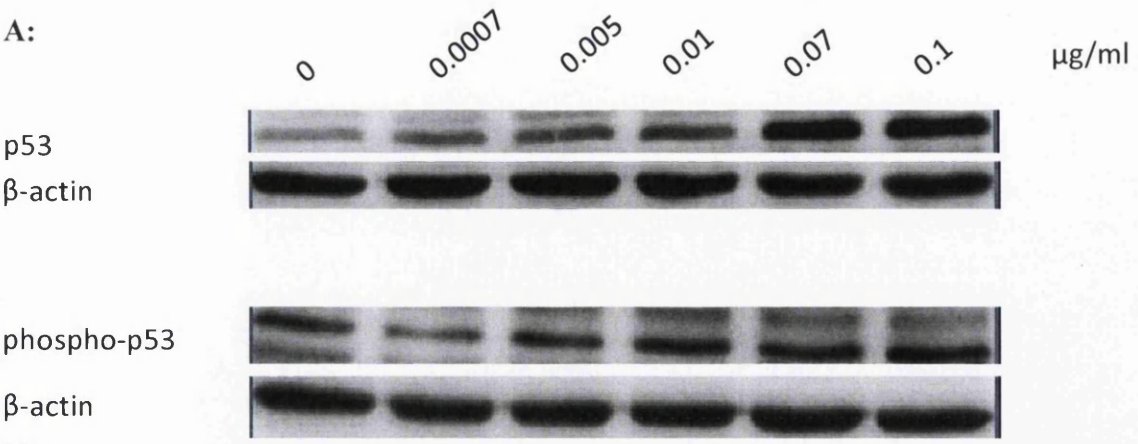

B:

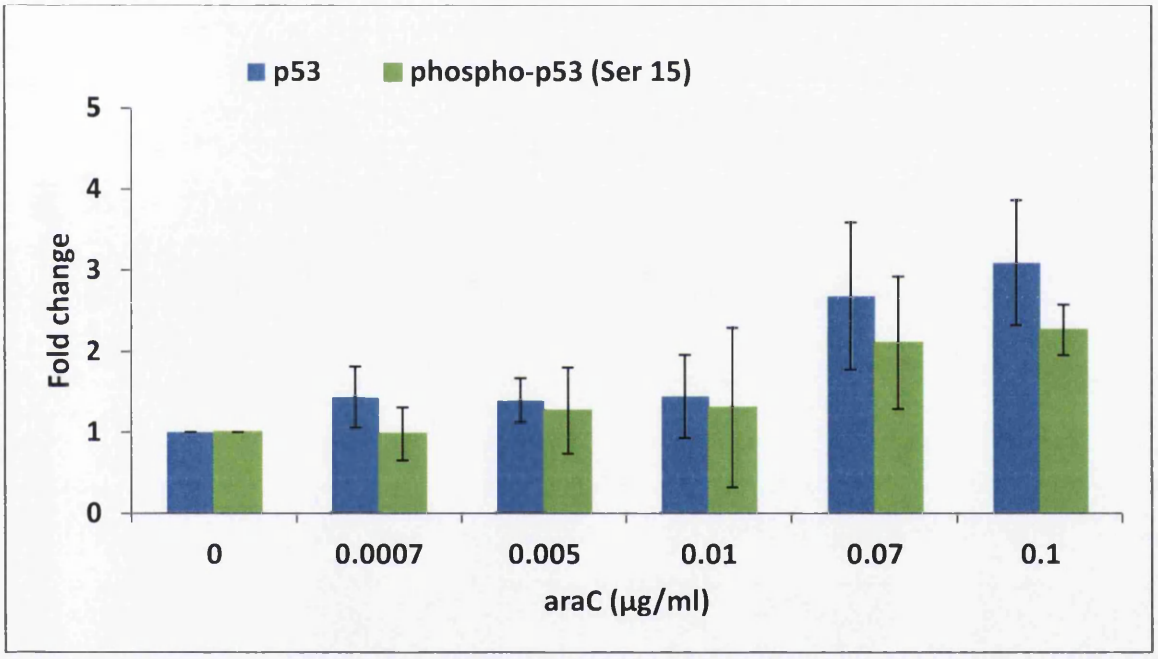

Figure 6.9: MCL-5 cells. A: Representative Western Blot for p53 and phospho-p53 (Ser15) following araC treatment. B: Relative fold change in protein expression (represents the ratio of β-actin normalised treated band density to the untreated control band density). Values represent mean ± SD (n=3)

p53 activation was observed in TK6 and MCL-5 cells at concentrations that caused increases in MN induction (see Chapter 5), whereas in AHH-1 cells an increase in total p53 was shown even at a concentration below the increase in MN frequency for chromosomal damage induction (see Chapter 5).

6.3.3 Induction of apoptosis in TK6 cells

Cell death (apoptosis) was investigated in TK6 cells treated with MMC (0 to 0.1µg/ml) for 4h or with araC (0 to 0.1µg/ml) for 24h at concentrations above and below the DNA damage induction. AnnexinV-FITC antibody staining was used for the detection of early apoptotic cells, while PI was used as a counterstain for dead cells. This allowed distinction on the flow cytometer between viable cells (negative for both AnnexinV-FITC and PI), early apoptotic cells (AnnexinV-FITC positive, PI negative), late apoptotic cells (AnnexinV-FITC and PI positive) and dead cells (PI positive, AnnexinV-FITC negative). Staurosporin was used as a positive control for early and late apoptotic cells.

TK6 cells treated with MMC for 4h showed 25% to 30% dead cells in all cultures, with no significant increases of dead cells over the background to the top dose of 0.1µg/ml MMC. Further no detection of apoptosis could be observed with the MMC treatment (Figure 6.10).

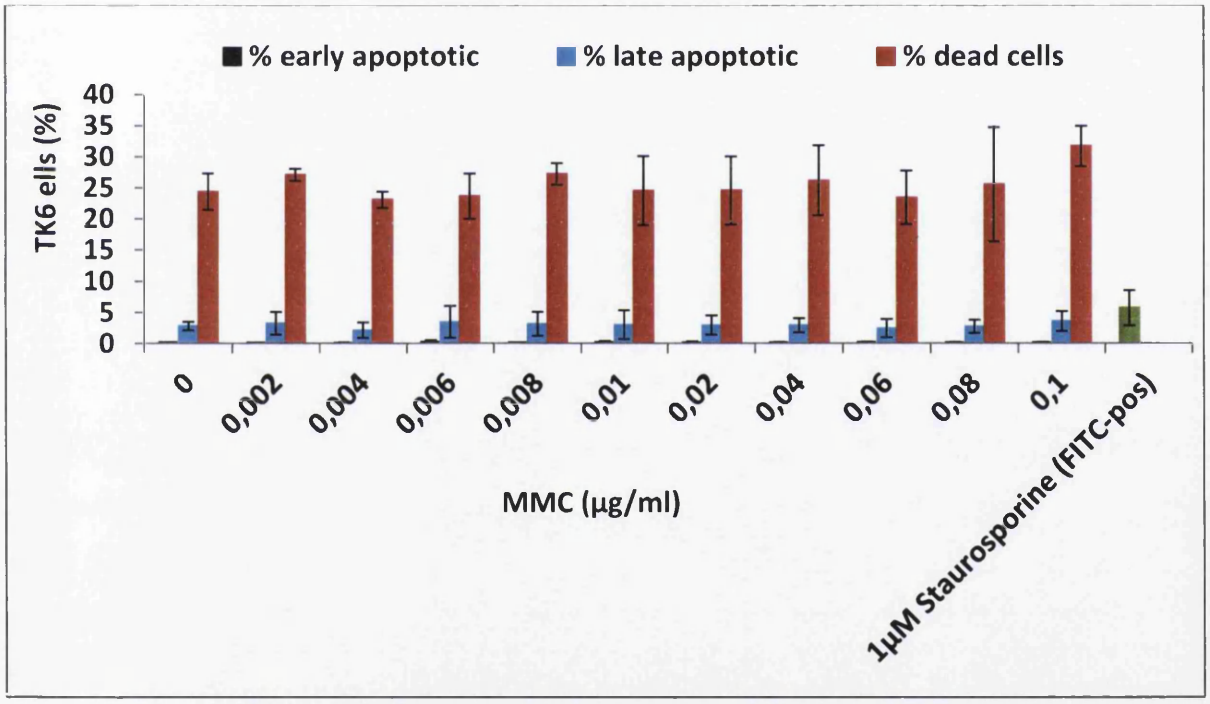

Figure 6.10: Flow cytometric analysis of apoptosis in TK6 cells treated with 4h of MMC. The graph shows the % of dead, late and early apoptotic cells in TK6 cultures treated with MMC. Staurosporin was used as a positive control. Values represent mean ± SD (n=3)

TK6 cells treated with araC for 24h showed increases in dead cells over the background levels at the top two concentrations at 0.07µg/ml and 0.1µg/ml araC, as well as an increase in late apoptotic cells at 0.07 and 0.1µg/ml araC (Figure 6.11).

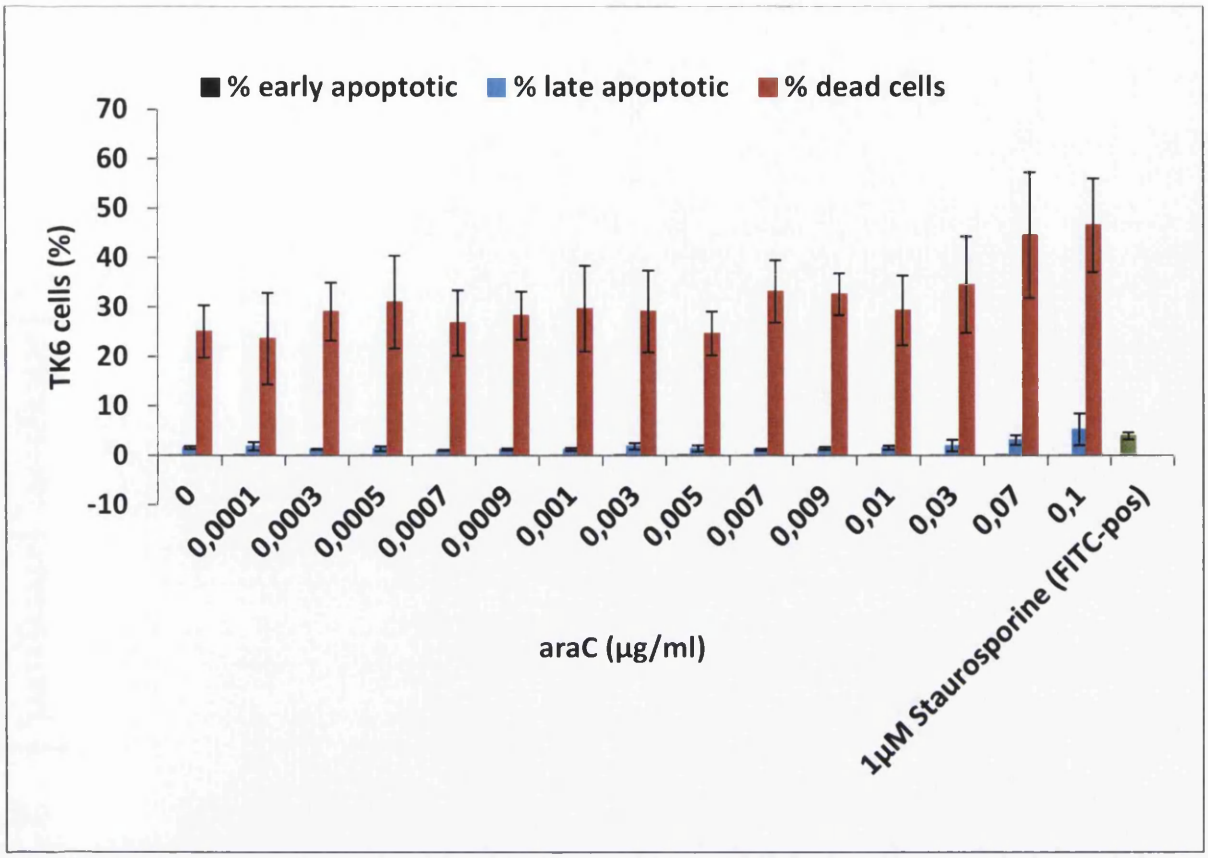

Figure 6.11: Flow cytometric analysis of apoptosis in TK6 cells treated with 24h of araC. The graph shows the % of dead, late and early apoptotic cells in TK6 cultures treated with araC. Staurosporin was used as a positive control. Values represent mean ± SD (n=3)

6.3.4 Cell cycle analysis in TK6 cells

PI was used as a DNA marker for the cell cycle analysis using flow cytometry. TK6 cells were treated with MMC for 4h over a range of concentrations between 0 and 0.1µg/ml. No significant changes in any of the cell cycle phases were observed, when comparing the control sample with the MMC treated samples (Figure 6.12).

A:

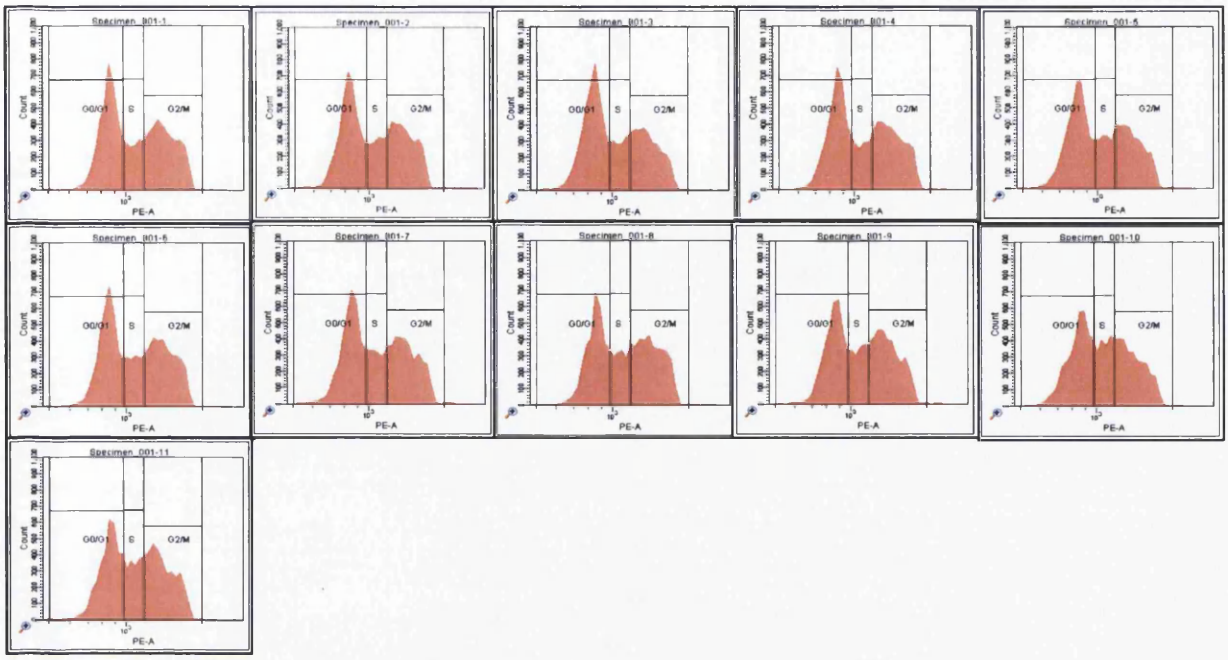

B:

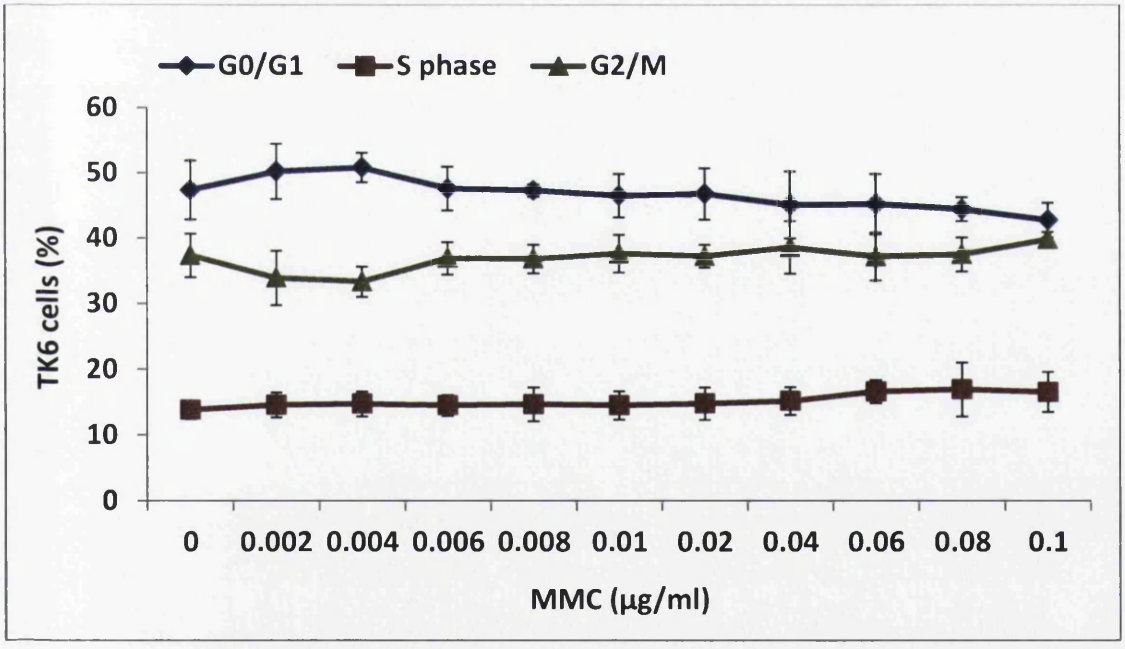

Figure 6.12: Cell cycle analysis in TK6 cells treated with MMC for 4h. A: Representative cell cycle plots for MMC (0 to 0.1µg/ml; from left to right) showing cells in G0/G1, S and G2/M phase. B: Graph presenting the % of cells in G0/G1, S and G2/M phase. Values represent mean ± SD (n=3)

In contrast, TK6 cells treated with MMC for 4h, followed by a recovery period of 18h, showed a decrease in the percentages of cells in the G0/G1 phase at the top concentration of 0.1µg/ml, with more cells being in the G2/M phase, when compared to the control (Figure 6.13).

A:

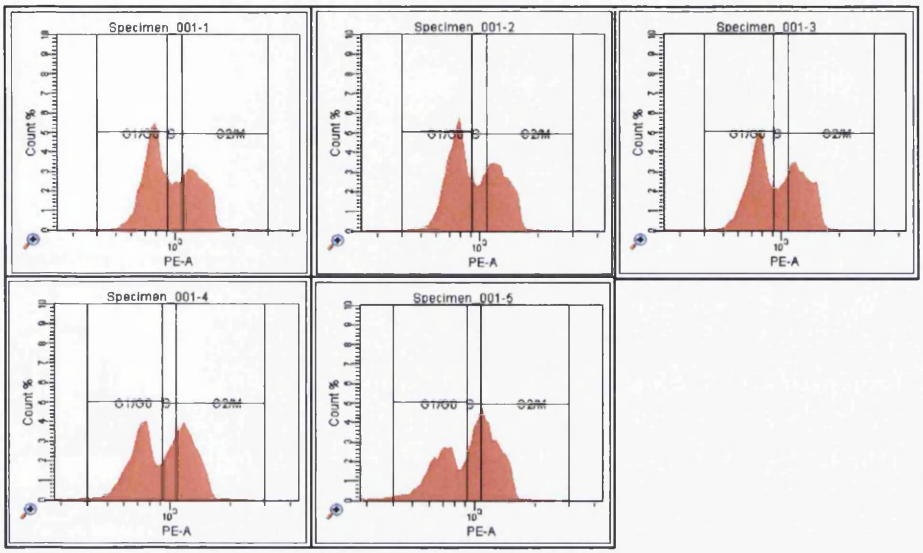

B:

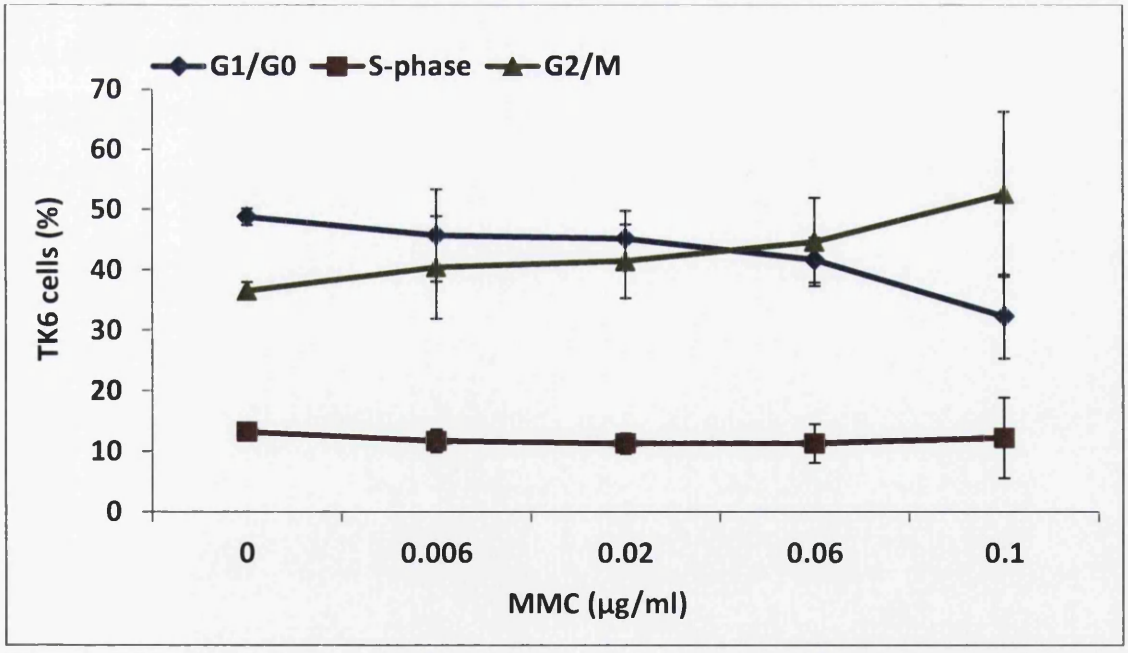

Figure 6.13: Cell cycle analysis in TK6 cells treated with MMC for 4h, followed by a recovery period of 18 h. A: Representative cell cycle plots for MMC (from left to right: 0, 0.006, 0.02, 0.06 and 0.1µg/ml) showing cells in G0/G1, S and G2/M phase. B: Graph presenting the % of cells in G0/G1, S and G2/M phase. Values represent mean ± SD (n=3)

No induction of apoptosis was observed in TK6 cells even at concentrations where chromosomal damage induction was observed (see Figure 6.10 and Chapter 3). However, an accumulation of cells at the G2/M checkpoint was shown at the higher range of concentrations in TK6 cells treated with MMC for 4h, followed by an 18h recovery period.
TK6 cells treated with araC for 24h over a range of concentrations between 0 and 0.1µg/ml showed an increase of cells in the G0/G1 phase and a decrease of cells in the G2/M phase at the higher concentration range, when compared to the control sample (Figure 6.14). However high toxicity was observed, when TK6 cells were treated above 0.07µg/ml of araC (see Chapter 5).

A:

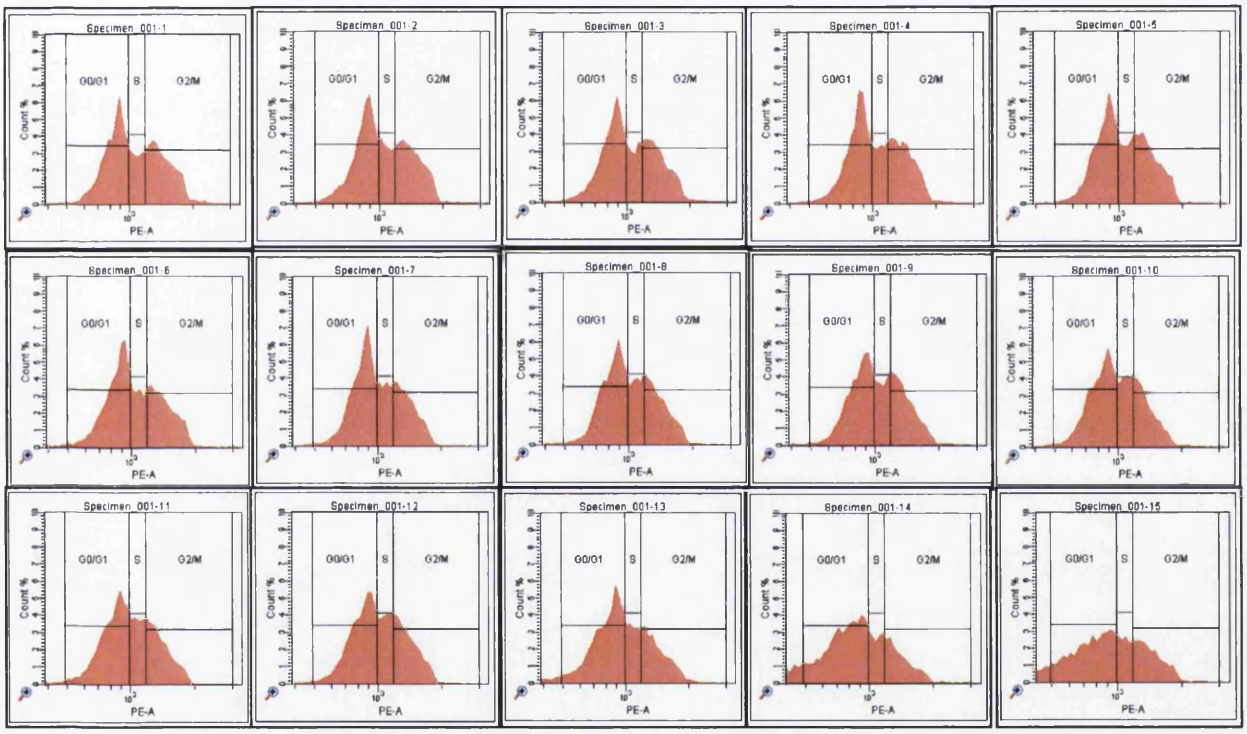

B:

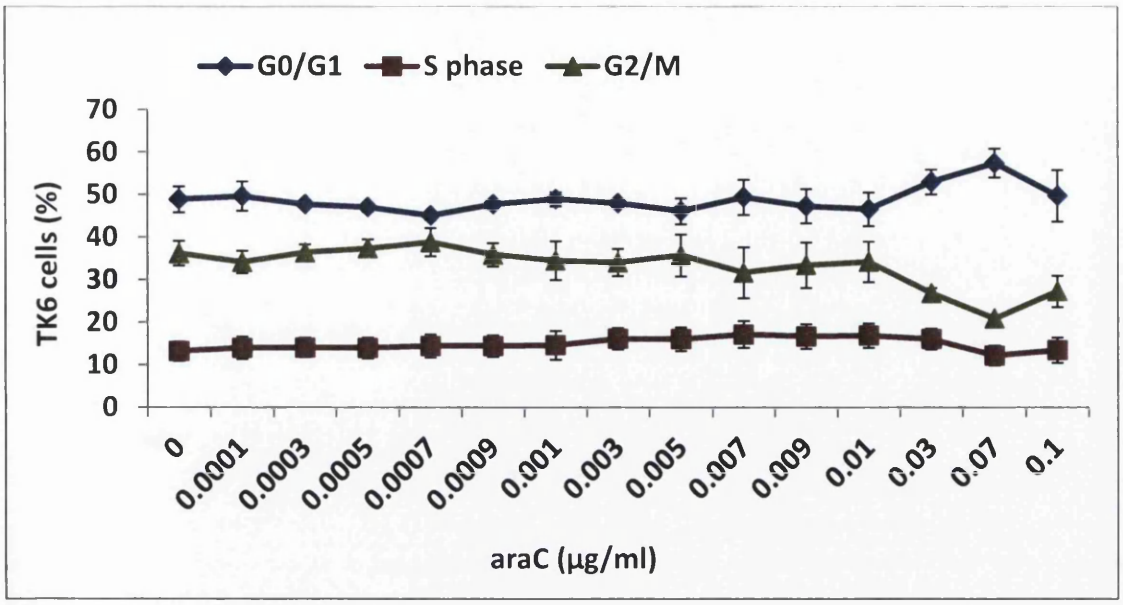

Figure 6.14: Cell cycle analysis in TK6 cells treated with araC for 24h. A: Representative cell cycle plots for araC (0 to 0.1µg/ml; from left to right) showing cells in G0/G1, S and G2/M phase. B: Graph presenting the % of cells in G0/G1, S and G2/M phase. Values represent mean ± SD (n=3)

Furthermore, TK6 cells treated with araC for 24h, followed by a recovery period of 18h, showed similar results as above, where an increase of cells in G0/G1 phase was observed, while cells in G2/M phase decreased (Figure 6.15).

A:

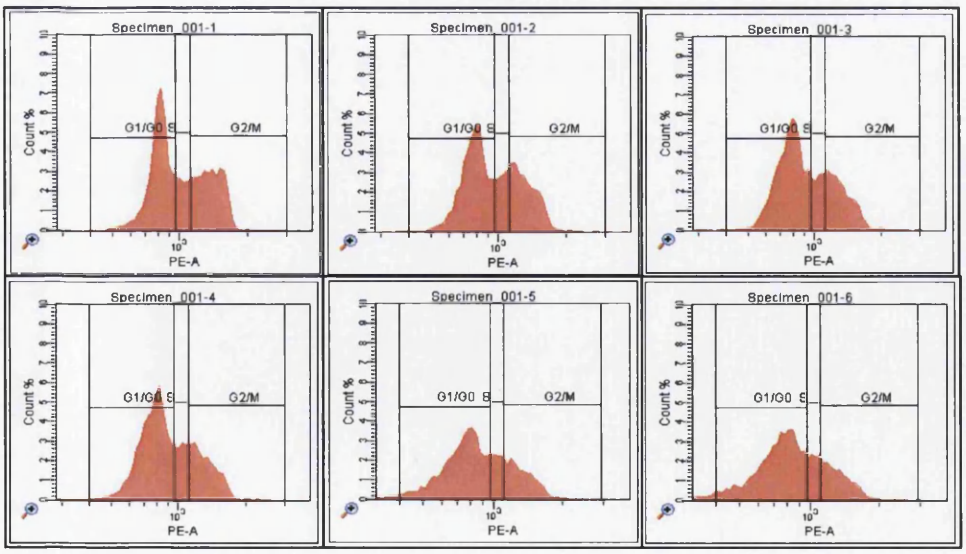

B:

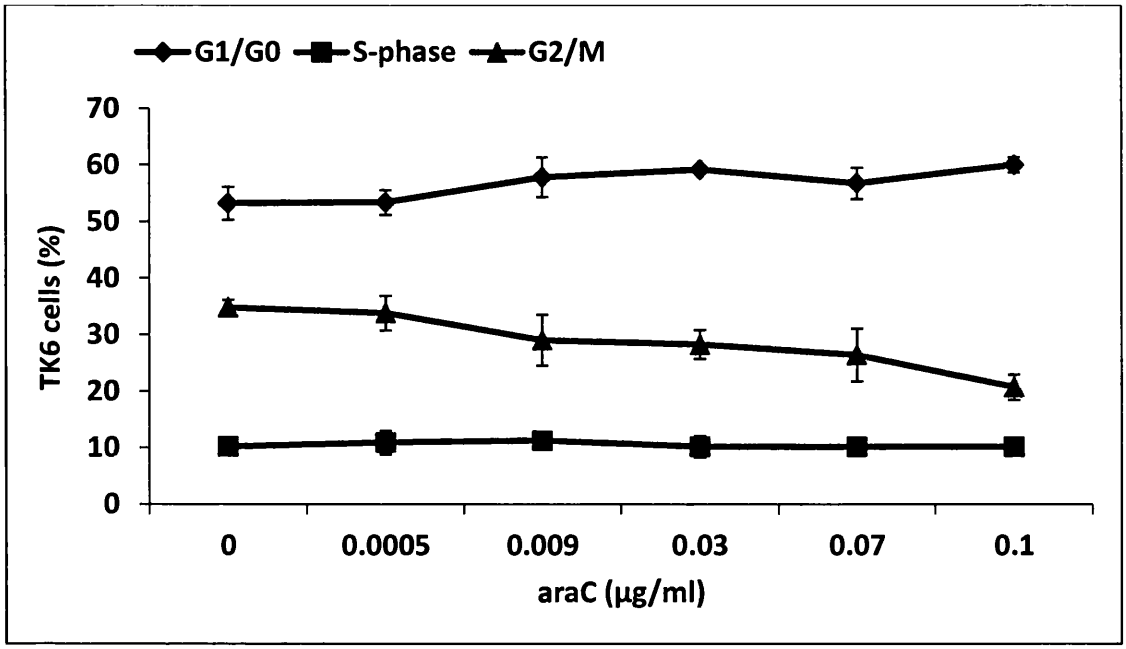

Figure 6.15: Cell cycle analysis in TK6 cells treated with araC for 24h, followed by a recovery period of 18 h. A: Representative cell cycle plots for araC (from left to right: 0, 0.0005, 0.009, 0.03, 0.07 and 0.1µg/ml) showing cells in G0/G1, S and G2/M phase. B: Graph presenting the % of cells in G0/G1, S and G2/M phase. Values represent mean ± SD (n=3)

Induction of apoptosis and an accumulation of cells at the G1/G0 checkpoint were observed in TK6 cells at doses where chromosomal damage induction and p53 activation was shown (see Figure 6.7, 6.11 and Chapter 5).

6.3.5 Chromosome aberration in NH32 cells after MMC and araC treatment

NH32 cells are a derivative of TK6 cells with a double p53 knockout (Chuang, et al., 1999; Hashimoto et al., 2011). p53 expression was checked in TK6 and NH32 cells after treatment with araC for 24h (0, 0.01 and 0.1µg/ml). As expected no p53 protein expression was observed in NH32 cells, whereas p53 was expressed in TK6 cells (Figure 6.16).

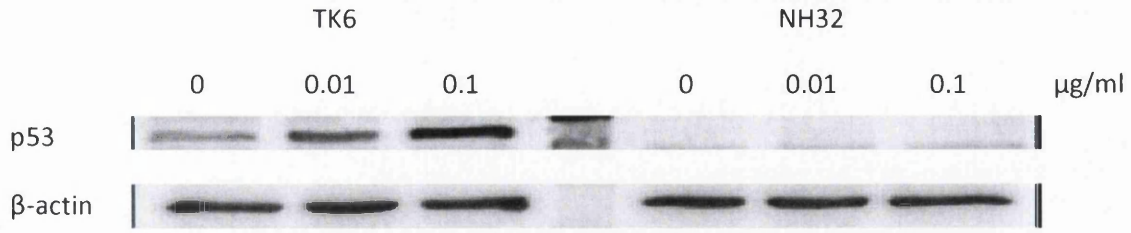

Figure 6.16: TK6 and NH32 cells. Representative Western Blot for p53 protein expression following araC treatment.

To compare the results gained in TK6 cells (p53 proficient) and to investigate the role of p53, NH32 cells (p53 deficient) were treated with MMC for 4h or with araC for 24h and chromosomal damage was examined, using the *in vitro* MN assay. The semi-automated scoring protocol for the Metafer-System (MetaSystems) was applied.

TK6 cells treated with MMC (0 to 0.1µg/ml) for 4h, followed by one cell cycle of cytochalasin B (18h) showed increases in MN induction at 0.04 to 0.06µg/ml and above. Further 45.8% toxicity was observed at 0.1µg/ml MMC (see Figure 3.6).

In comparison, NH32 cells treated with MMC for 4h, followed by one cell cycle of cytochalasin B (18h), showed increases in MN induction at 0.02 and 0.04µg/ml. Further 54.3% cell death and cytostasis were observed at 0.06µg/ml MMC (Figure 6.17).

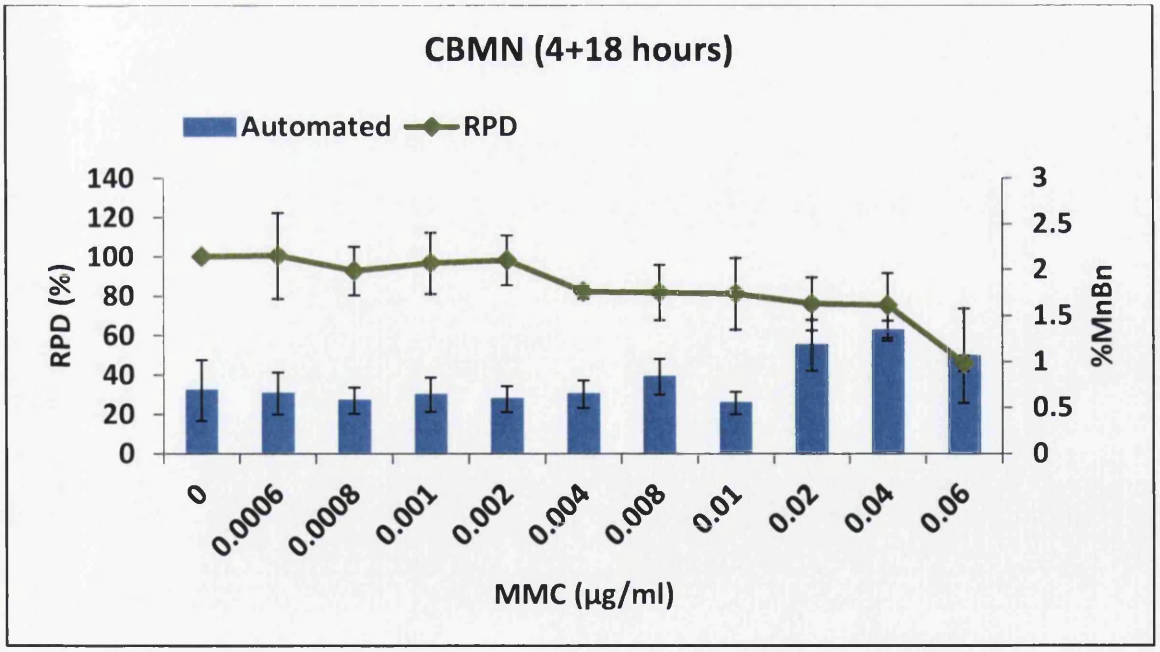

Figure 6.17: Effect of MMC on NH32 cells using the CBMN assay. NH32 cells were treated with MMC for 4h, followed by 18h of CytoB. Blue: percentage micronucleated binucleated cells, green: Relative population doubling (RPD). Values represent mean ± SD (n=3)

TK6 cells treated with araC (0 to 0.1µg/ml) for 24h, followed by one cell cycle of cytochalasin B (18h) showed significant increases in MN induction at 0.03µg/ml and above. Further >50±5% (62.5%) cell death and cytostasis were observed at 0.07µg/ml araC (see Figure 5.2).

In comparison, NH32 cells, treated with 24h of araC, followed by 18h of cytochalasin B, showed significant increases in MN induction at 0.007µg/ml and above, while >50±5% (90.6%) toxicity were observed at 0.03µg/ml araC (Figure 6.18).

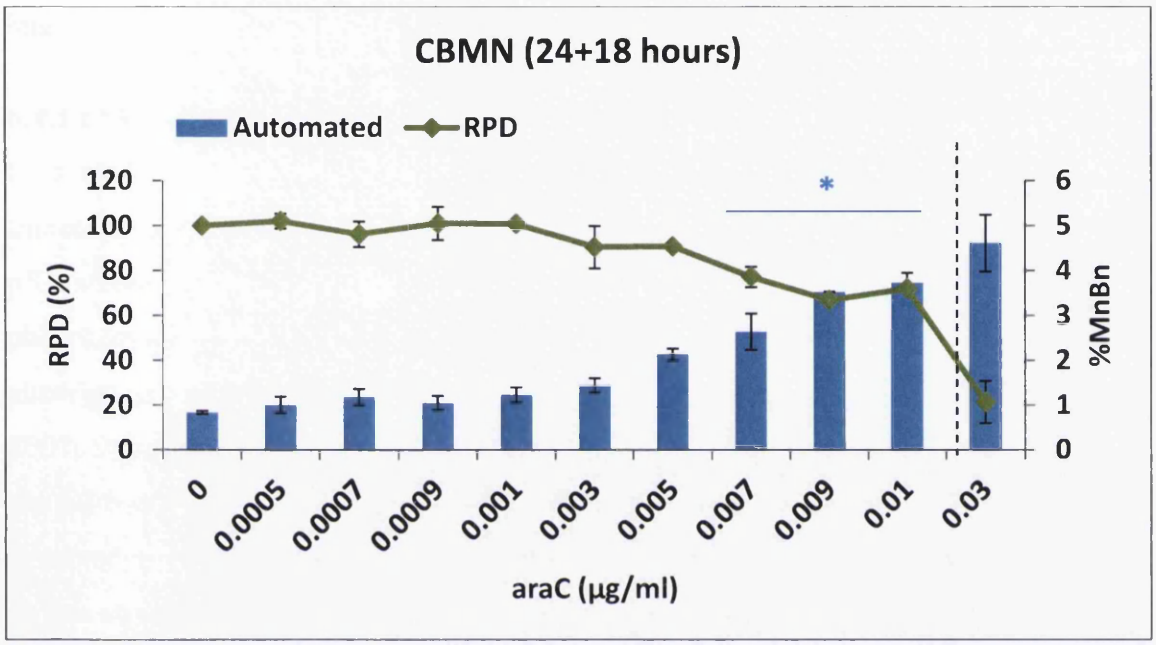

Figure 6.18: Effect of araC on NH32 cells using the CBMN assay. NH32 cells were treated with araC for 24h, followed by 18h of CytoB. Blue: percentage micronucleated binucleated cells, green: Relative population doubling (RPD). Values represent mean ± SD (n=3). (*) Represents $p<0.05$.

NH32 cells (p53 deficient) thus demonstrated to be more sensitive to toxicity than the p53 proficient parental cell line TK6. Furthermore NH32 cells treated with araC showed a higher magnitude for MN induction than TK6 cells treated with the analogue. However, NH32 cells treated with MMC showed a lower to a similar magnitude of MN induction compared to the parent TK6 cells line treated with the cross-linker.

6.4 Discussion

The role of the tumour suppressor gene *TP53* in the low dose region of MMC and araC exposure was investigated in this study. *TP53* encodes a phospho-protein, which is involved in cellular processes, such as cell cycle control (predominantly at the DNA damage checkpoint) and prevention of uncontrolled cell proliferation through apoptosis; thus the protein plays a crucial role for cellular integrity (Yang and Duerksen-Hughes, 1998; Arrowsmith, 1999). Inactivation of the gene by mutations is the most frequent alteration in human cancers (Kato et al., 2003).

6.4.1 p53 activation after genotoxic stress

It is well known that cellular stress including DNA damage, activate the p53 response. Increases in p53 protein levels as well as structural changes in the protein are hallmarks of p53 activation (Salazar et al., 2009). Furthermore post-translational modifications, like phosphorylation at serine residues ensure p53 stabilization and accumulation in the nucleus, allowing p53 to interact with sequence-specific sites on target genes (Joerger and Fersht, 2007; Salazar et al., 2009). Target genes include *p21*, which is involved in cell cycle arrest at the G1/S checkpoint, *Gadd45*, which plays a role in triggering DNA repair and *Bax*, which is involved in the apoptotic pathway (Yang and Duerksen-Hughes, 1998).

In this study p53 activation was investigated by *p21* gene expression and p53/ phospho-p53 (Ser15) protein expression analysis.

No significant increases in *p21* gene expression were observed in any of the cell lines after MMC or araC treatment. However increases in *p21* gene expression over the background with increasing concentrations were observed in TK6 cells treated with araC (see Figure 6.6). DNA damage induction triggers p53 activation, which leads to downstream signalling to target genes. *p21* gene expression was analysed in AHH-1 cells below the threshold for DNA damage induction level described in the previous chapters. Consequently, p53 protein levels might have been maintained at low levels, resulting in no p53 activation in AHH-1 cells at the low dose levels. Furthermore chromosomal damage was more strongly induced in TK6 cells treated with araC, when compared to the MMC treatment, resulting in increasing levels of *p21* in TK6 cells treated with araC. In addition *p21* is not the only target gene activated in the p53 response, suggesting that other target genes, like *Gadd45* or *Bax*, need to be investigated.

In parallel to the *p21* gene expression assessment, p53 activation was investigated by p53 and phopho-p53 (Ser15) protein expression analysis. As mentioned before DNA damage induces phosphorylation of p53 at serine residues, such as serine 15 or 20 (Lakin and Jackson, 1999). No increases in the protein levels of p53 and/or phospho-p53 (Ser15) were observed in AHH-1 cells treated with MMC for 4h. The results confirm that p53 is most likely not activated in AHH-1 cells at the low dose levels chosen. Natural defence mechanisms, like epithelial barriers to genotoxin entry, chemical detoxification, DNA redundancy or DNA repair (Jenkins et al., 2010) are most likely responsible for the low levels of MN induction seen in AHH-1 cells treated with MMC. Increases in phospho-p53 (Ser15) levels were observed in TK6 cells treated with MMC for 4h, showing that DNA damage occurs. However the overall p53 induction after MMC treatment was low. It was shown by Nelson and Kastan (1994) that DNA strand breaks might be critical to trigger p53 induction. They suggested that agents capable of directly causing strand breaks, in particular after short-term treatments, were more effective in activating p53 than agents that cause DNA cross-links (such as MMC), that induce DNA base modifications, intercalate into the DNA or cause interference with the cell cycle or cellular metabolism (Nelson and Kastan, 1994). DNA strand breaks, in particular DNA double strand breaks, can cause various problems for the cell, like relaxation of the torsional super helical strain in the DNA template required for transcriptional regulation, gene expression effects or chromosomal damage (Nelson and Kastan, 1994).

In addition, only the short-term treatment for MMC was investigated for p53 activation. Extended treatments, which showed high rates of chromosomal damage induction after MMC treatment might activate p53 more strongly, since it was shown previously that MMC is able to activate the p53 pathway (Champeil et al., 2010).

TK6 cells treated with araC for 24h showed high increases in p53 and phospho-p53 (Ser15) protein expression at 0.07µg/ml araC and above, whereas MCL-5 cells treated with araC for 24h showed high increases in p53 and phospho-p53 (Ser15) protein expression only at the top dose of 0.1µg/ml, while AHH-1 cells showed increases in p53 protein expression at 0.1µg/ml araC. These results suggest a direct relationship between p53 levels and the induction of MN. Significant increases in p53 expression were observed at concentrations that were found to be statistically significant for MN induction. Salazar *et al.* (2009) showed a direct relationship between p53 levels and the induction of MN in RKO cells treated with genotoxic chemicals, indicating that the level of p53 might be associated with chromosomal damage. Further, p53 binds directly to sites of DNA damage, such as mismatches and single-stranded DNA,

showing the potential of p53 as a direct DNA damage detector (Amundson et al., 1998) and as an endpoint for genotoxicity testing (Salazar et al., 2009).

In addition, it was shown by Fenech and Neville that araC inhibits the gap-filling step during excision repair, which results in the formation of single-strand breaks at repair sites. The single-strand breaks could then be converted to chromatid or chromosome breaks, confirming that DNA strand breaks might be critical to trigger for p53 induction (Fenech and Neville, 1992). Downstream effector genes transactivated by p53 determine the final outcome of p53 activation.

6.4.2 Cell cycle analysis and apoptosis in TK6 cells after MMC and araC treatment

Activation of p53 can lead to cell cycle arrest to prevent the proliferation of damaged cells and to allow DNA repair before replication and mitosis or induce apoptosis to eliminate irreparable damaged cells (Amundson et al., 1998).

TK6 cells exposed to MMC for 4h showed no changes in any phases of the cell cycle. However TK6 cells treated with MMC for 4h, followed by a recovery time of one cell cycle showed G2/M arrest in particular at 0.1µg/ml MMC.

A study by Islaih *et al.* (2005) analysed the cell cycle in TK6 cells after treatment with different genotoxins, such as MMC. The cells were exposed for 4h and cell cycle analysis was performed at 4h and 20h following treatment. Cells collected at the 8h time point showed significant increases in the percentage of cells in S phase, whereas cells collected at the 24h time point showed a strong G2/M arrest (Islaih et al., 2005). Furthermore a study by Lukamowicz *et al.* (2011) revealed a dose-dependent accumulation of cells in G2/M phase after MMC treatment. The G2/M checkpoint seems to be activated, when DNA synthesis is blocked to prevent segregation of damaged or incompletely synthesised DNA (Pucci et al., 2000). The cyclinB1/Cdc2 complex is the main regulatory factor for the entry into M phase and phosphorylation of cdc2 or inhibition of cyclinB1 can cause G2 arrest (Amundson et al., 1998). In addition p53-regulated genes can regulate the G2 arrest to a certain extent. Further experiments are required to clarify the mechanism behind the G2/M arrest induced by MMC.

TK6 cells exposed to araC for 24h with and without an extended recovery period of one cell cycle, showed dose-dependent increases in the percentage of cells in G1/G0 phase. p53 predominately acts at the DNA damage checkpoint in the cell cycle, influencing cell proliferation. The sequence-specific transactivation function of p53 clearly mediates the G1 arrest. Activation of p53 in this study was shown after araC treatment by increases in *p21* gene expression as well as p53 and phospho-p53 (Ser15) protein expression. p53 is activated

by DNA damage induced by araC and initiates the transcription of *p21*, a G1 cyclin dependent kinase inhibitor (CKI), which results in G1/G0 cell cycle arrest (Amundson et al., 1998; Pucci et al., 2000). Cell cycle progression is prevented by inhibition of phosphorylation of CDK2/cyclin-complexes by p21 and inhibition of further downstream signalling (Amundson et al., 1998). Hence the data support a general link between araC induced chromosome damage, p53 activation and G1/S phase block.

Activation of p53 can also lead to apoptosis to eliminate irreparable damaged cells. TK6 cells treated with MMC for 4h showed no induction of apoptosis over the low range of concentrations. Furthermore no increase in dead cells over the background level was observed. In contrast, TK6 cells treated with araC for 24h showed increases in dead cells at 0.07µg/ml araC and above, as well an increase in apoptotic cells at 0.1µg/ml araC.

It was proposed by Islaih *et al.* (2005) that TK6 cells have a prolonged cell cycle delay in response to genotoxins. Therefore it might be possible that damaged cells are rather stalled than eliminated through apoptosis (Sobol et al., 2012). However, it is important to note that the final outcome of p53 activation depends on many factors, such as the presence of growth factors and is mediated through the action of downstream effector genes, which are associated with growth control, cell cycle checkpoints, DNA repair and/or apoptosis (Amundson et al., 1998).

6.4.3 Chromosome aberration in NH32 (p53 deficient) cells after MMC and araC treatment

The human lymphoblastoid cell line TK6 has been extensively used in recent genotoxicity assays to examine its suitability for genotoxicology testing. Most studies revealed lower fold MN increase in TK6 cells than in the commonly used rodent cell lines (L5178Y, CHO and CHL) (Hashimoto et al., 2011). This was also confirmed is this study, when TK6 and L5178Y cells were treated with low doses of 4NQO (see Chapter 4). TK6 cells treated with 4NQO showed little to no induction of chromosome damage, while L5178Y showed significant increases in MN induction at very low doses, using the *in vitro* MN assay (see Chapter 4). TK6 cells are p53 proficient, whereas the rodent cell lines are p53 compromised and therefore more likely to survive and replicate with DNA damage, resulting in higher MN frequencies (Hashimoto et al., 2011). Furthermore, in our group it was observed that the human lymphoblastoid cell lines AHH-1 and MCL-5, which are heterozygous for TP53, showed a lower sensitivity to toxicity than TK6 cells and therefore allowed treatment with a

higher dose range (see Chapters 3 to 5). Consequently, p53 function might be a key factor for the cell-type dependent sensitivity for genotoxicity and cytotoxicity (Hashimoto et al., 2011). NH32 cells are an isogenic derivative of TK6 cells with a double TP53 knockout (Li et al., 2006). Thus, the DNA damage induction in TK6 and NH32 cells after MMC and araC treatment was compared to investigate, if p53 plays a central role in the low dose responses in human lymphoblastoid cells.

NH32 cells were more sensitive to cytotoxicity after both MMC and araC treatment than the proficient parent cell line TK6. Further NH32 cells treated with MMC for 4h showed a lower to a similar magnitude of MN induction compared to the parent TK6 cells line, when treated with the cross-linker MMC, whereas NH32 cells treated with araC for 24h showed a higher magnitude for MN induction than TK6 cells treated with the nucleoside analogue araC.

A study by Hashimoto *et al.* (2011) showed no differences in sensitivity to MN induction and cytotoxicity between p53 competent TK6 cells and p53-null NH32 cells after short and/or extended treatments with genotoxins. Further it was reported by Yu *et al.* (1997) that p53-null cells have similar characteristics to p53-competent cells, while p53-mutated cells show different characteristics, suggesting a dominant negative effect of abnormal p53 function (Yu et al., 1997; Hashimoto et al., 2011).

These results are in line with the results gained for MMC in our study. However it was shown that p53 induction in TK6 cells treated with MMC for 4h was low, suggesting that p53 might be insignificant under the chosen short treatment condition (because of low concentration). Natural defence mechanisms, like DNA repair seem to be responsible for the low DNA damage induction of MMC in NH32 cells. Furthermore NH32 cells were more sensitive to DNA damage and cytotoxicity after araC treatment, when compared to TK6 cells. p53 was highly activated in TK6 cells treated with araC for 24h and the cells showed G1 arrest in the cell cycle analysis, suggesting a central role for p53 in the dose response, since p53 plays an important function in cellular responses, such as cell cycle arrest at the G1 phase. In conclusion, p53 was more prominent in araC treated cell cultures and therefore p53 deficient cells showed a greater effect.

6.5 Summary

In this chapter the role of p53 in the low dose response relationships after treatment with the genotoxins MMC and araC was investigated by gene and protein expression analysis as well as apoptosis and cell cycle studies. Furthermore MN induction was compared between p53 competent TK6 cells and p53-null NH32 cells.

Low levels of p53 induction were observed in TK6 cells treated with MMC for 4h, since no significant increases in either *p21* gene expression or p53/ phospho-p53 (Ser15) protein expression were detected. Furthermore no cell cycle changes or induction of cell death were observed, suggesting that other defence mechanisms play a major role in the MMC dose response. This was further confirmed by the low DNA damage induction in NH32 cells.

On the other hand high p53 activity was shown in TK6 cells treated with araC for 24h. Increases in *p21* gene expression as well as high increases in total p53 and phospho-p53 (Ser53) were detected. Further the percentage of cells in G1/G0 phase increased over the dose range, suggesting a G1 arrest after araC treatment. In addition NH32 cells showed a higher magnitude of MN induction than TK6 cells. Consequently p53 played a central role in the DNA damage response in human lymphoblastoid cells treated with araC.

Furthermore the results gained in TK6, AHH-1 and MCL-5 cells suggested a direct relationship between the p53 levels and the induction of MN. High increases in p53 expression were only observed at concentrations that were found to be statistically significant for MN induction, showing the potential of p53 as a direct DNA damage detector and as a potential endpoint for genotoxicity testing.

Chapter 7

General Discussion

Genotoxicology deals with investigating the DNA damaging effects of substances that humans are exposed to and DNA damage is an underlying cause of mutations that have the potential to initiate carcinogenesis. The investigation of low dose responses in genotoxicology testing helps to improve health risk assessments by establishing if DNA reactive compounds follow linear or non-linear (thresholded) dose response relationships. The concepts of thresholds in genotoxicology have been discussed substantially and have been mainly accepted for aneuploidy based mechanistic experimental evidence (Elhajouji et al., 2011). However the assumption for direct acting genotoxins (including clastogens), such as MMC and 4NQO is that the relationship between exposure to these genotoxic chemicals, DNA damage formation and the induction of mutagenic change is linear (Henderson et al., 2000). Yet mutations are not produced directly by DNA adducts as DNA repair activity limits the proportion of adducts processed into mutational change. It is therefore possible that no observed effect levels (NOEL) may exist for some genotoxins (Jenkins et al., 2005). Furthermore, natural defence mechanisms, like epithelial barriers to genotoxin entry, chemical detoxification or DNA repair corroborate the theory of genotoxic thresholds (Jenkins et al., 2010).

The main aim of this thesis was therefore to assess low dose response relationships *in vitro* for a number of genotoxic agents (MMC, 4NQO and araC) and to establish if the DNA reactive compounds follow linear or non-linear (thresholded) dose responses, since it is important to investigate the biological significance of low dose exposures to improve health risk assessments. These studies used the newly installed semi-automated MN detection system at Swansea University to investigate DNA damage induction at the chromosomal level. Furthermore, the mechanism of action of each test component was further investigated by follow up experiments to gain mechanistic understanding of the dose response relationships, such as expression of DNA repair enzymes using Real-time PCR or protein analysis using Western blotting as well as cell cycle status analysis.

7.1 The Metafer-System: a semi-automated method for scoring MN

The *in vitro* and *in vivo* MN assay has been extensively used in genotoxicity studies and contributed to our understanding of the dose-relationships of genotoxins (Elhajouji et al.,

2011). A high demand for the automation of the MN assay exists, because visual scoring of MN can be time consuming and the results depend on subjective interpretation. Two types for automated MN scoring are commonly used: flow cytometry and MN scoring by image analysis (Varga et al., 2004). Several systems are commercially available, such as Metafer and Cellomics (Doherty et al., 2011).

One of the advantages of flow cytometry is the possibility of scoring a very large number of cells over a very short time. However the disadvantage of the methodology is, that no individual cells can be examined in detail to determine whether or not MN are the result of aneugenic or clastogenic events and furthermore samples cannot be re-analysed (Doherty et al., 2011). Consequently, it was decided to use the automated slide scoring platform Metafer in this laboratory. Advantages of the system are visual inspection of the images and cells, which allows MN distinction from other DNA fragments and slide preparations can be re-examined by conventional microscopy to clarify results (Doherty et al., 2011). In addition the Metafer software contains classifiers, which can be modified to determine the size and shape of nuclei and MN, allowing screening for MN in mononucleated and/or binucleated cells (Doherty et al., 2011).

The dose response curves and MN frequencies obtained with the Metafer-System after treatment of TK6 cells with MMC were compared to the conventional manual scoring of Giemsa stained slides (Chapter 3). Both the mono- and binucleated MN assay was performed. Very similar dose responses and MN frequencies were observed in TK6 cells treated with different doses of MMC for different time points, when comparing manual scoring with the Metafer-System for both the mononucleated and binucleated assay. Further both methods showed high correlation (see Chapter 3 and 4). Therefore the MMC study clearly demonstrated that the Metafer-System is an adequate system to provide rapid and accurate assessment of MN. Furthermore, the system proved to enhance reliability of results and to reduce scoring subjectivity of MN identification. In addition, the possibility to score high numbers of cells (between 2000 and 4000 cells per replicate were chosen in this study) in a short time advances the statistically power of the assay.

Minor difficulties were encountered in our laboratory during automated scoring with the Metafer-System due to the loss of cytoplasmic boundaries. Examples were the careful attention that needs to be paid to the distance of MN from the main nuclei and attention to the staining pattern and intensities of the two nuclei was required. Consequently, although the Metafer-System can be used as a fully automated system, it was decided to use a semi-automated approach with the final assessment being performed by visual examination under

the microscope. Further, it was notable that the mean response for the MN frequencies obtained with the Metafer-System was generally higher than for manual scoring. However that is possibly due to subjective manual scoring and the ability of the system to score higher total numbers of cells, coupled to the classifier settings, which determine the parameters for the identification of the mononucleated and binucleated cells and the MN. The slight increases in MN frequency were consistent across the different doses and different chemical treatments and so did not interfere with the low dose studies described here.

Further development of the technology was implemented in Chapter 4, where the human lymphoblastoid cell lines (TK6, AHH-1 and MCL-5) and the mouse lymphoma cell line L5178Y were treated with low doses of 4NQO. At AstraZeneca (Cheshire, UK) the mononucleated MN assay was performed and analysed by manual scoring and the Metafer-System. The results gained with the Metafer-System were again comparable to the results gained through manual scoring, proving once more that the Metafer-System was a biologically relevant method to score MN. It was noted that the Metafer-System at AstraZeneca detects slightly fewer MN than does the manual scoring, which might be due to the intensity of staining of the main nuclei and the small size of MN (Doherty, et al., 2011). However, the differences were consistent in all studies and the doses that caused significant increases in MN induction after 4NQO treatment were similar. However, clearly system setup in each laboratory influenced the performance of the Metafer-System and this requires attention in any new laboratory acquiring this equipment.

In conclusion, the Metafer-System is a very promising tool for improving risk assessment of human populations exposed to mutagens and thus the semi-automated scoring protocol for the Metafer-System was used for the assessment of chromosomal damage throughout this thesis.

7.2 Genotoxic thresholds for MMC, 4NQO and araC?

Dose response thresholds for genotoxins have implications for the setting of safe exposure levels. A threshold of genotoxic activity indicates that a compound will not produce mutations below a critical exposure level. Furthermore it reduces the risk for the induction of cancer or congenital abnormalities at these exposures. The main endpoints analysed for threshold dose responses have been DNA adduct formation, gene mutation and chromosomal aberration (Kirsch-Volders et al., 2003; Jenkins et al., 2010).

Redundant targets and protective mechanisms in the cells are the main mechanisms which can lead to genotoxic thresholds. Aneugens (non-DNA reactive genotoxins) show

thresholded dose response curves. Low levels of the compounds are tolerated, because deactivation of multiple targets is required to induce aneuploidy. However, thresholds of genotoxic activity have to be proven for direct acting genotoxins on a case-by-case basis. Experimental evidence (to date) of thresholded responses has only be demonstrated for spindle poisons, ionizing radiation, alkylating agents (methylmethanesulfonate (MMS), ethylmethanesulfonate (EMS)), topoisomerase II inhibitors and ROS inducers (Jenkins et al., 2005; Doak et al., 2007).

In this thesis the low dose response relationships of the direct acting agents MMC, 4NQO and araC in human lymphoblastoid cells were investigated. MMC cross-links the complementary strands of the DNA double helix, while 4NQO causes bulky DNA adducts and araC is a nucleoside analogue of both cytidine and deoxycytidine. Short-term as well as extended treatments were undertaken.

TK6 cells treated with MMC (0-0.1µg/ml) for 4h followed by 18h with cytochalasin B showed increases in MN frequency only at the higher doses (Chapter 3). Quantitative dose response assessment with the BMD model indicated a $BMDL_{10}$ for the manual data at 0.006µg/ml, whereas for the automated data the $BMDL_{10}$ was calculated at 0.007µg/ml. The $BMDL_{10}$ is considered an adequate point of departure (POD) for the extrapolation of dose response data (Gollapudi et al., 2013).

In conclusion, the short-term treatment of MMC in TK6 cells showed a clear non-linear dose response. In addition AHH-1 cells treated with MMC for 4h and one cell cycle of cytochalasin B showed a similar dose response to TK6 cells. Mechanistic experiments had to be applied to prove if MMC causes no adverse effects over the background at the low dose range in the short-term treatment.

Non-linear dose responses of araC were observed after extended treatments with the chemical in TK6, AHH-1 and MCL-5 cells with increases in MN induction only seen at the higher dose range (Chapter 5). Assessment with the BMD approach indicated a $BMDL_{10}$ in TK6 cells treated with araC at 0.0007µg/ml, in AHH-1 at 0.004µg/ml and in MCL-5 cells at 0.003µg/ml, which was in line with the observed genotoxicity data gained in this study.

Little to no chromosomal damage induction was observed in TK6 cells treated with 4NQO for short-term or extended treatment periods (Chapter 4). However, extending the recovery time after the short-term treatments in the CBMN assay from 18h to 42h and in the mononucleated assay from 24h to 40h increased the magnitude of MN induction at the top doses to a significant level. No induction of MN was observed in the low dose region with regard to any treatment regime. Furthermore AHH-1 and MCL-5 cells showed similar dose

response curves to TK6 cells. However gene mutation induction of 4NQO was observed in the *in vitro* HPRT assay and the *in vitro* comet assay revealed DNA damage induction by 4NQO at the higher dose region. Oxidative damage might be a cause for the mutagenicity of 4NQO. Further investigations into the mechanism of 4NQO have to be undertaken to get an understanding of the dose response relationships of 4NQO, such as DNA repair assays and gene and protein expression approaches. 4NQO induces three main adducts: dGuo-N2-AQO, dGuo-C8-AQO and dAdo-N6-AQO, which can be fixed as mutations (Inga et al., 1994). Further, it was shown that 4NQO induces apurinic/apyrimdinic sites and single-strand breaks, which originated probably from unstable adducts (Inga et al., 1994) and could be converted to double strand breaks and fixed as MN. Therefore studies investigating the adduct formation and mutation spectrum in TK6 cells after 4NQO treatment might help to understand the dose response of 4NQO. In conclusion, it was shown in this study that 4NQO is a weak clastogen in human lymphoblastoid cells, but has the potency to induce gene mutations and DNA damage.

These studies clearly demonstrated that direct acting genotoxic agents could exhibit thresholds or non-linear dose responses for chromosome aberrations *in vitro*. MMC, 4NQO and araC displayed dose ranges where there was no elevation of chromosomal damage above background levels and thus safe exposure levels might exist for these genotoxins. Investigations into the mechanisms of the thresholded effects are however needed to provide explanations for the results.

DNA repair is one of the natural defence mechanisms to cope with the exposure to genotoxins (Jenkins et al., 2010). MMC is a DNA cross-linking agent and the lesions induced are repaired by multiple repair pathways, including NER, BER and homologous recombination (Dronkert and Kanaar, 2001). Thus, the NOEL observed, could be due to DNA repair, which seems to be efficient at low doses of chemical compounds. Genes involved in different repair pathways were investigated for changes in gene expression (Chapter 3). However no significant changes in gene expression of any genes investigated could be observed. The base level expression of genes involved in DNA repair might be adequate to repair the damage caused by MMC to reduce DNA damage to background levels. In addition repair proteins could be modified by post-translational changes and these would not be picked up by gene expression approaches.

Apoptosis is another defence mechanism and the tumour suppressor gene TP53 encodes a phospho-protein, which is involved in cellular processes, such as cell cycle control and the prevention of uncontrolled cell proliferation through apoptosis. Therefore the role of p53 was

investigated in the low dose response of the genotoxins MMC and araC (Chapter 6). Low levels of p53 induction were observed in TK6 cells treated with MMC for 4h, since only small increases in either, *p21* gene expression or p53/ phospho-p53 (Ser15) were detected. Furthermore no cell cycle changes or induction of apoptosis were observed, suggesting that other defence mechanisms play a major role in the MMC dose response. Cellular and nuclear membranes might reduce the access of MMC to the nucleus. Consequently more studies into the mechanistic basis of the thresholded dose response of MMC need to be conducted.

MMC causes DNA damage through monofunctional DNA alkylation products and DNA cross-links (Abbas et al., 2002). However, the main cause of cytotoxicity is the interstrand MMC-DNA cross-links (Paz et al., 2004). Therefore investigations into MMC-induced adduct formation should be conducted. DNA cross-links cause damage to chromosomal DNA by blocking key DNA metabolisms, such as DNA replication and transcription (Lee et al., 2006). Further, alkylating agents, such as MMC are not capable of directly inducing strand breaks; thus they are rather the result of processing of lesions by different repair pathways (Morales-Ramirez et al., 2004). Therefore more investigations into the repair pathways induced by MMC have to be undertaken, by protein expression approaches or for example by the use of cell lines, which are deficient for certain repair pathways.

In addition, it was shown previously that MMC can activate the p53 pathway (Abbas et al., 2002; Champeil et al., 2010). However, only the short-term treatment for MMC was investigated for p53 activation here. Extended treatments, which showed high rates of chromosomal damage induction after MMC treatment might activate p53 more strongly than the short-term treatment.

High p53 activity was demonstrated in TK6 cells treated with araC. Increases in *p21* gene expression as well as increases in total p53 and phospho-p53 (Ser15) were detected. Further, the percentage of cells in G1/G0 phase increased over the dose range, suggesting a G1 arrest after araC treatment. Therefore p53 seems to play a central role in the DNA damage response in TK6 treated with araC, demonstrating the involvement of DNA repair pathways and apoptosis in the non-linear dose response relationships of araC. It was shown previously that araC slows down S-phase passage at low doses, whereas at higher concentrations araC inhibits the cell movement from G1 to S-phase (Valeriote, 1982). Further, araC is known for its inhibition of DNA synthesis in proliferating cells by incorporation into elongating DNA strands, resulting in retardation of DNA elongation as well as chain termination (Grant, 1998; Besirli et al., 2003). In addition, araC can inhibit enzymes involved in DNA synthesis and repair and furthermore can increase the generation of ROS (Grant, 1998; Besirli et al., 2003).

However, the exact mechanism of toxicity caused by araC is still unknown. Therefore more mechanistic studies need to be conducted to investigate the non-linear dose response of araC, such as investigating if DNA repair is involved in the dose responses seen.
In conclusion natural defence mechanisms seem to play an important role in the response of cells to exposure with direct acting genotoxins at the low dose level.

7.3 Importance of dose regime, accurate toxicity measurement and choice of cell type

Improvement of the *in vitro* mammalian cell assays is one of the priorities in genotoxicolgy testing because of the high rate of misleading positive results (Fowler et al., 2012; Fowler et al., 2012). It has become apparent that a number of chemicals that are not *in vivo* genotoxins lead to positive results *in vitro*. Reasons include the absence of detoxification processes *in vitro*, extreme culture conditions, which disturb the physiological conditions of the cell or DNA damage that can be inflicted through non-DNA target and processes within the cell (Scott et al., 1991; Fowler et al., 2012).
In this thesis the *in vitro* MN assay was used to investigate the low dose response relationships of genotoxins. Short-term as well as extended exposures of the chemical in the presence and absence of cytochalasin B are commonly used with this assay (OECD 487, 2007). However, dependent on the dose regime, linear and non-linear dose response relationships for MMC could be observed (Chapter 3). An extended treatment schedule of 24h in TK6 cells followed by one cell cycle of cytochalasin B (18h) showed significant increases in MN induction at low doses of MMC, demonstrating a linear dose response for MMC in the mononucleated and binucleated assay. The results are not unexpected since MMC is a cross-linking agent as well as an alkylating agent and therefore known to induce chromosomal aberrations (Greenwood et al., 2004; Schuler et al., 2010). Yet, an extended concurrent treatment of MMC and cytochalasin B in TK6 cells for one cell cycle showed no significant increases in MN frequency at the chosen dose regime. A possible interaction of cytochalasin B with MMC in the continuous treatment accounts for the lack of genotoxic effects. Cytochalasin B can reduce MN induction in combined treatments and has been shown for spindle poisons, like colchicine (Minissi et al., 1999). Cytochalasin B treatment might therefore interfere with the chromosome missegregation in human lymphocytes (Minissi et al., 1999).
Furthermore the cell cycle time might play a crucial role in the dose response of MMC. The average doubling of TK6 cells used in our lab was approximately 16 to 18 hours. It seems to be very likely that the treatment time and cell cycle length of TK6 cells are important to

produce genotoxic effects. It is therefore possible that the treatment time of 18h (one cell cycle) with no recovery time might not have been long enough to produce genotoxic effects and that at least 1.5 cell cycles are essential for DNA damage induction to be shown. In addition the time required for a lesion to be fixed as a mutation might play a role, as it was shown for alkylating agents *in vitro* (MMS) and *in vivo* (BCNU and Bus) that more than one cell division is needed to cause MN induction due to multiple rounds of error-prone lesion repair (Drabløs et al., 2004; Morales-Ramirez et al., 2004).

TK6 cells treated with MMC for 4h (short-term exposure) followed by one cell cycle with cytochalasin B showed a non-linear dose response.

Consequently, the dose regime seems to play a crucial role in the response of the cell to the exposure of genotoxins and in the induction of genotoxicity and cytotoxicity. Furthermore, a recent study from Sobol *et al.* (2012) showed that an extended recovery time after treatment with compounds with direct DNA reactivity in TK6 cells increased the magnitude of micronucleus induction. Similar observations were made in this study after the treatment of TK6 cells with 4NQO (Chapter 4). Short-term treatments (4h) and extended treatments (24h and 48h) without prolonged recovery time showed little to no chromosomal damage induction, whereas extending the recovery time after the short-term treatments in the CBMN assay from 18h to 42h and in the mononucleated assay from 24h to 40h increased the magnitude of MN induction at the top doses, demonstrating yet again the importance of the dose regime. TK6 cells might have a prolonged cell cycle delay in response to genotoxins (Islaih et al., 2005), resulting in the possibility of damaged cells being rather stalled than eliminated through apoptosis (Sobol et al., 2012). Consequently the extended recovery period would allow the stalled cells to progress into mitosis and hence to fix damage as a MN. In addition toxicity appeared to be higher in cells with the shorter recovery time than in cells with the extended recovery time, demonstrating higher cytostasis, which supports the proposition made by Islaih *et al.* (2005) and the findings from Sobol *et al.* (2012).

Consequently, cell cycle length, dose range, treatment time and recovery regimes should be taken into account when investigating dose response relationships and DNA damage induction.

Cytostasis and cell death together define the overall cytotoxicity of an agent in cell culture (Lorge et al., 2008). Appropriate measurements of cytotoxicity are crucial when selecting for test concentrations in *in vitro* genotoxicity assays, as underestimation of toxicity might lead to a selection of inappropriate toxic concentrations for analysis, which have the potential to generate misleading positive results in the chosen assays (Fellows et al., 2008).

Concentrations selected should have a maximum of 50±5% toxicity at the top dose, because necrotic and apoptotic cells often contain chromosome fragments. Different toxicity measures are available for the *in vitro* MN assay, including CBPI or PI for experiments with cytochalasin B and RPD, RICC and RCC for experiments with or without cytochalasin B (Fowler et al., 2012). RICC and RPD are appropriate measures of toxicity when compared with RI and CBPI (Schuler et al., 2010; Fowler et al., 2012), while RCC seems to underestimate toxicity and consequently higher concentrations for subsequent MN assay analysis could be selected (Fellows et al., 2008; Fowler et al., 2012). In the studies described in this thesis RPD was selected as the most suitable method to measure in toxicity, because of recent publications (Lorge et al., 2008; Fellows et al., 2008) and results gained in our laboratory (data not shown).

Another factor in the high rate of misleading positive results seems to be the choice of cell type and in particular the numbers of deficiencies that the cell lines carry, such as lack of normal metabolism, altered DNA-repair capability and impaired p53 function (Fowler et al., 2012).

A study by Fowler *et al.* (2012) showed that rodent cell lines, which are p53 deficient, were more susceptible to cytotoxicity and MN induction than p53 competent cells, resulting in misleading positive results (Fowler et al, 2012). In addition the mouse lymphoma cell line L5178Y treated with 4NQO in this thesis (Chapter 4) showed highly significant increases in MN induction with no decreases in cell viability, while the human lymphoblastoid cell lines TK6, AHH-1 and MCL-5 showed little to no induction of MN even up to 50±5% toxicity after 4NQO treatment. L5178Y cells are known for their dysfunctional p53 activity, since they have a missense mutation in exon 5 on chromosome 11a (amino acid change from a cysteine to an arginine) and a nonsense mutation in exon 4 on chromosome 11b (changing a glutamine to a stop codon) (Storer et al., 1997; Clark et al., 2004). From this it follows that the mouse lymphoma cells have no wild-type p53 allele. On the other hand TK6 cells are p53 competent, while AHH-1 and MCL-5 cells are heterozygous for p53 at the interface between the codons 281 and 282 of exon 8 (Guest and Parry, 1999).

The tumour suppressor gene TP53 is a transcriptional activator that regulates the expression of various genes involved in cell cycle arrest and apoptosis in response to genotoxic and cellular stress, which prevents damaged DNA from being replicated and plays an essential role in cellular integrity (Arrowsmith, 1999). Abnormal DNA binding properties and/or transcriptional activation through TP53 mutation can cause mal-functions in the DNA damage dependent cell death pathway (Guest and Parry, 1999). Consequently, the effects of

DNA damaging agents could become significant at low doses, where p53 competent cell lines would induce DNA damage dependent cell death (Guest and Parry, 1999).

Furthermore the DNA damage induction of MMC and araC in NH32 cells, which are an isogenic derivative of TK6 cells with a double p53 knockout were compared with TK6 cells (Li et al., 2006) (Chapter 6). NH32 cells were more sensitive to cytotoxicity after both MMC and araC treatment than the proficient parent cell line TK6. Furthermore NH32 cells showed a higher magnitude of MN induction than TK6 cells after araC treatment, demonstrating yet again that p53 plays a central role in the DNA damage response in human lymphoblastoid cells.

In conclusion in Chapter 4, it was shown that TK6 cells are more susceptible to cytotoxicity and further showed a smaller magnitude of MN induction than AHH-1 and MCL-5 cells and in particular to the mouse lymphoma cell line L5178Y. Cell lines with p53 mutations are more likely to survive and replicate with DNA damage, which can lead to higher MN frequencies, since p53 plays an important role in cell responses, like cell cycle arrest, apoptosis and DNA repair in response to DNA damage (Hashimoto et al., 2011). p53 function seems to be a key factor for the cell-type sensitivity for genotoxicity and cytotoxicity (Hashimoto et al., 2011). Subsequently, it is necessary to compare the ability of different cell types to lead to true positive and negative results (Fowler et al., 2012).

The data presented in this study demonstrated clearly the importance of dose-regime, accurate toxicity measurements and the choice of cell type for genotoxicity testing to reduce the detection of misleading positive compounds.

7.4 Conclusion

Non-linear dose response relationships after low dose exposure have been demonstrated for MMC (a cross-linking agent) and araC (a nucleoside analogue of cytidine and desoxycytidine), while 4NQO (a bulky adduct inducer) revealed to be a weak clastogen by investigating chromosomal damage, using the *in vitro* MN assay. The semi-automated scoring protocol for the Metafer-System proved to be an accurate protocol for scoring MN, when compared to the visually scoring protocol. However, dose regime, accurate toxicity measurements and choice of cell type are crucial for defining the dose response relationships and the induction of genotoxicity and cytotoxicity; thus they have to be taken into account when designing and analysing genotoxicology experiments.

DNA repair plays most likely a major role in these non-linear (thresholded) responses by removing genetic damage induced at low levels. Furthermore p53 was shown to be involved

in the DNA damage response in human lymphoblastoid cells, through cell cycle delay and the induction of apoptosis. In addition the potential of p53 as a direct DNA damage detector and as a potential endpoint for genotoxicity testing was noted and needs to be further validated.

References

Aaron, C.S., Bolcsfoldi, G., Glatt, H.-R., Moore, M., Nishi, Y., Stankowski, L., Theiss, J., Thompson, E. (1994) Mammalian cell gene mutation assays working group report. *Mutation Research.* **312:** 235-239

Abbas, T., Olivier, M., Lopez, J., Houser, S., Xiao, G., Kumar, G.S., Tomasz, M., Bargonetti, J. (2002) Differential Activation of p53 by Various Adducts of Mitomycin C. *The Journal of Biologican Chemistry.* **277(43):** 40513-40519

Ames, B.N., Shigenaga, M.K., Swirsky Gold, L. (1993) DNA Lesions, Inducible DNA Repair, and Cell Division: Three Key Factors in Mutagenesis and Carcinogenesis. *Environmental Health Perspectives.* **101(Suppl 5):** 35-44

Amundson, S.A., Myers, T.G., Fornace Jr., A.J. (1998) Roles for p53 in growth arrest and apoptosis: putting on the brakes after genotoxic stress. *Oncogene.* **17:** 3287-3299

araC structure. Available at: http://www.sigmaaldrich.com/catalog/product/sigma/c1768 (accessed: 09/01/2013)

Arima, Y., Nishigori, C., Takeuchi, T., Oka, S., Morimoto, K., Utani, A., Miyachi, Y. (2006) 4-Nitroquinoline 1-Oxide Forms 8-Hydroxydeoxyguanosine in Human Fibroblasts through Reactive Oxygen Species. *Toxicological Sciences.* **91(2):** 382-392

Arrowsmith, C.H. (1999) Structure and function in the p53 family. *Cell death and Differentiation.* **6:** 1169-1173

Auerbach, C., Robson, J.M. (1946) Chemical production of mutations. *Nature.* **157:** 302

Bailleul, B., Daubersies, P., Galiegue-Zouitina, S., Loucheux-Lefebvre, M.-H. (1989) Molecular Basis of 4-Nitroquinoline 1-Oxide Carcinogenesis. *Jpn. J. Cancer Research.* **80**: 691-697

Bargonetti, J., Champeil, E., Tomasz, M. (2010) Differential Toxicity of DNA Adducts of Mitomycin C. *Journal of Nucleic Acids.* **2010:** 1-6

Besirli, C.G., Deckwerth, T.L., Crowder, R.J., Freeman, R.S., Johnson Jr., E.M. (2003) Cytosine arabinoside rapidly activates Bax-dependent apoptosis and a delayed Bax-independent death pathway in sympathetic neurons. *Cell death and Differentiation.* **10:** 1045-1058

Bishop, J.O., Selman, G.G., Hickman, J., Black, L., Saunders, R.D., Clark, A.J. (1985) The 45-kb unit of major urinary protein gene organization is a gigantic imperfect palindrome. *Mol Cell Biol.* **5:** 1591-1600

Boamah, E.K., White, D.E., Talbott, K.E., Arva, N.C., Berman, D., Tomasz, M., Bargonetti, J. (2007) Mitomycin-DNA Adducts Induce p53-Dependent and p53-Independent Cell Death Pathways. *ACS Chem Biol.* **2(6):** 399-407

Boller, K., Schmid, W. (1970) Chemical mutagenesis in mammals. The Chinese hamster bone marrow as an *in vivo* test system. Hematological findings after treatment with trenimon. *Humangenetik.* **11:** 35-54

Bonetta, L. (2005) Prime time for real-time PCR. *Nature Methods.* **2(4):** 305-312

Bruin, J.E., Gerstein, H.C., Morrison, K.M., Holloway, A.C. (2008) Increased Pancreatic Beta-Cell Apoptosis following Fetal and Neonatal Exposure to Nicotine Is Mediated via the Mitochondria. *Toxicological Sciences.* **103(2).** 362-370

Burlinson, B., Tice, R.R., Speit, G., Agurell, E., Brendler-Schwaab, S. Y., Collins, A.R., Escobar, P., Honma, M., Kumaravel, T.S., Nakajima, M., Sasaki, Y.F., Thybaud, V., Uno, Y., Vasquez, M., Hartmann, A. (2007) Fourth International Workgroup on Genotoxicity testing: Results of the in vivo Comet assay workgroup. *Mutation Research.* **627:** 31-35

Bustin, S.A, Benes, V., Garson, J.A., Hellemans, J., Huggett, J., Kubista, M., Mueller, R., Nolan, T., Pfaffl, M.W., Shipley, G.L., Vandesompele, J., Wittwer, C.T. (2009) The MIQE Guidelines: Minimum Information for publication of Quantitative Real-Time PCR Experiments. *Clinical Chemistry.* **55(4):** 611-622

Calabrese, E.J. (2009) The road to linearity at low doses became the basis for carcinogen risk assessment. *Arch Toxicol.* **83:** 203-225

Cariou, O., Laroche-Prignet N., Ledieu S., Guizon, I., Paillard, F., Thybaud V. (2010) Cytosine arabinoside, vinblastine, 5-fluorouracil and 2-aminoanthracene testing in the *in vitro* micronucleus assay with L5178Y mouse lymphoma cells at Sanofi Aventis, with different cytotoxicity measurements, in support of the draft OECD Test Guideline on *In Vitro* Mammalian Cell Micronucleus Test. *Mutation Research.* **702:** 148-156

Carter S.B. (1967) Effects of cytochalasins on mammalian cells. *Nature.* **213:** 261-264

Champeil, E., Bargonetti, J., Tomasz, M. (2010) Differential Toxicity of DNA Adducts of Mitomycin C. *Journal of Nucleic Acids.* **2010:** 1-6

Cheng, Y-C., Capizzi, R.L. (1982) Enzymology of Cytosine Arabinoside. *Medical and Pediatric Oncology Supplement.* **1:** 27-31

Christmann, M., Tomicic, M.T., Roos, W.P., Kaina, B. (2003) Mechanisms of human DNA repair: an update. *Toxicology.* **193:** 3-34

Chuang, Y-Y.E., Chen, Q., Liber, H.L. (1999) Radiation-induced Mutations at the Autosomal Thymidine Kinase Locus Are Not Elevated in p53-null Cells. *Cancer Research.* **59:** 3073-3076

Cimino, M.C. (2006) Comparative Overview of Current International Strategies and Guidelines for Genetic Toxicology Testing for Regulatory Purposes. *Environmental and Molecular Mutagenesis.* **47:** 362-390

Clark, L.S., Harrington-Brock, K., Wang, J., Sargent, l., Lowry, D., Reynolds, S.H., Moore, M.M. (2004) Loss of P53 heterozygosity is not responsible for the small colony thymidine kinase mutant phenotype in L5178y mouse lymphoma cells. *Mutagenesis.* **19(4):** 263-268

Committee on Mutagenicity of Chemicals in Food, Consumer Products and the Environment (COM) (2000) Guidance on a strategy for testing of chemicals for mutagenicity. Department of Health, UK.
Available at: http://www.advisorybodies.doh.gov.uk/com/guidance.pdf. (Accessed: 03.03.12)

Committee on Mutagenicity of Chemicals in Food, Consumer Products and the Environment (COM) (2011) Guidance on a strategy for genotoxicity testing of chemical substances. Available at:
http://www.iacom.org.uk/guidstate/documents/COMGuidanceFINAL2.pdf.
(Accessed: 12.02.13)

Countryman, P.L., Heddle, J.A. (1976) The production of micronuclei from chromosome aberrations in irradiated cultures of human lymphocytes. *Mutation Research.* **41:** 321-332

Crebelli, R. (2000) Threshold-mediated mechanisms in mutagenesis: implications in the classification and regulation of chemical mutagens. *Mutation Research.* **464:** 129-135

Crespi, C.L., Gonzalez, D.T., Steimel, T.R., Turner, H.Y., Gelboin, B.W., Penman, R., Langenbach, A. (1991) A metabolically competent human cell line expressing five cDNAs encoding pro-carcinogen-activating enzymes: application to mutagenicity testing. *Chem. Res. Toxicol.* **4:** 566-572

Crofton-Sleigh, C., Doherty, A.T., Ellard, S., Parry, E.M., Venitt, V. (1993) Micronucleus assays using cytochalasin-blocked MCL-5 cells, a proprietary human cell line expressing five human cytochromes P-45 and microsomal epoxide hydrolase. *Mutagenesis.* **8:** 363-373

Danam, R., Howell, S.R., Brent, T.P., Harris, L.C. (2005) Epigenetic regulation of O^6-methylguanine-DNA methyltransferase gene expression by histone acetylation and methyl-CpG binding proteins. *Molecular Cancer Therapeutics.* **4:** 61-69

Danshiitsoodol, N., Azzariti de Pinho, C., Matoba, Y., Kumagai, T., Sugiyama, M. (2006) The Mitomycin C (MMC)-binding Protein from MMC-producing Microorganisms Protects from the Lethal Effect of Bleomycin: Crystallographic Analysis to Elucidate the Binding Mode of the Antibiotic to the Protein. *J.Mol.Biol.* **360:** 398-408

De Bont, R. and van Larebeke, N. (2004) Endogenous DNA damage in humans: a review of quantitative data. *Mutagenesis.* **19(3):** 169-185

Dearfield K.L., Auletta A.E., Cimino M.C., Moore M.M. (1991) Considerations in the U.S. Environmental Protection Agency's testing approach for mutagenicity. *Mutation Research.* **258:** 259-283

Dearfield, K.L., Cimino, M.C., McCarroll, N.E., Mauer, I., Valcovic, L.R. (2002) Genotoxicity risk assessment: a proposed classification strategy. *Mutation Research.* **521:** 121-135

Decordier I., Kirsch-Volders M. (2006) The *in vitro* micronucleus test: From past to future. *Mutation Research.* **607:** 2-4

Decordier, I., Papine, A., Plas, G., Roesems, S., Loock, K.V., Moreno-Palomo, J., Cemeli, E., Anderson, D., Fucic, A., Marcos, R., Soussaline, F., Kirsch-Volders, M. (2009) Automated image analysis of cytokinesis-blocked micronuclei: an adapted protocol and a validated scoring procedure for biomonitoring. *Mutagenesis.* **24:** 85-93

Decordier, I., Papine A., Vande Loock, K., Plas G., Soussaline, F., Kirsch-Volders, M. (2011) Automated image analysis of micronuclei by IMSTAR for biomonitoring. *Mutagenesis.* **26(1):** 163-168

Dertinger, S.D., Phonethepswath, S., Franklin, D., Weller, P., Torous, D.K., Bryce, S.M., Avlasevich, S., Bemis, J.C., Hyrien, O., Palis, J., MacGregor, J.T. (2010) Integration of Mutation and Chromosomal Damage Endpoints into 28-Day Repeat Dose Toxicology Studies. *Toxicological Sciences.* **115(2):** 401-411

Doak, S.H., Jenkins, G.J.S., Parry, E.M., Griffiths, A.P., Baxter, J.N., Parry, J.M. (2004) Differential expression of the MAD2, BUB1 and HSP27 genes in Barrett's oesophagus-their association with aneuploidy and neoplastic progression. *Mutation Research.* **547:** 133-144

Doak, S.H., Jenkins, G.J.S., Johnson, G.E., Quick, E., Parry, E.M., Parry, J.M. (2007) Mechanistic Influences for Mutation Induction Curves after Exposure to DNA-Reactive Carcinogens. *Cancer Res.* **67**: 3904-3911

Dobo, K.L., Eastmond, D.A., Grosovsky, A.J. (1997) The influence of cellular apoptotic capacity on N-nitrosodimethylamine-induced loss of heterozygosity mutation in human cells. *Carcinogenesis.* **18:** 1701-1707

Doherty, A.T., Hayes, J., Fellows, M., Kirk, S., O'Donovan, M. (2011) A rapid, semi-automated method for scoring micronuclei in mononucleated mouse lymphoma cells. *Mutation Research.* **726:** 36-41

Drabløs, F., Feyzi, E., Aas, P.A., Vaagbø, C.B., Kavli, B., Bratlie, M.S., Peña-Diaz, J., Otterlei, M., Slupphaug, G., Krokan, H.E. (2004) Alkylation damage in DNA and RNA-repair mechanisms and medical significance. *Elsevier.* **3:** 1389-1407

Drake, J.W., Allen, E.F., Forsberg, S.A., Preparat, R.M., Greenber, E.O. (1969) Spontaneous mutation. *Nature.* 221: 1128-1132

Dronkert, M.L. and Kanaar, R (2001) Repair of DNA interstrand cross-links. *Mutation Research.* **486(4):** 217-247

Elhajouli, A., van Hummelen, P., Kirsch-Volders, M. (1995) Indications for a threshold of chemically-induced aneuploidy in vitro in human lymphocytes. *Environ Mol Mutagen.* **26**: 292-304

Elhajouji, A., Tibaldi, F., Kirsch-Volders, M. (1997) Indication for thresholds of chromosome non-disjunction versus chromosome lagging induced by spindle inhibitors *in vitro* in human lymphocytes. *Mutagenesis.* **12:** 133-140

Elhajouji, A. (2010) Mitomycin C, 5-fluoruracil, colchicine and etoposide tested in the in vitro mammalian cell micronucleus test (Mnvit) in the human lymphoblastoid cell line TK6 at Novartis in support of OECD draft Test Guideline 487. *Mutat.Res.* **702:** 157-162

Elhajouji, A., Lukamowicz, M., Cammerer, Z., Kirsch-Volders, M. (2011) Potential thresholds for genotoxic effects by micronucleus scoring. *Mutagenesis.* **26(1):** 199-204

Elmore, S. (2007) Apoptosis: A Review of Programmed Cell Death. *Toxicol. Pathol.* **35(4):** 495-516

Endo, H., Ono, T. and Sugimura, T.: Chemistry and Biological Actions of 4-Nitroquinoline 1-Oxide. Springer-Verlag Berlin-Heidelberg-New York, 1971

Evans, H.J., Neary, G.J., Williamson, F.S. (1959) The relative biological efficiency of single doses of fast neutrons and gamma rays in Vicia faba roots and the effect of oxygen. Part II. Chromosome damage; the production of micronuclei. *Int.J.Rad.Biol.* **1:** 230-240

Fellows, M.G., O`Donovan, M.R., Lorge, E., Kirkland, D. (2008) Comparison of different methods for an accurate assessment of cytotoxicity in the *in vitro* micronucleus test II: Practical aspects with toxic agents. *Mutation Research.* **655:** 4-21

Fellows, M.D., O'Donovan, M.R. (2009) Etoposide, cadmium chloride, benzo[a]pyrene, cyclophosphamide and colchicines tested in the in vitro mammalian cell micronucleus test (MNvit) in the presence and absence of cytokinesis block using L5178Y mouse lymphoma cells and 2-aminoanthracene tested in MNvit in the absence of cytokinesis block using TK6 cells at AstraZeneca UK, in support of OECD draft Test Guideline 487. *Mutat.Res.* **702:** 163-170

Fenech, M and Morley, A.A. (1986) Cytokinesis-block micronucleus method in human lymphocytes: effect of in vivo ageing and low-dose X-irradiation. *Mutation Research.* **161:** 193-198

Fenech, M. and Neville, S. (1992) Conversion of excision-repairable DNA lesions to micronuclei within one cell cycle in human lymphocytes. *Environ. Mol. Mutagenesis.* **19:** 27-36

Fenech, M., Rinaldi, J., Surralles, J. (1994) The origin of micronuclei induced by cytosine arabinoside and its synergistic interation with hydroxyurea in human lymphocytes. *Mutagenesis.* **9(3):** 273-277

Fenech, M. (1997) The advantages and disadvantages of the cytokinesis-block micronucleus method. *Mutation Research.* **392:** 11-18

Fenech, M., Holland, N., Chang, W.P., Zeiger, E., Bonassi, S. (1999) The Human MicroNucleus Project-An international colloaborative study on the use of the micronucleus technique for measuring DNA damage in humans. *Mutat.Res.* **428:** 271-283

Fenech M. (2000) The in vitro micronucleus technique. *Mutation Research.* **455:** 81-95

Fenech, M., Chang, W.P., Kirsch-Volders, M., Holland, N., Bonassi, S., Zeiger, E. (2003) HUMN project: detailed description of the scoring criteria for the cytokinesis-block micronucleus assay using isolated human lymphocyte cultures. *Mutat.Res.* **534:** 65-75

Fowler, P., Whitwell, J., Jeffrey, L., Young, J., Smith, K., Kirkland, D. (2010) Etoposide; colchicine; mitomycin C and cyclophosphamide tested in the in vitro mammalian cell micronucleus test (MNvi) in Chinese hamster lung (CHL) cells at Covance laboratories, Harrogate UK in support of OECD draft Test Guideline 487. *Mutation research.* **702(2):** 175-180

Fowler, P., Smith K., Young, J., Jeffrey, L., Kirkland, D., Pfuhler, S., Carmichael, P. (2012) Reduction of misleading ("false") positive results in mammalian cell genotoxicity assays. I. Choice of cell type. *Mutation Research.* **742:** 11-25

Fowler, P., Smith, R., Smith, K., Young, J., Jeffrey, L., Kirkland, D., Pfuhler, S., Carmichael, P. (2012) Reduction of misleading ("false") positive results in mammalian cell genotoxicity assays. II. Importance of accurate toxicity measurement. *Mutation Research.* **747:** 104-117

Fukushima, S., Wanibuchi, H., Morimura, K., Iwai, S., Nakae, D., Kishida, H., Tsuda, H., Uehara, N., Imaida, K., Shirai, T., Tatematsu, M., Tsukamoto, T., Hirose, M. and Furukawa, F. (2004) Existence of a Threshold for Induction of Aberrant Crypt Foci in the Rat colon with Low Doses of 2-Amino-1-methyl-6-phenolimidazo[4,5-b]pyridine. *Toxicological Sciences.* **80**: 109-114

Fulda, S. and Debatin, K.-M. (2006) Extrinsic versus intrinsic apoptosis pathways in anticancer chemotherapy. *Oncogene.* **25:** 4798-4811

Galloway, S.M., Aardema, M.J., Ishidate, Jr. M., Ivett, J.L., Kirkland, D.J., Morita, T., Mosesso, P., Sofuni, T. (1994) Report from working group on in vitro tests for chromosomal aberrations. *Mutation Research.* **312:** 241-261

Gocke, E., Ballantyne, M., Whitwell, J., Müller, L. (2009) MNT and MutaMouse studies to define the *in vivo* dose response relations of the genotoxicity of EMS and ENU. *Toxicol. Lett.* 190: 286-297

Gocke, E., Mueller, L. (2009) *In vivo* studies in the mouse to define a threshold for the genotoxicity of EMS and ENU. *Mutation Research.* **678**: 101-107

Gollapudi, B.B., Johnson, G.E., Hernandez, L.G., Pottenger, L.H., Dearfield, K.L., Jeffrey, A.M., Julien, E., Kim, J.H., Lovell, D.P., MacGregor, J.T., Moore, M.M., van Benthem, J., white, P.A., Zeiger, E., Thybaud, V. (2013) Quantitative Approaches for assessing Dose-response relationships in Genetic Toxicology Studies. *Environmental and Molecular Mutagenesis.***54:** 8-18

Grant, S. (1998) Ara-C: cellular and molecular pharmacology. *Adv.Cancer.Res.* **72:** 197-233

Grawé, J., Abramsson-Zetterberg, L., Zetterberg, G. (1998) Low dose effects of chemicals as assessed by the flow cytrometric in vivo micronucleus assay. *Mutat.Res.* **405:** 199-208

Greenwood, S.K., Hill, R.B., Sun, J.T., Armstrong, M.J., Johnson, T.E., Gara, J.P., Galloway, S.M. (2004) Population doubling: a simple and more accurate estimation of cell growth suppression in the in vitro assay for chromosomal aberrations that reduces irrelevant positive results. *Environ.Mol.Mutagen.* **43:** 36-44

Greim, H. and Albertini, R.J., 2012. Introduction and Conclusion: The Rationale for Thresholds for Genotoxic Carcinogens. In: H. Greim and R.J. Albertini, ed 2012. The Cellular Response to the Genotoxic Insult. RSC Publishing. Chapter 1

Griffiths, A.F., Miller, J.H., Suzuki, D.T., Lewontin, R.C., Gelbart, W.M. An Introduction to Genetic Analysis. 7th edition. New York: W.H. Freeman; 2000

Guest, R.D. and Parry, J.M. (1999) P53 integrity in the genetically engineered mammalian cell lines AHH-1 and MCL-5. *Mutation Research.* **423:** 39-46

Hashimoto, K., Nakajima, Y., Uematsu, R., Matsumura, S., Chatani, F. (2011) Involvement of p53 function in different magnitude of genotoxic and cytotoxic responses in *in vitro* micronucleus assays. *Mutation Research.* **726:** 21-28

Harris, C.C. (1996) Structure and Function of the p53 Tumor Suppressor Gene: Clues for Rational Cancer Therapeutic Strategies. *Journal of the National Cancer Institute.* **88(20):** 1442-1455

Hata, T., Sano, Y., Sugawara, R., Matsumae, A., Kanomori, K., Shima, T., Hoshi, T. (1956) Mitomycin, a New Antibiotic from *Streptomyces.* I. *J Antibiot. Ser A.* **9:** 141-146

Hayashi, M., MacGregor, J.T., Gatehouse, D.G., Adler, I-D., Blakey, D.H., Dertinger, S.D., Krishna, G., Morita, T., Russo, A., Sutou, S.(2000) In Vivo Rodent Erythrocyte Micronucleus Assay. II. Some aspects of Protocol Design Including Repeated Treatments, Integration With Toxicity Testing, and Automated Scoring. *Environmental and Molecular Mutagenesis.* **35:** 234-252

Hayashi, M., MacGregor, J.T., Gatehouse, D.G., Blakey, D.H., Dertinger, S.D., Abramsson-Zetterberg, L., Krishna, G., Morita, T., Russo, A., Asano, N., Suszuki, H., Ohyama, W., Gibson, D. (2007) *In vivo* erythrocyte micronucleus assay III. Validation and regulatory acceptance of automated scoring and the use of rat-peripheral blood reticulocytes, with discussion of non-hematopoietic target cells and a single dose-level limit test. *Mutat. Res.* **627:** 10-30

Heddle J.A. (1973) A rapid in vivo test for chromosome damage. *Mutation Research.* **18:** 187-190

Heddle, J.A., Fenech, M., Hayashi, M., MacGregor, J.T. (2011) Reflections on the development of micronucleus assay. *Mutagenesis.* **26:** 3-10

Henderson, E.S. (1982) Introduction to the Symposium on High-Dose Cytosine Arabinoside. *Medical and Pediatric Oncology Supplement.* **1:** 1-3

Henderson, L., Alberini, S., Aardema, M. (2000) Thresholds in genotoxicity responses. *Mutation Research.* **464:** 123-128

Hengstler, J.G., Bogdanffy, M.S., Bolt, H.M., Oesch, F. (2003) Challenging dogma: thresholds for genotoxic carcinogens? The case of vinyl acetate. *Annu Rev Pharmacol Toxicol.* **43**: 485-520

Howell, W.H. (1890) The life-history of the formed elements of the blood, especially the red blood corpuscles. Journal of Morphology, New York, 1890-91, 4: 57-116.

Hu, T., Miller, C.M., Ridder, G.M., Aardema, M.J. (1999) Characterization of p53 in Chinese hamster cell lines CHO-K1, CHO-WBL, and CHL: implications for genotoxicity testing. *Mutation Research.* **426:** 51-62

Inga, A., Iannone, R., Degan, P., Campomenosi, P., Fronza, G., Abbondanddolo, A., Menichini, P. (1994) Analysis of 4-nitroquinoline-1-oxide induced mutations at the *hprt* locus in mammalian cells: possible involvement of preferential DNA repair. *Mutagenesis.* **9(19):** 67-72

International Conference on Harmonization (ICH) (1996b) Guideline for industry. Specific aspects for regulatory genotoxicity testing of pharmaceuticals. ICH 2SA, April 1996. Available at: http://www.ema.europa.eu/docs/en_GB/document_library/Scientific_guideline/2009/09/WC500003146.pdf. (Accessed: 27.02.12)

International Conference on Harmonization (ICH) (1997b) Guideline for industry. Genotoxicity: A standard battery for genotoxicity testing of pharmaceuticals. ICH 2SB, July 1997. Available at http://www.hc-sc.gc.ca/dhp-mps/prodpharma/applic-demande/guide-ld/ich/securit/s2b-eng.php. (Accessed: 27.02.12)

Islaih, M., Halstead, I.A., Kadura, B., Li, B., Reid-Hubbard, J.L., Flick, l., Altizer, J.L., Thom Deahl, J., Monteith, D.K., Newton, R.K., Watson, D.E. (2005) Relationships between genomic, cell cycle, and mutagenic responses of TK6 cells exposed to DNA damaging chemials. *Mutation Research.* **578:** 100-116

Iyer, V.N. and Szybalski, W. (1963) A MOLECULAR MECHANISM OF MITOMYCIN ACTION: LINKING OF COMPLEMENTARY DNA STRANDS. *Proc. N.A.S.*, **50:** 355-362

Iyer, V.N. and Szybalski, W. (1964) Mitomycins and porfiromycin: chemical mechanism of activation and cross-linking of DNA. *Science.* **145:** 55-58

Jackson, A.L., Loeb, L.A. (2001) The contribution of endogenous sources of DNA damage to the multiple mutations in cancer. *Mutation Research.* **477:** 7-21

Jenkins, G.J.S., Chaleshtori, M.H., Song, H., Parry, J.M. (1998) Mutation analysis using the restriction site mutation (RSM) assay. *Mutation Research.* **405:** 209-220

Jenkins, G.J.S., Doak, S.H., Johnson, G.E., Quick, E., Waters, E.M. and Parry, J.M. (2005) Do dose response thresholds exist for genotoxic alkylating agents?. *Mutagenesis.* **20**: 389-398

Jenkins, G.J.S., Zaïr, Z., Johnson, G.E., Doak, S.H. (2010) Genotoxic thresholds , DNA repair, and susceptibility in human populations. *Toxicology.* **278:** 305-310

Joerger, A.C. and Fersht, A.R. (2007) Structure-function-rescue: the diverse nature of common p53 cancer mutants. *Oncogene.* **26:** 2226-2242

Johnson, R.D., Jasin, M. (2000) Sister chromatid gene conversion is a prominent double-strand break repair pathway in mammalian cells. *EMBO J.* **19:** 3398-3407

Johnson, G.E., Doak, S.H., Griffiths, S.M., Quick, E.L., Skibinski, D.O.F., Zaïr, Z.M., Jenkins, G.J. (2009) Non-linear dose-response of DNA-reactive genotoxins: Recommendations for data analysis. *Mutat.Res.* **678:** 95-100

Johnson, G.E., 2012.Mammalian Cell *HPRT* Gene Mutation Assay: test Methods. In: J.M. Parry and E.M. Parry, ed. 2012. Genetic Toxicology: Principles and Methods, Methods in Molecular Biology, vol. 817. Springer. Chapter 4

Jolly, J.M.J. (1905) Sur la formation des globules rouges des mammifères. Comptes rendus de la Société de Biologie, Paris, 1905, **58:** 528-531

Jones, C.J., Edwards, S.M., Waters, R. (1989) The repair of identified large DNA adducts induced by 4-nitroquinoline-1-oxide in normal or xeroderma pigmentosum group A human fibroblasts, and the role of DNA polymerases α or δ. *Carcinogenesis.* **10(7):** 1197-1201

Kanojia, D. and Vaidya, M.M. (2006) 4-Nitroquinoline-1-oxide induced experimental oral carcinogenesis. *Oral Oncology.* **42:** 655-667

Kato, S., Han, S.-Y., Liu, W., Otsuka, K., Shibata, H., Kanamaru, R., Ishioka, C. (2003) Understanding the function-structure and function-mutation relationships of p53 tumor suppressor protein by high-resolution missense mutation analysis. *PNAS.* **100(14):** 8424-8429

Kawaguchi, S., Nakamura, T., Yamamoto, A., Honda, G., Sasaki, Y.F. (2010) Is the Comet assay a Sensitive Procedure for Detecting Genotoxicity?. *Journal of Nucleic Acids.* **2010:** 1-8

Kirkland, D.J., Aardema, M., Banduhn, N., Carmichael, P., Fautz, R., Meunier, J-R., Pfuhler, S. (2007) *In vitro* approaches to develop weight of evidence (WoE) and mode of action (MoA) discussions with positive *in vitro* genotoxicity results. *Mutagenesis.* **22(3):** 161-175

Kirsch-Volders, M., Elhajouji, A., Cundari, E., Van Hummelen, P. (1997) The in vitro micronucleus test: a multi-endpoint assay to detect simultaneously mitotic delay, apoptosis, chromosome breakage, chromosome loss and non-disjunction. *Mutat.Res.* **392:** 19-30

Kirsch-Volders, M., Sofuni, T., Aardema, M., Albertini, S., Eastmond, D., Fenech, M., Ishidate,Jr., M., Lorfe, E., Norppa, H., Surralles, J., von der Hude, W., Wakata, A. (2000) Report from the In Vitro Micronucleus Assay Working Group. *Environ.Mol.Mutagen.* **35:** 167-172

Kirsch-Volders, M., Aardema M., Elhajouji A. (2000) Concepts of threshold in mutagenesis and carcinogenesis. *Mutation Research.* **464:** 3-11

Kirsch-Volders, M. and Fenech, M. (2001) Inclusion of micronuclei in non-devided mononuclear lymphocytes and necrosis/apoptosis may provide a more comprehensive cytokinesis block micronucleus assay for biomonitoring purposes. *Mutagenesis.* **16(1):** 51-58

Kirsch-Volders, M., Vanhauwaert, A., Eichenlaub-Ritter, U., Decordier, I. (2003) Indirect mechanisms of genotoxicity. *Toxicology Letters.* **140-141:** 63-74

Kirsch-Volders, M., Sofuni, T., Aardema M., Albertini, S., Eastmond, D., Fenech, M., Ishidate, Jr., M., Kirchner, S., Lorge, E., Morita, T., Norppa, H., Surrales, J., Vanhauwaert, A., Wakata, A. (2003) Report from the in vitro micronucleus assay working group. *Mutation Research.* **540:** 153-163

Kirsch-Volders, M., Gonzalez, L., Carmichael, P., Kirkland, D. (2009) Risk assessment of genotoxic mutagens with thresholds: A brief introduction. *Mutat.Res.* **687:** 72-75

Koana, T., Takashima, Y., Okada, M.O., Ikehata, M., Miyakoshi, J. , Sakai, K. (2004) A threshold exists in the dose-response relationship for somatic mutation frequency induced by X irradiation of Drosophila. *Radiat. Res.* **161**: 391-396

Kohda, K., Kawazoe, Y., Minoura, Y., Tada, M. (1991) Separation and identification of N^4-(guanosi-7-yl)-4-aminoquinoline 1-oxide, a novel nucleic acid adduct of carcinogen 4-nitroquinoline 1-oxide. *Carcinogenesis.* **12(8):** 1523-1525

Krokan, H.E., Nilsen, H., Skorpen, F., Otterlei, M., Slupphaug, G. (2000) Base excision repair of DNA in mammalian cells. *FEBS Letters.* **476:** 73-77

Kufe, D.W., Major P.P. (1982) Studies on the Mechanism of Action of Cytosine Arabinoside. *Medical and Pediatric Oncology Supplement.* **1:** 49-67

Kumar, D., Khan, P.K., Sinha, S.P. (1995) Cytogenetic Toxicity and No-effect Limit Dose of Pesticides. *Fd Chem. Toxic.* **33**: 309-314

Kumaravel T.S., Vilhar B., Faux S.P., Jha A.N. (2009) Comet Assay measurements: a perspective. *Cell Biol Toxicol.* **25:** 53-64

Lakin, N.D. and Jackson, S.P. (1999) Regulation of p53 in response to DNA damage. *Oncogene.* **18:** 7644-7655

Lee, Y-J., Park, S-J., Ciccone S.L.M., Kim, C-R., Lee, S-H. (2006) An *in vivo* analysis of MMC-induced DNA damage and its repair. *Carcinogenesis.* **27(3):** 446-453

Levin, W.A.Y., Luz, H., Ryan, D., Wood, A.W., Kpitulnik, J., West, S., Huand, M.T., Conney, A.H., Thakker, D., Holder, G., Hogi, G., Jerina, D.M. (1977) Properties of the liver microsomal monoxygenase and epoxide hydrolase: factors influencing the metabolism and mutagenicity of benzo(a)pyrene. P659-682. In H.H. Hiatt and J.A. Watson (Ed) Origins of Human Cancer. Cold Spring Harbour Laboratory.N.Y

Li, C-Q., Pang, B., Kiziltepe, T., Trudel, L.J., Engelward, B.P., Dedon, P.C., Wogan, G.N. (2006) Thresholds Effects of Nitric Oxide-Induced Toxicity and Cellular Responses In Wild-Type and p53-Null Human Lymphoblastoid Cells. *Chem. Res. Toxicol.* **19:** 399-406

Lieber, R., Wise, T.W., Mizuta, R., Meek, K. (1998) The XRCC4 gene product is a target for and interacts with the DNA-dependent protein kinase. *J. Biol. Chem.* **273:** 1794-1801

Loeb, K.R. and Loeb, L.A. (2000) Significance of multiple mutations in cancer. *Carcinogenesis.* **21(3):** 379-385

Loeb, L.A., Loeb, K.R., Anderson, J.P. (2003) Multiple mutations and caner. *PNAS.* **100(3):** 776-781

Lorge, E., Hayashi, M., Alnertini, S., Kirkland, D. (2008) Comparison of different methods for an accurate assessment of cytotoxicity in the *in vitro* micronucleus test. *Mutation Research.* **655:** 1-3

Lovell, D.P. (2000) Dose-response and threshold-mediated mechanisms in mutagenesis: statistical models and study design. *Mutation Research.* **464**: 87-95

Lukamowicz, M., Woodward, K., Kirsch-Volders, M., Suter, W., Elhajouji, A. (2011) A Flow Cytometry Based In Vitro Micronucleus Assay in TK6 cells-Validation Using Early Stage Pharmaceutical Development Compounds. *Environmental and Molecular Mutagenesis.* **52:** 363-372

Lutz, W.K. (1998) Dose-response relationships in chemical carcinogenesis: superposition of different mechanisms of action, resulting in linear-non-linear curves, practical thresholds, J-shapes. *Mutation Research.* **405:** 117-124

Lutz, W.K. and Lutz, R.W. (2009) Statistical model to estimate a threshold dose and its confidence limits for the analysis of sublinear dose-response relationships, exemplified for mutagenicity data. *Mutation Research.* **678:** 118-122

Lynch, A., Harvey, J., Aylott, M., Nicholas, E., Burman, M., Siddiqui, A., Walker, S., Rees, R. (2003) Investigations into the concept of a threshold for topoisomerase inhibitor-induced clastogenicity. *Mutagenesis.* **18**: 345-353

MacGregor, J.T., Casciano, D., Müller, L. (2000) Strategies and testing methods for identifying mutagenic risks. *Mutation Research.* **455:** 3-20

Majno, G. and Joris, I. (1995) Apoptosis, Oncosis, Necrosis. *American Journal of Pathology.* **146 (1):** 3-15

Mao, Y., Varoglu, M., Sherman, D.H. (1999) Molecular characterization and analysis of the biosynthetic gene cluster for the antitumor antibiotic mitomycin C from Streptomyces lavendulae NRRL 2564. *Chemistry & Biology.* **6:** 251-263

Margison, G.P., Santibañez-Koref, M.F. (2002) O^6-Alkylguanine-DNA alkyltransferase: role in carcinogenesis and chemotherapy. *Bioessays.* **24:** 255-266

Marnett, L.J. and Plastaras, J.P. (2001) Endogenous DNA damage and mutation. *Trends in Genetics.* **17(4):** 214-221

McCann, J., Choi, E., Yamasaki, E., Ames, B.N. (1975) Detections of carcinognes as mutagens in the Salmonella/microsome test: assay of 300 chemicals. *Proc. Natl. Acad. Sci.* **72:** 5135-5139

Minissi, S., Gustavino, B., Degrassi, F., Tanzarella, C., Rizzoni, M. (1999) Effect of cytochalasin B on the induction of chromosome missegregation by colchicine at low concentrations in human lymphocytes. *Mutagenesis.* **14(1):** 43-49

MMC structure. Available at: http://www.sigma-aldrich.com/catalog/product/sigma/m4287 (accessed: 03/12/2012)

Modrich, P., Lahue, R. (1996) Mismatch repair in replication fidelity, genetic recombination, and cancer biology. *Annu. Rev. Biochem.* **65:** 101-133

Momparler, R.L. (1982) Biochemical Pharmacology of Cytosine Arabinoside. *Medical and Pediatric Oncology Supplement.* **1:** 45-48

Morales-Ramirez, P., Vallarino-Kelly, T., Cruz-Vallejo, V.L., López-Iturbe, R., Alvaro-Delgadillo, H. (2004) *In vivo* kinetics of micronuclei induction by bifunctional alkylating antineoplastics. *Mutagenesis.* **19(3):** 207-213

Morita, T., MacGregor, J.T., Hayashi, M. (2011) Micronucleus assays in rodent tissues other than bone marrow. *Mutagenesis.* **26:** 223-230

Morris, S.M., Manjanatha, M.G., Shelton, S.D., Domon, O.E., McGarrity, L.J., Casciano, D.A. (1996) A mutation in the *p53* tumor suppressor gene of AHH-1 $tk^{+/-}$ human lymphoblastoid cells. *Mutation Research.* **356:** 129-134

Morrow, C.S., Diah, S., Smitherman, P.K., Schneider, E., Townsend, A.J. (1998) Multidrug resistance protein and glutathione S-transferase P1-1 act in synergy to confer protection from 4-nitroquinoline 1-oxide toxicity. *Carcinogenesis.* **19(1):** 109-115

Mortelman, K. and Zeiger, E. (2000) The Ames *Salmonella*/microsome mutagenecity assay. *Mutation Research.* **455:** 29-60

Muller, H.J. (1927) Artificial transmutation of the gene. *Science.* **66:** 84-87

Nakahara, W., Fukuoka, F., Sugimura, T. (1957) Carcinogenic action of 4-nitroquinoline-N-oxide. *Gann.* **48:** 129-137

Nature Education 2012. Available at: http://www.nature.com/scitable/topicpage/mitosis-14046258 (accessed: 23/1/2013)

Nelson, W.G. and Kastan, M.B. (1994) DNA Strand Breaks: the DNA Template Alterations That Trigger p53-Dependent DNA Damage Response Pathways. *Molecular and Cellular Biology.* **14(3):** 1815-1823

Nesslany, F., Marzin, D., (2010) Cytosine arabinoside, vinblastine, diethylstilboestrol and 2-aminoanthracene tested in the *in vitro* human TK6 cell line micronucleus test (MNvit) at Intitut Pasteur de Lille in support of OECD draft test guideline 487. *Mutation Research.* **702:** 212-218

Nomura, T., Okamoto, E., Tateishi, N., Kimura, S., Isa, Y. (1974) Tumour induction in the progeny of mice receiving 4-Nitroquinoline oxide and N-methyl-N-nitrosoutethan during pregnancy or lactation. *Cancer Research.* **34(12):** 3373-3378

4NQO structure. Available at: http://www.sigmaaldrich.com/catalog/product/aldrich/n8141 (accessed: 2/1/2013)

Nüsse, M., Marx, K. (1997) Flow cytometric analysis of micronuclei in cell cultures and human lymphocytes: advantages and disadvantages. *Mutat.Res.* **392:** 109-115

Nunoshiba, T. and Demple, B. (1993) Potent Intracellular Oxidative Stress Exerted by the Carcinogen 4-Nitroquinoline-N-oxide. *Cancer Research.* **53:** 3250-3252

OECD, 1986b. Organisation of Economic Cooperation and Development. OECD guideline for testing chemicals. "Genetic Toxicology: Mouse Spot Test". No. 484, 23 October 1986

OECD, 1997a. Organisation of Economic Cooperation and Development. OECD guideline for testing of chemicals. Bacterial Reverse Mutation Test. No. 471, 21 July 1997.

OECD, 1997b. Organisation of Economic Cooperation and Development. OECD guideline for testing of chemicals. *In Vitro* Mammalian Chromosome Aberration Test. No. 473, 21 July 1997.

OECD, 1997d. Organisation of Economic Cooperation and Development. OECD guideline for testing of chemicals. Mammalian Bone Marrow Chromosome Aberration Test. No. 475, 21 July 1997.

OECD, 1997e. Organisation of Economic Cooperation and Development. OECD guideline for testing of chemicals. *In Vitro* Mammalian Cell Gene Mutation Test. No. 476, 21 July 1997.

OECD, 2005. Organisation of Economic Cooperation and Development. OECD guideline for the testing of chemicals (Sections 1-5). Available at http://www.oecd.org/document/22/0,2340,en_2649_34377_1916054_1_1_1_1,00.html (Accessed: 12.02.13)

OECD, 2007. Organisation of Econimic Cooperation and Deveopment. OECD guideline for the testing of chemicals, draft proposal for a new guideline 487: *In Vitro* Mammalian Cell Micronucleus Test (MNvit)

OECD, 2008. Organisation for Economic Cooperation and Development. Detailed Review Paper on Transgenic Rodent Mutation Assays. OECD Health and Environment Publications, Series on Testing and Assessment No. 103, Paris. Available at: http://www.oecd.org/dataoecd/43/38/40830957.pdf (Accessed: 12.02.13)

Olive, P.L., Banath, J.P., Durand, R.E. (1990) Detection of etoposide resistance by measuring DNA damage in individual Chinese hamster cells. *J Natl Cancer Inst.* **82(9):** 779-783

Parry, J.M. and Parry, E.M, 2012. Genetic Toxicology: Principles and Methods, Methods in Molecular Biology, vol. 817. Springer

Paz, M.M., Das, A., Tomasz, M. (1999) Mitomycin C Linked to DNA Minor Groove Binding Agents: Synthesis, Reductive Activation, DNA Binding and Cross-Linking Properties and In Vitro Antitumor Activity. *Bioorg.Med.Chem.* **7:** 2713-2726

Paz M.M., Kumar G.S., Glover M., Waring M.J., Tomasz M. (2004) Mitomycin Dimers: Polyfunctional Cross-Linkers of DNA. *J.Med.Chem.* **47:** 3308-3319

Paz, M.M., 2008. Antitumour Antibiotics. In: S. Missailidis, ed. 2008. Anticancer therapeutics. Oxford: Wiley-Blackwell. Chapter 8

Pfuhler, S., Kirst, A., Aardema, M., Banduhn, N., Goebel, C., Araki, D., Costabel-Farkas, M., Dufour, E., Fautz, R., Harvey, J., Hewitt, N.J., Hibatallah, J., Carmichael, P., Macfarlane, M., Reisinger, K., Rowland, J., Schellauf, F., Schepky, A., Scheel., J. (2010) A tiered approach to the use of alternatives to animal testing for the safety assessment of cosmetics: Genotoxicity. A COLIPA analysis. *Regulatory Toxicology and Pharmacology.* **57(2-3):** 315-324

Platel, A., Nesslany, F., Gervais, V., Marzin, D. (2009) Study of oxidative DNA damage in TK6 human lymphoblastoid cells by use of the *in vitro* micronucleus test: Dtermination of No-Observed-Effect Levels. *Mutation Research.* **678**: 30-37

Pucci, B., Kasten, M., Giordanao, A. (2000) Cell Cycle and Apoptosis. *Neoplasia.* **2(4):** 291-299

Ribeiro, D. A., Grilli, D.G., Salvadori, D.M.F. (2008) Genomic instability in blood cells is able to predict the oral cancer risk: an experimental stydy in rats. J Mol Hist. 39: 481-486

Rojas, E., Lopez, M.C., Valverde, M. (1999) Single cell gel eletrophoresis assay: methodology and applications. *Journal of Chromatography B.* **722:** 225-254

Rossnerova, A., Spatova, M., Schunck, C., Sram, R.J. (2011) Automated scoring of lymphocyte micronuclei by the MetaSystems Metafer image cytometry system and its application in studies of human mutagen sensitivity and biodosimetry of genotoxin exposure. *Mutagenesis.* **26:** 169-175

Salazar, A.M., Sordo, M., Ostrosky-Wegman, P. (2009) Relationship between micronuclei formation and p53 induction. *Mutation Research.* **672:** 124-128

Sancar, A. (1996) DNA excision repair. *Annu Rev Biochem.* **65:** 43-81

Sarasin, A. (2003) An overview of the mechanisms of mutagenesis and carcinogenesis. *Mutation Research.* **544:** 99-106

Schafer, K.A. (1998) The Cell Cycle: A Review. *Vet Pathol.* **35:** 461-478

Schmid W. (1975) The micronucleus test. *Mutation Research.* **31:** 9-15

Schuler, M., Gudi, R., Cheung, J., Kumar, S., Dickinson, D., Engel, M., Szkudlinska, A., Colman, M., Maduka, N., Sherman, J., Thiffeault, C. (2010) Evaluation of phenolphtalein, diazepam, and quinacrine dihydrochloride in the *in vitro* mammalian cell micronucleus test in Chinese hamster ovary (CHO) and TK6 cells. *Mutat.Res.* **702:** 219-229

Schwartz, J.L., Jordan, R., Evans, H.H., Lenarczyk, M., Liber, H.L. (2004) Baseline levels of chromosome instability in the human lymphoblastoid cell TK6. *Mutagenesis.* **19(6):** 477-482

Scott, D., Galloway, S.M., Marshall, R.R., Ishidate Jr.,M., Brusick, D., Ashby, J., Myhr, B.C. (1991) Genotoxicity under extreme culture conditions. A report from ICPEMC Task Group 9. *Mutation Research.* **257:**147-204

Seager, A.L, Shah, U.K, Mikhail, J.M, Nelson, B.C, Marquis, B.J, Doak, S.H, Johnson, G.E, Griffiths, S.M, Carmichael, P.L, Scott, S.J, Scott, A.D, Jenkins, G.J. (2012) Pro-oxidant induced DNA damage in human lymphoblastoid cells: homeostatic mechanisms of genotoxic tolerance. *Toxicol. Sci.* **128(2):** 387-397

Searle, C.E. (1976*) Chemical Carcinogens.* Washington DC, American chemical society.

Singh, N.P., McCoy, M.T., Tice, R.R., Schneider, E.L. (1988) A simple technique for quantification of low levels of DNA damage in individual cells. *Exp. Cell. Res.* **175:** 184-191

Smith, C.C., O'Donovan, M.R., Martin, E.A. (2006) hOGG1 recognizes oxidative damage using the comet assay with greater specificity than FPG or ENDOIII. *Mutagenesis.* **21(3):** 185-190

Snodgrass R.G., Collier A.C., Coon A.E., Pritsos C.A. (2010) Mitomycin C Inhibits Ribosomal RNA *A NOVEL CYTOTOXIC MECHANISM FOR BIOREDUCTIVE DRUGS. The Journal of Biological Chemistry.* **285:** 19068-19075

Snyderwine, E.G. and Bohr, V.A. (1992) Gene- and Strand-specific Damage and Repair in Chinese Hamster Ovary Cells Treated with 4-Nitroquinoline 1-Oxide. *Cancer research.* **52:** 4183-4189

Sobel, Z., Homiski, M.L., Dickinson, D.A., Spellman, R.A., Li, D., Scott, A., Cheung, J.R., Coffing, S.L., Munzner, J.B., Sanok, K.E., Gunther, W.C., Dobo, K.L., Schuler, M. (2012) Development and validation of an in vitro micronucleus assay platform in TK6 cells. *Mutation Research.* **746:** 29-34

Stankowski Jr., L.F., Roberts, D.J., Chen, H., Lawlor, T., McKeon, M., Murli, H., Thakur, A., Xu, Y. (2011) Integration of a Pig-a, Micronucleus, Chromosome Aberration, and Comet Assay endpoints in a 28-Day Rodent Toxicity Study With 4-Nitroquinoline-1-oxide. *Environmental and Molecular Mutagenesis.* **52:** 738-747

Storer, R.D., Kraynak, A.R., McKelvey, T.W., Elia, M.C., Goodrow, T.L., DeLuca, J.G. (1997) The mouse lymphoma L5178Y $Tk^{+/-}$ cell line is heterozygous for a codon 170 mutation in the p53 tumor suppressor gene. *Mutation Research.* **373:** 157-165

Sugimura, T., Okabe, K., Nagao, M. (1966) The Metabolism of 4-Nitroquinoline-1-Oxide, a Carcinogen III. An Enzyme Catalyzing the Conversion of 4-Nitroquinoline-1-Oxide to 4-Hydroxyaminoquinoline-1-Oxide in Rat Liver and Hepatomas. *Cancer research*: **26(1)** 1717-1721

Svenberg, J.A., Fryar-Tita, E., Jeong, Y.-C., Boysen, G., Starr, T., Walker, V.E., Albertini, R.J. (2008) Biomarkers in Toxicology and Risk Assessment: Informing Critical Dose-Response Relationships. *Chem. Res. Toxicol.* **21**: 253-265

Tada, M. and Tada, M. (1975) Seryl-tRNA synthetase and activation of the carcinogen 4-nitroquinoline 1-oxide. *Nature.* **255:** 510-512

Takata M., Sasaki M.S., Sonoda E., Morrison C., Hashimoto M., Utsumi H., Yamaguchi-Iwai Y., Shinohara A., Takeda S. (1998) Homologous recombination and non-homologous end-joining pathways of double strand break repair have overlapping roles in the maintenance of chromosomal integrity in vertebrate cells. *EMBO J.* **17:** 5497-5508

Tedeschi, G., Chen, S., Massey, V. (1995) DT-diaphorese. *The Journal of Biological Chemistry.* **270:** 1198-1204

Thoday, J.M. (1951) The effect of ionizing radiation on the broad bean root. Part IX. Chromosome breakage and the lethality of ionizing radiations to the root meristem. *Br.J.Radiol.* **24:** 276-572

Tice, R.R., Hayashi, M., MacGregor, J.T., Anderson, D., Blakey, D.H., Holden, H.E., Kirsch-Volders, M., Oleson Jr., F.B., Pacchierotti, F., Preston, R.J., Romagna, F., Shimada, H., Sutou, S., Vannier, B. (1994) Report from the working group on the in vivo mammalian bone marrow chromosomal aberration test. *Mutation Research.* **312:** 305-312

Tomasz, M. (1995) Mitomycin C: small, fast and deadly (but very selective). *Chemistry & Biology.* **2:** 575-579

Tomasz, M. and Palom, Y. (1997) The Mitomycin Bioreductive Antitumor Agents: Cross-Linking and Alkylation of DNA as the Molecular Basis of Their Activity. *Pharmacol. Ther.* **76:** 73-87

Umar, A., Kunkel, T.A. (1996) DNA-replication fidelity, mismatch repair and genome instability in cancer cells. *Eur. J. Biochem.* **238:** 297-307

Valentin-Severin, I., Le Hegarat, L., Lhuguenot, J.-C., Le Bon, A-M., Chagnon, M-C. (2003) Use of HepG2 cell line for direct or indirect mutagens screening : comparative investigation between comet and micronucleus assays. *Mutation Research.* 536: 79-90

Valeriote, F. (1982) Cellular Aspects of the Action of Cytosine Arabinoside. *Medical and Pediatric Oncology Supplement.* **1:** 5-26

Vanderkerken, K., Vanparijs, P.H.., Verschaeve, L., Kirsch-Volders, M. (1989) The mouse bone marrow micronucleus assay can be used to distinguish aneugens from clastogens. *Mutagenesis.* **4:** 6-11

Varga, D., Johannes, T., Jainta, S., Schuster, S., Schwarz-Boeger, U., Kiechle, M., Garcia, B.P., Vogel, W. (2004) An automated scoring procedure for the micronucleus test by image analysis. *Mutagenesis.* **19**: 391-397

Verhaegen, F., Vral, A., Seuntjens, J., Schipper, N.W., de Ridder, L., Thierens, H. (1994) Scoring of Radiation-Induced Micronuclei in Cytokinesis-Blocked Human Lymphocytes by Automated Image Analysis. *Cytometry.* **17:** 119-127

Vermeulen, K., Van Bockstaele, D.R., Berneman, Z.N. (2003) The cell cycle: a review of regulation, deregulation and therapeutic targets in cancer. *Cell. Prolif.* **36:** 131-149

Vig, B.K. and Swearngrin, S.E. (1986) Sequence of centromere separation: kinetochore formation in induced laggards and micronuclei. *Mutagenesis.* **1:** 461-465

Wanibuchi, H., Wei, M., Karim, M.R., Morimura, K., Doi, K., Kinoshita, S., Fukushima, S. (2006) Existence of No Hepatocarcinogenic Effect Levels of 2-amino-3,6-dimethylimidazo[4,5-f]quinoxaline with or without Coadministration with Ethanol. *Toxicologic Pathology.* **34**: 232-236

Whitwell, J., Fowler, P., Allars, S., Jenner, K., Lloyd, M., Wood, D., Smith, K., Young, J., Jeffrey, L., Kirkland, D. (2010) 5-Fluorouracil, colchicine, benzo[a]pyrene and cytosine arabinoside tested in the *in vitro* mammalian cell micronucleus test (MNvit) in Chinese hamster V79 cells at Covance Laboratories, Harrogate, UK in support of OECD draft Test Guideline 487. *Mutation Research.* **702:** 230-236

Yamamoto, K.I, Kikuchi, Y. (1980) A comparison of diameters of micronuclei induced by clastogens and by spindle poisons. *Mutation Research.* **71:** 127-131

Yang, J. and Duerksen-Hughes, P. (1998) A new approach to identifying genotoxic carcinogens: p53 induction as an indicator of genotoxic damage. *Carcinogenesis.* **19(6):** 1117-1125

Yu, Y., Li, C.Y., Little, J.B., (1997) Abbrogation of p53 function by HPV16 E6 gene delays apoptosis and enhances mutagenesis but does not alter radiosensitivity in TK6 human lymphoblast cells. *Oncogene.* **14:** 1661-1667

Yu, Z., Chen, J., Ford, B.N., Brackley, M.E., Glickman, B.W. (1999) Human DNA Repair systems: An Overview. *Environmental and Molecular Mutagenesis.* **33:** 3-20

Appendix I

Micronucleus assay raw data tables

Terminology for data tables:

Mono - number of mononucleated cells scored

Bi – number of binucleated cells scored

Tri – number of trinucleated cells scored

Tetra – number of tetranucleated cells scored

Multi – number of multinucleated cells scored

Tot Multi – total number of multinucleated cells scored

Total – total cells sored altogether

% Bi – frequency of binucleated cells

% Mono – frequency of mononucleated cells

MnBn – number of micronuclei scored in binucleated cells

%MnBn – frequency of micronuclei in binucleated cells

Mono – number of micronuclei scored in mononucleated cells

% MnMono – frequency of micronuclei in mononucleated cells

Table A.1: Results from MMC in TK6 cells (CBMN assay: 4+18h; manual data)

MMC (µg/ml)	Mono	Bi	Tri	Tetra	Multi	Tot Multi	Total	% Bi	% Mono	MnBn	%MnBn	MnMono
0	453	1067	5	24	4	33	1553	68.70573	29.16935	4	0.374883	1
0	474	1066	12	32	5	49	1589	67.08622	29.83008	3	0.281426	0
0	1163	1015	9	22	5	36	2214	45.84463	52.52936	14	1.37931	1
0	1006	1032	12	25	5	42	2080	49.61538	48.36538	7	0.678295	0
0	364	1030	8	28	20	56	1450	71.03448	25.10345	8	0.776699	2
0	692.00	1042.00	9.20	26.20	7.80	43.20	1777.20	60.46	37.00	7.20	0.70	0.80
0.002	429	1019	4	24	3	31	1479	68.89790	29.00609	6	0.588813	0
0.002	503	1036	7	22	7	36	1575	65.77778	31.93651	6	0.579151	2
0.002	351	1036	11	34	12	57	1444	71.74515	24.30748	5	0.482625	1
0	427.67	1030.33	7.33	26.67	7.33	41.33	1499.33	68.81	28.42	5.67	0.55	1.00
0.004	554	1032	9	4	6	19	1605	64.29907	34.51713	3	0.290698	1
0.004	478	1010	13	14	1	28	1516	66.62269	31.53034	2	0.19802	2
0.004	389	1035	7	24	6	37	1461	70.84189	26.6256	6	0.57971	2
0.004	473.67	1025.67	9.67	14.00	4.33	28.00	1527.33	67.25	30.89	3.67	0.36	1.67
0.006	494	1026	11	17	3	31	1551	66.15087	31.85042	7	0.682261	0
0.006	451	1047	8	19	3	30	1528	68.52094	29.51571	6	0.573066	0
0.006	360	1029	8	24	5	37	1426	72.15989	25.24544	4	0.388727	1
0.006	435.00	1034.00	9.00	20.00	3.67	32.67	1501.67	68.94	28.87	5.67	0.55	0.33
0.008	507	1138	8	17	7	32	1677	67.85927	30.23256	6	0.527241	1
0.008	567	1013	8	27	3	38	1618	62.60816	35.04326	3	0.29615	0
0.008	318	1023	2	34	11	47	1388	73.70317	22.91066	10	0.977517	2
0.008	464.00	1058.00	6.00	26.00	7.00	39.00	1561.00	68.06	29.40	6.33	0.60	1.00
0.01	471	1041	10	18	8	36	1548	67.24806	30.42636	3	0.288184	0
0.01	546	1050	11	12	3	26	1622	64.7349	33.66215	5	0.47619	4
0.01	338	1018	3	26	8	37	1393	73.07968	24.26418	6	0.589391	2
0.01	451.67	1036.33	8.00	18.67	6.33	33.00	1521.00	68.35	29.45	4.67	0.45	2.00

0.02	990	1021	15	15	3	33	2044	49.95108	48.43444	4	0.391773	7
0.02	984	1020	10	31	4	45	2049	49.78038	48.02343	5	0.490196	5
0.02	354	1023	14	24	11	49	1426	71.73913	24.82468	6	0.58651	1
0.02	776.00	1021.33	13.00	23.33	6.00	42.33	1839.67	57.16	40.43	5.00	0.49	4.33
0.04	958	1055	11	15	3	29	2042	51.66503	46.91479	6	0.56872	9
0.04	1003	1021	21	15	5	41	2065	49.4431	48.57143	5	0.489716	2
0.04	470	1032	13	16	5	34	1536	67.1875	30.59896	10	0.968992	1
0.04	810.33	1036.00	15.00	15.33	4.33	34.67	1881.00	56.10	42.03	7.00	0.68	4.00
0.06	947	1022	23	14	8	45	2014	50.74479	47.02085	16	1.565558	7
0.06	928	988	28	19	3	50	1966	50.25432	47.20244	20	2.024291	24
0.06	557	1034	7	14	6	27	1618	63.90606	34.42522	10	0.967118	4
0.06	810.67	1014.67	19.33	15.67	5.67	40.67	1866.00	54.97	42.88	15.33	1.52	11.67
0.08	1394	1015	36	14	2	52	2461	41.2434	56.64364	16	1.576355	10
0.08	1455	1015	30	18	4	52	2522	40.24584	57.69231	13	1.280788	20
0.08	493	1027	11	21	18	50	1570	65.41401	31.40127	15	1.460565	1
0.08	1114.00	1019.00	25.67	17.67	8.00	51.33	2184.33	48.97	48.58	14.67	1.44	10.33
0.1	1285	1023	34	15	8	57	2365	43.25581	54.33404	21	2.052786	8
0.1	1194	1033	26	21	5	52	2279	45.3269	52.3914	17	1.645692	14
0.1	576	1018	21	27	5	53	1647	61.80935	34.97268	12	1.178782	2
0.1	1018.33	1024.67	27.00	21.00	6.00	54.00	2097.00	50.13	47.23	16.67	1.63	8.00

Table A.2: Results from MMC in TK6 cells (CBMN assay 4+18h; automated data)

MMC (µg/ml)	Bi	MnBn	%MnBn
0	2016	10	0.496032
0	2008	10	0.498008
0	2000	11	0.55
0	5013	41	0.817874
0	2101	12	0.571157
0	2876	17	0.591099
0	2669.00	16.83	0.59
0.002	4119	37	0.898276
0.002	4102	25	0.609459
0.002	4204	28	0.666032
0.002	2107	7	0.332226
0.002	3633.00	24.25	0.63
0.004	4112	23	0.559339
0.004	2002	6	0.2997
0.004	4202	26	0.618753
0.004	2113	13	0.615239
0.004	3107.25	17.00	0.52
0.006	4107	16	0.389579
0.006	4110	26	0.632603
0.006	4076	29	0.711482
0.006	2110	11	0.521327
0.006	3600.75	20.50	0.56
0.008	4181	24	0.574025
0.008	4108	18	0.438169
0.008	4206	27	0.64194
0.008	2105	12	0.570071
0.008	3650.00	20.25	0.56
0.01	2008	6	0.298805
0.01	2013	10	0.496771
0.01	2102	15	0.713606
0.01	2110	11	0.521327
0.01	2058.25	10.50	0.51
0.02	5900	49	0.830508
0.02	4102	25	0.609459
0.02	6310	37	0.586371
0.02	5109	48	0.939518
0.02	5355.25	39.75	0.74
0.04	4111	31	0.754074
0.04	4194	42	1.001431
0.04	4121	36	0.873574
0.04	2102	25	1.189343
0.04	3632.00	33.50	0.95
0.06	2006	25	1.246261
0.06	2134	34	1.593252
0.06	5699	45	0.789612
0.06	2029	38	1.872844
0.06	2967.00	35.50	1.38
0.08	3701	57	1.540124
0.08	3605	42	1.165049
0.08	3781	50	1.322401
0.08	2111	31	1.468498
0.08	3299.50	45.00	1.37
0.1	2128	32	1.503759
0.1	2137	34	1.591015
0.1	2405	33	1.372141
0.1	2385	38	1.593291
0.1	2263.75	34.25	1.52

Table A.3: Results from MMC in TK6 cells (CBMN assay: 24+18h; manual data)

MMC (µg/ml)	Mono	Bi	Tri	Tetra	Multi	Tot Multi	Total	% Bi	%Mono	MnBn	%MnBn	MnMono
0	483	1023	4	10	1	15	1521	67.25838	31.75542	3	0.293255	0
0	495	1027	12	9	2	23	1545	66.47249	32.03883	9	0.876339	3
0	452	1023	7	20	3	30	1505	67.97342	30.03322	5	0.488759	3
0	685	1028	9	17	1	27	1740	59.08046	39.36782	5	0.486381	2
0	528.75	1025.25	8.00	14.00	1.75	23.75	1577.75	65.20	33.30	5.50	0.54	2.00
0.002	563	1073	7	12	3	22	1658	64.71653	33.95657	8	0.745573	1
0.002	464	1029	6	9	1	16	1509	68.19085	30.74884	4	0.388727	2
0	513.50	1051.00	6.50	10.50	2.00	19.00	1583.50	66.45	32.35	6.00	0.57	1.50
0.004	580	1026	5	15	3	23	1629	62.98343	35.60467	6	0.584795	1
0.004	437	1048	19	21	2	42	1527	68.6313	28.61821	19	1.812977	4
0.004	508.50	1037.00	12.00	18.00	2.50	32.50	1578.00	65.81	32.11	12.50	1.20	2.50
0.006	552	1028	13	24	0	37	1617	63.57452	34.13729	10	0.972763	5
0.006	514	1045	10	11	2	23	1582	66.05563	32.49052	11	1.052632	3
0.006	533.00	1036.50	11.50	17.50	1.00	30.00	1599.50	64.82	33.31	10.50	1.01	4.00
0.008	514	1045	10	11	2	23	1582	66.05563	32.49052	11	1.052632	3
0.008	543	1035	19	16	3	38	1616	64.04703	33.60149	15	1.449275	5
0.008	528.50	1040.00	14.50	13.50	2.50	30.50	1599.00	65.05	33.05	13.00	1.25	4.00
0.01	560	1034	16	16	4	36	1630	63.43558	34.35583	16	1.547389	3
0.01	604	1178	24	18	1	43	1825	64.54795	33.09589	17	1.443124	4
0.01	582.00	1106.00	20.00	17.00	2.50	39.50	1727.50	63.99	33.73	16.50	1.50	3.50
0.02	641	1058	80	40	7	127	1826	57.94085	35.10405	46	4.347826	7
0.02	607	1055	78	32	6	116	1778	59.33633	34.13948	44	4.170616	16
0.02	624.00	1056.50	79.00	36.00	6.50	121.50	1802.00	58.64	34.62	45.00	4.26	11.50
0.04	1282	1112	196	144	18	358	2752	40.40698	46.5843	97	8.723022	34
0.04	1100	1093	232	166	12	410	2603	41.99001	42.25893	87	7.959744	25
0.04	1191.00	1102.50	214.00	155.00	15.00	384.00	2677.50	41.20	44.42	92.00	8.34	29.50

0.06	1063	1189	300	250	24	574	2826	42.0736	37.615	189	15.89571	59
0.06	1570	1155	301	283	34	618	3343	34.54981	46.9638	150	12.98701	41
0.06	1316.50	1172.00	300.50	266.50	29.00	596.00	3084.50	38.31	42.29	169.50	14.44	50.00
0.08	1951	1223	433	455	34	922	4096	29.8584	47.63184	218	17.82502	70
0.08	1822	1243	425	384	30	839	3904	31.83914	46.67008	236	18.98632	80
0.08	1886.50	1233.00	429.00	419.50	32.00	880.50	4000.00	30.85	47.15	227.00	18.41	75.00
0.1	1717	1156	430	475	36	941	3814	30.30939	45.01835	270	23.3564	77
0.1	1963	1244	509	455	44	1008	4215	29.51364	46.57177	320	25.72347	128
0.1	1840.00	1200.00	469.50	465.00	40.00	974.50	4014.50	29.91	45.80	295.00	24.54	102.50

Table A.4: Results from MMC in TK6 (CBMN assay: 24+18h; automated data)

MMC (µg/ml)	Bi	MnBn	%MnBn
0	2011	27	1.342616
0	2004	26	1.297405
0	2008	30	1.494024
0	2010	28	1.393035
0	2008.25	27.75	1.38
0.002	2007	38	1.893373
0.002	2007	41	2.04285
0.002	2007.00	39.50	1.97
0.004	2005	46	2.294264
0.004	2012	58	2.882704
0.004	2008.50	52.00	2.59
0.006	2024	52	2.56917
0.006	2023	61	3.015324
0.006	2023.50	56.50	2.79
0.008	2001	63	3.148426
0.008	2009	83	4.131409
0.008	2005.00	73.00	3.64
0.01	2014	72	3.574975
0.01	2007	66	3.28849
0.01	2010.50	69.00	3.43
0.02	2010	155	7.711443
0.02	2009	135	6.719761
0.02	2009.50	145.00	7.22
0.04	2064	260	12.5969
0.04	2198	294	13.3758
0.04	2131.00	277.00	12.99
0.06	1691	326	19.27853
0.06	1324	245	18.50453
0.06	1507.50	285.50	18.89
0.08	1487	302	20.30935
0.08	1286	234	18.19596
0.08	1386.50	268.00	19.25
0.1	1088	286	26.28676
0.1	1326	267	20.13575
0.1	1207.00	276.50	23.21

Table A.5: Results from MMC in TK6 cells (Mononucleated assay: 24+24h; manual data)

MMC (µg/ml)	Mono	Bi	Tri	Tetra	Multi	Tot Multi	Total	% Bi	% Mono	MonoMn	% MonoMn	MnBn
0	2021	96	5	1	1	7	2124	4.519774	95.15066	3	0.1484414	2
0	2025	71	3	2	0	5	2101	3.379343	96.38267	9	0.4444444	5
0	2112	118	7	7	15	29	2259	5.22355	93.4927	4	0.1893939	8
0	1643	112	6	0	4	10	1765	6.345609	93.08782	6	0.3651856	8
0	1950.25	99.25	5.25	2.50	5.00	12.75	2062.25	4.87	94.53	5.50	0.29	5.75
0.002	2054	100	12	5	2	19	2173	4.60193	94.5237	20	0.9737098	11
0.002	2046	81	6	1	2	9	2136	3.792135	95.78652	11	0.5376344	7
0	2050.00	90.50	9.00	3.00	2.00	14.00	2154.50	4.20	95.16	15.50	0.76	9.00
0.004	2037	110	8	2	3	13	2160	5.092593	94.30556	25	1.227295	11
0.004	2033	106	5	2	6	13	2152	4.925651	94.47026	20	0.9837678	13
0.004	2035.00	108.00	6.50	2.00	4.50	13.00	2156.00	5.01	94.39	22.50	1.11	12.00
0.006	2049	101	10	2	6	18	2168	4.658672	94.51107	33	1.6105417	9
0.006	2044	106	10	3	5	18	2168	4.889299	94.28044	20	0.9784736	11
0.006	2046.50	103.50	10.00	2.50	5.50	18.00	2168.00	4.77	94.40	26.50	1.29	10.00
0.008	2055	170	11	1	7	19	2244	7.575758	91.57754	36	1.7518248	20
0.008	2065	144	10	0	3	13	2222	6.480648	92.93429	39	1.8886199	21
0.008	2060.00	157.00	10.50	0.50	5.00	16.00	2233.00	7.03	92.26	37.50	1.82	20.50
0.01	2043	160	14	1	2	17	2220	7.207207	92.02703	26	1.2726383	20
0.01	2045	122	8	0	2	10	2177	5.604042	93.93661	36	1.7603912	20
0.01	2044.00	141.00	11.00	0.50	2.00	13.50	2198.50	6.41	92.98	31.00	1.52	20.00
0.02	2111	319	22	10	15	47	2477	12.87848	85.22406	76	3.6001895	60
0.02	2070	294	34	8	5	47	2411	12.19411	85.85649	65	3.1400966	55
0.02	2090.50	306.50	28.00	9.00	10.00	47.00	2444.00	12.54	85.54	70.50	3.37	57.50
0.04	2154	544	47	11	8	66	2764	19.68162	77.93054	147	6.8245125	129
0.04	2185	616	58	14	17	89	2890	21.31488	75.60554	175	8.0091533	152
0.04	2169.50	580.00	52.50	12.50	12.50	77.50	2827.00	20.50	76.77	161.00	7.42	140.50

0.06	2209	624	93	14	12	119	2952	21.13821	74.83062	192	8.6917157	167
0.06	2318	754	96	17	20	133	3205	23.52574	72.32449	223	9.6203624	186
0.06	2263.50	689.00	94.50	15.50	16.00	126.00	3078.50	22.33	73.58	207.50	9.16	176.50
0.08	2237	735	82	19	16	117	3089	23.79411	72.41826	229	10.236924	229
0.08	2237	784	121	27	13	161	3182	24.63859	70.3017	222	9.9240054	238
0.08	2237.00	759.50	101.50	23.00	14.50	139.00	3135.50	24.22	71.36	225.50	10.08	233.50
0.1	2077	925	194	25	19	238	3240	28.54938	64.10494	283	13.625421	364
0.1	1933	798	123	19	13	155	2886	27.65073	66.97852	231	11.950336	299
0.1	2005.00	861.50	158.50	22.00	16.00	196.50	3063.00	28.10	65.54	257.00	12.79	331.50

Table A.6: Results from MMC in TK6 cells (Mononucleated assay: 24+24h; automated data)

MMC (µg/ml)	Mono	MonoMn	% MonoMn
0	3929	47	1.19623314
0	3864	51	1.31987578
0	3915	38	0.9706258
0	3864	41	1.0610766
0	3893.00	44.25	1.14
0.002	3886	96	2.47040659
0.002	3898	65	1.66752181
0.002	3892.00	80.50	2.07
0.004	3899	81	2.07745576
0.004	3873	64	1.65246579
0.004	3886.00	72.50	1.86
0.006	3905	121	3.09859155
0.006	3873	94	2.42705913
0.006	3889.00	107.50	2.76
0.008	3927	131	3.33587981
0.008	3881	86	2.21592373
0.008	3904.00	108.50	2.78
0.01	3909	194	4.96290611
0.01	3919	160	4.08267415
0.01	3914.00	177.00	4.52
0.02	3987	290	7.27363933
0.02	3937	242	6.14681229
0.02	3962.00	266.00	6.71
0.04	4334	519	11.9750808
0.04	3962	243	6.13326603
0.04	4148.00	381.00	9.05
0.06	3975	444	11.1698113
0.06	3968	241	6.07358871
0.06	3971.50	342.50	8.62
0.08	3640	387	10.6318681
0.08	3747	351	9.367494
0.08	3693.50	369.00	10.00
0.1	2829	242	8.55425946
0.1	5187	431	8.30923463
0.1	4008.00	336.50	8.43

Table A.7: Results from MMC in TK6 cells (CBMN assay: 18h combined; manual data)

MMC (µg/ml)	Mono	Bi	Tri	Tetra	Multi	Tot Multi	Total	% Bi	% Mono	MnBn	% MnBn	MnMono
0	335	1039	13	26	18	57	1431	72.60657	23.4102	5	0.481232	0
0	327	1018	12	66	7	85	1430	71.18881	22.86713	1	0.098232	1
0	278	1031	10	75	13	98	1407	73.27647	19.75835	6	0.581959	1
0	239	1008	13	72	4	89	1336	75.4491	17.88922	4	0.396825	1
0	344	1024	18	63	6	87	1455	70.37801	23.64261	7	0.683594	1
0	304.60	1024.00	13.20	60.40	9.60	83.20	1411.80	72.58	21.51	4.60	0.45	0.80
0.002	376	1018	17	12	14	43	1437	70.84203	26.16562	4	0.392927	2
0.002	410	1036	14	58	9	81	1527	67.84545	26.85003	3	0.289575	1
0.002	449	1034	15	53	10	78	1561	66.23959	28.76361	5	0.483559	1
0.002	411.67	1029.33	15.33	41.00	11.00	67.33	1508.33	68.31	27.26	4.00	0.39	1.33
0.004	331	1044	8	7	19	34	1409	74.0951	23.49184	3	0.287356	1
0.004	301	1094	6	67	9	82	1477	74.06906	20.37915	6	0.548446	1
0.004	397	1042	17	45	10	72	1511	68.96095	26.27399	8	0.767754	4
0.004	343.00	1060.00	10.33	39.67	12.67	62.67	1465.67	72.38	23.38	5.67	0.53	2.00
0.006	359	1026	10	12	14	36	1421	72.20267	25.2639	9	0.877193	1
0.006	379	1119	12	39	13	64	1562	71.63892	24.26376	0	0	2
0.006	379	1014	6	25	8	39	1432	70.81006	26.46648	3	0.295858	3
0.006	372.33	1053.00	9.33	25.33	11.67	46.33	1471.67	71.55	25.33	4.00	0.39	2.00
0.008	297	1022	8	12	8	28	1347	75.87231	22.049	6	0.587084	2
0.008	421	1074	8	30	5	43	1538	69.83095	27.37321	5	0.465549	1
0.008	365	1034	9	41	7	57	1456	71.01648	25.06868	5	0.483559	1
0.008	361.00	1043.33	8.33	27.67	6.67	42.67	1447.00	72.24	24.83	5.33	0.51	1.33
0.01	371	1017	7	39	11	57	1445	70.38062	25.67474	6	0.589971	4
0.01	421	1024	10	30	13	53	1498	68.35781	28.10414	5	0.488281	2
0.01	331	1019	5	31	7	43	1393	73.15147	23.76167	5	0.490677	1
0.01	374.33	1020.00	7.33	33.33	10.33	51.00	1445.33	70.63	25.85	5.33	0.52	2.33

0.02	431	1032	9	44	15	68	1531	67.40692	28.15153	9	0.872093	2
0.02	472	1015	5	14	1	20	1507	67.35236	31.3205	1	0.098522	0
0.02	461	1026	10	23	4	37	1524	67.32283	30.24934	6	0.584795	4
0.02	454.67	1024.33	8.00	27.00	6.67	41.67	1520.67	67.36	29.91	5.33	0.52	2.00
0.04	676	1033	8	25	8	41	1750	59.02857	38.62857	9	0.871249	4
0.04	672	1060	10	11	2	23	1755	60.39886	38.2906	6	0.566038	2
0.04	734	1117	8	21	3	32	1883	59.32023	38.98035	6	0.537153	3
0.04	694.00	1070.00	8.67	19.00	4.33	32.00	1796.00	59.58	38.63	7.00	0.66	3.00
0.06	813	1033	6	35	6	47	1893	54.56947	42.9477	15	1.452081	2
0.06	850	1026	9	14	3	26	1902	53.94322	44.6898	10	0.974659	3
0.06	846	1049	15	19	5	39	1934	54.23992	43.74354	14	1.334604	4
0.06	836.33	1036.00	10.00	22.67	4.67	37.33	1909.67	54.25	43.79	13.00	1.25	3.00
0.08	777	1018	8	27	4	39	1834	55.50709	42.36641	7	0.687623	3
0.08	904	1027	12	12	1	25	1956	52.50511	46.21677	9	0.876339	2
0.08	973	1027	12	7	4	23	2023	50.76619	48.09689	9	0.876339	3
0.08	884.67	1024.00	10.67	15.33	3.00	29.00	1937.67	52.93	45.56	8.33	0.81	2.67
0.1	1023	1014	14	32	6	52	2089	48.53997	48.9708	7	0.690335	0
0.1	1142	1030	6	5	2	13	2185	47.13959	52.26545	15	1.456311	5
0.1	1075	1024	7	13	3	23	2122	48.25636	50.65975	9	0.878906	5
0.1	1080.00	1022.67	9.00	16.67	3.67	29.33	2132.00	47.98	50.63	10.33	1.01	3.33

Table A.8: Results from MMC in TK6 cells (CBMN assay: 18h combined; automated data)

MMC (µg/ml)	Bi	MnBn	%MnBn
0	2107	14	0.664452
0	2014	16	0.794439
0	2007	14	0.697559
0	2009	10	0.49776
0	2006	15	0.747757
0	2028.60	13.80	0.68
0.002	2112	13	0.61553
0.002	2005	11	0.548628
0.002	2009	20	0.99552
0.002	2042.00	14.67	0.72
0.004	2105	10	0.475059
0.004	2015	16	0.794045
0.004	2010	7	0.348259
0.004	2043.33	11.00	0.54
0.006	2105	10	0.475059
0.006	2004	20	0.998004
0.006	2006	7	0.348953
0.006	2038.33	12.33	0.61
0.008	2107	11	0.522069
0.008	2011	9	0.447539
0.008	2008	13	0.64741
0.008	2042.00	11.00	0.54
0.01	2106	20	0.949668
0.01	1999	5	0.250125
0.01	2010	12	0.597015
0.01	2038.33	12.33	0.60
0.02	4207	18	0.427858
0.02	2012	23	1.143141
0.02	2013	16	0.794834
0.02	2744.00	19.00	0.79
0.04	2101	20	0.951928
0.04	2272	34	1.496479
0.04	2006	13	0.648056
0.04	2126.33	22.33	1.03
0.06	2312	24	1.038062
0.06	2478	23	0.928168
0.06	2355	25	1.061571
0.06	2381.67	24.00	1.01
0.08	2100	19	0.904762
0.08	2050	34	1.658537
0.08	2506	30	1.197127
0.08	2218.67	27.67	1.25
0.1	2325	17	0.731183
0.1	2078	32	1.539942
0.1	2729	37	1.355808
0.1	2377.33	28.67	1.21

Table A.9: Results from MMC in AHH-1 cells (CBMN assay: 4+22h; automated data)

MMC (µg/ml)	Bi	MnBn	% MnBn
0	2098	32	1.525262
0	2105	28	1.330166
0	2105	29	1.377672
0	2102.67	29.67	1.41
0.002	2109	37	1.754386
0.002	2105	36	1.710214
0.002	2103	28	1.331431
0.002	2105.67	33.67	1.60
0.004	2101	31	1.475488
0.004	2102	25	1.189343
0.004	2105	29	1.377672
0.004	2102.67	28.33	1.35
0.006	2100	27	1.285714
0.006	2105	30	1.425178
0.006	2113	22	1.041174
0.006	2106.00	26.33	1.25
0.008	2104	27	1.28327
0.008	4205	75	1.783591
0.008	4213	66	1.56658
0.008	3507.33	56.00	1.54
0.01	2107	33	1.566208
0.01	4205	76	1.807372
0.01	4189	55	1.312963
0.01	3500.33	54.67	1.56
0.02	2106	31	1.471985
0.02	2101	39	1.856259
0.02	2103	33	1.569187
0.02	2103.33	34.33	1.63
0.04	2101	27	1.285102
0.04	2101	35	1.665873
0.04	2101	33	1.570681
0.04	2101.00	31.67	1.51
0.06	2192	42	1.916058
0.06	2111	48	2.273804
0.06	2105	41	1.947743
0.06	2136.00	43.67	2.05
0.08	2028	34	1.676529
0.08	4210	66	1.567696
0.08	4205	112	2.663496
0.08	3481.00	70.67	1.97
0.1	2112	43	2.035985
0.1	2100	56	2.666667
0.1	2100	47	2.238095
0.1	2104.00	48.67	2.31

Table A.10: Results from 4NQO in TK6 cells (CBMN assay: 4+18h; automated data)

4NQO (µg/ml)	Bi	MnBn	% MnBn
0	3000	38	1.266667
0	3008	40	1.329787
0	3010	20	0.664452
0	3006.00	32.67	1.09
0.0005	3042	38	1.249178
0.0005	3008	25	0.831117
0.0005	3015	19	0.630182
0.0005	3021.67	27.33	0.90
0.0007	3153	38	1.205201
0.0007	3007	31	1.030928
0.0007	3012	19	0.63081
0.0007	3057.33	29.33	0.96
0.0009	3005	30	0.998336
0.0009	3016	23	0.762599
0.0009	3012	12	0.398406
0.0009	3011.00	21.67	0.72
0.001	3066	37	1.206784
0.001	3148	37	1.175349
0.001	3019	18	0.596224
0.001	3077.67	30.67	0.99
0.003	3199	39	1.219131
0.003	3010	35	1.162791
0.003	3010	28	0.930233
0.003	3073.00	34.00	1.10
0.005	3094	37	1.195863
0.005	2997	25	0.834168
0.005	3018	23	0.762094
0.005	3036.33	28.33	0.93
0.007	3167	52	1.641932
0.007	3005	37	1.231281
0.007	3003	32	1.065601
0.007	3058.33	40.33	1.31
0.009	3029	67	2.211951
0.009	3038	26	0.855826
0.009	3018	27	0.894632
0.009	3028.33	40.00	1.32
0.01	3075	49	1.593496
0.01	3001	37	1.232922
0.01	3008	18	0.598404
0.01	3028.00	34.67	1.14
0.02	3150	53	1.68254
0.02	3138	34	1.083493
0.02	3044	33	1.0841
0.02	3110.67	40.00	1.28
0.03	3053	55	1.801507
0.03	3087	46	1.49012
0.03	3015	56	1.85738
0.03	3051.67	52.33	1.72

Table A.11: Results from 4NQO in TK6 cells (CBMN assay: 24+18h; automated data)

4NQO (µg/ml)	Bi	MnBn	% MnBn
0	4231	27	0.638147
0	4219	37	0.876985
0	4213	26	0.617137
0	4221.00	30.00	0.71
0.0005	4214	26	0.616991
0.0005	4215	33	0.782918
0.0005	4215	29	0.688019
0.0005	4214.67	29.33	0.70
0.0007	4215	24	0.569395
0.0007	4226	39	0.922858
0.0007	4204	29	0.689819
0.0007	4215.00	30.67	0.73
0.0009	4198	18	0.428776
0.0009	4221	34	0.805496
0.0009	4208	24	0.570342
0.0009	4209.00	25.33	0.60
0.001	4212	25	0.593542
0.001	4207	39	0.927026
0.001	4210	24	0.570071
0.001	4209.67	29.33	0.70
0.003	4192	24	0.572519
0.003	4202	40	0.951928
0.003	4208	28	0.665399
0.003	4200.67	30.67	0.73
0.005	4198	18	0.428776
0.005	4204	36	0.856327
0.005	4211	31	0.736167
0.005	4204.33	28.33	0.67
0.007	4212	20	0.474834
0.007	4220	40	0.947867
0.007	4214	40	0.949217
0.007	4215.33	33.33	0.79
0.009	4228	27	0.6386
0.009	4207	48	1.140956
0.009	4213	33	0.78329
0.009	4216.00	36.00	0.85
0.01	4202	24	0.571157
0.01	4226	72	1.703739
0.01	4196	37	0.881792
0.01	4208.00	44.33	1.05
0.02	4226	30	0.709891
0.02	4212	72	1.709402
0.02	4203	94	2.236498
0.02	4213.67	65.33	1.55
0.03	4208	63	1.497148
0.03	4221	52	1.231936
0.03	4202	61	1.45169
0.03	4210.33	58.67	1.39

Table A.12: Results from 4NQO in TK6 cells (CBMN assay: 48+18h; automated data)

4NQO (µg/ml)	Bi	MnBn	% MnBn
0	4204	22	0.523311
0	4220	40	0.947867
0	4206	37	0.879696
0	4210.00	33.00	0.78
0.0005	4204	24	0.570885
0.0005	4032	38	0.94246
0.0005	4209	30	0.712758
0.0005	4148.33	30.67	0.74
0.0007	4216	22	0.521822
0.0007	4213	29	0.688346
0.0007	4217	23	0.545411
0.0007	4215.33	24.67	0.59
0.0009	4198	23	0.54788
0.0009	4203	34	0.808946
0.0009	4207	34	0.808177
0.0009	4202.67	30.33	0.72
0.001	4200	20	0.47619
0.001	4217	33	0.782547
0.001	4213	35	0.830762
0.001	4210.00	29.33	0.70
0.003	4219	24	0.568855
0.003	4201	26	0.6189
0.003	4209	27	0.641483
0.003	4209.67	25.67	0.61
0.005	4216	24	0.56926
0.005	4208	17	0.403992
0.005	4227	31	0.733381
0.005	4217.00	24.00	0.57
0.007	4193	21	0.500835
0.007	4215	26	0.616845
0.007	4217	35	0.829974
0.007	4208.33	27.33	0.65
0.009	4198	20	0.476417
0.009	4223	45	1.065593
0.009	4218	37	0.877193
0.009	4213.00	34.00	0.81
0.01	4228	33	0.780511
0.01	4210	31	0.736342
0.01	4212	46	1.092118
0.01	4216.67	36.67	0.87
0.02	4213	21	0.498457
0.02	4218	33	0.782361
0.02	4217	26	0.616552
0.02	4216.00	26.67	0.63
0.03	4203	38	0.904116
0.03	4213	34	0.807026
0.03	4202	58	1.380295
0.03	4206.00	43.33	1.03

Table A.13: Results from 4NQO in TK6 cells (CBMN assay: 4+42h; automated data)

4NQO (µg/ml)	Bi	MnBn	% MnBn
0	4220	37	0.876777
0	4213	29	0.688346
0	4228	50	1.182592
0	4220.33	38.67	0.92
0.001	4219	26	0.61626
0.001	4204	26	0.618459
0.001	4218	48	1.13798
0.001	4213.67	33.33	0.79
0.003	4208	26	0.617871
0.003	4194	33	0.786838
0.003	4216	48	1.13852
0.003	4206.00	35.67	0.85
0.01	4210	38	0.902613
0.01	4215	48	1.13879
0.01	4209	29	0.689
0.01	4211.33	38.33	0.91
0.03	4209	64	1.520551
0.03	4217	57	1.351672
0.03	4212	71	1.68566
0.03	4212.67	64.00	1.52

Table A.14: Results from 4NQO in AHH-1 cells (CBMN assay: 4+22h; automated data)

4NQO (µg/ml)	Bi	MnBn	% MnBn
0	4214	36	0.854295
0	4213	31	0.735818
0	8429	81	0.960968
0	5618.67	49.33	0.85
0.003	4217	28	0.663979
0.003	4215	34	0.806643
0.003	8419	86	1.021499
0.003	5617.00	49.33	0.83
0.007	4218	38	0.900901
0.007	4214	32	0.759374
0.007	4212	17	0.403609
0.007	4214.67	29.00	0.69
0.01	4206	34	0.808369
0.01	4216	38	0.901328
0.01	4197	32	0.762449
0.01	4206.33	34.67	0.82
0.03	4244	47	1.107446
0.03	4216	22	0.521822
0.03	4199	24	0.571565
0.03	4219.67	31.00	0.73
0.07	4207	45	1.069646
0.07	4214	28	0.664452
0.07	4199	28	0.666825
0.07	4206.67	33.67	0.80
0.1	4224	27	0.639205
0.1	4212	52	1.234568
0.1	4222	40	0.947418
0.1	4219.33	39.67	0.94
0.3	4213	62	1.471635
0.3	3455	49	1.418234
0.3	4206	55	1.307656
0.3	3958.00	55.33	1.40
0.7	4078	35	0.858264
0.7	1470	17	1.156463
0.7	4205	58	1.37931
0.7	3251.00	36.67	1.13

Table A.15: Results from 4NQO in MCL-5 cells (CBMN assay: 4+22h; automated data)

4NQO (µg/ml)	Bi	MnBn	% MnBn
0	4148	34	0.819672
0	4204	37	0.880114
0	4209	58	1.378
0	4187.00	43.00	1.03
0.003	4201	29	0.690312
0.003	4209	30	0.712758
0.003	4217	51	1.209391
0.003	4209.00	36.67	0.87
0.007	4195	56	1.334923
0.007	4216	29	0.687856
0.007	4221	55	1.303009
0.007	4210.67	46.67	1.11
0.01	4018	41	1.020408
0.01	4203	35	0.832739
0.01	4207	54	1.283575
0.01	4142.67	43.33	1.05
0.03	4202	67	1.594479
0.03	4209	51	1.211689
0.03	4205	41	0.97503
0.03	4205.33	53.00	1.26
0.07	4207	59	1.402425
0.07	3864	28	0.724638
0.07	4207	58	1.378655
0.07	4092.67	48.33	1.17
0.1	4213	51	1.210539
0.1	3908	45	1.151484
0.1	4203	72	1.713062
0.1	4108.00	56.00	1.36
0.3	4778	70	1.465048
0.3	3276	34	1.037851
0.3	3981	84	2.110023
0.3	4011.67	62.67	1.54
0.7	2866	34	1.186322
0.7	3489	14	0.401261
0.7	3348	54	1.612903
0.7	3234.33	34.00	1.07

Table A.16: Results from 4NQO in AHH-1 cells (CBMN assay: 4+46h; automated data)

4NQO (µg/ml)	Bi	MnBn	% MnBn
0	4207	41	0.974566
0	4213	29	0.688346
0	4237	39	0.920463
0	4219.00	36.33	0.86
0.003	4212	47	1.115859
0.003	4199	28	0.666825
0.003	4204	24	0.570885
0.003	4205.00	33.00	0.78
0.03	4220	45	1.066351
0.03	4208	50	1.188213
0.03	4218	67	1.588431
0.03	4215.33	54.00	1.28
0.1	4200	102	2.428571
0.1	4206	65	1.545411
0.1	4224	85	2.012311
0.1	4210.00	84.00	2.00
0.3	4464	59	1.321685
0.3	6316	96	1.519949
0.3	3951	100	2.531005
0.3	4910.33	85.00	1.79

Table A.17: Results from 4NQO in MCL-5 cells (CBMN assay: 4+46h; automated data)

4NQO (µg/ml)	Bi	MnBn	% MnBn
0	4207	34	0.808177
0	4211	43	1.021135
0	3914	29	0.74093
0	4110.67	35.33	0.86
0.003	4210	45	1.068884
0.003	4213	52	1.234275
0.003	4197	43	1.024541
0.003	4206.67	46.67	1.11
0.03	4213	52	1.234275
0.03	4215	30	0.711744
0.03	4195	61	1.454112
0.03	4207.67	47.67	1.13
0.1	4224	57	1.349432
0.1	4214	47	1.11533
0.1	4209	84	1.995723
0.1	4215.67	62.67	1.49
0.3	3731	72	1.929778
0.3	4202	106	2.522608
0.3	2565	63	2.45614
0.3	3499.33	80.33	2.30

Table A.18: Results from 4NQO in TK6 cells (MonoMn assay (AZ): 24+24h; manual data)

4NQO (µg/ml)	Mono	Bi	Tri	Tetra	Multi	Tot Multi	Total	% Bi	%Mono	Mono Mn	% MonoMn	MnBn
0	1000	20	3	1	0	4	1024	1.953125	97.65625	9	0.9	5
0	1000	21	0	2	1	3	1024	2.050781	97.65625	4	0.4	4
0	1000.00	20.50	1.50	1.50	0.50	3.50	1024.00	2.00	97.66	6.50	0.65	4.50
0.0025	1000	22	3	2	1	6	1028	2.14008	97.27626	5	0.5	5
0.0025	1000	15	5	2	1	8	1023	1.46628	97.75171	11	1.1	2
0.0025	1000.00	18.50	4.00	2.00	1.00	7.00	1025.50	1.80	97.51	8.00	0.80	3.50
0.005	1000	24	3	2	1	6	1030	2.330097	97.08738	11	1.1	3
0.005	1000	31	5	2	0	7	1038	2.986513	96.33911	12	1.2	9
0.005	1000.00	27.50	4.00	2.00	0.50	6.50	1034.00	2.66	96.71	11.50	1.15	6.00
0.0075	993	27	3	0	0	3	1023	2.639296	97.06745	11	1.10775428	8
0.0075	1000	32	4	1	0	5	1037	3.085824	96.43202	16	1.6	10
0.0075	996.50	29.50	3.50	0.50	0.00	4.00	1030.00	2.86	96.75	13.50	1.35	9.00
0.01	1000	21	3	0	0	3	1024	2.050781	97.65625	23	2.3	6
0.01	1000	30	7	3	1	11	1041	2.881844	96.06148	16	1.6	8
0.01	1000.00	25.50	5.00	1.50	0.50	7.00	1032.50	2.47	96.86	19.50	1.95	7.00
0.015	1000	26	3	1	0	4	1030	2.524272	97.08738	17	1.7	6
0.015	1000	27	6	1	0	7	1034	2.611219	96.7118	14	1.4	5
0.015	1000.00	26.50	4.50	1.00	0.00	5.50	1032.00	2.57	96.90	15.50	1.55	5.50
0.02	1000	33	5	0	0	5	1038	3.179191	96.33911	17	1.7	12
0.02	1000	37	5	0	0	5	1042	3.550864	95.96929	20	2	11
0.02	1000.00	35.00	5.00	0.00	0.00	5.00	1040.00	3.37	96.15	18.50	1.85	11.50
0.03	1000	39	3	1	1	5	1044	3.735632	95.78544	15	1.5	10
0.03	1000	56	6	3	1	10	1066	5.253283	93.80863	15	1.5	12
0.03	1000.00	47.50	4.50	2.00	1.00	7.50	1055.00	4.49	94.80	15.00	1.50	11.00

Table A.19: Results from 4NQO in TK6 cells (MonoMn assay (AZ): 24+24h; automated data)

4NQO (µg/ml)	Mono	MonoMn	%MonoMn
0	1649	8	0.4851425
0	2263	12	0.5302696
0	1956.00	10.00	0.51
0.0025	2322	11	0.4737295
0.0025	2315	12	0.5183585
0.0025	2318.50	11.50	0.50
0.005	2309	14	0.6063231
0.005	2372	10	0.4215852
0.005	2340.50	12.00	0.512711
0.0075	2373	12	0.505689
0.0075	2374	13	0.547599
0.0075	2373.50	12.50	0.53
0.01	2129	15	0.7045561
0.01	2274	15	0.6596306
0.01	2201.50	15.00	0.68
0.015	2325	17	0.7311828
0.015	2093	13	0.621118
0.015	2209.00	15.00	0.68
0.02	2249	12	0.5335705
0.02	2378	24	1.0092515
0.02	2313.50	18.00	0.77
0.03	2337	19	0.8130081
0.03	2317	16	0.6905481
0.03	2327.00	17.50	0.75

Table A.20: Results from 4NQO in TK6 cells (MonoMn assay (AZ): 4+40h; manual data)

4NQO (µg/ml)	Mono	Bi	Tri	Tetra	Multi	Tot Multi	Total	% Bi	%Mono	Mono Mn	%MonoMn	MnBn
0	1000	22	2	1	0	3	1025	2.146341	97.56098	5	0.5	4
0	1000	26	3	1	0	4	1030	2.524272	97.08738	9	0.9	4
0	1000.00	24.00	2.50	1.00	0.00	3.50	1027.50	2.34	97.32	7.00	0.70	4.00
0.0025	1000	24	3	2	0	5	1029	2.33236	97.18173	7	0.7	5
0.0025	1000	19	4	2	0	6	1025	1.85366	97.56098	6	0.6	7
0.0025	1000.00	21.50	3.50	2.00	0.00	5.50	1027.00	2.09	97.37	6.50	0.65	6.00
0.005	1000	27	2	0	0	2	1029	2.623907	97.18173	10	1	4
0.005	1000	27	5	2	0	7	1034	2.611219	96.7118	8	0.8	8
0.005	1000.00	27.00	3.50	1.00	0.00	4.50	1031.50	2.62	96.95	9.00	0.90	6.00
0.0075	1000	27	4	1	0	5	1032	2.616279	96.89922	14	1.4	11
0.0075	1000	22	0	2	0	2	1024	2.148438	97.65625	17	1.7	8
0.0075	1000.00	24.50	2.00	1.50	0.00	3.50	1028.00	2.38	97.28	15.50	1.55	9.50
0.01	1000	21	1	0	0	1	1022	2.054795	97.84736	14	1.4	9
0.01	1000	31	4	0	0	4	1035	2.995169	96.61836	13	1.3	9
0.01	1000.00	26.00	2.50	0.00	0.00	2.50	1028.50	2.52	97.23	13.50	1.35	9.00
0.015	1000	18	9	3	0	12	1030	1.747573	97.08738	19	1.9	7
0.015	1000	41	3	0	0	3	1044	3.927203	95.78544	14	1.4	13
0.015	1000.00	29.50	6.00	1.50	0.00	7.50	1037.00	2.84	96.44	16.50	1.65	10.00
0.02	1000	32	5	1	0	6	1038	3.082852	96.33911	22	2.2	14
0.02	1000	32	2	2	0	4	1036	3.088803	96.5251	26	2.6	8
0.02	1000.00	32.00	3.50	1.50	0.00	5.00	1037.00	3.09	96.43	24.00	2.40	11.00
0.03	1000	44	10	2	0	12	1056	4.166667	94.69697	28	2.8	17
0.03	1000	43	7	0	0	7	1050	4.095238	95.2381	30	3	10
0.03	1000.00	43.50	8.50	1.00	0.00	9.50	1053.00	4.13	94.97	29.00	2.90	13.50

Table A.21: Results from 4NQO in TK6 cells (MonoMn assay (AZ): 4+40h; automated data)

4NQO (µg/ml)	Mono	MonoMn	%MonoMn
0	1697	9	0.53034767
0	2374	15	0.63184499
0	2035.50	12.00	0.58
0.0025	2375	18	0.75789474
0.0025	2255	16	0.70953437
0.0025	2315.00	17.00	0.73
0.005	2308	23	0.9965338
0.005	2170	17	0.78341014
0.005	2239.00	20.00	0.89325592
0.0075	2397	19	0.79265749
0.0075	2321	9	0.38776389
0.0075	2359.00	14.00	0.59
0.01	2395	20	0.83507307
0.01	2316	14	0.6044905
0.01	2355.50	17.00	0.72
0.015	1972	13	0.65922921
0.015	2390	18	0.75313808
0.015	2181.00	15.50	0.71
0.02	2327	24	1.03137086
0.02	2320	29	1.25
0.02	2323.50	26.50	1.14
0.03	2294	24	1.0462075
0.03	2288	27	1.18006993
0.03	2291.00	25.50	1.11

Table A.22: Results from 4NQO in L5178Y cells (MonoMn assay (AZ): 4+24h; manual data)

4NQO (µg/ml)	Mono	Bi	Tri	Tetra	Multi	Tot Multi	Total	% Bi	%Mono	Mono Mn	%MonoMn	MnBn
0	1000	7	1	0	0	1	1008	0.694444	99.20635	7	0.7	0
0	992	11	2	0	0	2	1005	1.094527	98.70647	3	0.302419	0
0	996.00	9.00	1.50	0.00	0.00	1.50	1006.50	0.89	98.96	5.00	0.50	0.00
0.005	1001	7	0	1	0	1	1009	0.69376	99.20714	8	0.799201	0
0.005	1000	13	1	0	0	1	1014	1.28205	98.61933	3	0.3	0
0.005	1000.50	10.00	0.50	0.50	0.00	1.00	1011.50	0.99	98.91	5.50	0.55	0.00
0.0075	1000	9	1	0	0	1	1010	0.891089	99.0099	9	0.9	0
0.0075	1000	10	0	0	0	0	1010	0.990099	99.0099	13	1.3	1
0.0075	1000.00	9.50	0.50	0.00	0.00	0.50	1010.00	0.94	99.01	11.00	1.10	0.50
0.01	1000	8	1	0	0	1	1009	0.792864	99.10803	7	0.7	0
0.01	1000	15	2	0	0	2	1017	1.474926	98.32842	15	1.5	1
0.01	1000.00	11.50	1.50	0.00	0.00	1.50	1013.00	1.13	98.72	11.00	1.10	0.50
0.02	1000	9	0	1	0	1	1010	0.891089	99.0099	16	1.6	0
0.02	1000	15	0	0	0	0	1015	1.477833	98.52217	18	1.8	1
0.02	1000.00	12.00	0.00	0.50	0.00	0.50	1012.50	1.18	98.77	17.00	1.70	0.50
0.03	1000	14	2	0	0	2	1016	1.377953	98.4252	22	2.2	2
0.03	1000	17	1	3	0	4	1021	1.665034	97.94319	27	2.7	2
0.03	1000.00	15.50	1.50	1.50	0.00	3.00	1018.50	1.52	98.18	24.50	2.45	2.00
0.04	1000	27	2	2	0	4	1031	2.618817	96.99321	30	3	1
0.04	1000	11	0	0	0	0	1011	1.088032	98.91197	31	3.1	0
0.04	1000.00	19.00	1.00	1.00	0.00	2.00	1021.00	1.85	97.95	30.50	3.05	0.50
0.05	1000	22	1	1	0	2	1024	2.148438	97.65625	34	3.4	3
0.05	1000	18	3	2	0	5	1023	1.759531	97.75171	37	3.7	2
0.05	1000.00	20.00	2.00	1.50	0.00	3.50	1023.50	1.95	97.70	35.50	3.55	2.50

Table A.23: Results from 4NQO in L5178Y cells (MonoMn assay (AZ): 4+24h; automated data)

4NQO (µg/ml)	Mono	MonoMn	%MonoMn
0	2339	4	0.171013
0	2350	5	0.212766
0	2344.50	4.50	0.19
0.005	2305	8	0.347072
0.005	2192	7	0.319343
0.005	2248.50	7.50	0.33
0.0075	2243	10	0.445831
0.0075	2290	9	0.393013
0.0075	2266.50	9.50	0.419148
0.01	2362	11	0.465707
0.01	2340	9	0.384615
0.01	2351.00	10.00	0.43
0.02	2349	15	0.63857
0.02	2282	16	0.701139
0.02	2315.50	15.50	0.67
0.03	2267	29	1.279224
0.03	2276	22	0.966608
0.03	2271.50	25.50	1.12
0.04	2291	35	1.527717
0.04	2221	30	1.350743
0.04	2256.00	32.50	1.44
0.05	2233	45	2.015226
0.05	2324	37	1.592083
0.05	2278.50	41.00	1.80

Table A.24: Results from araC in TK6 cells (CBMN assay: 24+18h; automated data)

araC (µg/ml)	Bi	MnBN	%MnBn
0	4218	38	0.900901
0	4218	32	0.758653
0	4208	24	0.570342
0	4214.67	31.33	0.74
0.0001	4210	33	0.783848
0.0001	4219	46	1.090306
0.0001	4206	12	0.285307
0.0001	4211.67	30.33	0.72
0.0003	4214	29	0.688182
0.0003	4226	28	0.662565
0.0003	4233	23	0.54335
0.0003	4224.33	26.67	0.63
0.0005	4203	25	0.594813
0.0005	4210	47	1.11639
0.0005	4199	24	0.571565
0.0005	4204.00	32.00	0.76
0.0007	4214	40	0.949217
0.0007	4208	42	0.998099
0.0007	4199	31	0.738271
0.0007	4207.00	37.67	0.90
0.0009	4199	30	0.714456
0.0009	4204	34	0.808754
0.0009	4195	26	0.619785
0.0009	4199.33	30.00	0.71
0.001	4219	32	0.758474
0.001	4200	36	0.857143
0.001	4212	20	0.474834
0.001	4210.33	29.33	0.70
0.003	4218	23	0.545282
0.003	4217	53	1.256818
0.003	4209	17	0.403896
0.003	4214.67	31.00	0.74
0.005	4223	35	0.828795
0.005	4222	43	1.018475
0.005	4224	30	0.710227
0.005	4223.00	36.00	0.85
0.007	4230	57	1.347518
0.007	4074	60	1.472754
0.007	4221	29	0.687041
0.007	4175.00	48.67	1.17
0.009	4202	42	0.999524
0.009	4155	58	1.395909
0.009	4211	30	0.71242
0.009	4189.333	43.33	1.04
0.01	4222	43	1.018475
0.01	4217	72	1.707375
0.01	4225	52	1.230769
0.01	4221.33	55.67	1.32
0.03	4202	96	2.284626
0.03	4211	139	3.300879
0.03	4200	95	2.261905
0.03	4204.33	110.00	2.62
0.07	4207	102	2.424531
0.07	4235	182	4.297521
0.07	4211	132	3.134647
0.07	4217.67	138.67	3.29
0.1	4155	105	2.527076
0.1	2468	92	3.727715
0.1	4032	118	2.926587
0.1	3551.67	105.00	3.06

Table A.25: Results from araC in TK6 cells (CBMN assay: 48+18h; automated data)

araC (µg/ml)	Bi	MnBN	%MnBn
0	4220	25	0.592417
0	4207	35	0.831947
0	4212	26	0.617284
0	4213.00	28.67	0.68
0.0001	4211	27	0.641178
0.0001	4217	19	0.450557
0.0001	4213	22	0.522193
0.0001	4213.67	22.67	0.54
0.0003	4222	22	0.52108
0.0003	4200	31	0.738095
0.0003	4203	26	0.618606
0.0003	4208.33	26.33	0.63
0.0005	4215	24	0.569395
0.0005	4021	9	0.223825
0.0005	4213	13	0.308569
0.0005	4149.67	15.33	0.37
0.0007	4209	18	0.427655
0.0007	4170	16	0.383693
0.0007	4222	31	0.734249
0.0007	4200.33	21.67	0.52
0.0009	4224	19	0.449811
0.0009	4201	26	0.6189
0.0009	4212	30	0.712251
0.0009	4212.33	25.00	0.59
0.001	4202	22	0.52356
0.001	4212	31	0.735992
0.001	4226	32	0.757217
0.001	4213.33	28.33	0.67
0.003	4204	26	0.618459
0.003	4211	37	0.878651
0.003	4189	26	0.620673
0.003	4201.33	29.67	0.71
0.005	4217	32	0.758833
0.005	4221	34	0.805496
0.005	4223	46	1.089273
0.005	4220.33	37.33	0.88
0.007	4222	25	0.592136
0.007	4212	35	0.830959
0.007	4215	44	1.043891
0.007	4216.33	34.67	0.82
0.009	3987	51	1.279157
0.009	3728	33	0.885193
0.009	4206	30	0.713267
0.009	3973.667	38	0.959206
0.01	4207	31	0.736867
0.01	4199	44	1.047869
0.01	4201	37	0.880743
0.01	4202.33	37.33	0.89
0.03	4218	61	1.446183
0.03	4173	71	1.701414
0.03	4196	73	1.739752
0.03	4195.67	68.33	1.63
0.07	4203	88	2.093743
0.07	3809	137	3.596745
0.07	4198	100	2.382087
0.07	4070.00	108.33	2.69
0.1	3459	103	2.977739
0.1	4568	199	4.356392
0.1	4070	95	2.334152
0.1	4032.33	132.33	3.22

Table A.26: Results from araC in AHH-1 cells (CBMN assay: 24+22h; automated data)

araC (µg/ml)	Bi	MnBN	%MnBn
0	8428	61	0.723778
0	8422	63	0.748041
0	8425	56	0.664688
0	8425.00	60.00	0.71
0.0001	4205	41	0.97503
0.0001	4214	41	0.972947
0.0001	4195	19	0.45292
0.0001	4204.67	33.67	0.80
0.0003	4220	40	0.947867
0.0003	4224	38	0.899621
0.0003	4195	25	0.595948
0.0003	4213.00	34.33	0.81
0.0005	4220	30	0.7109
0.0005	4220	28	0.663507
0.0005	4208	17	0.403992
0.0005	4216.00	25.00	0.59
0.0007	4218	27	0.640114
0.0007	4208	34	0.807985
0.0007	4198	20	0.476417
0.0007	4208.00	27.00	0.64
0.0009	4200	24	0.571429
0.0009	4211	39	0.926146
0.0009	4204	31	0.737393
0.0009	4205.00	31.33	0.74
0.001	4212	30	0.712251
0.001	4219	31	0.734771
0.001	4208	23	0.546578
0.001	4213.00	28.00	0.66
0.003	4208	31	0.736692
0.003	4219	26	0.61626
0.003	4192	24	0.572519
0.003	4206.33	27.00	0.64
0.005	4204	22	0.523311
0.005	4238	25	0.589901
0.005	4207	40	0.950796
0.005	4216.33	29.00	0.69
0.007	4209	33	0.784034
0.007	4218	26	0.616406
0.007	4196	29	0.691134
0.007	4207.67	29.33	0.70
0.009	4119	23	0.558388
0.009	4219	32	0.758474
0.009	4202	24	0.571157
0.009	4180	26.33333	0.629339
0.01	4211	37	0.878651
0.01	4204	26	0.618459
0.01	4197	21	0.500357
0.01	4204.00	28.00	0.67
0.03	4214	44	1.044139
0.03	4216	49	1.162239
0.03	4210	24	0.570071
0.03	4213.33	39.00	0.93
0.07	4113	99	2.407002
0.07	4218	45	1.066856
0.07	4207	43	1.022106
0.07	4179.33	62.33	1.50
0.1	4212	93	2.207977
0.1	4211	67	1.591071
0.1	4211	34	0.807409
0.1	4211.33	64.67	1.54
0.12	4230	85	2.009456
0.12	4068	60	1.474926
0.12	4123	92	2.231385
0.12	4140.33	79.00	1.91
0.15	4218	61	1.446183
0.15	4116	99	2.405248
0.15	4266	91	2.133146
0.15	4200.00	83.67	1.99
0.2	2882	40	1.387925
0.2	5575	82	1.470852
0.2	4266	124	2.906704
0.2	4241.00	82.00	1.92

Table A.27: Results from araC in MCL-5 cells (CBMN assay: 24+22h; automated data)

araC (µg/ml)	Bi	MnBN	%MnBn
0	4224	40	0.94697
0	4198	33	0.786089
0	4208	28	0.665399
0	4210.00	33.67	0.80
0.0001	4221	33	0.781805
0.0001	4214	43	1.020408
0.0001	4219	31	0.734771
0.0001	4218.00	35.67	0.85
0.0003	4218	36	0.853485
0.0003	4200	44	1.047619
0.0003	4203	40	0.951701
0.0003	4207.00	40.00	0.95
0.0005	4207	34	0.808177
0.0005	4199	45	1.071684
0.0005	4202	44	1.04712
0.0005	4202.67	41.00	0.98
0.0007	4210	29	0.688836
0.0007	4197	34	0.810102
0.0007	4208	30	0.712928
0.0007	4205.00	31.00	0.74
0.0009	4227	29	0.686066
0.0009	4206	43	1.022349
0.0009	4217	24	0.569125
0.0009	4216.67	32.00	0.76
0.001	4203	38	0.904116
0.001	4204	40	0.951475
0.001	4201	27	0.642704
0.001	4202.67	35.00	0.83
0.003	4201	41	0.975958
0.003	4217	35	0.829974
0.003	4211	24	0.569936
0.003	4209.67	33.33	0.79
0.005	4200	38	0.904762
0.005	4204	48	1.14177
0.005	4214	37	0.878026
0.005	4206.00	41.00	0.97
0.007	4206	41	0.974798
0.007	4210	42	0.997625
0.007	4209	40	0.950344
0.007	4208.33	41.00	0.97
0.009	4197	42	1.000715
0.009	4202	47	1.118515
0.009	4216	30	0.711575
0.009	4205	39.66667	0.943602
0.01	4202	54	1.285102
0.01	4206	40	0.951022
0.01	4222	58	1.373757
0.01	4210.00	50.67	1.20
0.03	4203	68	1.617892
0.03	4204	80	1.90295
0.03	4205	106	2.520809
0.03	4204.00	84.67	2.01
0.07	4030	122	3.027295
0.07	4206	96	2.282454
0.07	4201	101	2.404189
0.07	4145.67	106.33	2.57
0.1	4209	151	3.58755
0.1	4195	83	1.978546
0.1	4097	132	3.22187
0.1	4167.00	122.00	2.93

Table A.28: Results from MMC in NH32 cells (CBMN assay: 4+18h; automated data)

MMC (µg/ml)	Bi	MnBN	%MnBn
0	4203	19	0.452058
0	4207	23	0.546708
0	4222	45	1.065846
0	4210.67	29.00	0.69
0.0006	4212	26	0.617284
0.0006	4212	19	0.451092
0.0006	4221	38	0.900261
0.0006	4215.00	27.67	0.66
0.0008	4327	24	0.554657
0.0008	4227	31	0.733381
0.0008	4214	19	0.450878
0.0008	4256.00	24.67	0.58
0.001	4213	18	0.427249
0.001	4200	31	0.738095
0.001	4214	32	0.759374
0.001	4209.00	27.00	0.64
0.002	4193	25	0.596232
0.002	4216	31	0.735294
0.002	4219	19	0.450344
0.002	4209.33	25.00	0.59
0.004	4178	20	0.478698
0.004	4205	32	0.760999
0.004	4244	30	0.70688
0.004	4209.00	27.33	0.65
0.008	4278	27	0.631136
0.008	4217	43	1.019682
0.008	4217	36	0.853687
0.008	4237.33	35.33	0.83
0.01	4157	20	0.481116
0.01	4203	29	0.689983
0.01	4200	20	0.47619
0.01	4186.67	23.00	0.55
0.02	4134	60	1.451379
0.02	4205	50	1.189061
0.02	4234	38	0.897496
0.02	4191.00	49.33	1.18
0.04	4124	50	1.212415
0.04	4222	58	1.373757
0.04	4222	60	1.421127
0.04	4189.33	56.00	1.34
0.06	4374	71	1.623228
0.06	4210	26	0.617577
0.06	4221	40	0.947643
0.06	4268.333	45.66667	1.062816

Table A.29: Results from araC in NH32 cells (CBMN assay: 24+18h; automated data)

araC (µg/ml)	Bi	MnBN	%MnBn
0	4219	35	0.82958
0	4216	34	0.806452
0	4223	37	0.876154
0	4219.33	35.33	0.84
0.0005	4207	47	1.117186
0.0005	4228	34	0.804163
0.0005	4215	47	1.115065
0.0005	4216.67	42.67	1.01
0.0007	4204	41	0.975262
0.0007	4225	54	1.278107
0.0007	4231	55	1.299929
0.0007	4220.00	50.00	1.18
0.0009	4220	37	0.876777
0.0009	4219	50	1.185115
0.0009	4225	46	1.088757
0.0009	4221.33	44.33	1.05
0.001	4209	50	1.187931
0.001	4210	60	1.425178
0.001	4212	46	1.092118
0.001	4210.33	52.00	1.24
0.003	4207	53	1.259805
0.003	4228	65	1.53737
0.003	4223	65	1.53919
0.003	4219.33	61.00	1.45
0.005	4212	95	2.255461
0.005	4222	91	2.155377
0.005	4212	84	1.994302
0.005	4215.33	90.00	2.14
0.007	4294	132	3.074057
0.007	4216	108	2.56167
0.007	4215	96	2.27758
0.007	4241.67	112.00	2.64
0.009	4169	147	3.526025
0.009	4207	148	3.517946
0.009	4215	149	3.534994
0.009	4197.00	148.00	3.53
0.01	4215	168	3.985765
0.01	4222	151	3.576504
0.01	4214	153	3.630755
0.01	4217.00	157.33	3.73
0.03	4200	224	5.333333
0.03	4171	176	4.219612
0.03	4096	175	4.272461
0.03	4155.667	191.6667	4.608469

Appendix II

HPRT assay raw data table

Table A.30: HPRT assay data set for TK6 cells treated with 4NQO for 24h

4NQO (µg/ml)	MF	PE
H2O	75	84.40
H2O	136	48.34
H2O	33	130.93
H2O	81.33	87.89
DMSO	109	138.63
DMSO	171	29.66
DMSO	171	59.18
DMSO	150.33	75.82
0.0009	185	103.10
0.0009	122	88.35
0.0009	124	73.40
0.0009	143.67	88.28
0.003	103	120.40
0.003	364	42.57
0.003	234	71.33
0.003	233.67	78.10
0.01	386	94.16
0.01	944	18.63
0.01	558	80.59
0.01	629.33	64.46
0.02	871	55.05
0.02	1081	17.83
0.02	337	137.30
0.02	976.00	36.44

Terminology for data table:

MF – Mutation frequency $*10^{-6}$

PE – Plate effiency

Appendix III

Comet assay raw data table

Table A.31: Comet assay data for TK6 cells treated with 4NQO for 3h (AZ)

4NQO (µg/ml)	%TI -hOGG1	%TI +hOGG1
0	1.711076	1.37494
0	0.92976	0.916257
0	1.320418	1.145599
0.007	2.367384	4.050035
0.007	0.72723	1.71772
0.007	1.547307	2.883877
0.009	4.464567	3.76769
0.009	1.512453	1.314716
0.009	2.98851	2.541203
0.02	1.631675	2.151925
0.02	1.066499	1.55795
0.02	1.349087	1.854937
0.04	5.442586	5.535046
0.04	4.091848	2.951205
0.04	4.767217	4.243126
0.06	6.757332	8.284068
0.06	7.584607	10.01188
0.06	7.17097	9.147972

Terminology for data table:

%TI – % Tail intensity

Appendix IV

Pan centromeric staining raw data tables

Terminology for data table:

MN- – Micronuclei without staining (clastogenic)

%Mn- – Frequency of micronuclei without staining (clastogenic)

MN+ – Micronuclei with staining (aneugenic)

%Mn+ – Frequency of micronuclei with staining (aneugenic)

Total – Total number of micronuclei scored

Table A.32: Results from MMC in TK6 cells (Pan centromeric staining: 4+18h)

MMC (µg/ml)	MN -	MN +	Total	% MN -	% MN +
0	30	21	51	58.82353	41.17647
0	27	25	52	51.92308	48.07692
0	28.50	23.00	51.50	55.37	44.63
0.002	38	21	59	64.40678	35.59322
0.002	28	22	50	56	44
0.002	33.00	21.50	54.50	60.20	39.80
0.004	34	19	53	64.15094	35.84906
0.004	26	24	50	52	48
0.004	30.00	21.50	51.50	58.08	41.92
0.006	23	12	35	65.71429	34.28571
0.006	27	26	53	50.9434	49.0566
0.006	25.00	19.00	44.00	58.33	41.67
0.008	48	14	62	77.41935	22.58065
0.008	28	21	49	57.14286	42.85714
0.008	38.00	17.50	55.50	67.28	32.72
0.01	45	8	53	84.90566	15.09434
0.01	33	24	57	57.89474	42.10526
0.01	39.00	16.00	55.00	71.40	28.60
0.02	38	14	52	73.07692	26.92308
0.02	37	16	53	69.81132	30.18868
0.02	37.50	15.00	52.50	71.44	28.56
0.04	42	11	53	79.24528	20.75472
0.04	41	10	51	80.39216	19.60784
0.04	41.50	10.50	52.00	79.82	20.18
0.06	46	7	53	86.79245	13.20755
0.06	36	13	49	73.46939	26.53061
0.06	41.00	10.00	51.00	80.13	19.87
0.08	49	11	60	81.66667	18.33333
0.08	39	11	50	78	22
0.08	44.00	11.00	55.00	79.83	20.17
0.1	45	9	54	83.33333	16.66667
0.1	37	12	49	75.5102	24.4898
0.1	41.00	10.50	51.50	79.42	20.58

Table A.33: Results from 4NQO in TK6 cells (Pan centromeric staining: 24+18h)

4NQO (µg/ml)	MN -	MN +	Total	% MN -	% MN +
0	34	19	53	64.15094	35.84906
0	31	22	53	58.49057	41.50943
0	32.50	20.50	53.00	61.32	38.68
0.0007	34	17	51	66.66667	33.33333
0.0007	36	14	50	72	28
0.0007	35.00	15.50	50.50	69.33	30.67
0.001	39	11	50	78	22
0.001	31	19	50	62	38
0.001	35.00	15.00	50.00	70.00	30.00
0.005	37	14	51	72.54902	27.45098
0.005	35	16	51	68.62745	31.37255
0.005	36.00	15.00	51.00	70.59	29.41
0.009	37	13	50	74	26
0.009	38	13	51	74.5098	25.4902
0.009	37.50	13.00	50.50	74.25	25.75
0.02	47	10	57	82.45614	17.54386
0.02	43	7	50	86	14
0.02	45.00	8.50	53.50	84.23	15.77
0.03	42	10	52	80.76923	19.23077
0.03	40	12	52	76.92308	23.07692
0.03	41.00	11.00	52.00	78.85	21.15

Table A.34: Results from araC in TK6 cells (Pan centromeric staining: 24+18h)

araC (µg/ml)	MN -	MN +	Total	% MN -	% MN +
0	32	20	52	61.53846	38.46154
0	30	20	50	60	40
0	31.00	20.00	51.00	60.77	39.23
0.0001	25	21	46	54.34783	45.65217
0.0001	31	20	51	60.78431	39.21569
0.0001	28.00	20.50	48.50	57.57	42.43
0.0003	31	19	50	62	38
0.0003	35	15	50	70	30
0.0003	33.00	17.00	50.00	66.00	34.00
0.0005	30	20	50	60	40
0.0005	32	18	50	64	36
0.0005	31.00	19.00	50.00	62.00	38.00
0.0007	34	16	50	68	32
0.0007	35	16	51	68.62745	31.37255
0.0007	34.50	16.00	50.50	68.31	31.69
0.0009	32	19	51	62.7451	37.2549
0.0009	28	23	51	54.90196	45.09804
0.0009	30.00	21.00	51.00	58.82	41.18
0.001	37	14	51	72.54902	27.45098
0.001	31	19	50	62	38
0.001	34.00	16.50	50.50	67.27	32.73
0.003	34	18	52	65.38462	34.61538
0.003	33	17	50	66	34
0.003	33.50	17.50	51.00	65.69	34.31
0.005	38	12	50	76	24
0.005	36	14	50	72	28
0.005	37.00	13.00	50.00	74.00	26.00
0.007	34	17	51	66.66667	33.33333
0.007	34	18	52	65.38462	34.61538
0.007	34.00	17.50	51.50	66.03	33.97
0.009	45	14	59	76.27119	23.72881
0.009	36	15	51	70.58824	29.41176
0.009	40.50	14.50	55.00	73.43	26.57
0.01	46	15	61	75.40984	24.59016
0.01	37	13	50	74	26
0.01	41.50	14.00	55.50	74.70	25.30
0.03	40	16	56	71.42857	28.57143
0.03	38	12	50	76	24
0.03	39.00	14.00	53.00	73.71	26.29
0.07	36	15	51	70.58824	29.41176
0.07	33	17	50	66	34
0.07	34.50	16.00	50.50	68.29	31.71

Appendix V

RT² Profiler™ PCR Array (PAH-042)

The Human DNA Repair RT² *Profiler*™ PCR Array profiles the expression of 84 key genes encoding the enzymes that repair damaged DNA (http://www.sabiosciences.com)

Array Layout

APEX1 A01	APEX2 A02	ATM A03	ATR A04	ATXN3 A05	BRCA1 A06	BRCA2 A07	BRIP1 A08	CCNH A09	CCNO A10	CDK7 A11	DDB1 A12
DDB2 B01	DMC1 B02	ERCC1 B03	ERCC2 B04	ERCC3 B05	ERCC4 B06	ERCC5 B07	ERCC6 B08	ERCC8 B09	EXO1 B10	FEN1 B11	LIG1 B12
LIG3 C01	LIG4 C02	MGMT C03	MLH1 C04	MLH3 C05	MMS19 C06	MPG C07	MRE11A C08	MSH2 C09	MSH3 C10	MSH4 C11	MSH5 C12
MSH6 D01	MUTYH D02	NEIL1 D03	NEIL2 D04	NEIL3 D05	NTHL1 D06	OGG1 D07	PARP1 D08	PARP2 D09	PARP3 D10	PMS1 D11	PMS2 D12
PNKP E01	POLB E02	POLD3 E03	POLL E04	PRKDC E05	RAD18 E06	RAD21 E07	RAD23A E08	RAD23B E09	RAD50 E10	RAD51 E11	RAD51C E12
RAD51B F01	RAD51D F02	RAD52 F03	RAD54L F04	RFC1 F05	RPA1 F06	RPA3 F07	SLK F08	SMUG1 F09	TDG F10	TOP3A F11	TOP3B F12
TREX1 G01	UNG G02	XAB2 G03	XPA G04	XPC G05	XRCC1 G06	XRCC2 G07	XRCC3 G08	XRCC4 G09	XRCC5 G10	XRCC6 G11	XRCC6BP1 G12
B2M H01	HPRT1 H02	RPL13A H03	GAPDH H04	ACTB H05	HGDC H06	RTC H07	RTC H08	RTC H09	PPC H10	PPC H11	PPC H12

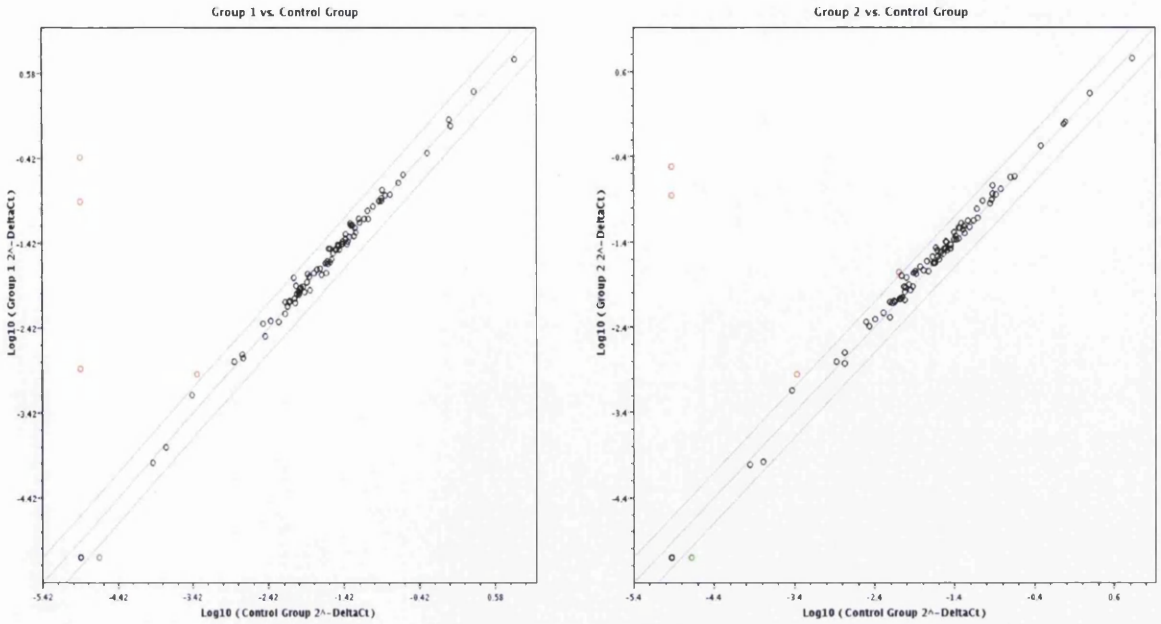

Figure A.1: DNA Repair RT^2 Profiler^{TM} PCR Array Scatter Plot of TK6 cells treated with MMC for 2h. Normalized expression of every gene of the array was compared between the control group and treated group 1 A: 0.004µg/ml or group 2 B: 0.08µg/ml. Black dots: Genes with no changes in gene expression; red dots: Genes with up-regulation of gene expression; green dots: Genes with down-regulation in gene expression.

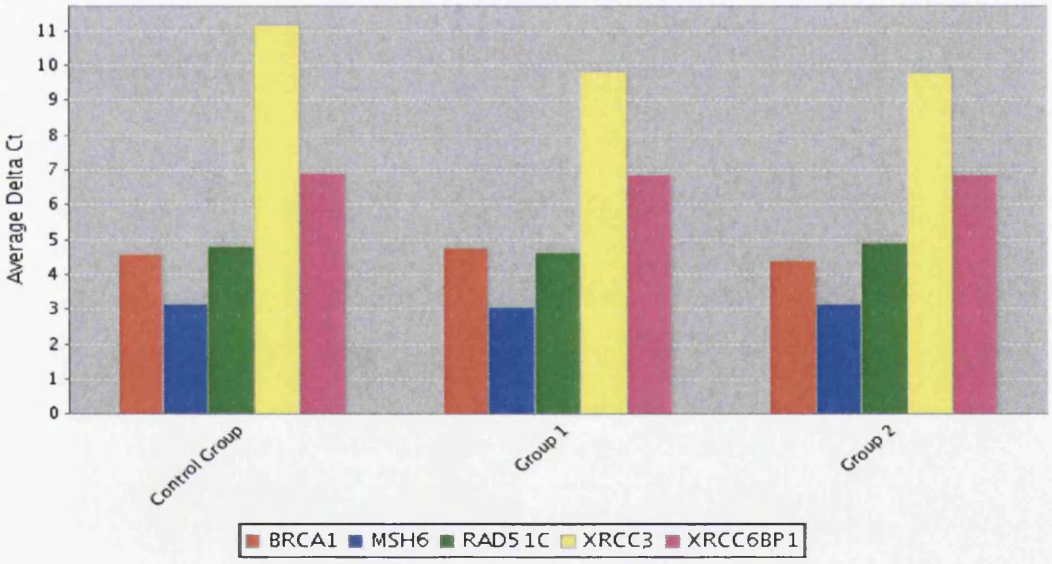

Figure A.2: DNA Repair RT^2 Profiler^{TM} PCR Array Multigroup Plot of TK6 cells treated with MMC for 2h. Expression changes of a selected set of genes across the control group and the treated groups 1 (0.004µg/ml) and 2 (0.08µg/ml).

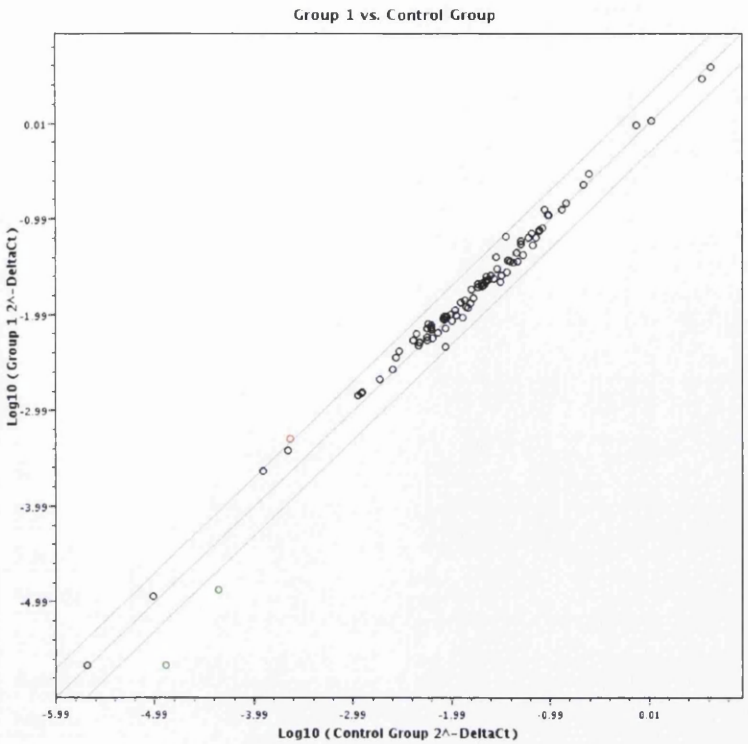

Figure A.3: DNA Repair RT^2 Profiler^{TM} PCR Array Scatter Plot of TK6 cells treated with MMC for 24h. Normalized expression of every gene of the array was compared between the control group and treated group 1 A: 0.02µg/ml. Black dots: Genes with no changes in gene expression; red dots: Genes with up-regulation of gene expression; green dots: Genes with down-regulation in gene expression.

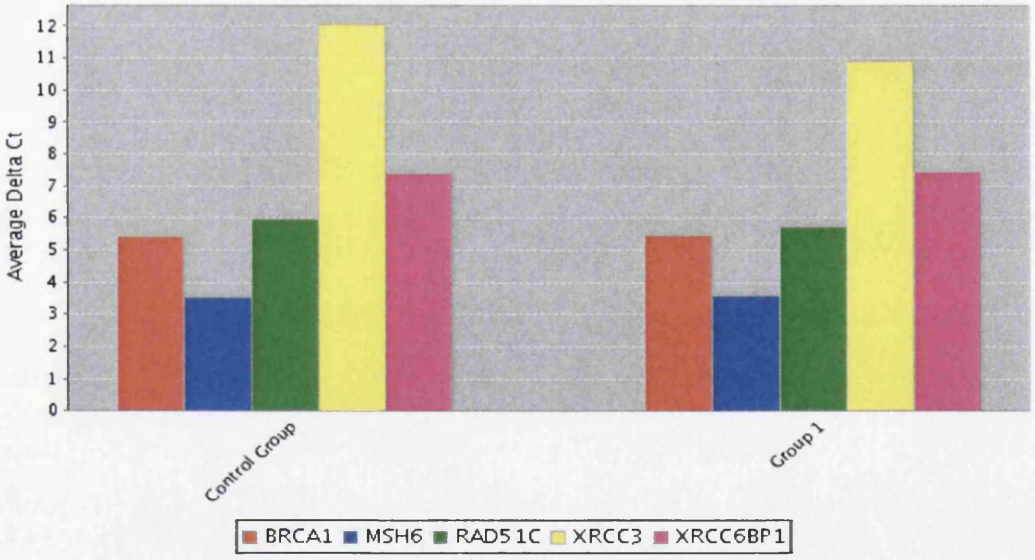

Figure A.4: DNA Repair RT^2 Profiler^{TM} PCR Array Multigroup Plot of TK6 cells treated with MMC for 24h. Expression changes of a selected set of genes across the control group and the treated group 1 (0.02µg/ml).

Appendix VI

Real-time PCR raw data

Table A.35: C_T-values of *XRCC3* gene expression, following exposure (4h) with increasing concentrations of MMC in TK6 cells

	C_T-values					
	Replicate 1		Replicate 2		Replicate 3	
	beta-actin	XRCC3	beta-actin	XRCC3	beta-actin	XRCC3
Standard	14.98	26.71	14.02	26.70	7.77	24.17
Standard	14.98	26.34	13.97	26.33	7.57	24.04
Standard	15.32	26.75	14.36	26.75	7.63	
Standard (10-1)	19.40	30.76	18.43	30.75	12.04	26.69
Standard (10-1)	17.58	29.72	16.65	29.71	11.85	26.63
Standard (10-1)						
Standard (10-2)	21.61	33.42	20.66	33.41	16.17	30.10
Standard (10-2)	21.55	34.25	20.59	34.24	15.44	29.94
Standard (10-2)	21.47	32.69	20.48	32.68		
Standard (10-3)	25.12	36.33	24.13	36.32	20.11	32.69
Standard (10-3)	24.87	36.56	23.87	36.55	19.86	32.83
Standard (10-3)	24.70	36.97	23.72	36.97	19.52	
0µg/ml	15.91	24.66	12.58	23.99	7.55	23.68
0µg/ml	15.82	25.09	12.47	24.14	7.61	23.70
0µg/ml	15.76	25.81	12.44	24.21	7.78	23.79
0.004µg/ml	15.47	25.45	12.53	23.30	8.69	23.58
0.004µg/ml	15.32	25.38	12.90	23.28	7.56	23.52
0.004µg/ml	15.61	25.67	13.16	23.46	7.85	23.42
0.008µg/ml	15.71	25.15	13.70	24.75	8.78	23.79
0.008µg/ml	15.18	25.09	13.43	24.67	7.79	23.72
0.008µg/ml	15.45	25.37	13.78	24.79	7.80	23.98
0.02µg/ml	14.19	24.79	12.81	24.76	7.55	22.11
0.02µg/ml	14.11	24.69	13.22	24.91	7.87	21.76
0.02µg/ml	14.55	24.70	13.30	24.92	7.63	22.48
0.04µg/ml	14.55	25.47	13.12	24.68	7.83	23.82
0.04µg/ml	14.45	25.31	12.94	24.60	7.66	23.67
0.04µg/ml	14.56	25.51	12.97	24.58	8.47	23.84
0.08µg/ml	14.11	23.94	13.72	23.39	7.81	24.22
0.08µg/ml	14.21	24.08	13.23	23.70	7.60	24.10
0.08µg/ml	14.53	23.97	13.33	23.86	7.78	24.43

Table A.36: Relative fold changes in *XRCC3* gene expression, following exposure (4h) with increasing concentrations of MMC in TK6 cells

Replicate 1	SQ mean			
MMC (µg/ml)	Beta actin	XRCC3	Normalization	Fold change
0	6.05E-01	3.01E+00	4.98E+00	1
0.004	7.83E-01	2.31E+00	2.95E+00	0.59225993
0.008	8.03E-01	2.84E+00	3.53E+00	0.70941145
0.02	1.82E+00	3.93E+00	2.16E+00	0.43311328
0.04	1.53E+00	2.42E+00	1.58E+00	0.3171478
0.08	1.82E+00	6.52E+00	3.57E+00	0.71696133
Replicate 2	SQ mean			
MMC (µg/ml)	Beta actin	XRCC3	Normalization	Fold change
0	3.260579	5.97233	1.831677781	1
0.004	2.551601	10.15145	3.978463888	2.172032619
0.008	1.45473	3.881497	2.668189662	1.456691614
0.02	2.130362	3.555878	1.669142557	0.911264293
0.04	2.259236	4.210245	1.863569712	1.017411322
0.08	1.696445	8.294559	4.889375902	2.669342803
Replicate 3	SQ mean			
MMC (µg/ml)	Beta actin	XRCC3	Normalization	Fold change
0	1.05E+00	1.23E+00	1.18E+00	1
0.004	8.71E-01	1.46E+00	1.68E+00	1.4289034
0.008	8.25E-01	1.14E+00	1.38E+00	1.1718763
0.02	1.03E+00	4.46E+00	4.33E+00	3.6853925
0.04	8.81E-01	1.19E+00	1.35E+00	1.1453629
0.08	1.00E+00	8.19E-01	8.17E-01	0.6953486

Table A.37: C_T-values of *Rad51C* gene expression, following exposure (4h) with increasing concentrations of MMC in TK6 cells

	C_T-values					
	Replicate 1		Replicate 2		Replicate 3	
	beta-actin	XRCC3	beta-actin	XRCC3	beta-actin	XRCC3
Standard	14.98	26.71	14.02	26.70	7.77	24.17
Standard	14.98	26.34	13.97	26.33	7.57	24.04
Standard	15.32	26.75	14.36	26.75	7.63	
Standard (10-1)	19.40	30.76	18.43	30.75	12.04	26.69
Standard (10-1)	17.58	29.72	16.65	29.71	11.85	26.63
Standard (10-1)						
Standard (10-2)	21.61	33.42	20.66	33.41	16.17	30.10
Standard (10-2)	21.55	34.25	20.59	34.24	15.44	29.94
Standard (10-2)	21.47	32.69	20.48	32.68		
Standard (10-3)	25.12	36.33	24.13	36.32	20.11	32.69
Standard (10-3)	24.87	36.56	23.87	36.55	19.86	32.83
Standard (10-3)	24.70	36.97	23.72	36.97	19.52	
0µg/ml	15.91	24.66	12.58	23.99	7.55	23.68
0µg/ml	15.82	25.09	12.47	24.14	7.61	23.70
0µg/ml	15.76	25.81	12.44	24.21	7.78	23.79
0.004µg/ml	15.47	25.45	12.53	23.30	8.69	23.58
0.004µg/ml	15.32	25.38	12.90	23.28	7.56	23.52
0.004µg/ml	15.61	25.67	13.16	23.46	7.85	23.42
0.008µg/ml	15.71	25.15	13.70	24.75	8.78	23.79
0.008µg/ml	15.18	25.09	13.43	24.67	7.79	23.72
0.008µg/ml	15.45	25.37	13.78	24.79	7.80	23.98
0.02µg/ml	14.19	24.79	12.81	24.76	7.55	22.11
0.02µg/ml	14.11	24.69	13.22	24.91	7.87	21.76
0.02µg/ml	14.55	24.70	13.30	24.92	7.63	22.48
0.04µg/ml	14.55	25.47	13.12	24.68	7.83	23.82
0.04µg/ml	14.45	25.31	12.94	24.60	7.66	23.67
0.04µg/ml	14.56	25.51	12.97	24.58	8.47	23.84
0.08µg/ml	14.11	23.94	13.72	23.39	7.81	24.22
0.08µg/ml	14.21	24.08	13.23	23.70	7.60	24.10
0.08µg/ml	14.53	23.97	13.33	23.86	7.78	24.43

Table A.38: Relative fold changes in *Rad51C* gene expression, following exposure (4h) with increasing concentrations of MMC in TK6 cells

Replicate 1	SQ mean			
MMC (µg/ml)	Beta actin	Rad51C	Normalization	Fold change
0	7.39E-01	7.59E-01	1.03E+00	1
0.004	5.22E-01	2.35E-01	4.51E-01	0.4392208
0.008	1.10E+00	7.83E-01	7.13E-01	0.6943003
0.02	1.18E+00	7.57E-01	6.39E-01	0.6218035
0.04	9.24E-01	6.74E-01	7.30E-01	0.7099223
0.08	1.52E+00	9.20E-01	6.05E-01	0.5886604
Replicate 2	SQ mean			
MMC (µg/ml)	Beta actin	Rad51C	Normalization	Fold change
0	3.01E+00	1.10E+00	3.67E-01	1
0.004	2.03E+00	8.30E-01	4.09E-01	1.11560277
0.008	1.30E+00	7.48E-01	5.77E-01	1.57415662
0.02	2.10E+00	1.22E+00	5.82E-01	1.58684942
0.04	2.23E+00	9.66E-01	4.34E-01	1.18287783
0.08	1.61E+00	8.49E-01	5.28E-01	1.44091701
Replicate 3	SQ mean			
MMC (µg/ml)	Beta actin	Rad51C	Normalization	Fold change
0	1.05E+00	1.39E+00	1.32E+00	1
0.004	8.71E-01	1.27E+00	1.45E+00	1.09811002
0.008	8.25E-01	1.37E+00	1.66E+00	1.25568453
0.02	1.03E+00	1.26E+00	1.22E+00	0.92140745
0.04	8.81E-01	1.12E+00	1.27E+00	0.96178885
0.08	1.00E+00	1.52E+00	1.52E+00	1.15028963

Table A.39: C_T-values of *MSH6* gene expression, following exposure (4h) with increasing concentrations of MMC in TK6 cells

	C_T-values					
	Replicate 1		Replicate 2		Replicate 3	
	beta-actin	MSH6	beta-actin	MSH6	beta-actin	MSH6
Standard	14.58	20.08	12.18	23.65	11.20	18.81
Standard	14.36	19.88	11.96	23.47	11.43	18.62
Standard	14.61	19.93	12.42	23.50	11.72	18.77
Standard (10-1)	19.13	25.03	15.95	27.57	14.93	22.28
Standard (10-1)	18.99	24.77	15.56	27.04	14.60	22.19
Standard (10-1)	18.36	24.46			14.26	21.72
Standard (10-2)	22.32	29.36	18.84	30.72	17.99	26.01
Standard (10-2)	21.99	28.64	18.61	30.57	17.99	25.71
Standard (10-2)	21.91	27.63	18.61	30.44	17.66	
Standard (10-3)	25.97	32.35	22.07	34.01	21.90	29.45
Standard (10-3)	25.70	32.67	21.91	34.43	21.38	29.40
Standard (10-3)	24.71	31.83	21.76	33.88	21.00	28.39
0µg/ml	13.49	19.05	12.92	24.14	11.68	18.39
0µg/ml	13.76	19.16	12.19	23.88	11.36	18.31
0µg/ml	13.89	19.68	12.76	24.46	11.47	18.88
0.004µg/ml	13.11	19.16	12.75	24.42	11.16	18.58
0.004µg/ml	13.39	18.88	12.83	24.00	10.96	18.64
0.004µg/ml	13.73	19.32	12.60	24.56	11.09	18.77
0.008µg/ml	14.29	19.17	13.69	24.49	11.21	18.35
0.008µg/ml	14.10	18.96	13.54	24.25	10.89	18.24
0.008µg/ml	14.20	19.39	12.91	24.53	11.17	18.70
0.02µg/ml	14.03	19.24	13.55	24.19	11.27	18.80
0.02µg/ml	13.81	19.18	12.70	24.13	11.52	18.34
0.02µg/ml	14.45	19.53	12.97	24.14	11.50	18.80
0.04µg/ml	14.66	19.63	12.65	24.67	11.20	18.71
0.04µg/ml	14.22	19.28	12.23	24.64	11.20	18.56
0.04µg/ml	14.84	19.91	12.99	24.67	11.86	18.73
0.08µg/ml	14.12	19.26	13.15	25.04	11.42	18.68
0.08µg/ml	15.11	19.49	13.16	24.85	11.32	18.69
0.08µg/ml	15.47	19.64	13.76	24.98	11.65	18.94

Table A.40: Relative fold changes in *MSH6* gene expression, following exposure (4h) with increasing concentrations of MMC in TK6 cells

Replicate 1	SQ mean			
MMC (µg/ml)	Beta actin	MSH6	Normalization	Fold change
0	2.02E+00	1.76E+00	8.68E-01	1
0.004	2.47E+00	1.93E+00	7.81E-01	0.89940381
0.008	1.48E+00	1.87E+00	1.26E+00	1.45534746
0.02	1.59E+00	1.72E+00	1.08E+00	1.24443378
0.04	1.18E+00	1.47E+00	1.25E+00	1.43758815
0.08	1.01E+00	1.59E+00	1.57E+00	1.80910599
Replicate 2	SQ mean			
MMC (µg/ml)	Beta actin	MSH6	Normalization	Fold change
0	8.06E-01	7.05E-01	8.75E-01	1
0.004	7.31E-01	6.32E-01	8.64E-01	0.98806
0.008	4.72E-01	5.88E-01	1.24E+00	1.423209
0.02	5.89E-01	6.99E-01	1.19E+00	1.356298
0.04	8.07E-01	5.01E-01	6.22E-01	0.710719
0.08	4.75E-01	4.14E-01	8.71E-01	0.995261
Replicate 3	SQ mean			
MMC (µg/ml)	Beta actin	MSH6	Normalization	Fold change
0	9.08E-01	1.14E+00	1.25E+00	1
0.004	1.22E+00	1.03E+00	8.42E-01	0.670742914
0.008	1.21E+00	1.21E+00	1.00E+00	0.796919787
0.02	9.52E-01	1.05E+00	1.10E+00	0.878764726
0.04	9.77E-01	1.03E+00	1.05E+00	0.836789746
0.08	9.33E-01	9.60E-01	1.03E+00	0.820284645

Table A.41: C_T-values of *BRCA1* gene expression, following exposure (4h) to increasing concentrations of MMC in TK6 cells

	C_T-values					
	Replicate 1		Replicate 2		Replicate 3	
	beta-actin	BRCA1	beta-actin	BRCA1	beta-actin	BRCA1
Standard	14.58	20.65	12.18	22.82	11.20	21.82
Standard	14.36	20.43	11.96	22.91	11.43	21.79
Standard	14.61	20.56	12.42	23.10	11.72	22.19
Standard (10-1)	19.13	24.98	15.95	26.93	14.93	25.74
Standard (10-1)	18.99	25.01	15.56	27.10	14.60	24.49
Standard (10-1)	18.36	24.30		26.65	14.26	
Standard (10-2)	22.32	28.37	18.84	30.56	17.99	29.11
Standard (10-2)	21.99	28.04	18.61	30.30	17.99	27.81
Standard (10-2)	21.91		18.61	30.00	17.66	32.51
Standard (10-3)	25.97	31.67	22.07	33.95	21.90	31.65
Standard (10-3)	25.70	31.11	21.91	33.64	21.38	31.64
Standard (10-3)	24.71	30.88	21.76	33.62	21.00	
0µg/ml	13.49	18.88	12.92	23.14	11.68	21.25
0µg/ml	13.76	19.14	12.19	23.02	11.36	21.28
0µg/ml	13.89	19.46	12.76	23.26	11.47	22.11
0.004µg/ml	13.11	18.86	12.75	23.18	11.16	21.59
0.004µg/ml	13.39	18.86	12.83	23.20	10.96	21.50
0.004µg/ml	13.73	19.19	12.60	23.38	11.09	21.76
0.008µg/ml	14.29	19.09	13.69	23.94	11.21	21.34
0.008µg/ml	14.10	18.90	13.54	23.75	10.89	21.24
0.008µg/ml	14.20	19.25	12.91	23.75	11.17	21.77
0.02µg/ml	14.03	18.90	13.55	23.10	11.27	21.80
0.02µg/ml	13.81	19.13	12.70	23.15	11.52	21.85
0.02µg/ml	14.45	19.72	12.97	23.14	11.50	22.56
0.04µg/ml	14.66	19.00	12.65	23.67	11.20	21.55
0.04µg/ml	14.22	19.19	12.23	23.56	11.20	21.66
0.04µg/ml	14.84	19.88	12.99	23.76	11.86	21.95
0.08µg/ml	14.12	19.14	13.15	23.59	11.42	21.73
0.08µg/ml	15.11	19.16	13.16	23.61	11.32	21.75
0.08µg/ml	15.47	19.53	13.76	23.96	11.65	22.06

Table A.42: Relative fold changes in *BRCA1* gene expression, following exposure (4h) to increasing concentrations of MMC in TK6 cells

Replicate 1	SQ mean			
MMC (µg/ml)	Beta actin	BRCA1	Normalization	Fold change
0	2.02E+00	3.06E+00	1.51E+00	1
0.004	2.47E+00	3.43E+00	1.39E+00	0.918286
0.008	1.48E+00	3.19E+00	2.16E+00	1.427359
0.02	1.59E+00	2.91E+00	1.83E+00	1.208449
0.04	1.18E+00	2.73E+00	2.32E+00	1.534094
0.08	1.01E+00	2.81E+00	2.78E+00	1.842273
Replicate 2	SQ mean			
MMC (µg/ml)	Beta actin	BRCA1	Normalization	Fold change
0	8.06E-01	9.73E-01	1.21E+00	1
0.004	7.31E-01	9.05E-01	1.24E+00	1.025691
0.008	4.72E-01	6.32E-01	1.34E+00	1.1093
0.02	5.89E-01	9.78E-01	1.66E+00	1.375556
0.04	8.07E-01	6.94E-01	8.60E-01	0.712509
0.08	4.75E-01	6.74E-01	1.42E+00	1.175801
Replicate 3	SQ mean			
MMC (µg/ml)	Beta actin	BRCA1	Normalization	Fold change
0	9.08E-01	1.30E+00	1.43E+00	1
0.004	1.22E+00	1.20E+00	9.80E-01	0.687028
0.008	1.21E+00	1.35E+00	1.12E+00	0.782901
0.02	9.52E-01	8.97E-01	9.42E-01	0.660405
0.04	9.77E-01	1.12E+00	1.15E+00	0.803423
0.08	9.33E-01	1.02E+00	1.10E+00	0.770086

Table A.43: CT-values of *XRCC6BP1* gene expression, following exposure (4h) with increasing concentrations of MMC in TK6 cells

	C_T-values					
	Replicate 1		Replicate 2		Replicate 3	
	beta-actin	XRCC6BP1	beta-actin	XRCC6BP1	beta-actin	XRCC6BP1
Standard	12.38	24.84	11.76	19.18	14.27	22.76
Standard	12.10	24.72	11.79	19.03	13.94	22.68
Standard		24.94	11.78	19.12	14.14	22.59
Standard (10-1)	15.04	27.95	15.87	22.55	16.37	26.55
Standard (10-1)	14.64	28.38	15.42	22.60	15.65	26.11
Standard (10-1)		27.87	14.60			
Standard (10-2)	18.07	31.14	18.55	26.48	19.20	29.92
Standard (10-2)	17.95	30.65	18.13	25.86	19.18	29.52
Standard (10-2)			18.14	25.56	18.61	
Standard (10-3)	20.99	35.35	21.83	30.02	22.19	32.58
Standard (10-3)	21.22	35.88	21.87	30.24	21.86	33.12
Standard (10-3)			21.67		22.24	32.88
0µg/ml	11.95	23.07	12.69	19.08	10.83	21.51
0µg/ml	12.01	23.13	12.33	18.89	10.60	21.34
0µg/ml	11.92	23.06	12.20	18.62	10.80	21.45
0.004µg/ml	10.74	22.56	12.15	19.38	10.49	21.34
0.004µg/ml	10.41	22.47	11.89	19.42	10.43	21.32
0.004µg/ml	10.43	22.22	11.93	19.27	10.66	21.38
0.008µg/ml	10.81	22.09	12.55	19.55	10.39	21.30
0.008µg/ml	10.67	22.31	11.71	19.52	10.38	21.34
0.008µg/ml	10.61	22.48		19.69	10.29	
0.02µg/ml	10.76	22.56	12.04	19.30	10.80	20.83
0.02µg/ml	10.77	22.38	11.88	18.99	10.79	21.32
0.02µg/ml	9.89	22.36	11.92	19.03	10.72	
0.04µg/ml	11.42	23.83	12.34	19.67	10.49	21.59
0.04µg/ml	11.43	23.88	12.23	19.04	10.61	21.55
0.04µg/ml	11.43	23.64	12.59		10.32	21.68
0.08µg/ml	11.22	23.15	11.95	18.70	10.71	21.28
0.08µg/ml	11.31	22.83	12.63	19.19	10.86	21.55
0.08µg/ml	10.86	22.41	12.65	19.55	11.19	21.97

Table A.44: Relative fold changes in *XRCC6BP1* gene expression, following exposure (4h) with increasing concentrations of MMC in TK6 cells

Replicate 1	SQ mean			
MMC (µg/ml)	Beta actin	XRCC6BP1	Normalization	Fold change
0	1.11E+00	2.77E+00	2.51E+00	1
0.004	3.37E+00	4.34E+00	1.29E+00	0.51335614
0.008	2.94E+00	4.71E+00	1.60E+00	0.63896158
0.02	3.69E+00	4.28E+00	1.16E+00	0.46105969
0.04	1.67E+00	1.76E+00	1.05E+00	0.41878544
0.08	2.12E+00	3.43E+00	1.62E+00	0.64354456
Replicate 2	SQ mean			
MMC (µg/ml)	Beta actin	XRCC6BP1	Normalization	Fold change
0	6.79E-01	1.10E+00	1.62E+00	1
0.004	9.00E-01	8.00E-01	8.89E-01	0.549336
0.008	8.47E-01	6.90E-01	8.14E-01	0.503048
0.02	9.25E-01	9.39E-01	1.02E+00	0.627327
0.04	6.82E-01	8.15E-01	1.20E+00	0.738833
0.08	6.86E-01	9.34E-01	1.36E+00	0.84141
Replicate 3	SQ mean			
MMC (µg/ml)	Beta actin	XRCC6BP1	Normalization	Fold change
0	1.44E+01	2.50E+00	1.74E-01	1
0.004	1.74E+01	2.66E+00	1.53E-01	0.87851011
0.008	2.00E+01	2.70E+00	1.35E-01	0.77619614
0.02	1.40E+01	3.23E+00	2.31E-01	1.32612183
0.04	1.82E+01	2.22E+00	1.22E-01	0.7027906
0.08	1.25E+01	2.27E+00	1.82E-01	1.0457999

Table A.45: C_T-values of *p21* gene expression, following exposure (4h) with increasing concentrations of MMC in TK6 cells

	C_T-values					
	Replicate 1		Replicate 2		Replicate 3	
	beta-actin	p21	beta-actin	p21	beta-actin	p21
Standard	13.78	20.77	12.60	18.57	15.73	20.69
Standard	13.86	20.83	13.59	19.25	15.91	20.95
Standard		20.61				
Standard (10-1)	17.99	24.76	17.88	24.14	18.26	24.80
Standard (10-1)	17.55	24.15	17.85	23.87	18.15	24.55
Standard (10-1)			17.48			
Standard (10-2)	21.67	27.48	20.54	27.12	21.40	26.89
Standard (10-2)	21.38	27.32	20.29	26.25	20.77	26.59
Standard (10-2)					20.65	
Standard (10-3)	23.58	30.69	23.59	30.03	23.96	31.28
Standard (10-3)	23.61	30.66	23.49	29.72	23.89	30.98
Standard (10-3)	23.23				23.65	
0µg/ml	14.31	19.89	16.13	21.00	14.21	20.06
0µg/ml	14.35	19.76	15.94	20.70	14.34	19.74
0µg/ml	14.87	19.61	16.90	20.64	14.51	20.16
0.004µg/ml	13.82	20.16	15.47	19.13	15.02	20.00
0.004µg/ml	14.01	20.05	15.34	19.12	14.98	19.53
0.004µg/ml	14.37	20.11	15.50	18.89	15.18	19.56
0.008µg/ml	14.13	19.78	13.57	19.27	14.97	20.22
0.008µg/ml	13.91	19.83	14.67	19.62	15.17	19.83
0.008µg/ml	14.36	19.76	15.84			20.82
0.02µg/ml	13.91	19.86	16.00	20.53	14.67	19.38
0.02µg/ml	13.95	19.66	16.08	20.38	14.73	19.13
0.02µg/ml	14.57	19.60	16.34	20.93	14.85	19.65
0.04µg/ml	14.33	19.81	15.64	20.36	13.81	18.41
0.04µg/ml	14.22	19.82	15.93	20.27	13.50	18.37
0.04µg/ml	14.51	19.69		20.18	13.83	18.67
0.08µg/ml	13.28	18.97	12.96	17.87	14.07	17.84
0.08µg/ml	13.16	19.02	13.10	18.17	13.91	17.99
0.08µg/ml	13.71	19.25	13.43	18.28	14.70	18.60

Table A.46: Relative fold changes in *p21* gene expression, following exposure (4h) with increasing concentrations of MMC in TK6 cells

Replicate 1	SQ mean			
MMC (µg/ml)	Beta actin	p21	Normalization	Fold change
0	8.65E-01	2.18E+00	2.516313	1
0.004	1.18E+00	1.69E+00	1.426477	0.56689167
0.008	1.12E+00	2.11E+00	1.879715	0.7470114
0.02	1.13E+00	2.24E+00	1.986417	0.78941554
0.04	9.53E-01	2.14E+00	2.24004	0.89020693
0.08	1.94E+00	3.48E+00	1.796278	0.71385305
Replicate 2	SQ mean			
MMC (µg/ml)	Beta actin	p21	Normalization	Fold change
0	1.76E-01	4.49E-01	2.554029	1
0.004	3.10E-01	1.37E+00	4.432752	1.735592
0.008	6.22E-01	1.07E+00	1.71805	0.672682
0.02	1.93E-01	5.04E-01	2.614411	1.023642
0.04	2.45E-01	6.21E-01	2.532755	0.99167
0.08	1.48E+00	2.53E+00	1.71544	0.67166
Replicate 3	SQ mean			
MMC (µg/ml)	Beta actin	p21	Normalization	Fold change
0	3.11E+00	1.90E+00	0.610326	1
0.004	1.69E+00	2.33E+00	1.378748	2.259035
0.008	1.68E+00	1.59E+00	0.945399	1.549006
0.02	2.21E+00	2.89E+00	1.306243	2.140239
0.04	5.40E+00	5.40E+00	1.001071	1.640224
0.08	3.58E+00	6.99E+00	1.952407	3.198958

Table A.47: C_T-values of *p21* gene expression, following exposure (4h) with increasing concentrations of MMC in AHH-1 cells

	C_T-values					
	Replicate 1		Replicate 2		Replicate 3	
	beta-actin	p21	beta-actin	p21	beta-actin	p21
Standard	13.78	20.77	12.60	18.57	15.73	20.69
Standard	13.86	20.83	13.59	19.25	15.91	20.95
Standard		20.61				
Standard (10-1)	17.99	24.76	17.88	24.14	18.26	24.80
Standard (10-1)	17.55	24.15	17.85	23.87	18.15	24.55
Standard (10-1)			17.48			
Standard (10-2)	21.67	27.48	20.54	27.12	21.40	26.89
Standard (10-2)	21.38	27.32	20.29	26.25	20.77	26.59
Standard (10-2)					20.65	
Standard (10-3)	23.58	30.69	23.59	30.03	23.96	31.28
Standard (10-3)	23.61	30.66	23.49	29.72	23.89	30.98
Standard (10-3)	23.23				23.65	
0µg/ml	12.79	19.69	12.52	18.50	13.75	19.80
0µg/ml	12.79	19.62	12.58	19.02	13.87	19.69
0µg/ml	13.41	19.99	13.62	20.03	14.27	20.00
0.004µg/ml	12.84	19.65	14.47	21.66	13.85	19.72
0.004µg/ml	12.84	19.41	14.38	21.76	13.74	19.77
0.004µg/ml	13.19	19.67	14.34	22.14	14.03	20.30
0.008µg/ml	12.55	19.35	13.31	18.91	14.99	20.26
0.008µg/ml	12.30	19.20	13.54	19.18	14.73	20.06
0.008µg/ml	12.50	19.60	13.81	19.51	15.34	20.64
0.02µg/ml	13.46	19.95	14.01	19.48	14.69	20.06
0.02µg/ml	13.27	19.96	13.90	19.58	14.61	20.12
0.02µg/ml	13.72	19.97	14.23	19.50	15.37	20.54
0.04µg/ml	13.91	20.08	13.81	20.23	15.04	20.45
0.04µg/ml	13.83	20.26	13.97	20.93	14.86	20.60
0.04µg/ml	14.50	20.11	14.82	20.76	15.15	20.81
0.08µg/ml	13.41	19.70	14.38	19.83	16.05	20.94
0.08µg/ml	13.06	19.80	13.91	19.72	16.05	21.16
0.08µg/ml	13.75	19.86	14.72	20.07	16.65	21.64

Table A.48: Relative fold changes in *p21* gene expression, following exposure (4h) with increasing concentrations of MMC in AHH-1 cells

Replicate 1	SQ mean			
MMC (µg/ml)	Beta actin	p21	Normalization	Fold change
0	2.572307	2.15745	0.838722	1
0.004	2.608381	2.456625	0.94182	1.12292236
0.008	3.740781	2.817722	0.753244	0.89808581
0.02	1.792782	1.875219	1.045983	1.24711541
0.04	1.184305	1.64485	1.388874	1.65594038
0.08	1.914941	2.117818	1.105944	1.3186068
Replicate 2	SQ mean			
MMC (µg/ml)	Beta actin	p21	Normalization	Fold change
0	1.85E+00	1.36E+00	0.735704	1
0.004	6.31E-01	2.25E-01	0.35642	0.484461
0.008	1.13E+00	1.26E+00	1.107045	1.504742
0.02	8.05E-01	1.01E+00	1.255649	1.706731
0.04	7.54E-01	4.98E-01	0.660799	0.898186
0.08	6.75E-01	8.05E-01	1.194012	1.622952
Replicate 3	SQ mean			
MMC (µg/ml)	Beta actin	p21	Normalization	Fold change
0	4.407694	2.106465	0.477906	1
0.004	4.707765	1.98525	0.421697	0.882384
0.008	1.791605	1.513517	0.844783	1.767673
0.02	2.033471	1.592654	0.783219	1.638854
0.04	1.762811	1.216742	0.690229	1.444275
0.08	0.625903	0.797646	1.274393	2.666615

Table A.49: C_T-values of *p21* gene expression, following exposure (24h) with increasing concentrations of araC in TK6 cells

	C_T-values					
	Replicate 1		Replicate 2		Replicate 3	
	beta-actin	p21	beta-actin	p21	beta-actin	p21
Standard	12.96	22.02	12.59	22.50	14.42	16.85
Standard	12.94	22.54	12.72	22.53	14.13	16.81
Standard			12.66	22.39		17.20
Standard (10-1)	17.21	27.10	18.18	28.05	17.07	20.14
Standard (10-1)	17.06	25.78	17.85	27.22	16.28	19.99
Standard (10-1)	17.07		17.74			
Standard (10-2)	20.17	29.59	20.95	31.27	20.21	23.11
Standard (10-2)	19.74	29.19	20.78	30.59	19.71	22.64
Standard (10-2)			20.58		19.53	22.22
Standard (10-3)	22.98	32.65	23.04	34.37	24.15	26.57
Standard (10-3)	22.55	32.92	22.82	33.62	23.48	26.36
Standard (10-3)						
0µg/ml	13.37	21.54	12.74	22.23	16.25	17.44
0µg/ml	13.17	21.38	12.73	21.66	15.87	17.38
0µg/ml	13.37	21.16	12.87	21.67	16.16	17.38
0.0007µg/ml	13.09	20.94	12.81	21.41	15.40	17.05
0.0007µg/ml	13.13	20.66	12.72	21.18	15.33	16.76
0.0007µg/ml	13.24	20.42	12.96	21.24	16.07	17.01
0.005µg/ml	12.21	19.75	13.05	21.31	15.19	16.88
0.005µg/ml	12.13	19.54	12.79	20.99	15.55	16.91
0.005µg/ml	12.31	19.50	12.87	21.09	15.90	17.12
0.01µg/ml	13.24	20.04	12.93	22.11	15.74	16.86
0.01µg/ml	13.16	20.32	12.88	21.90	16.61	16.48
0.01µg/ml	13.45	20.95	12.79	22.17	16.48	16.98
0.07µg/ml	12.03	18.87	12.59	20.48	15.84	16.44
0.07µg/ml	12.08	18.78	12.43	20.14	15.84	16.42
0.07µg/ml	12.54	18.73	12.59	20.27	16.10	16.36
0.1µg/ml	11.90	19.33	11.42	18.95	15.85	15.78
0.1µg/ml	12.79	19.33	11.54	18.80	15.74	15.82
0.1µg/ml	13.84	19.33	12.12	19.03	16.55	16.01

Table A.50: Relative fold changes in *p21* gene expression, following exposure (24h) with increasing concentrations of araC in TK6 cells

Replicate 1	SQ mean			
araC (µg/ml)	Beta actin	p21	Normalization	Fold change
0	1.11E+00	2.24E+00	2.022245417	1
0.0007	1.23E+00	3.56E+00	2.890254164	1.429230172
0.005	2.42E+00	7.25E+00	2.99636522	1.48170207
0.01	1.12E+00	4.26E+00	3.786876183	1.872609601
0.07	2.45E+00	1.24E+01	5.05478457	2.499590073
0.1	1.79E+00	8.65E+00	4.820452615	2.383712963
Replicate 2	SQ mean			
araC (µg/ml)	Beta actin	p21	Normalization	Fold change
0	1.58E+00	1.92E+00	1.22E+00	1
0.0007	1.52E+00	2.68E+00	1.76E+00	1.445972
0.005	1.45E+00	2.93E+00	2.02E+00	1.656356
0.01	1.49E+00	1.68E+00	1.13E+00	0.929404
0.07	1.85E+00	4.81E+00	2.60E+00	2.13737
0.1	3.31E+00	1.09E+01	3.29E+00	2.70406
Replicate 3	SQ mean			
araC (µg/ml)	Beta actin	p21	Normalization	Fold change
0	1.98E-01	6.76E-01	3.413017	1
0.0007	2.91E-01	9.57E-01	3.291488	0.964392
0.005	3.00E-01	9.35E-01	3.118143	0.913603
0.01	1.79E-01	1.09E+00	6.102837	1.788106
0.07	2.23E-01	1.42E+00	6.350254	1.860598
0.1	2.11E-01	2.13E+00	10.09687	2.958341

Table A.51: C_T-values of *p21* gene expression, following exposure (24h) with increasing concentrations of araC in AHH-1 cells

	C_T-values					
	Replicate 1		Replicate 2		Replicate 3	
	beta-actin	p21	beta-actin	p21	beta-actin	p21
Standard	12.96	22.02	12.54	19.61	12.91	19.57
Standard	12.94	22.54	12.26	19.64	12.99	19.60
Standard			12.65	20.02	12.73	19.66
Standard (10-1)	17.21	27.10	17.13	24.53	16.20	22.99
Standard (10-1)	17.06	25.78	17.02	24.34	15.42	22.76
Standard (10-1)	17.07		15.96	23.68		22.20
Standard (10-2)	20.17	29.59	20.10	27.23	19.63	26.27
Standard (10-2)	19.74	29.19	19.62	26.95	18.69	25.32
Standard (10-2)			19.24	26.60	18.62	
Standard (10-3)	22.98	32.65	23.22	30.70	22.38	29.61
Standard (10-3)	22.55	32.92	22.95	29.45	21.91	29.24
Standard (10-3)						
0µg/ml	11.10	21.15	12.36	20.38	12.66	18.82
0µg/ml	10.87	20.99	12.75	20.38	12.65	18.73
0µg/ml	11.08	21.09	12.80	20.56	13.02	18.60
0.0007µg/ml	11.99	21.85	12.69	19.76	12.61	18.83
0.0007µg/ml	11.93	21.83	12.43	20.57	12.64	18.61
0.0007µg/ml	12.01	21.81	12.97	21.38	12.95	18.49
0.005µg/ml	12.82	21.84	13.65	20.30	12.10	19.03
0.005µg/ml	12.61	21.73	13.60	20.55	12.14	18.70
0.005µg/ml	12.86	21.80	13.67	20.99	12.27	18.46
0.01µg/ml	12.28	21.26	13.15	19.46	12.18	18.07
0.01µg/ml	12.04	21.44	13.29	19.79	12.20	18.52
0.01µg/ml	12.18	21.34	14.02	20.16	12.35	18.36
0.07µg/ml	12.97	21.87	14.06	20.94	12.71	18.44
0.07µg/ml	13.01	21.91	14.07	20.93	12.69	18.19
0.07µg/ml	13.37	21.88	14.60	20.73	12.93	18.02
0.1µg/ml	10.86	20.48	14.17	20.45	13.66	19.28
0.1µg/ml	10.74	20.50	14.03	21.35	13.59	18.62
0.1µg/ml	11.07	20.67	14.70	20.46	13.62	18.31

Table A.52: Relative fold changes in *p21* gene expression, following exposure (24h) with increasing concentrations of araC in AHH-1 cells

Replicate 1	SQ mean			
araC (µg/ml)	Beta actin	p21	Normalization	Fold change
0	5.74E+00	2.70E+00	0.469849065	1
0.0007	2.87E+00	1.62E+00	0.565511724	1.203602956
0.005	1.63E+00	1.67E+00	1.022824181	2.176920754
0.01	2.51E+00	2.25E+00	0.897359587	1.909889055
0.07	1.28E+00	1.57E+00	1.229710472	2.617245757
0.1	6.29E+00	3.83E+00	0.60885054	1.295842825
Replicate 2	SQ mean			
araC (µg/ml)	Beta actin	p21	Normalization	Fold change
0	1.095581	0.830061	0.757645	1
0.0007	1.053292	0.834506	0.792284	1.045719
0.005	0.559313	0.749696	1.340388	1.76915
0.01	0.636871	1.296683	2.03602	2.687301
0.07	0.380185	0.620268	1.63149	2.153371
0.1	0.368611	0.69544	1.88665	2.490151
Replicate 3	SQ mean			
araC (µg/ml)	Beta actin	p21	Normalization	Fold change
0	1.05E+00	1.74E+00	1.67E+00	1
0.0007	1.08E+00	1.84E+00	1.71E+00	1.025488153
0.005	1.63E+00	1.75E+00	1.07E+00	0.641065661
0.01	1.55E+00	2.34E+00	1.51E+00	0.904441648
0.07	1.04E+00	2.50E+00	2.40E+00	1.440217606
0.1	5.50E-01	1.79E+00	3.24E+00	1.944379143

Table A.53: C_T-values of *p21* gene expression, following exposure (24h) with increasing concentrations of araC in MCL-5 cells

	C_T-values					
	Replicate 1		Replicate 2		Replicate 3	
	beta-actin	p21	beta-actin	p21	beta-actin	p21
Standard	12.50	21.49	11.61	19.56	12.59	22.50
Standard	12.29	21.79	11.52	19.40	12.72	22.53
Standard			11.79	19.58	12.66	22.39
Standard (10-1)	16.82	26.01	14.88	23.38	18.18	28.05
Standard (10-1)	16.32	25.95	14.79	23.06	17.85	27.22
Standard (10-1)			14.60	22.67	17.74	
Standard (10-2)	19.99	29.50	17.65	25.85	20.95	31.27
Standard (10-2)	19.63	28.91	17.59	25.99	20.78	30.59
Standard (10-2)			17.62	25.58	20.58	
Standard (10-3)	22.36	33.12	20.92	29.68	23.04	34.37
Standard (10-3)	22.48	32.79	21.01	29.37	22.82	33.62
Standard (10-3)	21.88					
0µg/ml	13.10	21.28	13.60	22.80	12.52	21.98
0µg/ml	12.79	21.87	13.67	22.49	12.73	22.34
0µg/ml	13.21	22.09	13.87	22.62	12.96	22.77
0.0007µg/ml	12.65	21.48	13.56	22.92	12.32	23.08
0.0007µg/ml	11.90	21.34	13.51	22.77	12.29	22.88
0.0007µg/ml	12.46	21.36	13.59	22.98	12.82	22.83
0.005µg/ml	12.20	21.83	13.64	22.01	12.80	22.97
0.005µg/ml	12.57	21.55	13.41	21.81	12.81	23.04
0.005µg/ml	12.66	21.13	13.79	21.96	12.98	23.30
0.01µg/ml	12.04	21.12	12.88	20.96	12.29	23.01
0.01µg/ml	12.18	21.14	13.02	20.94	12.57	22.70
0.01µg/ml	12.47	21.58	13.02	21.20	13.05	23.12
0.07µg/ml	12.70	20.88	13.11	20.88	12.54	22.06
0.07µg/ml	12.47	20.84	12.96	20.85	12.55	21.67
0.07µg/ml	12.66	20.84	13.53	20.77	12.93	22.00
0.1µg/ml	11.67	20.10	12.80	19.76	12.76	22.07
0.1µg/ml	11.63	20.05	12.72	20.33	12.75	21.91
0.1µg/ml	12.12	20.38	13.23	20.30	12.84	22.01

Table A.54: Relative fold changes in *p21* gene expression, following exposure (24h) with increasing concentrations of araC in MCL-5 cells

Replicate 1	SQ mean			
araC (µg/ml)	Beta actin	p21	Normalization	Fold change
0	8.95E-01	1.11E+00	1.235675	1
0.004	1.50E+00	1.34E+00	0.895119	0.724397
0.008	1.33E+00	1.27E+00	0.955133	0.772965
0.02	1.59E+00	1.46E+00	0.916573	0.741759
0.04	1.20E+00	1.88E+00	1.559399	1.261982
0.08	2.16E+00	2.87E+00	1.329965	1.076306
Replicate 2	SQ mean			
araC (µg/ml)	Beta actin	p21	Normalization	Fold change
0	2.10E-01	1.15E-01	0.545692	1
0.0007	2.36E-01	9.55E-02	0.404323	0.740937
0.005	2.27E-01	1.89E-01	0.829647	1.520359
0.01	3.65E-01	3.55E-01	0.97324	1.783498
0.07	3.12E-01	4.08E-01	1.305081	2.39161
0.1	3.86E-01	6.82E-01	1.769863	3.24334
Replicate 3	SQ mean			
araC (µg/ml)	Beta actin	p21	Normalization	Fold change
0	1.63E+00	1.42E+00	8.73E-01	1
0.0007	1.95E+00	9.99E-01	5.13E-01	0.587396
0.005	1.49E+00	8.99E-01	6.04E-01	0.692178
0.01	1.77E+00	9.94E-01	5.63E-01	0.644797
0.07	1.70E+00	1.84E+00	1.08E+00	1.237394
0.1	1.57E+00	1.74E+00	1.11E+00	1.270464

Appendix VII

Western Blots

Figure A.5: Representative Western Blots for p53 and phosphos-p53 following MMC treatment in TK6 cells (Replicate 1 to 3)

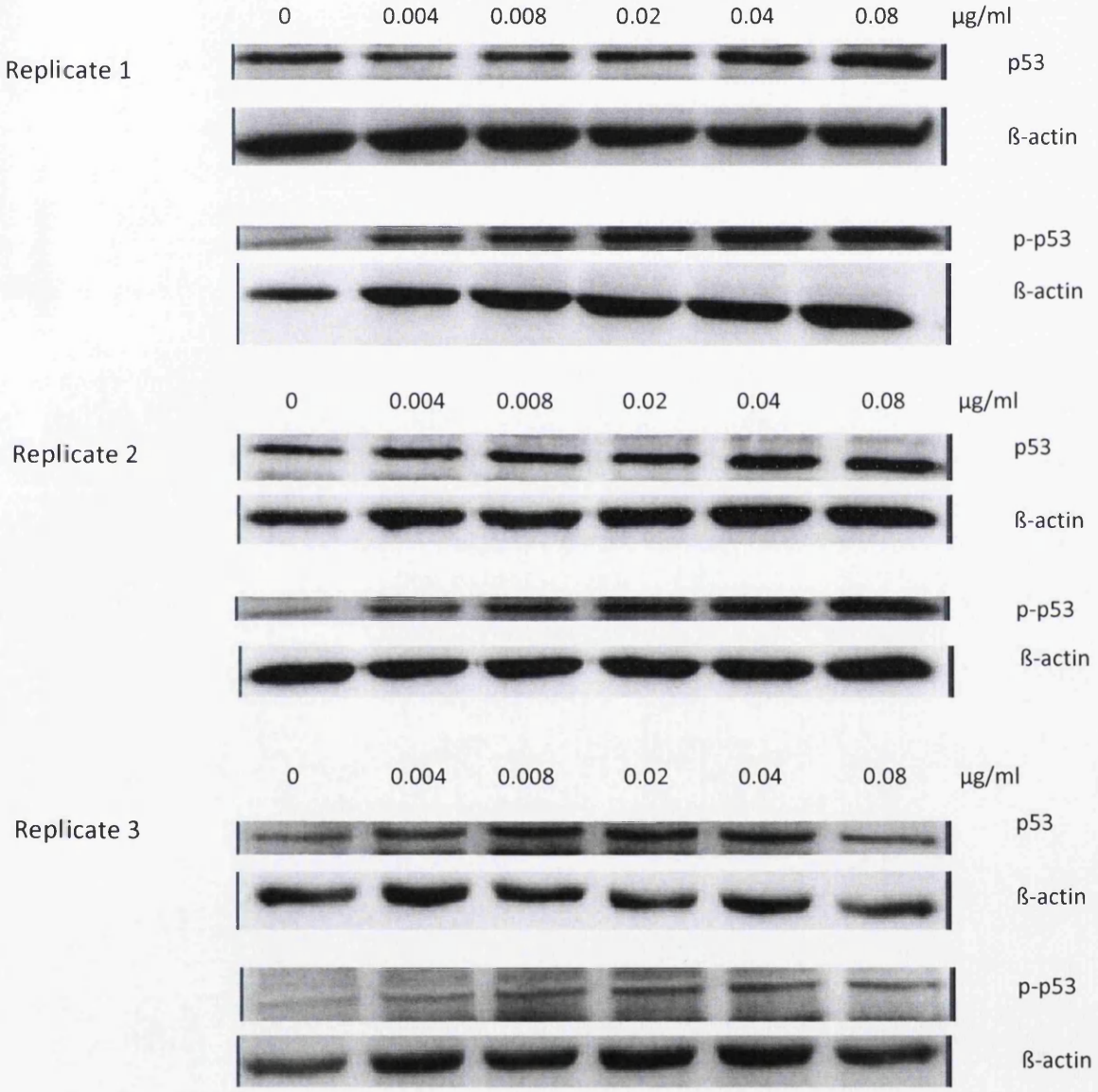

Figure A.6: Representative Western Blots for p53 and phosphos-p53 following MMC treatment in AHH-1 cells (Replicate 1 to 3)

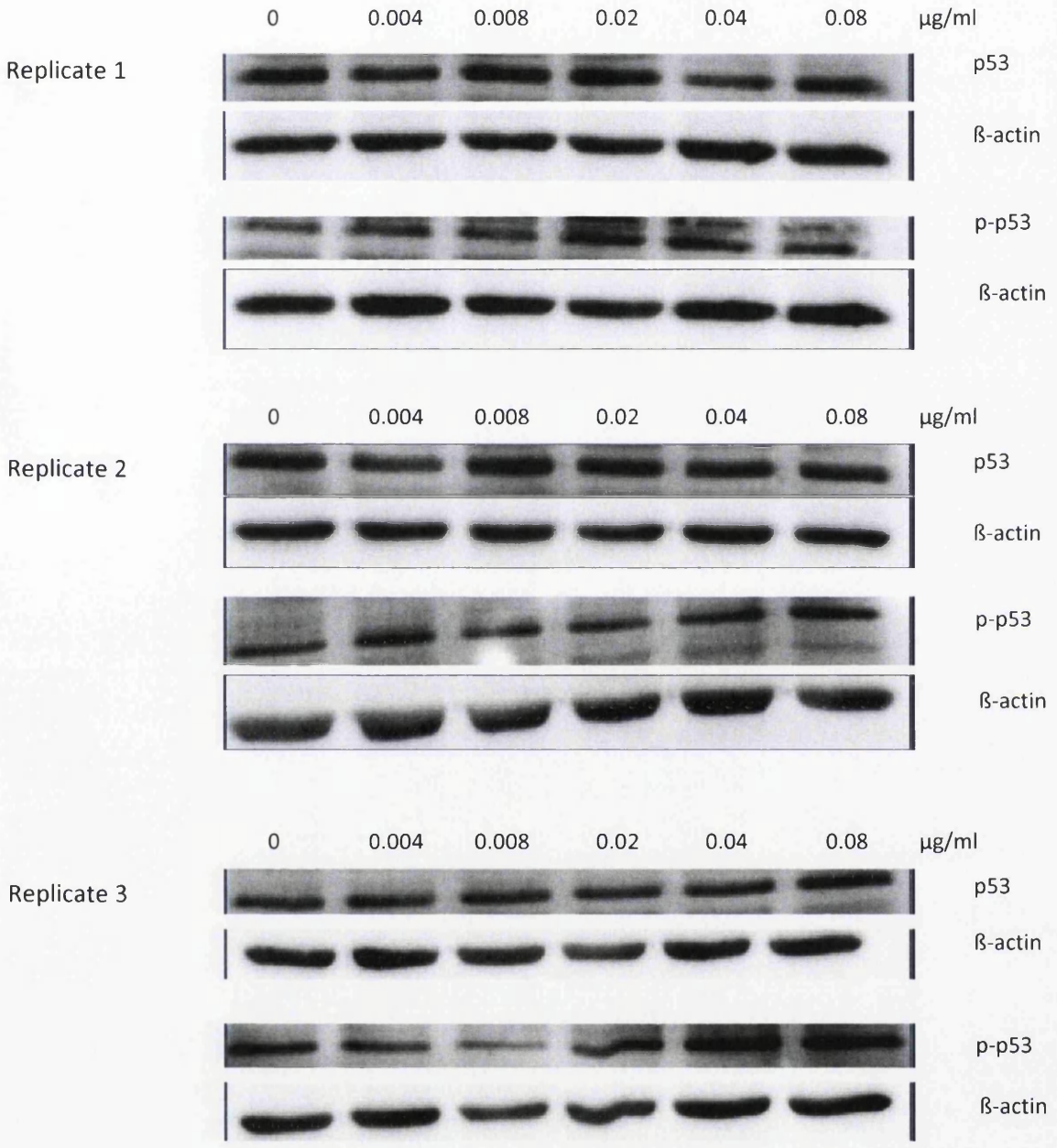

Figure A.7: Representative Western Blots for p53 and phosphos-p53 following araC treatment in TK6 cells (Replicate 1 to 3)

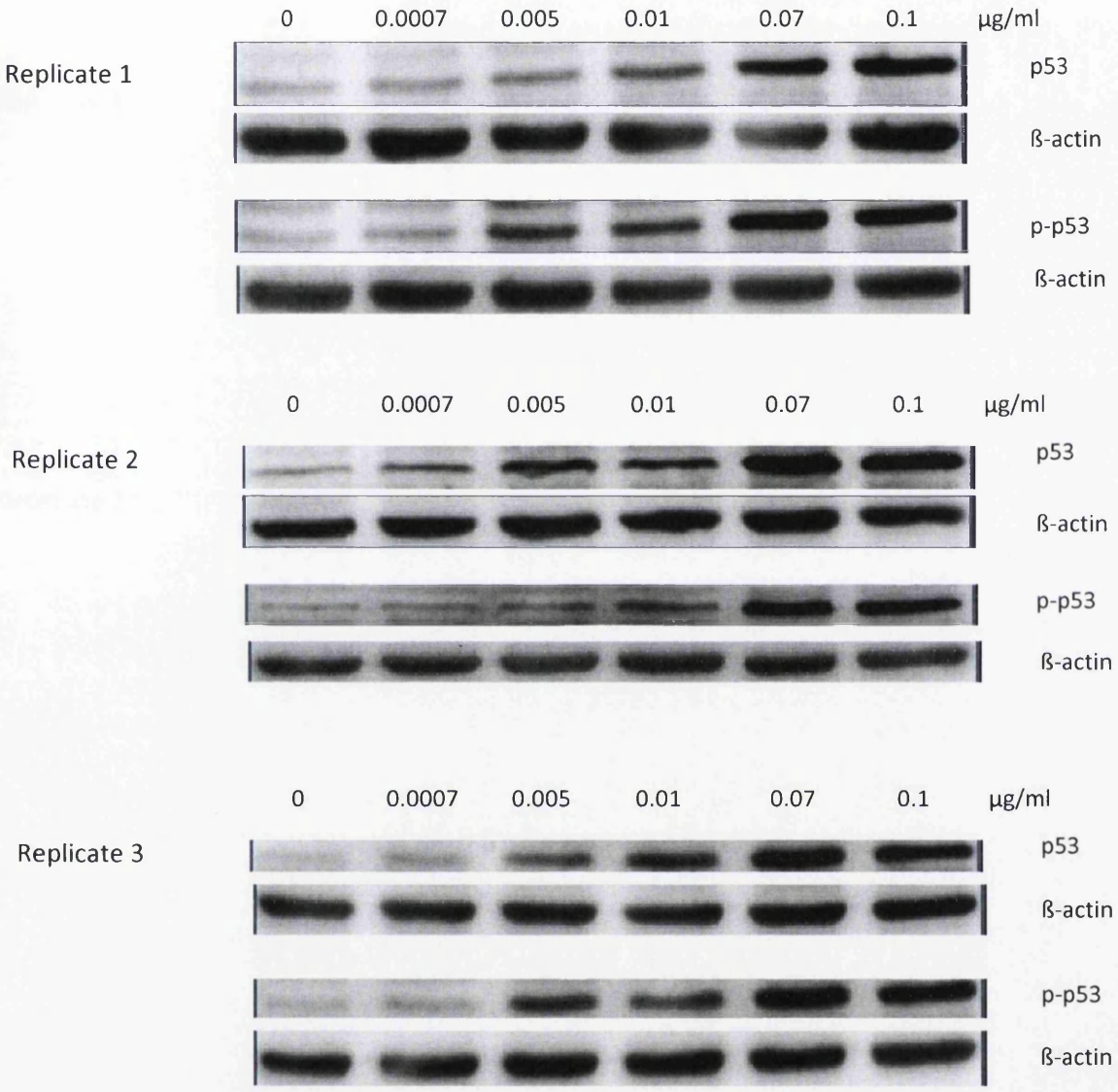

Figure A.8: Representative Western Blots for p53 and phosphos-p53 following araC treatment in AHH-1 cells (Replicate 1 to 3)

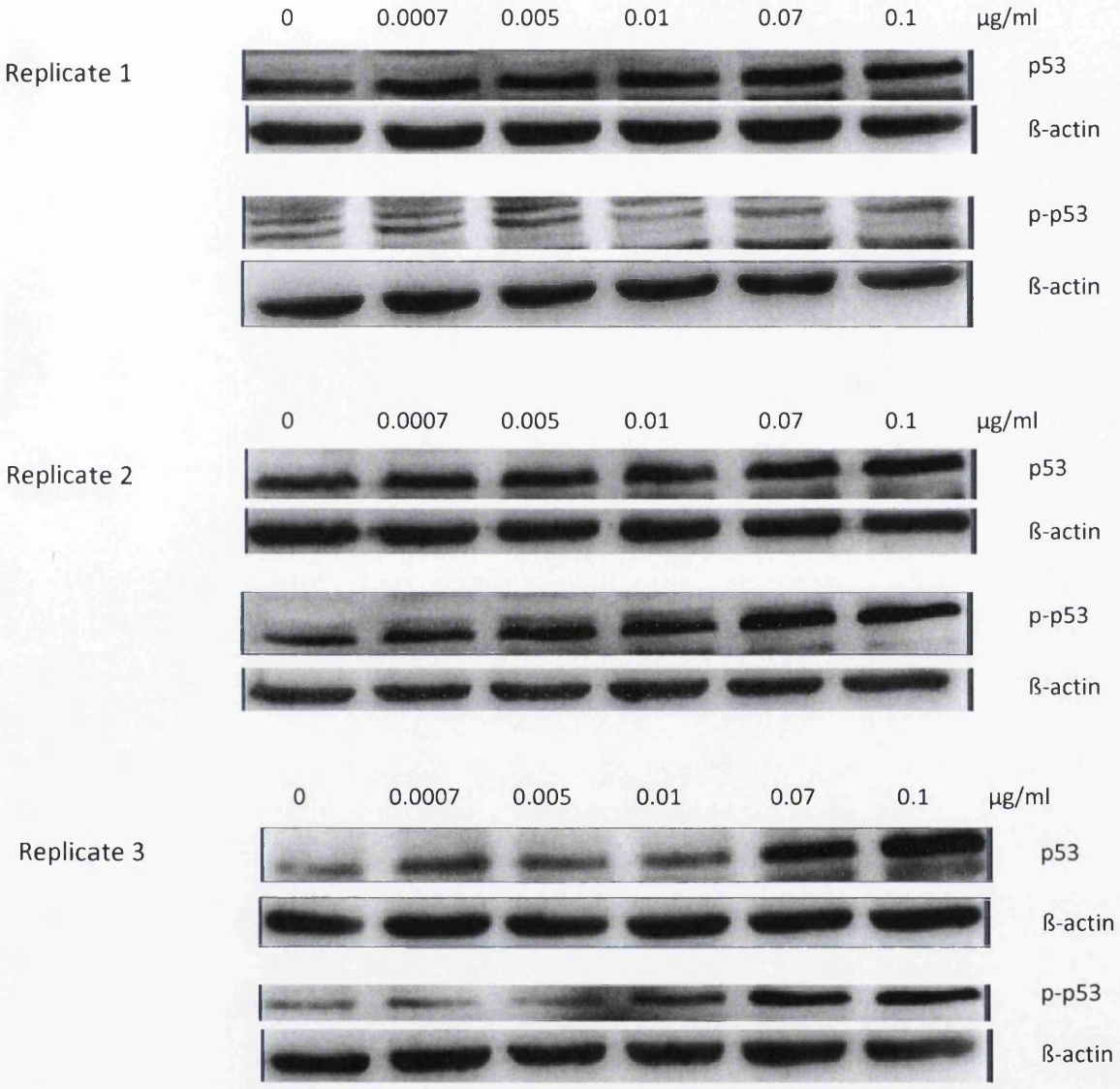

Figure A.9: Representative Western Blots for p53 and phosphos-p53 following araC treatment in MCL-5 cells (Replicate 1 to 3)

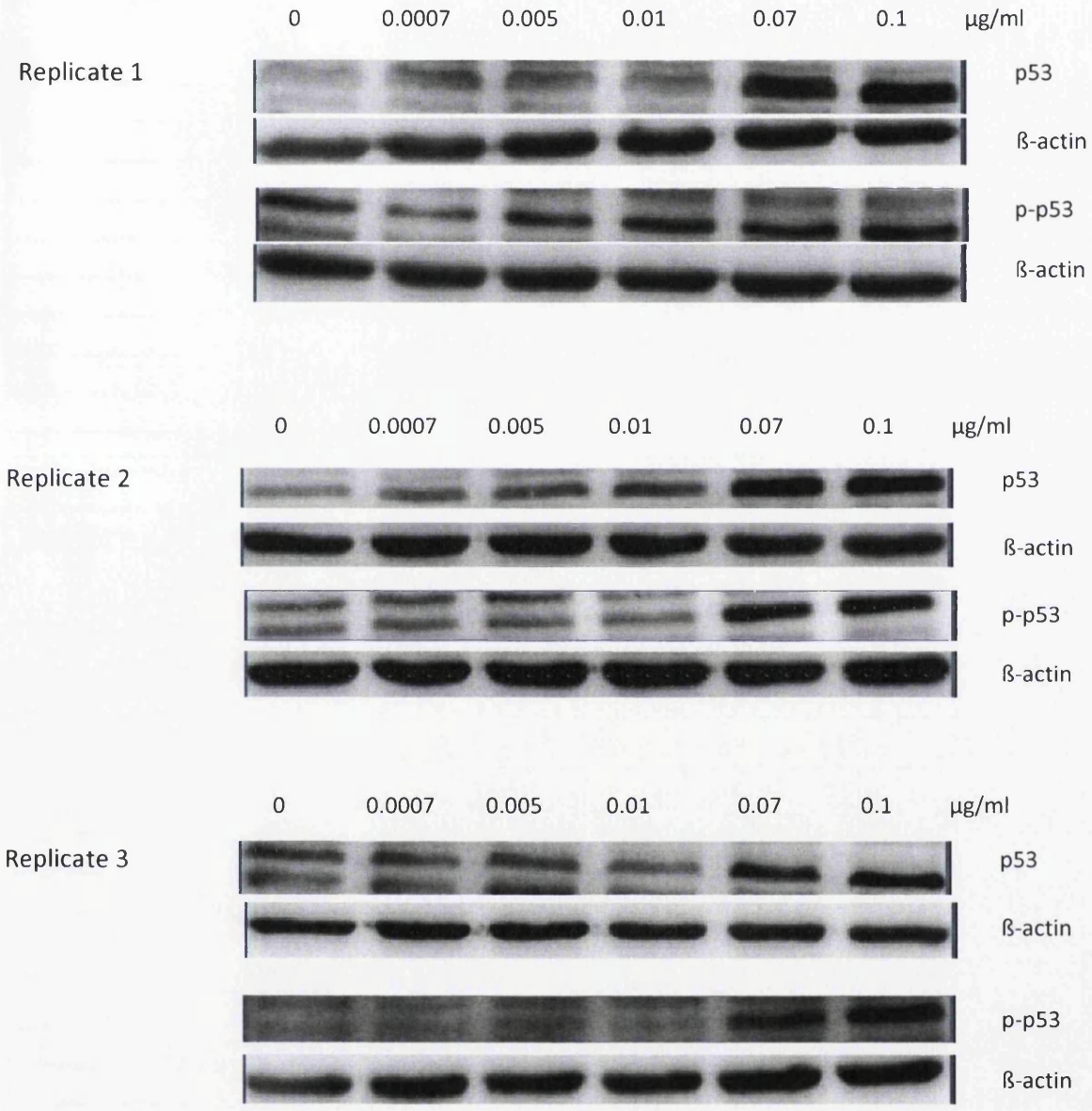

Appendix VIII

Apoptosis results

Table A.55: Flow cytometric analysis of apoptosis in TK6 cells treated with 4h of MMC. Staurosporin was used as a positive control.

MMC (µg/ml)	% early apoptotic	% late apoptotic	%dead cells
0	0.205581778	2.804680183	24.4112812
0.002	0.169598731	3.22034498	27.1388548
0.004	0.127322486	2.115392439	23.1531928
0.006	0.286247854	3.45387751	23.7130678
0.008	0.153506919	3.150629666	27.2894347
0.01	0.202130496	3.002960705	24.5793689
0.02	0.159741045	2.93954491	24.626641
0.04	0.188918268	2.920127671	26.244557
0.06	0.20734541	2.407648329	23.4933976
0.08	0.169269517	2.72810154	25.5900046
0.1	0.161842952	3.578054799	31.7730298
1µM Staurosporine (FITC-pos)	5.712631356		

Table A.56: Flow cytometric analysis of apoptosis in TK6 cells treated with 24h of araC. Staurosporin was used as a positive control.

araC (µg/ml)	% early apoptotic	% late apoptotic	% dead cells
0	0.05663	1.595473	25.05149
0.0001	0.055515	1.890797	23.62957
0.0003	0.053539	1.270249	29.08727
0.0005	0.048329	1.385316	31.02858
0.0007	0.031296	1.050755	26.78154
0.0009	0.028512	1.22981	28.2823
0.001	0.038313	1.216312	29.66936
0.003	0.069749	1.870813	29.13842
0.005	0.061986	1.424695	24.666
0.007	0.048805	1.132638	33.16454
0.009	0.072746	1.447228	32.58757
0.01	0.078127	1.545029	29.30622
0.03	0.048481	1.963403	34.51287
0.07	0.081076	3.095258	44.52838
0.1	0.069369	5.24765	46.5181
1µM Staurosporine (FITC-pos)	3.931486		

Appendix IX

Cell cycle results

Table A.57: Cell cycle analysis in TK6 cells treated with MMC for 4h

MMC (μg/ml)	G0/G1	S-phase	G2/M
0	47.3	13.7666667	37.3
0.002	50.1333333	14.5	33.8333333
0.004	50.7333333	14.6666667	33.2666667
0.006	47.5	14.4333333	36.8333333
0.008	47.2	14.6	36.7333333
0.01	46.4	14.4333333	37.5333333
0.02	46.7	14.7	37.1666667
0.04	45	15.1	38.5
0.06	45.1333333	16.5333333	37.1
0.08	44.3333333	16.8666667	37.4333333
0.1	42.6666667	16.4333333	39.7

Table A.58: Cell cycle analysis in TK6 cells treated with MMC for 4h +18h recovery

MMC (μg/ml)	G1/G0	S-phase	G2/M
0	48.7666667	13.1666667	36.5
0.006	45.7	11.6666667	40.4
0.02	45.1666667	11.2666667	41.4333333
0.06	41.6333333	11.3	44.6333333
0.1	32.2666667	12.2	52.5666667

Table A.59: Cell cycle analysis in TK6 cells treated with araC for 24h

araC (µg/ml)	G0/G1	S-phase	G2/M
0	48.8666667	13.2	36.1666667
0.0001	49.6	13.9666667	34.1333333
0.0003	47.7	14.0333333	36.4
0.0005	47.0333333	13.9666667	37.3333333
0.0007	45.0666667	14.4	38.8
0.0009	47.7	14.4	35.8666667
0.001	48.9	14.6	34.4666667
0.003	47.9333333	16.1	34.0333333
0.005	46.1	16.0333333	35.7
0.007	49.3666667	17.1333333	31.6333333
0.009	47.2666667	16.6666667	33.4
0.01	46.5333333	16.8666667	34.1666667
0.03	52.9333333	16.0333333	26.8333333
0.07	57.4	12.1666667	20.8666667
0.1	49.6666667	13.4	27.2333333

Table A60: Cell cycle analysis in TK6 cells treated with araC for 24h +18h recovery

araC (µg/ml)	G1/G0	S-phase	G2/M
0	53.2	10.2	34.7666667
0.0005	53.3666667	10.9	33.8
0.009	57.8	11.2333333	29
0.03	59.1333333	10.1666667	28.2333333
0.07	56.7333333	10.1666667	26.4
0.1	60	10.1666667	20.7